UNIVERSITY OF PARDUBICE
FACULTY OF CHEMICAL TECHNOLOGY
DEPARTMENT OF ORGANIC CHEMISTRY AND TECHNOLOGY

Mechanisms of ring transformations of isothiouronium salts derived from bromolactones

DISSERTATION THESIS

Author: Ing. Jiří Váňa
Supervisor: prof. Ing. Miloš Sedlák, DrSc.

2012

UNIVERZITA PARDUBICE
FAKULTA CHEMICKO-TECHNOLOGICKÁ
ÚSTAV ORGANICKÉ CHEMIE A TECHNOLOGIE

Studium transformačních reakcí isothiouroniových solí odvozených od bromlaktonů

DISERTAČNÍ PRÁCE

Autor práce: Ing. Jiří Váňa

Vedoucí práce: prof. Ing. Miloš Sedlák, DrSc.

2012

Prohlašuji:

Tuto práci jsem vypracoval samostatně. Veškeré literární prameny a informace, které jsem v práci využil, jsou uvedeny v seznamu použité literatury. Práce byla vypracována na Ústavu organické chemie a technologie.

Byl jsem seznámen s tím, že se na moji práci vztahují práva a povinnosti vyplývající ze zákona č. 121/2000 Sb., autorský zákon, zejména se skutečností, že Univerzita Pardubice má právo na uzavření licenční smlouvy o užití této práce jako školního díla podle § 60 odst. 1 autorského zákona, a s tím, že pokud dojde k užití této práce mnou nebo bude poskytnuta licence o jejím použití jinému subjektu, je Univerzita Pardubice oprávněna ode mne požadovat přiměřený příspěvek na úhradu nákladů, které na vytvoření díla vynaložila, a to podle okolností až do její skutečné výše.

Souhlasím s prezenčním zpřístupněním své práce v Univerzitní knihovně Univerzity Pardubice.

I declare:

This work has been made independently. All used literature resources and information's are written in the reference section. This work has been elaborated at the Institute of Organic Chemistry and Technology.

I was informed about rights and responsibilities connected with the law 121/2000 Sb., authors law. Mainly with the fact that University of Pardubice is entitled to conclude a license agreement of usage of this work as a school work in accordance with § 60 paragraph 1 of authors law. If the work will be used by me or the license will be provided to another subject, the University of Pardubice is authorized to demand adequate fee for compensation of the costs invested to the work depending on circumstances to the real extent.

I agree with making my work available for the attendance lending in the University Library.

Pardubice 9.1.2012 Ing. Jiří Váňa

Acknowledgement

I would like to thank to my supervisor prof. Miloš Sedlák for leadership, valuable advices and multilateral help during my work. To doc. Jiří Hanusek for stimulating consultations, constructive remarks and help with my work. To Dr. Andrew Laws for enabling me to acquire work experiences in the foreign country. To doc. Jana Roithová for measuring of IRMPD spectra and help with the “gas phase” chemistry.

I would like to thank to Éliška, Panovič, Šurik and all the collective of the Institute of Organic Chemistry for creation of the nice and inspiriting atmosphere in the lab.

I would like to thank to Paul for the help with my English.

Finally I would like to thank to my all family and friends for the encouragement.

Contents

Summary

The kinetics and mechanism of rearrangement of *S*-(2-oxotetrahydrofuran-3-yl)-*N*-(4-methoxyphenyl)isothiouronium bromide (**1b**) into 5-(2-hydroxyethyl)-2-[(4-methoxyphenyl)imino]-1,3-thiazolidin-4-one (**2b**) have been studied under pseudo-first order reaction conditions in aqueous buffer solutions (pH 2 – 9) in hydrochloric acid solutions (0.001-0.3 mol·l^{-1}) and sodium hydroxide solutions at 25 °C and at constant ionic strength (I = 1 mol·l^{-1}). Multiple breaks in the measured pH profile establish the formation of three different kinetically detectable intermediates $\mathbf{T}^{\pm}$, $\mathbf{T}^{0}$ and $\mathbf{T}^{-}$, whose rate of formation and breakdown to the product are pH dependent. Treatment of the isothiouronium salt **1a** (pK_a = 6.7) with base produces reactive isothiourea which undergoes cyclization to give the zwitterionic intermediate $\mathbf{T}^{\pm}$ (rate limiting step at pH < 2). Intermediate $\mathbf{T}^{\pm}$ then undergoes either general acid-catalyzed, concerted (α = –0.47) breakdown to product (r.l.s. at pH 2-3) or a water-mediated proton switch to $\mathbf{T}^{0}$ which is followed by its general acid-catalyzed breakdown (pH 3-6). The last reaction pathway involves the formation of the anionic intermediate $\mathbf{T}^{-}$ either from $\mathbf{T}^{\pm}$ or from $\mathbf{T}^{0}$ (pH > 6). The first possibility involving reaction of $\mathbf{T}^{\pm}$ via $\mathbf{T}^{-}$ to **2b** seems to be more likely because it is in accordance with kinetics observed in basic amine buffers, where the non-linear increase of the observed rate constant with the total buffer concentration changes to a linear increase as a general-base catalyzed pathway is introduced. Coexistence of all three kinetically detectable intermediates is very rare and is possible due to relatively enhanced stability of these intermediates *i.e.* fast intramolecular step leading to the production of $\mathbf{T}^{\pm}$ and the presence of a relatively poor leaving group (alkoxide) necessitates participation of an acid for progression to products. These observations have been compared to the rearrangement of *S*-(2-oxotetrahydrofuran-3-yl)-*N*-(4-methoxybenzyl)isothiouronium bromide (**1p**) which shows the same character. Only the reaction rate is one order of magnitude lower.

Influence of the additional Cu(II) ions on the reaction rate has been followed. The reaction acceleration depends which Cu(II) salt have been used, its concentration and the pH of the solution. The highest influence has been observed at low Cu(II) ion concentration. With increasing concentration the influence of the Cu(II) ions decreases and the reaction rate becomes Cu(II) independent. Coordination of the copper(II) to the carbonyl oxygen which makes this group more reactive towards nucleophiles has been proposed as an explanation

of the reaction acceleration. Also stabilisation of the leaving group by copper(II) coordination facilitates the rearrangement.

3-Bromophtalide has been used instead of 2-bromobutyrolactone for the preparation of isothiouronium salts in the next part of my work. Measuring of the pK_as of the prepared salts shows surprisingly high influence of the substitution on the benzene ring. The values of the so obtained Hammett constants are approximately of 2.5. The sulphur bridge effect is the most probable explanation for this observation.

The influence of substitution in the thiourea moiety of the molecule on the formation of transformation products has been observed. Rearrangement of unsubstituted (**3**) and monosubstituted (**5**) isothiouronium salts leads to *N*-substituted-1-hydroxy-3-oxo-1,3-dihydro-2*H*-isoindol-2-carbothioamides (**4**,**6)**, however, the rearrangement of *N*,*N*´-disubstituted salts (**9**) gives 1,3-disubtituted-1-(3-oxo-1,3-dihydro-2-benzofuran-1-yl)thioureas (**10**). The mechanism proceeding *via* attack of the imino group of the free base of thiourea on the carbonyl group followed by breakdown of the so formed zwitterionic intermediate to the aldehyde and its subsequent cyclization has been proposed for the rearrangement of the unsubstituted (**3**) and monosubstituted (**5**) salts.

The transformation of *N*,*N*´-disubstituted salts (**9**) offers more explanation. This *S* to *N* alkyl migration could proceed as a S_N1 type reaction where carbocationic intermediate is formed in the first reaction step. The frontside type of S_N2 reaction is the second possibility and the "double-displacement" mechanism with the double inversion is the third alternative. Measuring of the IRMPD spectra together with other observations indicates presence of the carboxylic acid type intermediate ***XXVI*** and offers the last mechanism as the most probable.

Keywords: transformation reaction, reaction mechanism, acid-base catalysis, metal ion catalysis, isothiouronium salts, lactones, phthalides, 2-iminothiazolidinones

Souhrn

Transformační reakce *S*-(2-oxotetrahydrofuran-3-yl)-*N*-(4-methoxyfenyl)isothiouronium bromidu (**1b**) na 5-(2-hydroxyethyl)-2-[(4-methoxyfenyl)imino]-1,3-thiazolidin-4-on (**2b**) byla sledována spektrofotometricky za podmínek pseudoprvního řádu ve vodných roztocích pufrů (pH 2 – 9), kyseliny chlorovodíkové a hydroxidu sodného při 25 °C a konstantní iontové síle (I = 1 mol·l^{-1}). pH Profil reakce ukazuje několik zlomů, jejichž přítomnost lze vysvětlit uplatněním tří různých intermediátů $\mathbf{T}^{\pm}$, $\mathbf{T}^{0}$ and $\mathbf{T}^{-}$. Rychlost jejich vzniku a rozpadu závisí na pH prostředí. Reaktivním species je volná isothiomočovina vznikající z isothiouroniové soli **1b** (pK_a = 6.7) působením báze. Iminový atom dusíku atakuje karbonylový uhlík za vzniku tetraedrálního intermediátu $\mathbf{T}^{\pm}$ (rychlost určující krok při pH < 2). Intermediát $\mathbf{T}^{\pm}$ dále podléhá obecně kysele katalyzovanému součinnému (α = –0.47) rozpadu na produkt (r.u.k. při pH 2-3) a nebo přenosu protonu za vzniku intermediátu $\mathbf{T}^{0}$. Ten se dále působením obecné kyseliny rozpadá na produkt (pH 3-6). Poslední reakční cesta zahrnuje vznik anionického intermediátu $\mathbf{T}^{-}$ buď z $\mathbf{T}^{\pm}$ a nebo $\mathbf{T}^{0}$ (pH > 6). První možnost se jeví jako pravděpodobnější díky měření v aminových pufrech. Zde byl pozorován nelineární nárůst pozorované rychlostní konstanty v závislosti na koncetraci pufru kdy se reakce mění z obecně bázicky katalyzované na specificky katalyzovanou. Současná existence tří kineticky detekovatelných intermediátů je velmi vzácná a v tomto případě je zřejmě způsobena jejich zvýšenou stabilitou vedoucí k delší době života – to je umožněno rychlým intramolekulárním vznikem intermediátu $\mathbf{T}^{\pm}$ a přítomností relativně špatné odstupující alkoxidové skupiny. Tyto výsledky byly srovnány s přesmykem *S*-(2-oxotetrahydrofuran-3-yl)-*N*-(4-methoxybenzyl)isothiouronium bromidu (**1p**). Reakce se chová obdobě, pouze je přibližně o řád pomalejší.

V další části práce byl porovnán vliv přídavku měďnatých iontů na rychlost reakce. Urychlení závisí na druhu použité soli, její koncentraci a pH prostředí. Největší vliv byl pozorován při malých koncentrací iontů. S jejich rostoucí koncentrací vliv klesá a reakce se stává na koncentraci iontů nezávislou. Urychlení lze vysvětlit koordinací mědi na kyslík karbonylové skupiny. Ta se pak stává reaktivnější vůči nukleofilnímu ataku. Druhým účinkem měďnatého iontu je koordinace na odstupující alkoxidový atom kyslíku.

V další části práce byla obměněna struktura laktonové části molekuly a 2-brombutyrolakton byl 3-bromftalidem. Měření disociačních konstant ukazuje velký vliv substituce na benzenovém jádře. Hammettova závislost má směrnici přibližně 2,5. Tento vliv lze vysvětlit můstkovým efektem atomu síry.

Vliv substituce isothiouroniové části molekuly zásadním rozdílem ovlivňuje reaktivitu solí a typ vznikajících produktů. Přesmyk nesubstituovaných (**3**) a monosubstituovanných (**5**) isothiouroniových solí vede ke vzniku *N*-substituovaných 1-hydroxy-3-oxo-1,3-dihydro-2*H*-isoindol-2-karbothioamidů (**4**,**6**). Naopak přesmyk *N*,*N´*-disubstituovaných solí (**9**) poskytuje 1,3-dimethyl-1-(3-oxo-1,3-dihydro-2-benzofuran-1-yl)thiomočoviny (**10**). Mechanismus vzniku prvního typu produktu lze vysvětlit atakem volné iminoskupiny na skupinu karbonylovou za vzniku zwitterionického intermediátu. Ten se následně rozpadá na aldehyd. Konečný produkt reakce poskytuje intramolekulární cyklizace takto vzniklého aldehydu.

Na transformaci *N*,*N´*-disubstituovaných solí (**9**) lze nahlížet jako na migraci alkylu z atomu síry na atom dusíku. V úvahu připadají tři možné vysvětlení. Prvním je reakce typu S_N1, kdy v prvním kroku molekula disociuje za vzniku karbokationtu, který následně reaguje s dusíkem odstoupivší thiomočoviny za vzniku produktu. Druhou možností je mechanismus blízký reakci S_N2, kdy dochází k "frontside" ataku atomu dusíku na reakční centrum za současného odstoupení atomu síry. Třetí možností je "double-displacement mechanismus", kdy v prvním kroku opět dochází k ataku atomu dusíku na reakční centrum. Odsupující skupinou je v tomto případě karboxylát, který v druhém reakčním kroku zpětně napadá benzylový uklík. Měření IRMPD spekter ukazuje na možný vznik intermediátu karboxylátového typu ***XXVI*** a spolu s dalšímii poznatky ukazuje na třetí mechanismus jako na nejpravděpodobnější.

Klíčová slova: transformační reakce, reakční mechanismus, azidobazická katalýza, katalýza ionty kovů, isothiouroniové soli, laktony, ftalidy, 2-iminothiazolidinony

1 Introduction

It is well known that intramolecular reactions bear a striking resemblance to the reactions of enzymes and can give an insight into their analogous enzymatic process.[1-4] Small molecules undergoing intramolecular cyclization reactions have frequently been used as models for understanding the nature of preorganizational effects and their relative contributions to the enhanced rates observed in enzymatic reactions.[5-7] Acyl groups have a prominent position in biochemistry and biology and their biochemical relevance alone has made acyl group transfer one of the most studied reactions in all of organic chemistry.[8-14]

Intramolecular aminolysis are a specially important class of acyl-transfer reactions and are of great importance in biochemistry and medicinal chemistry. A large amount of research has been devoted to this area.[15-25] Isothiouronium salts are very useful for the study of intramolecular reactions, especially due to the fact that they are prepared in a nonreactive protonated form that they can be consider for a "masked" or "protected" amino group. After transfer to the reaction media and addition of the base, the amino group is released and can react with the desired functional groups. The pK_as of the salts are very close to physiological systems, which makes them very useful for mimicking processes occurring in living organisms.

Rearrangements of heterocyclic compounds are also of great significance; providing new routes to otherwise difficult-to-prepare biologically active compounds. This new approach to the synthesis of heterocycles has rapidly grown recently[26-36] and in many cases such transformations are subject to general acid-base catalysis and proceed under very mild conditions; even at physiological pH. These findings have great importance, not only for the synthesis of these compounds but also for their potential application in medicine (pro-drug approach).

Recently our group studied the structure[37,38] and reactivity[39-41] of substituted *S*-(1-phenylpyrrolidin-2-on-3-yl) isothiouronium salts which, in weakly basic medium, undergo an intramolecular rearrangement to give substituted 2-imino-5-[2-(phenylamino)ethyl]-1,3-thiazolidin-4-ones (Scheme 1).

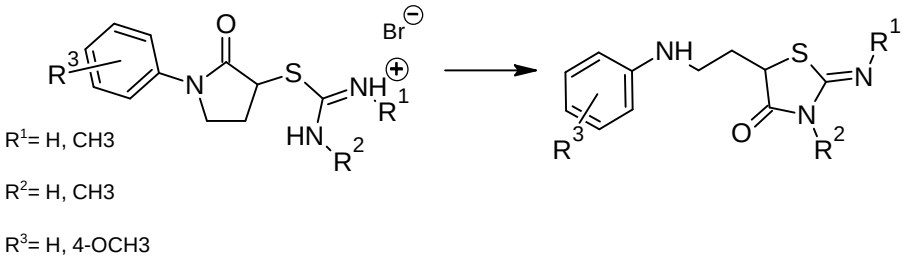

Scheme 1 – Transformation of *S*-(1-phenylpyrrolidin-2-on-3-yl) isothiouronium salts.

More recently the scope of this transformation have been extended: replacing the γ-lactam ring with a γ-lactone ring.[42] The *S*-(2-oxotetrahydrofuran-3-yl)-*N*-(subst. phenyl) isothiouronium bromides underwent rearrangement in acidic and basic medium to give 5-(2-hydroxyethyl)-2-phenylimino-1,3-thiazolidin-4-ones or 5-(2-hydroxyethyl)-2-phenylamino-4,5-dihydro-1,3-thiazol-4-ones in very good yields (Scheme 2).

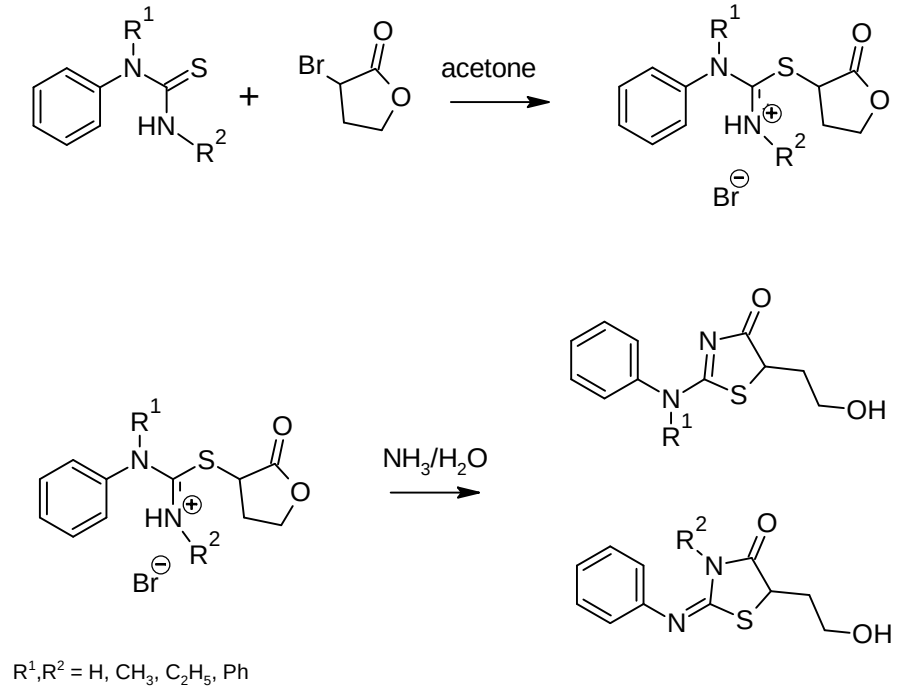

Scheme 2 – Transformation of *S*-(2-oxotetrahydrofuran-3-yl)-*N*-(subst. phenyl) isothiouronium bromides.

The aim of this work was to prepare the series of derivates, measure the kinetics of its transformation in the widest possible pH area and try to in detail investigate and propose the reaction mechanism. According to the literature[43] there is possibility of the reaction acceleration by the transition metal ions. This possibility should be also examined. In the second part of the work 3-bromophtalide should be used instead of the 2-bromobutyrolactone. This alteration should cause the change in the mechanism and reaction should lead to the different types of the products. These products should be identified and mechanism of their formation should be proposed.

2 Theoretical background

2.1 Reactions accelerated by transition metals ions

The influence of additional copper ions on reaction rate of isomerisation and rearrangement has been observed in the reaction of (*E*) and (*Z*)-phenylhydrazones of 3-benzoyl-5-phenyl-1,2,4-oxadiazole (Scheme 3).[43,44] Acceleration and mechanism of the reactions depends not only on the concentration of added copper ions but also on the anions presented in the solution.

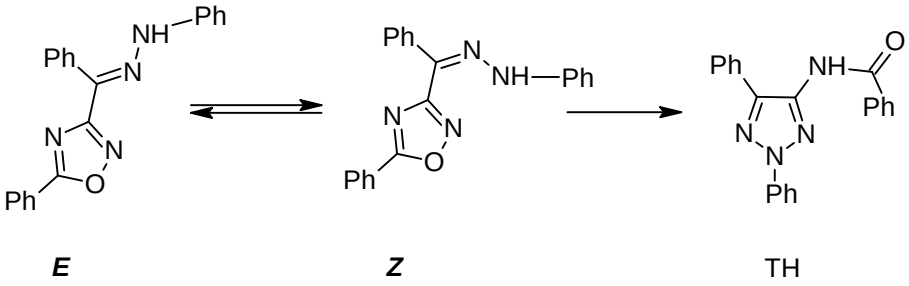

Scheme 3 – Isomerisation and rearrangement of (*E*) and (*Z*)-phenylhydrazones of 3-benzoyl-5-phenyl-1,2,4-oxadiazole.

All plots of observed rate constants of isomerisation ($k_{E,Z}$ and $k_{Z,E}$) versus the copper(II) concentration show a hyperbolic trend that was explained by the two step mechanism. An adduct of copper with the substrate is formed in the first step followed by the rate limiting isomerisation of the double bond. The reaction scheme could be written as:

$$E + \mathrm{Cu(II)} \underset{}{\overset{(K_E)\mathrm{Cu}}{\rightleftharpoons}} E/\mathrm{Cu(II)}$$

$$E/\mathrm{Cu(II)} \underset{(k_{Z,E})\mathrm{Cu}}{\overset{(k_{E,Z})\mathrm{Cu}}{\rightleftharpoons}} Z/\mathrm{Cu\ (II)}$$

Where E/Cu means complex of ligand with the Cu(II) ion. This scheme leads to the equation:

$$k_{E,Z} = \frac{\left(k_{E,Z}\right)_{\mathrm{Cu}}\left(K_E\right)_{\mathrm{Cu}}\left[\mathrm{Cu(II)}\right]}{1+\left(K_E\right)_{\mathrm{Cu}}\left[\mathrm{Cu(II)}\right]} \qquad (1)$$

The decrease of double bond character of the imino bond after the coordination of the copper to the imino nitrogen is proposed. This decrease allows rotation around the bond and formation of the opposite isomer.

Significant dependence on the type of anion was observed during the rearrangement of the starting compounds. If copper(II) acetate was used as a catalyst, a hyperbolic trend was observed; otherwise, copper(II) chloride and bromide as a catalyst shows a parabolic trend.

In the presence of copper(II) acetate - bifunctional catalysis is proposed. The copper ion coordinates to hydrazonic nitrogen and brings acetate oxygen to the close proximity of the hydrogen, which can then act as a Lewis base and accelerate the reaction (Scheme 5a). Below is the kinetic equation (2) for the transformation equivalent to the former for isomerisation.

$$k_{Z,T} = \frac{(K_z)_{\mathrm{Cu}}(k_{Z,T})_{\mathrm{Cu}}[\mathrm{Cu(II)}]}{1+(K_z)_{\mathrm{Cu}}[\mathrm{Cu(II)}]} \qquad (2)$$

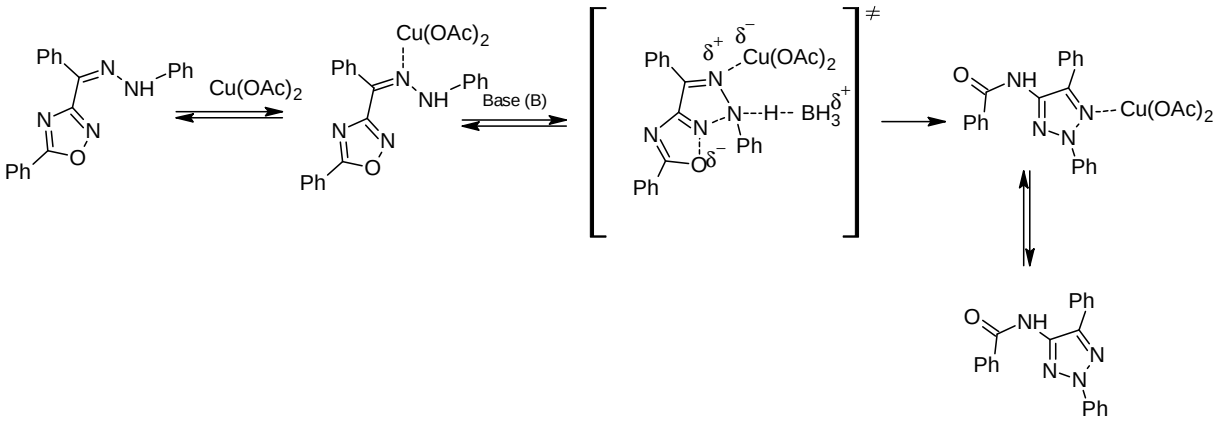

Scheme 4 – Proposed mechanism for the rearrangement catalyzed by copper(II) acetate.

Parabolic dependence for copper halides could be explained by the necessity of formation of binuclear copper complexes (Scheme 5b). Both types of dependences were observed in the ionic liquids used as a solvent.[45]

$$k_{Z,T} = k_u + k_{II}[\mathrm{CuX_2}]^2 \qquad (3)$$

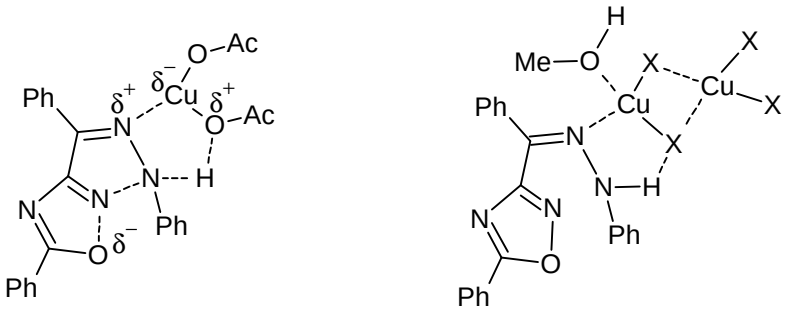

a **b**

Scheme 5 – Transition state (**a**) for the transformation catalyzed by copper(II) acetate and complex (**b**) for the reaction catalyzed by copper(II) chloride.

The participation of heavy metal ions in hydrolysis of amino acid esters was studied by H. Kroll.[46] The reaction was followed in amino buffers in a pH range of 7.5 – 8.5. Non-catalyzed hydrolysis is very slow in this pH area but with the addition of metal ions it was accelerated dramatically. The dependence of the observed rate constant plotted against the added metal ion concentration shows a saturation kinetic with the slope decreasing from the values higher than one for low ion concentration to zero at higher ion concentrations. The break corresponds to the ligand : metal ratio 1:1. This indicates the fast formation of the metal ion - amino acid ester complex in the first reaction step. It is necessary that the presence of the amino acid must be in the form of free base to form the complex. Measuring in a variety of buffers shows the dependence of the reaction rate on pH. One unit change in pH increases the reaction rate fourfold. The reaction rate stays constant with changing buffer concentration indicating general base catalysis. Those observations indicate that the addition of hydroxide ion to the carbonyl group is the rate-limiting step.
The formation of a chelate complex in the first step has been proposed. The metal ion coordinates to the amino and carbonyl group. This causes a decrease in electron density on the carbonyl carbon atom and a following hydroxide attack is facilitated. Various heavy metal ions were tested. The ability to accelerate the reaction grows in order of Mg^{2+}, Ca^{2+}, Mn^{2+}, Co^{2+} and Cu^{2+}. The tightness of the complex should be a reasonable explanation for this observation.

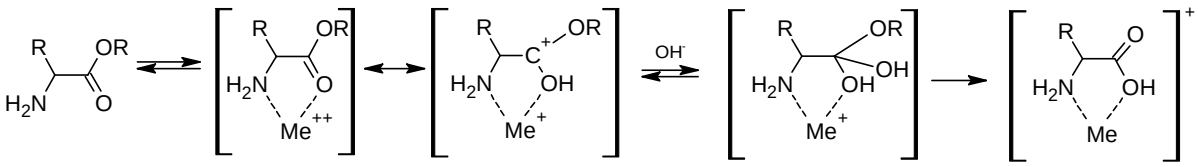

Scheme 6 – Hydrolysis of amino acid esters accelerated by addition of heavy metal ions.

The influence of the amino acid aliphatic chain substitution has been probed. The highest reaction rate was measured for glycine esters. Electron-withdrawing substituents (serine, phenylalanine) are hydrolyzed at approximately the same rate. Hydrolysis of esters with electron donating substituents (proline, alanine, leucine) is slower and reaction rate decreases with the growing accumulation of alkyl substituents.

Table 1: Relative rate constants for hydrolysis of amino acid esters catalyzed by Co(II) ions.

amino acid ester	k_{rel}
glycine	1.00
alanine	0.74
leucine	0.38
phenylalanine	0.90
tyrosine	0.38
cysteine	0.46
arginine	0.56
histidine	0.45
aspartic acid	0.65
serine	0.96
proline	0.71

More problematic is the situation for esters containing an additional group able to form complexes with metal ions. The formation of a competitive, catalytically non-active complex is possible resulting in a decrease in the reaction rate (Scheme 7).

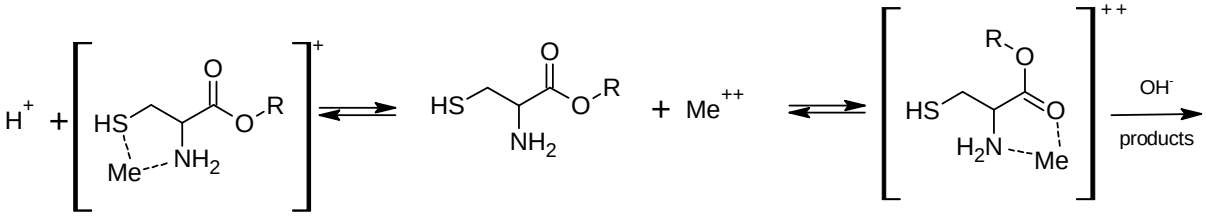

Scheme 7 – Two possible complexes acting in hydrolysis of cysteine ester.

The influence of Cu(II) ions on the hydrolysis of glycine esters was studied by Bender.[47] Measurements in TRIS buffers did not follow first order kinetics. It was due to the formation of stable complexes between copper and the product. Because of this the kinetics were followed in glycine buffers. It was found that the rate of hydrolysis in the presence of copper was 6 orders of magnitude higher than with only base catalyzed hydrolysis. Such a big difference indicates the coordination of copper to the carbonyl group because the protonation two atoms away from the carbonyl should increase the rate constant maximally of 3 orders.[48] A similar mechanism as described in a previous case was proposed.

Different results were obtained by Li who studied the interaction of glycine and cysteine esters with Cu(II) and Ni(II) ions.[49] Logarithms of reaction rates of complex formations for glycine and glycine ethyl ester with Ni(II) ions differ by 6 units, thus indicating a remarkable difference in the structure of complexes. It is proposed that glycine complexes to both nitrogen atoms and to the carbonyl group, otherwise glycine ester coordinates only to nitrogen. The value of the constants is similar to ammonia. Only two orders of magnitude difference was found for the nickel complex with cysteine. The author proposes binding between amino and sulfhydryl group.

2.2 Reactions of thioureas with functional and substitution derivates of *o*-toluic acid

2.2.1 Reactions of thioureas with *o*-halomethylbenzoyl halides and aldehydes

1-Oxo-1,3-dihydro-2*H*-isoindol-2-carbothioamides were prepared by the reaction of *o*-chloromethylbenzoyl chloride with thiourea in presence of Na_2CO_3 in acetone[50] (Scheme 8).

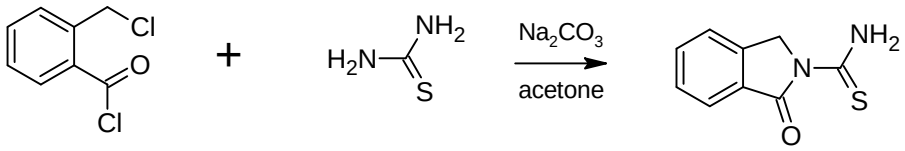

Scheme 8 – Reaction of 2-chloromethylbenzoyl chloride with thiourea.

On the other hand an attempt for the cyclization of analogous isothiouronium salt (Scheme 9) leads to decomposition followed by cyclization to thiophthalide.

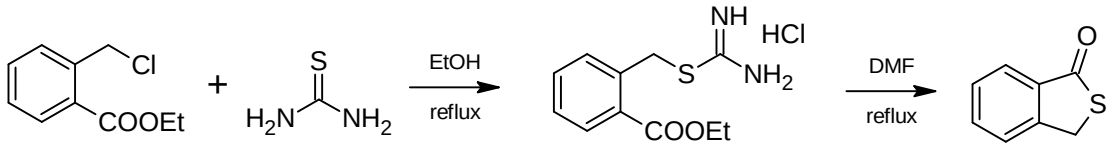

Scheme 9 – Reaction of ethyl 2-chloromethylbenzoate with thiourea.

If *N*,*N*´-disubstituted thioureas were used, seven-membered derivates of 2,4-benzothiazepin-5(1*H*)-one or 2,4-benzodiazepin-1-one were isolated (Scheme 10). The ratio of both products depends on thiourea substitution. The major product for 1,3-dimethyl and diphenyl thiourea is benzodiazepine. For diallyl, diisopropyl, dicyklohexyl and di-*o*-tolyl, thiazepine is the major product. If a bromo derivative instead of a chloro derivative is used, the product ratio can be changed.

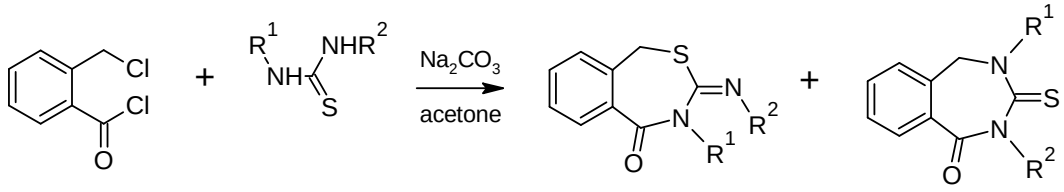

Scheme 10 – Reaction of *N*,*N*´-disubstituted thioureas with 2-chloromethylbenzoyl chloride.

The reaction of benzene-1,2-dicarbaldehyde with urea in an ionic liquid [bmim]BF_4 catalyzed by TMSCl gives 1-oxo-1,3-dihydro-2*H*-isoindol-2-carboxamides[51] (Scheme 11).

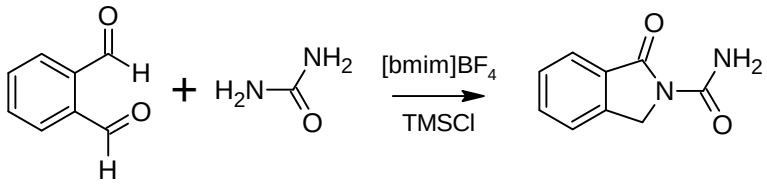

Scheme 11 – Reaction of benzene-1,2-dicarbaldehyde with urea.

In the case of thiourea as a starting material, the formation of analogous products has not been observed. If *N*-methylthiourea was used the reaction would occur classically by forming *N*-methyl-1-oxo-1,3-dihydro-2*H*-isoindol-2-carboxamides (Scheme 12).

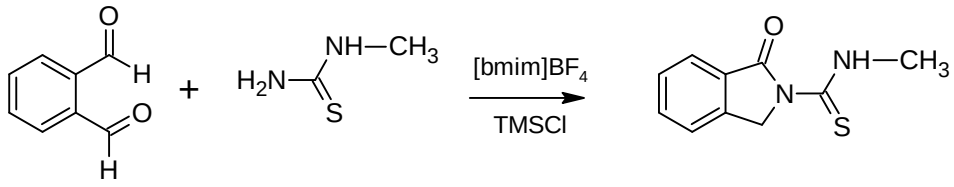

Scheme 12 – Reaction of benzene-1,2-dicarbaldehyde with *N*-methylthiourea.

The formation of the main product was accompanied by the formation of seven-membered rings that can not be distinguished by ^1H and ^{13}C NMR (Scheme 13).

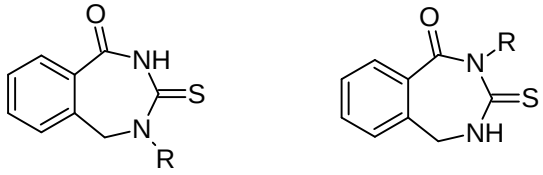

Scheme 13 – Side products of the reaction.

2.2.2 Reaction of phthalaldehydic acid with nucleophiles

Two tautomeric structures of phthalaldehydic acid are possible (Scheme 14). An open form with carboxylic and aldehydic group and a cyclic lactol form.[52-54] The presence of both of them depends on solvent, temperature and pH. NMR spectroscopy indicates that there are

signals present representing CH at δ 6.65 ppm and CHO at δ 10.58 in $CDCl_3$. Addition of *p*-toluensulfonic acid shifts the equilibrium to the cyclic form and no aldehydic signal is observed.

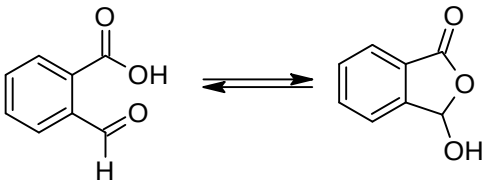

Scheme 14 – Tautomeric forms of phthalaldehydic acid.

The reaction of phthalaldehydic acid with different nucleophiles leads to diverse products depending on the basicity and nucleophility of the nucleophile (Scheme 15).

The reaction with the least basic anilines gives 3-anilinophthalides (**a**) as a product.[55] The same compound could by prepared by the reaction of 3-halophthalides with anilines. The reaction with aliphatic amines depends on the molar ratio of starting compounds. If the molar ratio of alkylhalide to amine was 2:1, the dialkylation product (3,3´-(*N*-dialkylimino)diphthalide) (**b**) was isolated and higher amounts of amine lead to the salts of imines (**c**).

A further reaction with ureas and amides also gives appropriate products substituted in position 3 (**d**).

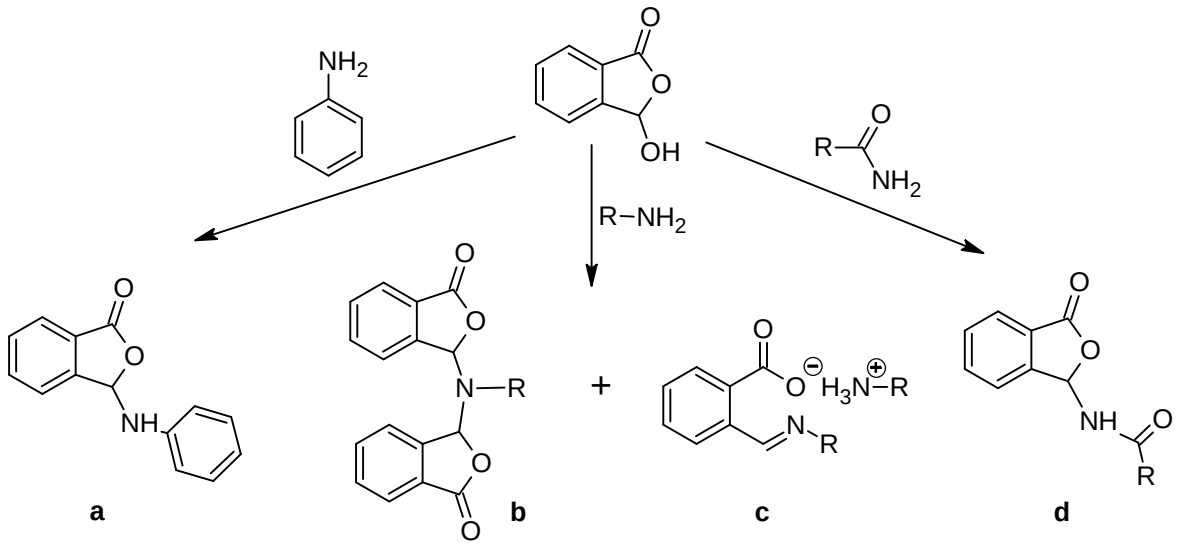

Scheme 15 – Reactions of phthalaldehydic acid with amines.

More interestingly however, is the reaction with phenylhydrazines; depending on the reaction conditions two different products could be isolated (Scheme 16).

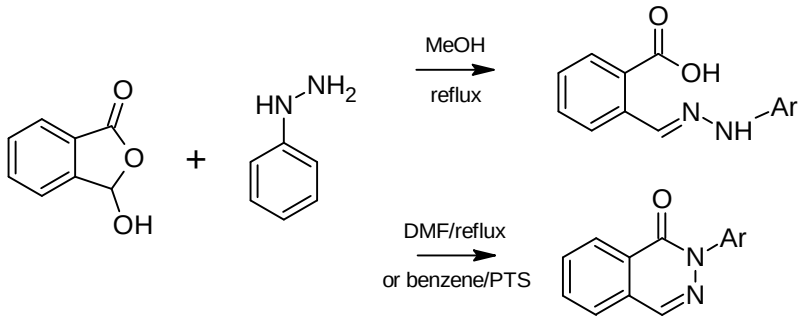

Scheme 16 – Reaction of phthalaldehydic acid with phenylhydrazine.

Those reactions and combinations of them can be used for the construction of various heterocycles (Scheme 17).

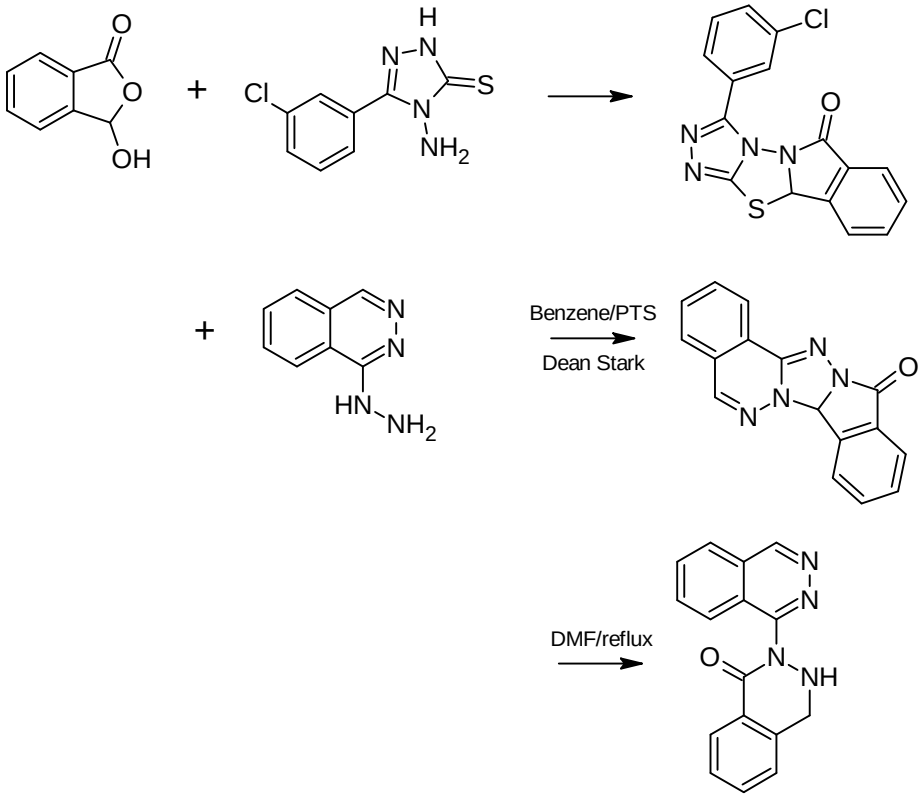

Scheme 17 – Reactions of phthalaldehydic acid.

2.2.3 Reaction of 3-halophthalides with nucleophiles

A different situation is observed in the reactions of 3-halophthalides. These compounds act as ambident electrophiles and can be attacked on the carbonyl carbon atom (acylation of the nucleophile) or on the carbon next to the halo atom (alkylation of the nucleophile). It was shown that strong nucleophiles usually attack the carbonyl group while the reaction with weak nucleophiles gives products of alkylation.[56,57] Also, the influence of the leaving group has been observed: the better the leaving group, the higher the amount of alkylation product produced.

In the case of primary amines, an ammonia rearrangement of alkylation product is observed and appropriate 3-hydroxyisoquinolones are the products of the reaction (Scheme 18).

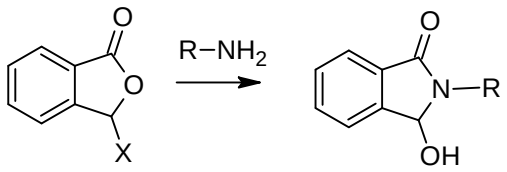

Scheme 18 – Reaction of halophthalides with primary amines.

According to this, a reaction of secondary amines (piperidine, pyrrolidine, imidazole, methylaniline and morpholine) with 3-hydroxyphthalide, 3-chlorophthalide and 3-iodophthalide gives both types of products (Scheme 19). Only products of alkylation were observed for 3-hydroxyphthalide. The reaction of 3-chlorophthalide with the more nucleophilic piperidine, pyrrolidine and morpholine gives acylated products while the reaction with the less nucleophilic imidazole and methylaniline gives alkylated products. The same products were isolated for 3-iodophthalide as a starting compound. Only piperidine and morpholine give a mixture of both of them.

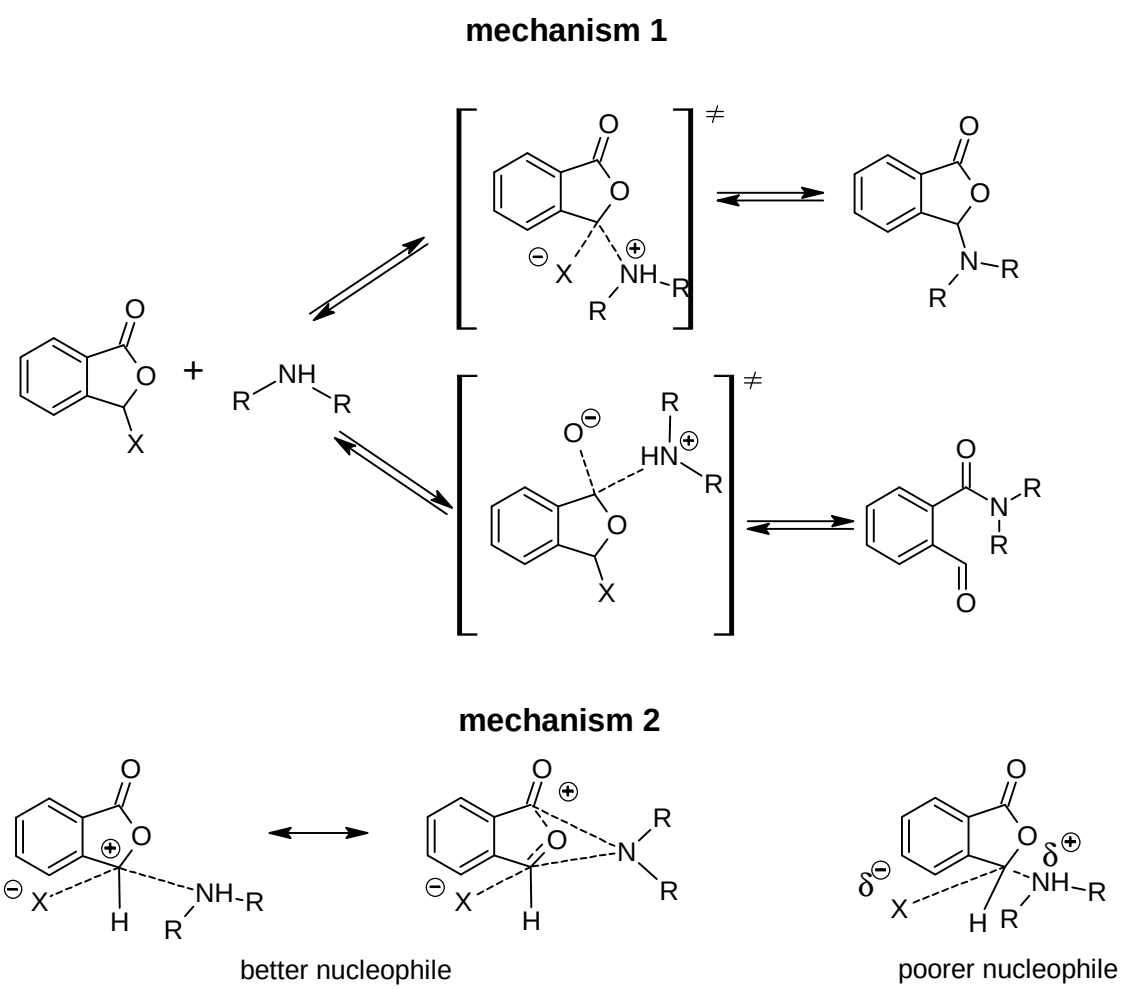

Scheme 19 – Proposed mechanisms for the reaction of 3-halophthalides with secondary amines.

Two mechanisms have been proposed and discussed by the authors to explain this behaviour. The first one involves the direct attack of the amine to the 1 or 3 position, with product distribution in this case depending only on the type of nucleophile. According to this; methylaniline and imidazole should be better alkyl halide nucleophiles while piperidine and morpholine being better carbonyl nucleophiles, But this observation is not consistent with previous observations and the nucleophility scale N^+ for carbonyl.

Due to these observations another mechanism has been proposed. The nucleophile in all cases attacks the alkyl halide carbon. The originating positive charge on the carbon can redistribute between atoms 1 an 3 and if there this is enough time for redistribution (looser transition state), the product of acylation can be formed. According to the Westaway[58], the

stronger the nucleophile, the looser the transition state and more acylation products are formed.

When a higher amount of amine is used, the product of acylation can transform to alkylated products. The question is however, if the rearrangement is inter or intramolecular. Reaction of acylated morpholino product with pyrrolidine gives only alkylated pyrrolidine product. It indicates rearrangement occurring with intermolecular attack (Scheme 20).

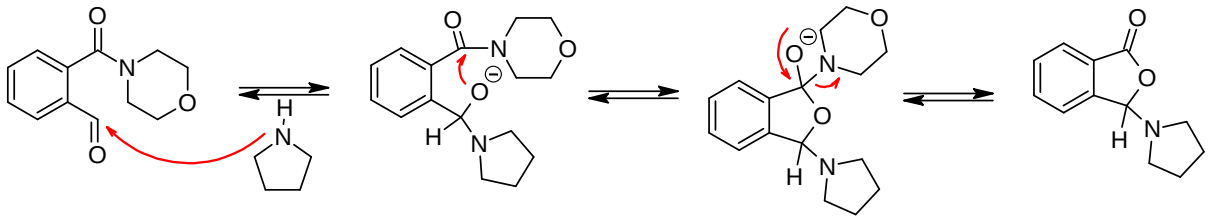

Scheme 20 – Reaction of 3-morpholinophthalide with pyrrolidine.

Similar trends in reactivity were observed for the reaction of halophthalides with substituted phenols.[59]

The reaction of halophthalides with *O*-alkyl xanthates[60] leads to the alkylation product (Scheme 21) and the reaction was followed spectrofotometrically for 3-chloro and 3-bromophthalide as starting compounds. The presence and absence of absorption at 392 nm characteristic for –C(=O)SC(=S) chromophore indicates two possible reaction pathways. During the reaction of 3-bromo phthalide with xanthate this band did not appear and so the direct alkylation mechanism is proposed. Otherwise, occurrence of this band was observed in the case of 3-chlorophthalide and the mechanism proceeding through an aldehyde intermediate has been proposed. The reaction with dithiocarbamates proceeds in a similar manner.

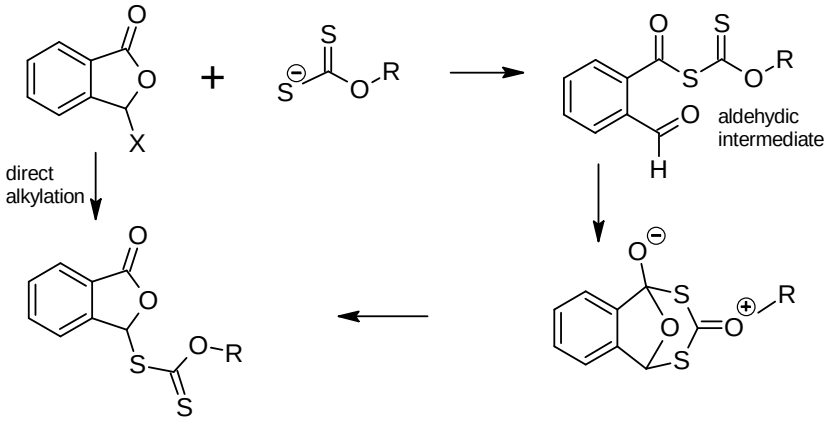

Scheme 21 – Reaction of 3-halophthalides with xanthates.

A combination of intramolecular and nucleophilic catalysis was observed during the hydroxide ion and morpholine catalyzed hydrolysis of methyl *o*-formylbenzoate (Scheme 22) and 3-methoxyphthalide.[61] In the case of morpholine, 3-morpholinophthalide as a reaction intermediate was isolated, characterized and the kinetics of its conversion was measured and compared with the reaction rate for morpholinolysis.

No general catalysis was observed during the hydrolysis of methyl *o*-formylbenzoate. The reaction was followed in the pH range of 0 – 9.23 and a typical V-shape was observed which could be explained by the catalysis of protons, water and hydroxide ions. A different situation was observed for 3-methoxyphthalide which, in the pH range of 4 – 9 is independent of pH. This plateau could be explained in a manner of the much important "water" catalyzed reaction in contrast to the previous substrate. An identical pH profile was observed for the hydrolysis of 3-morpholinophthalide, the only difference is the rate of the reaction which is 3 orders faster in this case.

It was found that the reaction rate for hydrolysis of 3-morpholinophthalide is the same as for the second step of morpholinolysis of methyl *o*-formylbenzoate. This observation confirmed the same mechanism for both of the reactions. Also the reversibility of the first step of morpholinolysis was studied in methanol. It was found, contrary to the second step, the first step is irreversible.

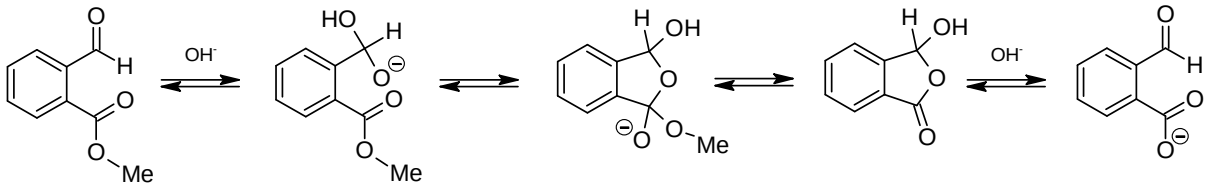

Scheme 22 – Intramolecular hydrolysis of methyl *o*-formylbezoate.

The reaction scheme for water catalyzed hydrolysis is depicted (Scheme 23). The water catalyzed reaction of 3-morpholinophthalide could be explained as a concerted process with the transition state stabilized by the resonance of the formyl group.

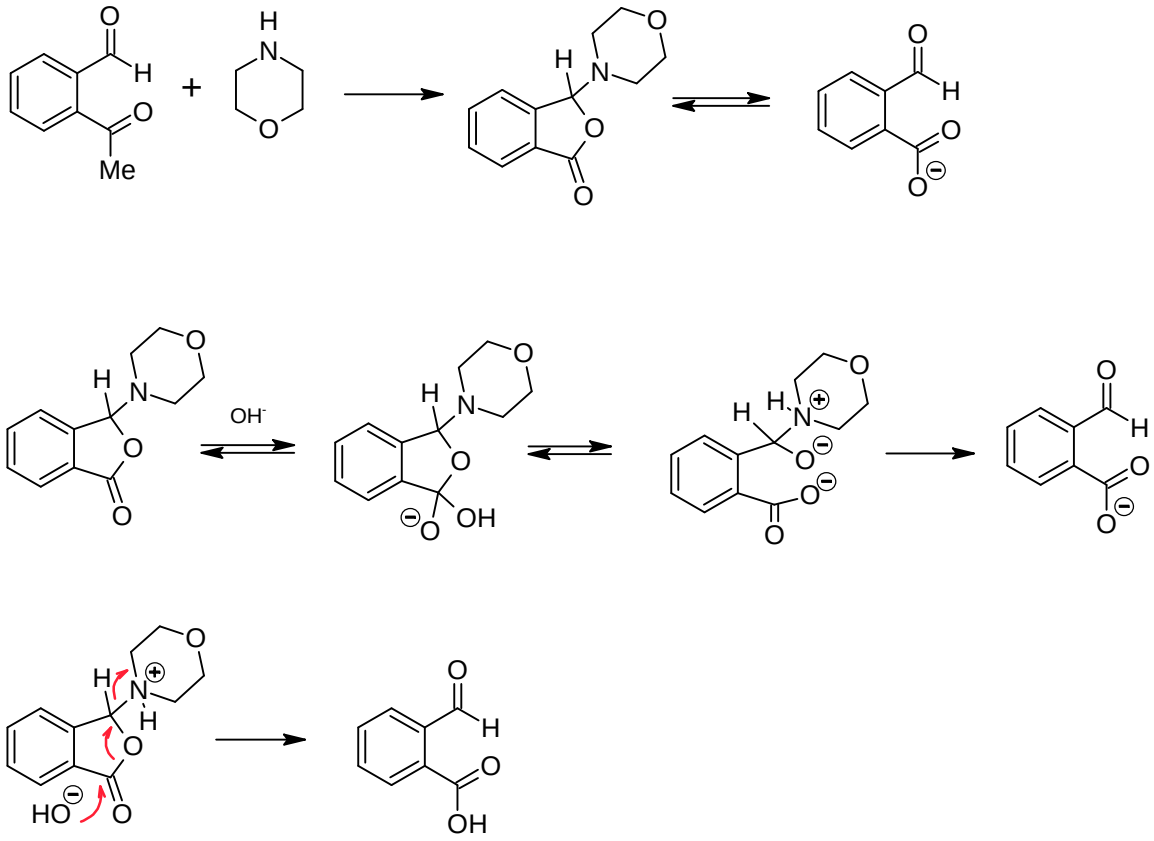

Scheme 23 – Morpholinolysis of methyl *o*-formylbenzoate.

2.3 Possible mechanisms proposed for aliphatic nucleophilic substitution

2.3.1 Classical view

As Ingold showed, there are two limiting mechanisms for nucleophilic substitution on aliphatic carbon atoms; those being: bimolecular S_N2 (A_ND_N)[62] and monomolecular S_N1 $(D_N + A_N)$.

In the classical S_N2 reaction, nucleophile attacks the molecule of substrate from the opposite side to the leaving group (backside attack) and the configuration on the reaction centre is inverted (Walden inversion). The reaction is first order in respect to the concentration of substrate and the nucleophile (4) and occurs in one intermediate-free reaction step.

$$v = k \cdot [RX] \cdot [Nu] \tag{4}$$

In the limiting S_N1 reaction the molecule of substrate dissociates spontaneously, carbocation is formed and subsequently attacked by the nucleophile or solvent molecule. The hybridisation on the central carbon atom changes from tetrahedral sp^3 to planar sp^2. Attack of the nucleophile is possible from both sides due to this fact, and the reaction proceeds with racemisation on the stereogenic centre. The reaction is first-order in regards to the substrate (5) and occurs in two steps with the carbocationic intermediate. The reaction rate does not depend on the concentration and the structure of the nucleophile.

$$v = k \cdot [RX] \tag{5}$$

2.3.2 Winstein explanation

Expansion of the theory and explanation of the partial racemisation during the reaction comes from Winstein. Carbocations need not be fully dissociated, but reactions can occur thorough the ionic pairs and in the case when there is only a small separation between the ions – the so called intimate ionic pair (R^+X^-) plays the main role. One side of the substrate is still blocked by the leaving group and so a product of the inversion is formed. In case of a more stable carbocation, the leaving group leaves easily and carbocation could be partially solvated and a so-called solvent separated ionic pair is formed $R^+ \| X^-$. There are two possibilities in a reaction of this kind of carbocation: a reaction with an external

molecule of the solvent that leads to the inversion of configuration or a reaction with the solvating molecule inserted into an ionic pair. Retention is observed in this case, and according to this model, partial racemisation occurs. Stable carbocations $R^+ + X^-$ could be attacked from the both directions with the same probability and completely racemisation is observed.

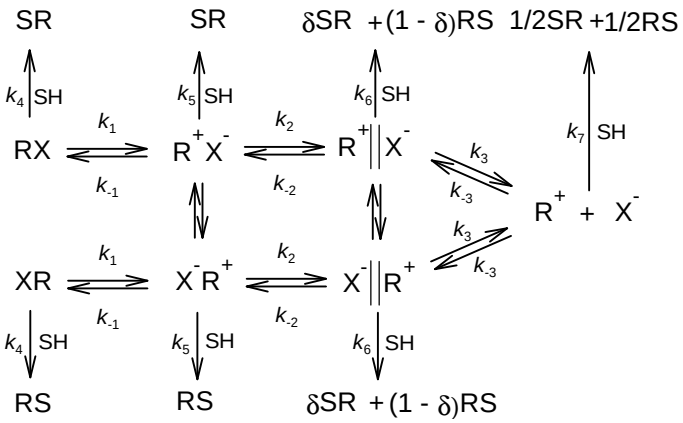

Scheme 24 – Winstein scheme for nucleophilic substitution reactions. Where: R-alkyl, *S*-nucleophile or solvent molecule, X-leaving group.

2.3.3 General Winstein scheme

General Winstein scheme for nucleophilic substitution (Scheme 25).[63]

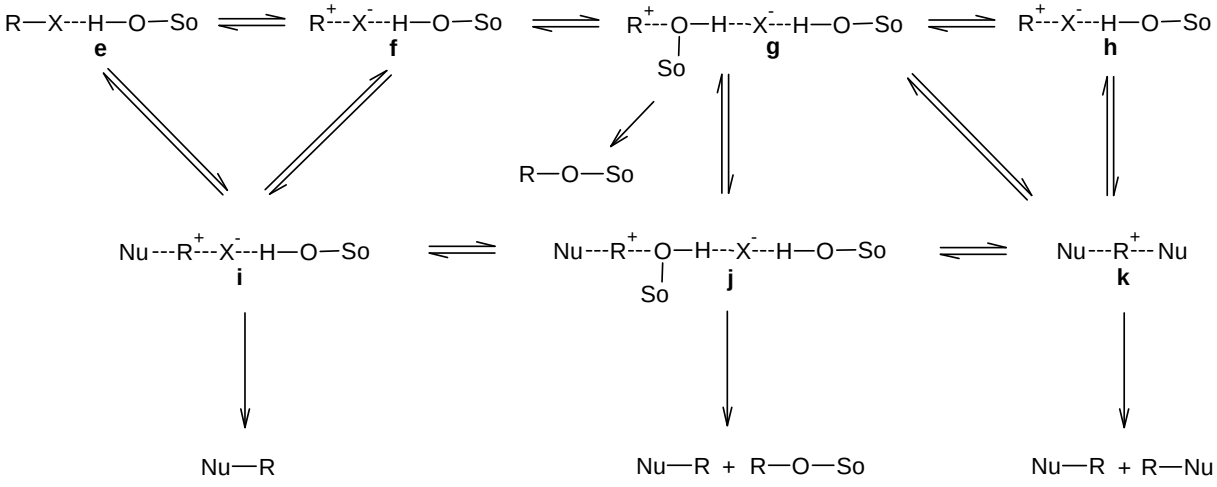

Scheme 25 – General Winstein scheme.

Basic G-W intermediates (**e**-**h**) were extended for solvent molecule solvating leaving group. Structures (**i**-**k**) could be both back side solvated intermediates and transition states of direct one-step reaction of intermediates (**e**-**h**) to products, and the structure of the substrate, type of nucleophile and reaction conditions defines which alternative is true.

Intermediate (**g**) can be used to easily explain the formation of the product with retention of configuration; it happens when back side attack of nucleophile is blocked or disfavoured in combination of very slow dissociation on the free carbocation (**h**) or (**k**). Under such circumstances the intermediate would collapse to the product with retention of configuration.

The reaction path starting from intermediate (**e**) with transition state (**i**) is a classical S_N2 reaction. Sneen and Larsen suggested an ionic alternative of S_N2 reaction that consisted of formation of structure (**f**) and its breakdown through transition state (**i**).

The solvent separated ionic pair could be (**j**) or could not be (**g**) solvated by the molecule of the nucleophile. There are two possible paths of the breakdown of intermediate (**g**): in the presence of nucleophile the product with inversion of configuration being formed and when the molecule of the nucleophile is missing the solvolysis reaction occurs and the product with retention of configuration is formed. The last reaction path includes the formation of a carbocation symmetrically surrounded by the nucleophile (**h**) or solvated by the solvent (**g**) and its reaction giving a racemic product.

As the overall scheme shows, the problem of nucleophilic substitution is a very complex problem and it cannot easily be decided which mechanism plays the dominant role.

2.3.4 Mechanism $S_N2(C^+)$

The next possible mechanism is so called $S_N2(C^+)$ ($D_N{}^*A_N$).[64] A stable carbocation formed in the first step is coordinated and attacked by the molecule of the nucleophile in the second step. Reaction rates for the both steps are similar and the reaction behaves bimolecularly with the rate limiting second step. An example being the reaction of triphenylmethylchloride with different nucleophiles in nitromethane.

2.3.5 Possible unification of mechanisms S_N1 a S_N2

A possible unification of limiting S_N1 and S_N2 was suggested by Sneen[65,66] and is illustrated in Scheme 26 for solvolysis of the substrate in the presence of an azide ion.

Sneen supposed the formation of an ionic pair R^+X^- as the reaction intermediate in both limiting cases and only its stability determines which mechanism dominates.

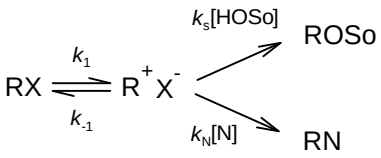

Scheme 26 – Reaction scheme with ionic pair as an intermediate.

Equation (6) for the ratio of formed products depending on nucleophile concentration can be deduced as follows:

$$\frac{[\mathrm{RN}]}{[\mathrm{ROSo}]} = \frac{k_\mathrm{N}[\mathrm{N}]}{k_\mathrm{S}} = m[\mathrm{N}] \tag{6}$$

$$\frac{k_{\mathrm{exp}\,t}}{k_\mathrm{NA}} = \frac{((k_{-1}/k_S)+1)(1+k_\mathrm{N}[\mathrm{N}]/k_S)}{((k_{-1}/k_S)+1+(k_\mathrm{N}[\mathrm{N}])/k_S)} = \frac{(x+1)(1+m[\mathrm{N}])}{(\mathrm{x}+1+m[\mathrm{N}])} \tag{7}$$

Where k_NA is the rate constant of solvolysis measured without the presence of an external azide ion.

In the case of the breakdown of the ionic pair in rate limiting step $k_{-1} \gg k_\mathrm{S}$ – a second equation can be written as (8)

$$\lim(x \to \infty)\frac{k_{\mathrm{exp}\,t}}{k_\mathrm{NA}} = 1 + m[\mathrm{N}] \tag{8}$$

And the reaction behaves as a classical S_N2 reaction.

In the case of the formation of an ionic pair in rate limiting step $k_\mathrm{S} \gg k_{-1}$ – the equation simplifies to (9)

$$\lim(x \to 0)\frac{k_{\mathrm{exp}\,t}}{k_\mathrm{NA}} = 1 \tag{9}$$

And the reaction behaves like a classical S_N1 reaction.

If both constants are similar, a borderline mechanism is observed.

An example is solvolysis of 2-octylmesylate in 25 % water:dioxane solution (Fig. 1).

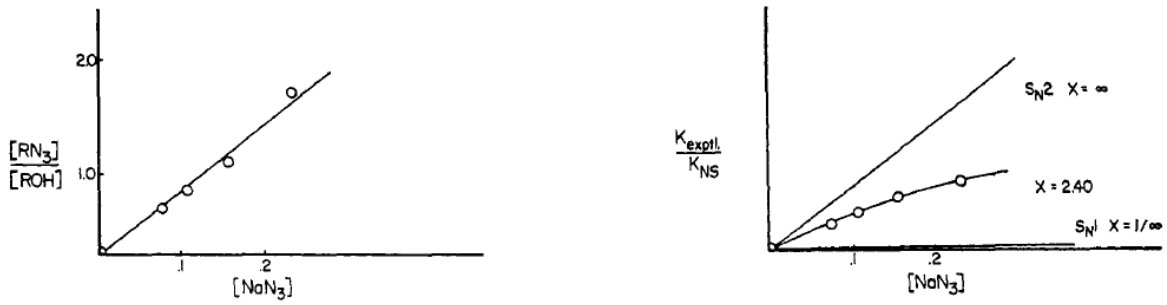

Figure 1 - Dependence of the rate constant on azide ion concentration.[65]

The first diagram shows the ratio of products as a dependence on azide concentration and the calculated value *m* of the slope is 8.22. The dependence of the ratio of the rate constants for the reaction with and without the presence of the nucleophile on the azide concentration is depicted on second diagram (right, the theoretical curve was calculated from the equation (7)). Also hypothetical dependences for both limiting mechanisms S_N1 and S_N2 are depicted.

Another representation of the continuous crossing between both limiting mechanisms is the More O´Ferrall diagram for aliphatic nucleophilic substitution[67-69] (Fig. 2). The limiting S_N1 mechanism proceeding to a fully developed carbocation is depicted by the wings of the diagram and the limiting S_N2 reaction goes through the central part of the diagram. The reaction coordinates for the other mechanisms are combinations of the previously mentioned reactions and moves in the borders of these two limiting paths.

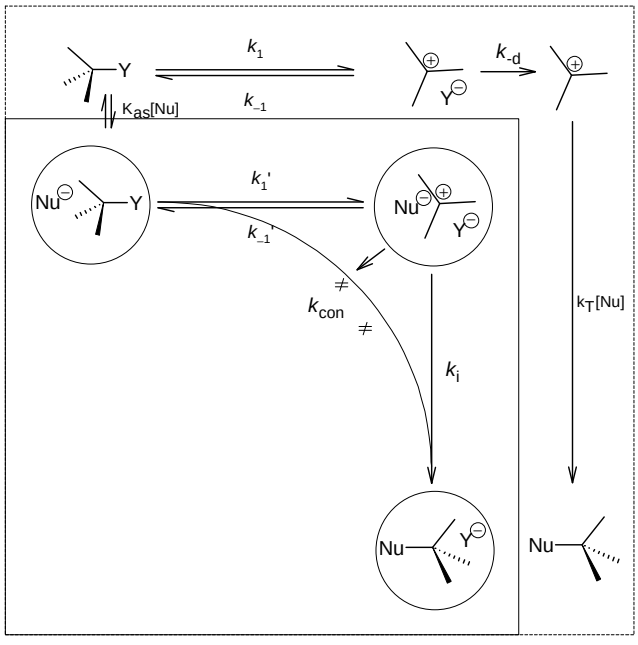

Figure 2 - More O´Ferrall diagram for aliphatic nucleophilic substitution.

The gradual crossing of the limiting cases illustrates the following scheme of reaction profiles: the stability of carbocations as intermediates decreases and the reaction changes from consecutive, to the reaction with only one reaction step with one transition state.

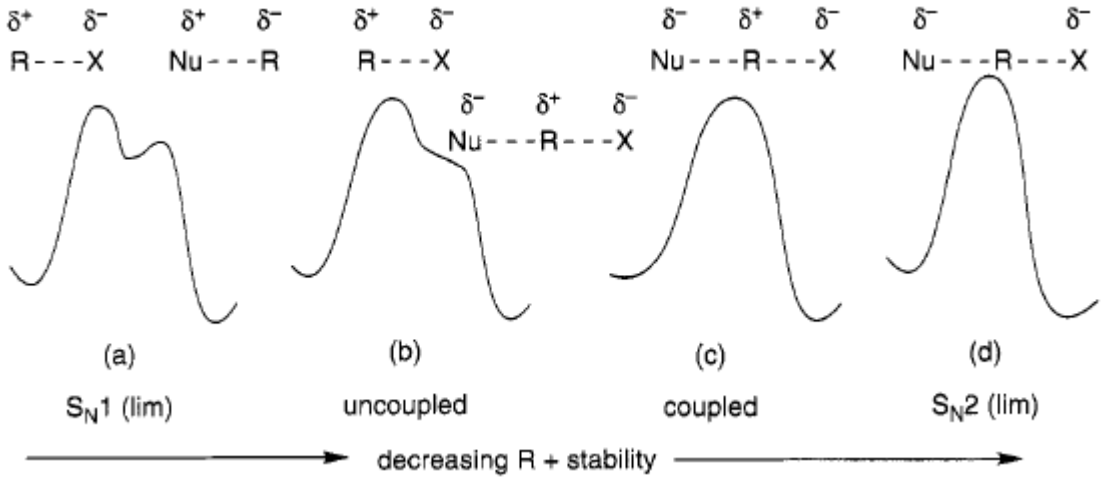

Figure 3 **-** Reaction coordinates for different types of substitution reactions.[70]

There is a big schism between authors; some arguments show that there is no continuous crossing between the two limiting mechanisms, but there is a competition between these two reaction paths in the borderline area. One of these arguments is an example of Menschutkin reaction of benzyl-4-toluenesulfonates with *N*,*N*-dimethylanilines. Dependences of the observed rate constants plotted against nucleophile concentration could be fitted by the equation (10)

$$k_{obs} = k_1 + k_2 \cdot [\mathrm{Nu}] \tag{10}$$

Where k_1 is rate constant for monomolecular substitution S_N1 and k_2 is rate constant for bimolecular substitution S_N2. The value of the constant k_1 is not influenced by the nucleophility of the nucleophile, however, the value of the constant k_2 is. Also, the Yukawa-Tsuno correlation of the constant k_1 with parameters $\rho = -5.2$ and $r = 1.3$ supports the S_N1 mechanism, and the correlation of the constants k_2 with Brown σ^+ shows low curvature.

There is still a large amount of discussion about which mechanisms really occur. Some authors believe that there is a sandwich transition state[71-73], and some of them deny the S_N2 mechanism [74] or vice versa (S_N1)[75] in traditional form.

2.3.6 Characterization of the reaction intermediates

The mechanism which dominates depends on the stability and lifetime of the possibly forming carbocationic intermediate. For the stable carbocations, a S_N1 mechanism dominates and as the stability decreases, ionic pair mechanisms start to play a major role and finally a pure S_N2 mechanism could be observed.

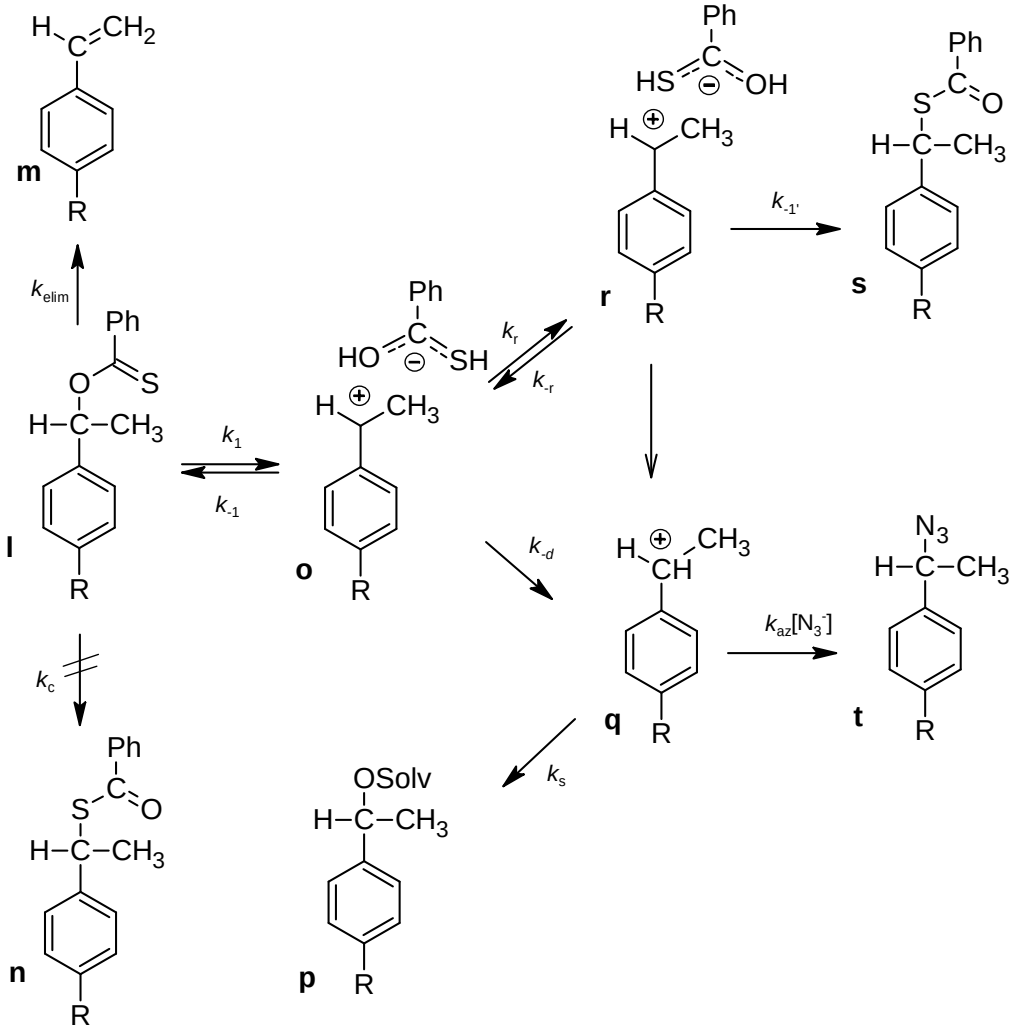

Scheme 27 – Reaction paths during azidolysis of 1-phenethylthionobenzoates.

Substituted 1-phenethylthionobenzoates (**l**) have been found as suitable models for the study of stability and dynamic behaviour of carbocations and ionic pairs (Scheme 27).[76] Depending on the type of substitution, added nucleophiles and the solvent used, different types of reactions and formation of different products could be observed:

- Elimination that leads to formation of styrenes (**m**).

- Formation of an ionic pair (**o**). This could reorganized to ionic pair (**r**) followed by formation of a stable 1-phenethyl-thionobenzote (**s**). Ionic pair **o** could also dissociate forming free carbocation (**q**). This can be trapped by the molecule of solvent forming the corresponding product or trapped by the molecule of nucleophile added into the reaction mixture (**t**). This method is called "azide clocks"[77-82] and is used for the determining reaction rates of separate reactions. The value of the so determined reaction rate constant for reorganization k_r is $1 \cdot 10^{11}$ s^{-1} and is six times higher than the value of the rate constant for diffusion of an ionic pair to free ions $k_{-d} = 1.6 \cdot 10^{10}$ s^{-1}. It is possible to say that every reorganization of an ionic pair leads to the formation of 1-phenethyl-thionobenzoate.

2.3.7 Oxygen scrambling

A similar example used for the study of mechanisms of substitution reactions with ionic pairs as a possible intermediates is the trifluoroethanolysis of ^{18}O labeled 2-butyl-4-bromobenzensulfonates[83] (Scheme 28).

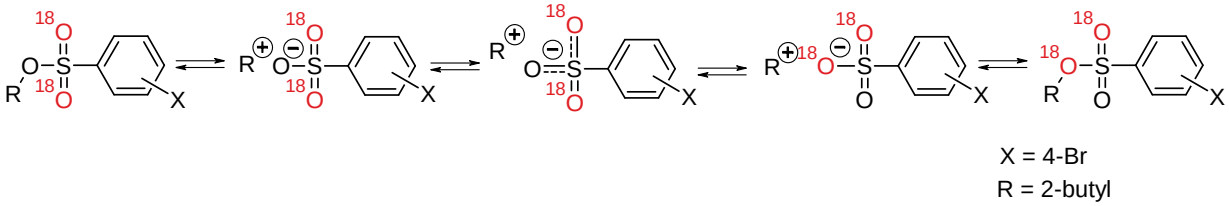

Scheme 28 – Oxygen scrambling of 2-butyl-4-bromobenzensulfonates.

The exchange of both oxygen atoms bonded to alkyl carbon was observed with the reaction rate value of $4.9 \cdot 10^{-7}$ s^{-1}. When optically pure starting compounds were used no racemisation has been observed. It indicates that the reaction is processing through a concerted S_N2 mechanism or through a very intimate ionic pair that enables rotation of the leaving group, but does not permit inversion of the carbocation. This could be explained by the fact that the bond angle in the tetrahedral anion is 110° and to the reach this type of transition state a rotation of 55° is necessary, while for planar carbocation a rotation of 90° is required; a concerted one-step mechanism with an "exploded" transition state is the most probable explanation. This reaction can also be considered as a suprafacial 1,3-sigmatropic rearrangement with a transition state depicted in (Fig. 4).[84]

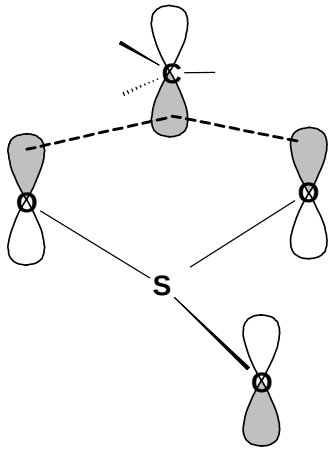

Figure 4 - Transition state demonstrated with the use of molecular orbitals.

2.3.8 Activation parameters

The determination of activation parameters of a reaction is an important criteria used in the study of reaction mechanisms.[85] This importance is highlighted in the study of the mechanisms of benzylic systems. Hammett correlations are not linear[86] but L[87] or U and V[88] shaped. Interpretation without activation parameters shows a S_N2 type of reaction. According to this, electron withdrawing substituents should cause a decrease of activation enthalpy or this should at least be independent, however, the experiments show an opposite trend indicating that activation enthalpy grows with growing withdrawing capability of substituents and is compensated by the decrease of entropy. An ionic pair as an intermediate is a good explanation for this observation.

2.4 Stereochemistry of substitution reactions

The stereochemistry of a reaction is another important feature being used when studying reaction mechanisms. Limiting S_N2 reaction processes with 100 % inversion of configuration. This is caused by the attack of nucleophile from the opposite side than the leaving group leaves (backside attack). Limiting S_N1 reaction processes with racemisation on reaction centre. This is due to the formation of a planar carbocation which is attacked from both sides with the same probability.

2.4.1 Possibility of frontside attack in S_N2 reactions

The possibility of the front side attack (nucleophile comes from the same side as leaving group leaves) of the nucleophile was studied for S_N2 type reactions. This attack causes the retention of configuration on the reaction centre. There is still not clear evidence for this mechanism, but some similar mechanisms have been described.

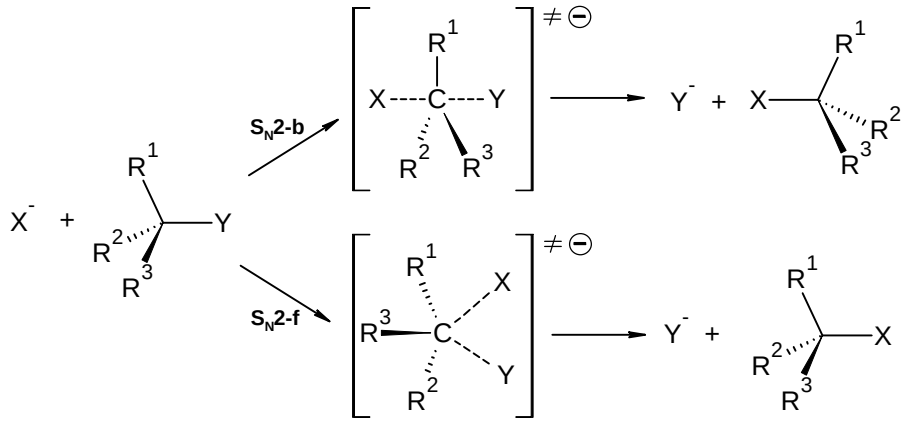

Scheme 29 – Backside and frontside attack for S_N2 substitution reaction.

Potential energy surfaces (PES) for both types of S_N2 reactions were calculated using quantum chemical methods.[89-94] The reaction barrier for frontside attack is 170-200 $kJ \cdot mol^{-1}$ higher compared to backside attack. This difference decreases for protonated alcohols with the increasing size of the aliphatic part of the molecule.[95] A difference of only 10 $kJ \cdot mol^{-1}$ was calculated for *t*-butyl alcohol and a similar situation exists for protonated amines[96] and trends in reactivity are similar as for classical S_N2 reactions. The reactivity of nucleophiles decreases in the order of F^-, Cl^-, Br^- and I^- and the reactivity of substrate grows in the opposite direction, with the highest observed influence being

observed for protonated fluorides.[97] The energy difference of transition states decrease in the following order Me > Et > *i*-Pr > *t*-Bu and there is no energy difference of transition states for *t*-butyl. According to this observation the author comes with the new insight on nucleophilic aromatic substitution. The stereochemical course of S_N1 and S_N2 reactions could be explained as a competition of frontside and backside attacks with most of the calculations being made in the gas phase which means that circumstances significantly different from the reactions in the lab existed. Precise modelling of reactions in liquid phase is complicated with many factors and interactions, so the results are not in good agreement with reality.

2.4.2 Mechanism S_Ni

A well-known substitution reaction with retention of configuration is the reaction of alcohols with thionyl chloride.[98] Two basic mechanisms were proposed: through a cyclic transition state proceeding S_Ni (intramolecular nucleophilic substitution) (Scheme 30)[99] and a mechanism proceeding through the ionic pair route.

Intramolecular attack of the chlorine atom causes a simultaneous leaving of the SO_2 molecule in the S_Ni mechanism.

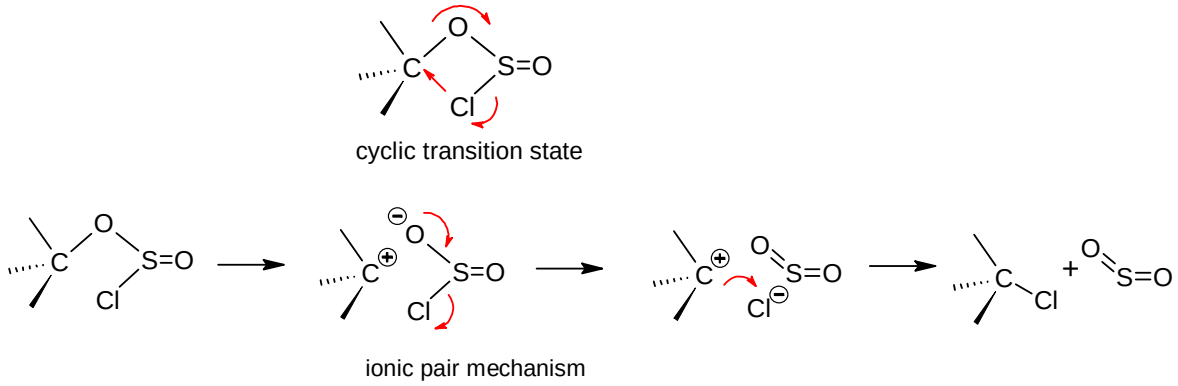

Scheme 30 – Possible mechanisms for the reactions of alcohols with thionyl chloride.

In the first step of the ionic pair mechanism, chlorosulphite dissociates to an ionic pair. The lifetime of both the parts (intermediates) is longer than the time for one molecular vibration and the leaving group decomposes forming a chloride anion in the next step. This anion attacks the carbocation from the same site and a stable product is formed. The breakdown followed by attack is faster than the attack of other nucleophilic species present

in the reaction media due to mutual proximity and preorganisation and a retention of configuration is observed due to this fact. An analogous mechanism has been proposed for similar substrates (Fig. 5).[100]

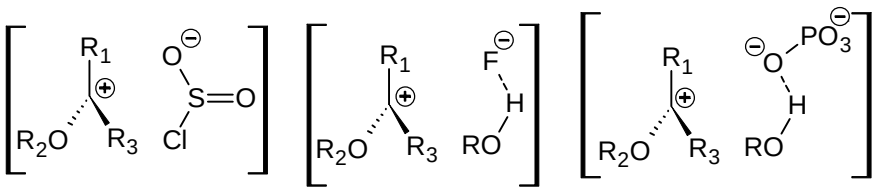

Figure 5 - Intermediates of substrates reacting with the similar mechanism as thionyl chloride with alcohols.

Detailed experiments and quantum chemistry calculations show[101] more complicated behaviour depending on carbon type. Breaking of the sulphur – chlorine bond in the first reaction step has been observed for the primary alkyl substrates. This is what is called a S_N2i mechanism. Otherwise the S_N1i mechanism with alkyl-oxygen bond breaking in the first step has been observed for substrates able to form stable carbocations (Scheme 31). This was supported by NMR experiments.

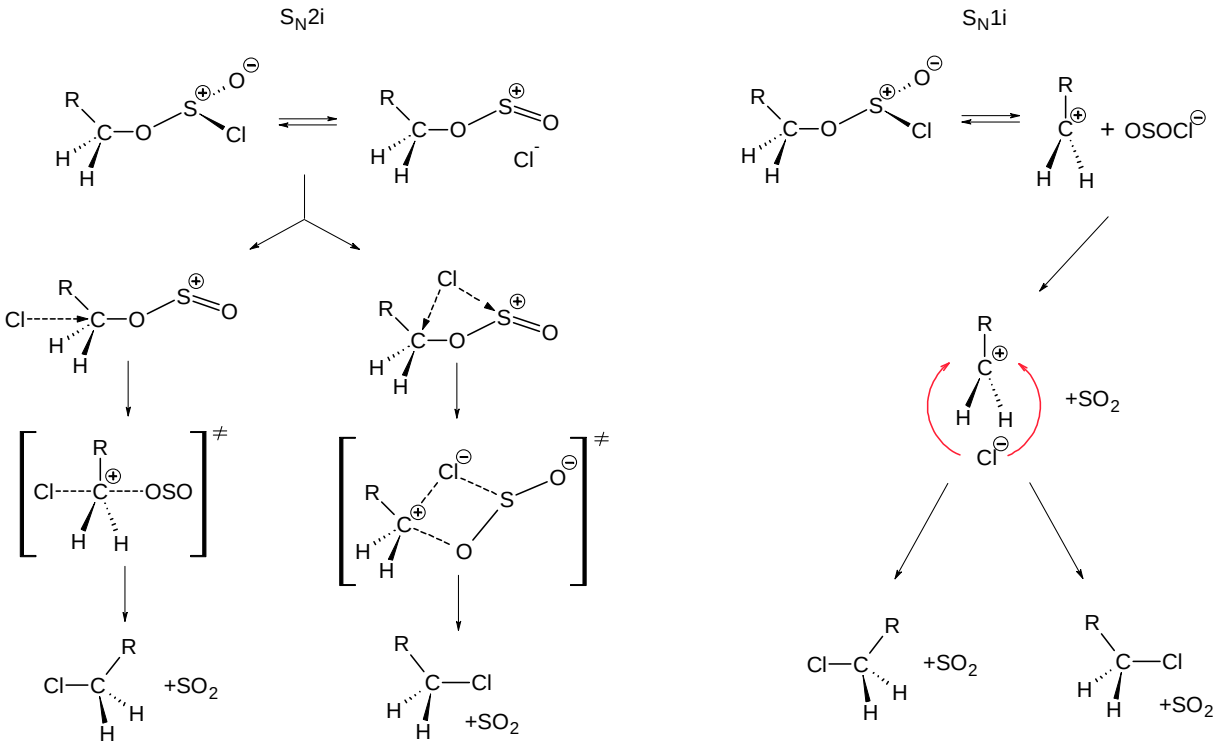

Scheme 31 – S_N2i a S_N1i reaction intermediates.

2.4.3 Reactions mechanism explained using frontside nucleophilic attack

One of the reaction mechanisms explained by the nucleophilic frontside attack is the reaction of cumylarensulphonates with anilines.[102] Cross interaction constants and kinetic isotopic effect were used to support this attack. Cross interaction parameters are defined in equation (11).[103]

$$\log(k_{XZ} / k_{HH}) = \rho_X \sigma_X + \rho_Z \sigma_Z + \rho_{XZ} \sigma_X \sigma_Z \tag{11}$$

$$\rho_{XZ} = \frac{\partial \rho_Z}{\partial \sigma_X} = \frac{\partial \rho_X}{\partial \sigma_Z} \tag{12}$$

where X means attacking nucleophile and the Z leaving group. For a strong nucleophile $\partial \sigma_X < 0$ and better leaving group $\partial \sigma_Z > 0$ an early transition state is observed when ρ_{XZ} is higher than zero ($\partial \rho_Z > 0$ and $\partial \rho_X < 0$). The higher value of the coefficient ρ_{XZ} the higher the interaction of nucleophile and leaving group is. The usage of deuteroanilines showed a trend in the value of KIE. KIE is close to zero when strong nucleophiles or good leaving groups take part in the reaction (degree of bond dissociation is higher). When using weaker nucleophiles or poor leaving groups (closer transition state) KIE becomes less than one. This could be caused by the steric hindrance in the transition state. This is the absolute opposite of reactions proceeding with the classical backside attack. An unusual value for the cross interaction coefficient $\rho_{XZ} = -0.75$ together with the value of KIE indicates the proximity of the nucleophile and the leaving group in the transition state. Frontside attack with the later transition state could be a good explanation for this observation (Scheme 32).

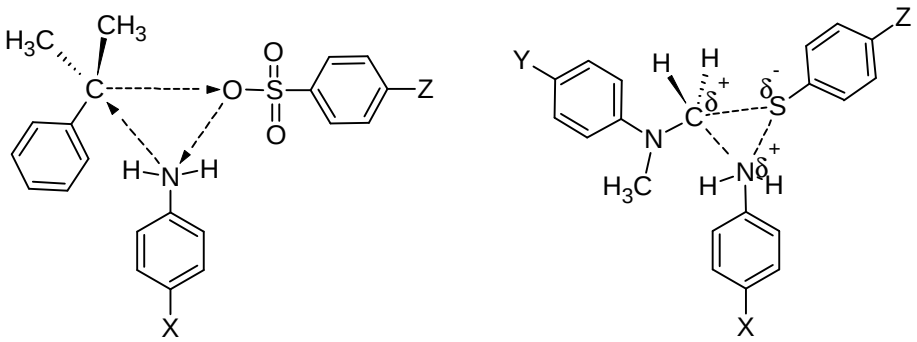

Scheme 32 – Transition states of reactions of cumylarensulphonates and anilinothioethers with anilines.

The reaction of anilinothioethers with anilines in methanol is another similar case.[104] The value of cross coefficient is ρ_{XZ} = –0.17 and β_{XZ} = –0.27. A value of SKIE k_H/k_D = 0.84 - 0.88 together with an activation enthalpy of $\Delta H^{\neq}$ = 4.2 - 5.2 kcal·mol^{-1} and entropy $\Delta S^{\neq}$ = –46 to –59 e.u. confirms this mechanism.

2.4.4 Frontside attack on another types of reaction centre

Nucleophilic substitution reactions could proceed on reaction centres other than carbon for example those which contains phosphorus atom. Some of the mechanisms propose frontside attack. The KIEs and cross interaction coefficients are also used as an evidence. It is generally true[105-106] that a coefficient ρ_{XZ} is smaller than zero for concerted S_N2 mechanism (or stepwise mechanism with the bond formation in the rate limiting step) and higher than zero for a stepwise mechanism with the leaving of the leaving group being the rate limiting step. The size of this coefficient is inversely related to the distance of the nucleophile from the leaving group in the transition state. A KIE higher than one indicates proton transfer in the transition state of the rate limiting step (frontside attack) otherwise a KIE smaller than one is typical for classical backside S_N2 mechanism.

Table 2: Table of substrates and proposed mechanisms.[105]

Table 1 Summary of selectivity parameters (ρ_X, β_X, ρ_Y and ρ_{XY}), deuterium kinetic isotope effects (k_H/k_D) and proposed mechanisms for the reactions of $R_1R_2P(=A)$; A = O or S)Cl with $XC_6H_4NH_2(D_2)$ in acetonitrile at 55.0 °C

A(R_1,R_2)[a]	$-\rho_X$	β_X	ρ_Y	ρ_{XY}	k_H/k_D	Proposed mechanism	ref.
O(YPhO,PhO)	3.42–4.63	1.24–1.68	0.22–0.87	–1.31	0.61–0.87	Concerted S_N2; late TS; mainly backside attack[d]	18a
S(YPhO,PhO)	3.81–4.01	1.34–1.41	0.67–0.89	–0.22	1.11–1.33	Concerted S_N2; backside and frontside attack[e]	18c
O(YPhO,EtO)	3.09–3.40	1.09–1.20	0.41–0.90	–0.60	1.07–1.80	Concerted S_N2; backside and frontside attack	18f
S(YPhO,EtO)	3.14–3.40	1.10–1.19	0.74–0.95	–0.28	1.06–1.27	Concerted S_N2; backside and frontside attack	18f
O(EtO,EtO)	2.99/2.80[b]	1.06/0.993	—	—	0.714–0.919	Concerted S_N2; mainly backside attack	18g
S(EtO,EtO)	2.75/2.70	0.977/0.957	—	—	1.01–1.10	Concerted S_N2; backside and frontside attack	18g
O(MeO,MeO)	2.72/2.56	0.962/0.907	—	—	0.798–0.979	Concerted S_N2; backside and frontside attack	18g
S(MeO,MeO)	2.81/2.73	0.993/0.963	—	—	0.945–1.06	Concerted S_N2; backside and frontside attack	18g
S(YPhS,Ph)	3.35–3.47	1.21–1.25	0.29–0.50	–0.31	1.15–1.59	Concerted S_N2; mainly frontside attack	18h
O(Ph,Ph)	4.78/4.56	1.69/1.62	—	—	1.42–1.82	Concerted S_N2; mainly frontside attack	18d
S(Ph,Ph)	3.97/3.94	1.40/1.40	—	—	1.00–1.10	Concerted S_N2; backside and frontside attack	18e
O(Ph,Me)	2.49/2.28	0.88/0.81	—	—	1.62–2.10	Concerted S_N2; mainly frontside attack	18i
O(Me,Me)[c]	4.59/4.42	1.62/1.56	—	—	0.703–0.899	Concerted S_N2; mainly backside attack	18i

[a] The substrates, $R_1R_2P(=O)Cl$ and $R_1R_2P(=S)Cl$, are denoted as O(R_1R_2) and S(R_1R_2), respectively. [b] Calculated from k_H/calculated from k_D. [c] Selectivity parameters and DKIEs are at 15.0 °C. [d] Backside attack indicates that the reaction proceeds through in-line type TS I. [e] Frontside attack indicates that the reaction proceeds through a hydrogen-bonded, four-center-type TS II.

In Figure 6 is depicted the geometry of transition states for frontside and backside attack. The important feature for distinguishing the mechanism is hydrogen bond formation between hydrogen on the nucleophile and the leaving group. The mechanisms for individual substrates could change in depending on the power of the nucleophile.

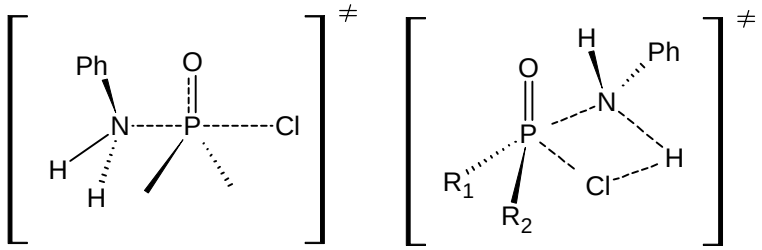

Figure 6 - Transition states geometry for backside a frontside attack.

2.4.5 Oxidative addition in view of frontside S_N2

Oxidative addition of the atoms of transient metals on alkylhalogenides could be considered as an interesting kind of frontside S_N2 mechanism.[107]

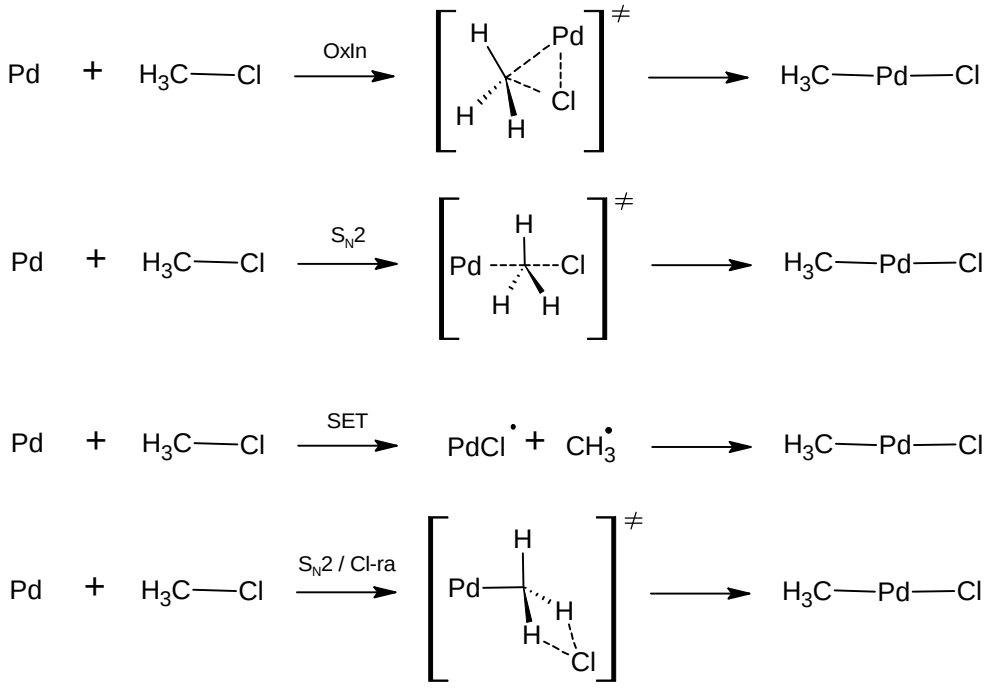

Scheme 33 – Possible mechanisms for oxidative addition.

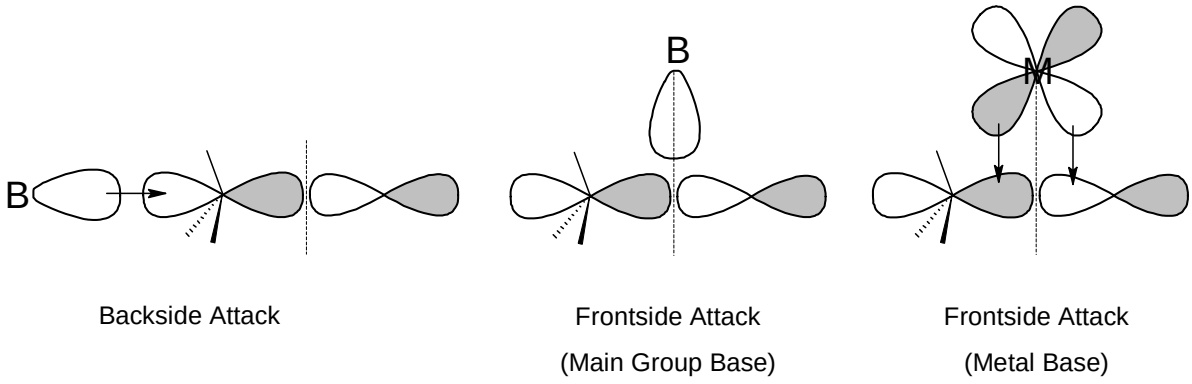

Figure 7 - Orbital overlay for possible attacks on reaction centre.

Oxidative addition of a palladium atom to chloromethane has been modelled in a gas phase using the DFT method. Four different types of mechanisms were taken into consideration and PESs were calculated for each of them. The first one is oxidative insertion (*cis* oxidative addition - OxIn). The second is a classical backside S_N2 reaction. The third one is single electron transfer (SET) and the last is an alternative of S_N2 reaction where the chloride anion as a leaving group, migrates on the palladium (Scheme 33).

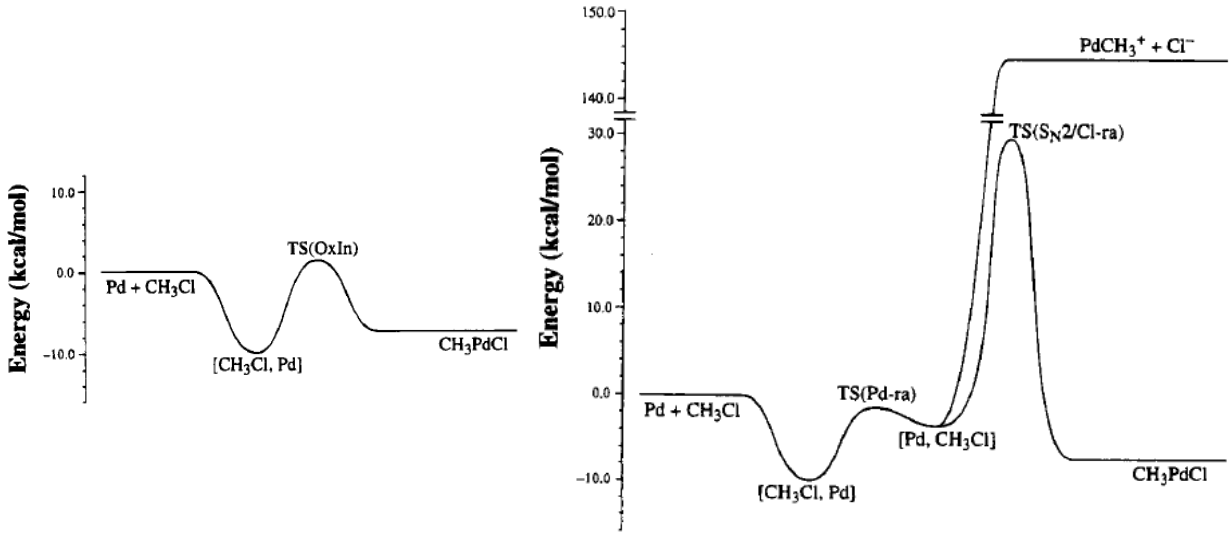

Figure 8 - Energetic profiles for oxidative insertion and classical nucleophilic substitution.[107]

Energetic profiles (Fig. 8) show oxidative addition with the activation energy of 1.7 kcal·mol^{-1} favoured. A mechanism of classical nucleophilic substitution with a nonsolvated

chloride anion recombining into the product in the next step is energetically unfavoured. The most favourable mechanism seems to be mechanism 4 with simultaneous migration of this anion to the molecule of palladium. However, the situation changes after including the influence of solvation as the enthalpy for a classical S_N2 mechanism drops under the enthalpy of the mechanism 4. But energy for oxidative insertion is still the lowest.

An explanation of this fact is depicted in Fig. 7. There is an advantageous overlap of *p* or sp^x HOMO orbitals of the nucleophile with σ^*_{CCl} orbitals of the substrate in the backside attack. Otherwise during the frontside attack HOMO orbitals of the nucleophile approaches the nodal plane of the orbitals of substrate; which makes the attack very disadvantageous. The opposite situation is in the case of "metal" bases (nucleophiles). The organization of their *d* type HOMO orbitals is very advantageous for the overlap with orbitals of substrate. From this point of view it could be said that a mechanism of oxidative addition may be considered analogous to a frontside S_N2 mechanism.

2.5 Nucleophilic substitution of enzyme catalyzed reactions

2.5.1 Glycosyltransferases

Glycosyltransferases[108-116] are enzymes using a phosphate group activated sugars as donors. Typical examples are nucleotide diphosphates, monophosphates, lipidic phosphates and in some cases also nonsubstituted phosphates. Most common acceptors are sacharides but it is also possible to transfer to lipids, nucleic acids, proteins, antibiotics and other small molecules.

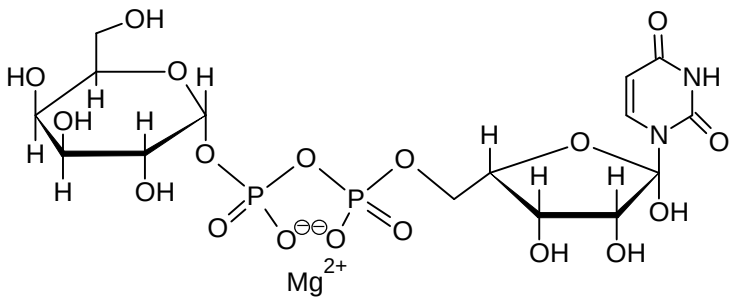

Figure 9 - UDP Gal.

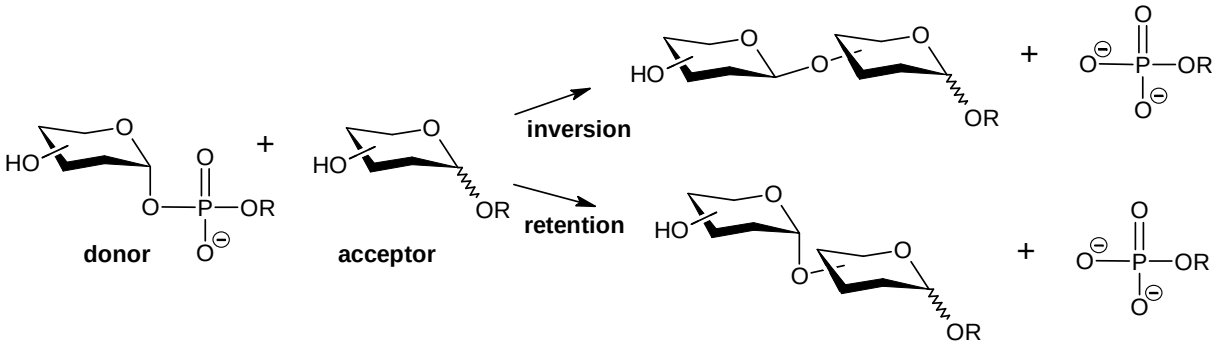

Scheme 34 – Inversion and retention of configuration.

The mechanism of action for invert glycosyltransferases is analogous to the mechanisms proposed for glycosidases – direct displacement S_N2. The question is: a mechanism of action for retentive glycosyltransferases. There is not observed evidence for the expected double-displacement mechanism. All methods used for glycosidases as capture by the fluoride substituted substrates or changes in catalytic place of enzyme did not succeed. The next argument against a double-displacement mechanism is the absence of a nucleophilic

group in the active site of the enzyme. These observations does not disprove double-displacement mechanism however, but it does mean that new question arise as to if there is no possibility of another reaction mechanism. Some authors propose so called S_Ni-like (internal return like) mechanism analogical to the S_Ni (internal return) mechanism of decomposition of alkylchlorosulphites (Chapter 2.4.2).

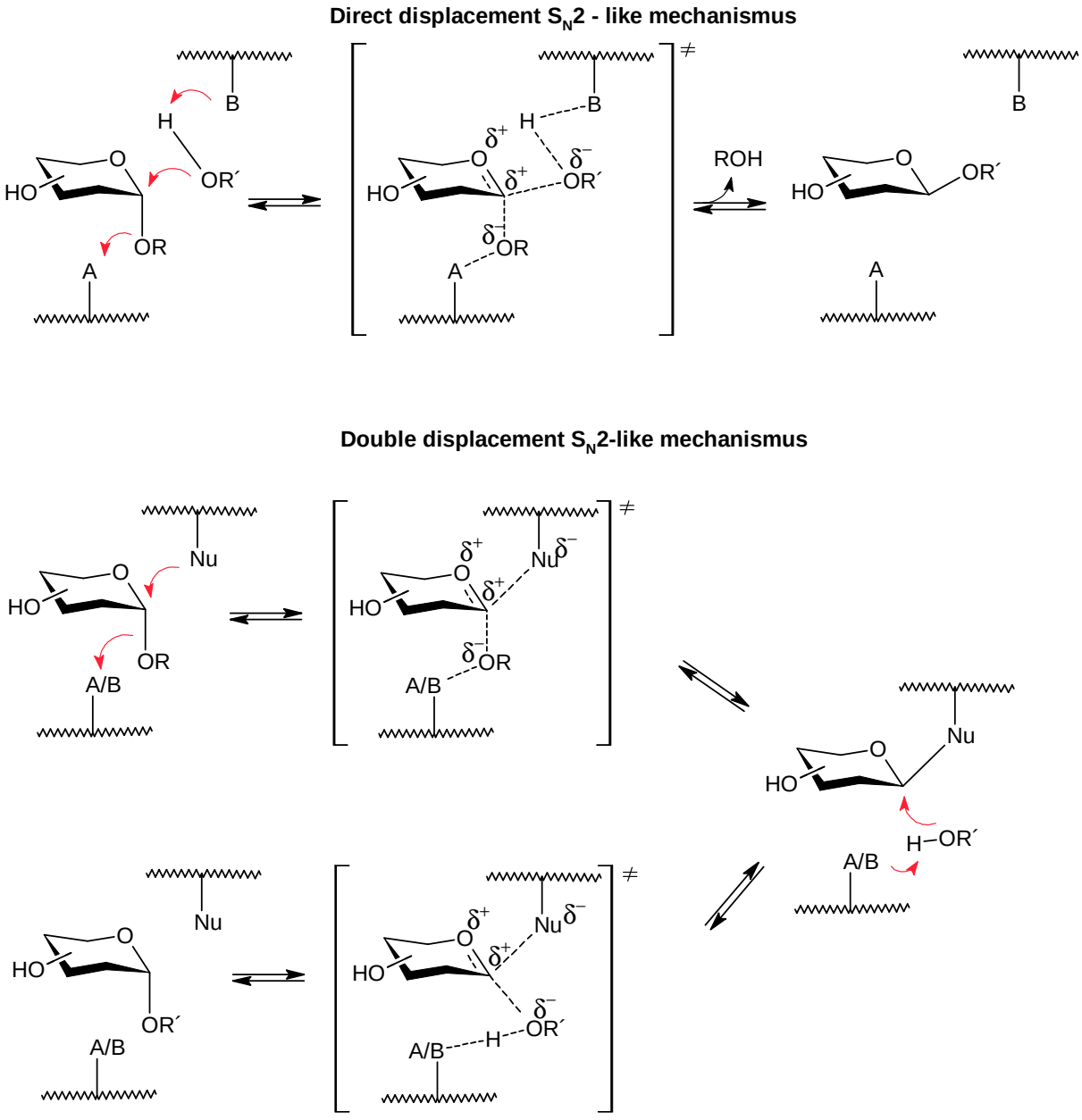

Scheme 34 – Direct-displacement and double-displacement S_N2-like mechanisms.

2.5.2 S_Ni-like mechanism

Authors of the term S_Ni-like ($D_N{}^*A_{Nss}$) are M. L. Sinnott and W. P. Jencks[117], who studied solvolysis D-glukopyranosyl derivates in ethanol a 2,2,2-trifluorethanol solutions.[118,119] Retention of the configuration occurred during the reactions of some substrates. They proposed mechanism with similar stereoelectronic requirements as S_Ni however; attacking nucleophile is not covalently bonded to the substrate. This is the reason why the word "like" is used in the name of mechanism - it is only a stereoelectronic analogy of the S_Ni mechanism.

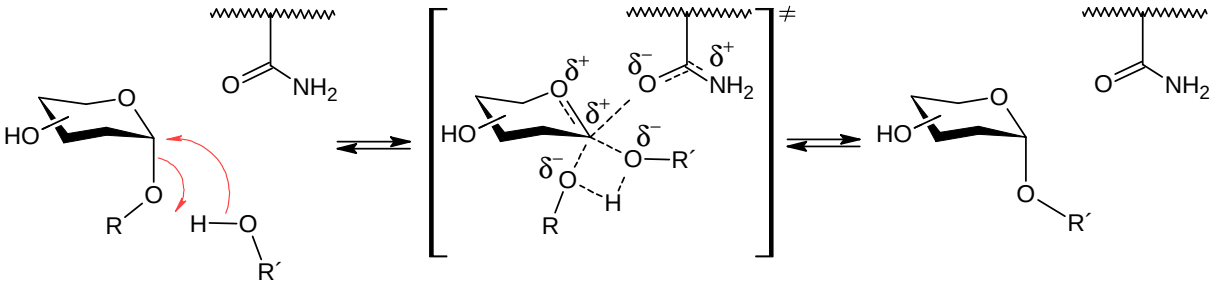

Scheme 35 - S_Ni-like mechanism for glycosyltransferases.

This mechanism was proposed for glycogen phosphorylases at first, but some experiments disprove it.[120] Making some changes this could be applied for glycosyltransferases (Scheme 35) but there is still no evidence of them and it is only accepted because the double-displacement mechanism has not yet been proven.

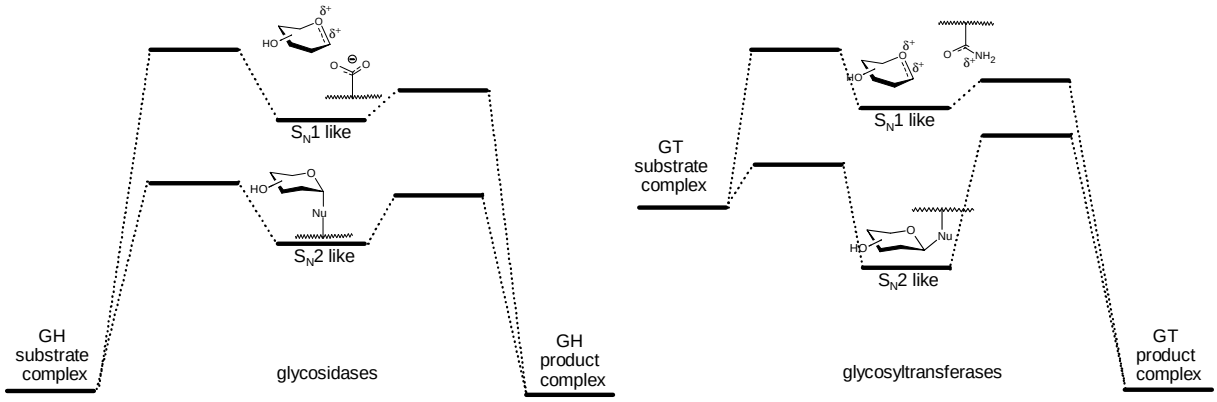

Scheme 36 – Energetic profiles for reactions catalyzed by glycosidases and glycosyltransferases.

One of the arguments why the active site allows formation of active site enabling S_Ni-like mechanism instead of double-displacement being developed in glycosyltransferases, is the difference of energy of starting complexes of enzyme and substrate in connection with the activation energy of the first step (Scheme 36).

While glycosidic bonds hydrolyzed by glycosidases are very stable, a much more energy rich and unstable phosphoglycosidic bond is the substrate for glycosyltransferases. The acidity of the leaving group is also very important. The pK_a of leaving glycides during glycolysis is approximately 14, otherwise pK_a of the leaving phosphate group is about 7. These circumstances cause a decrease of the activation barrier in the first step of S_Ni-like mechanism and so enables this reaction path.

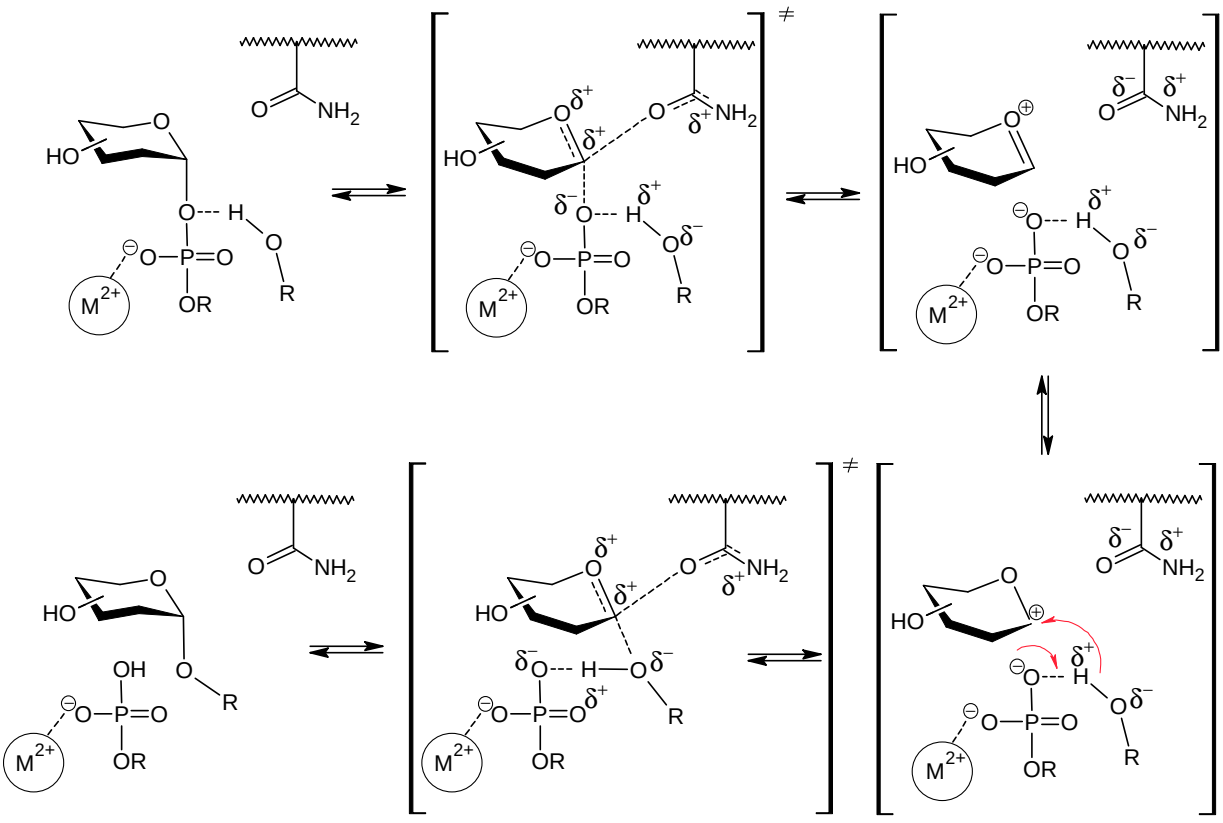

Scheme 37 – Proposed mechanism of glycosyltransferases action.

The most probable is the situation analogous to the classical nucleophilic substitution[121] where mechanisms S_N1 a S_N2 are only borders and the reaction occur in the area somewhere between them (Scheme 18). An ionic pair with a short lifetime requiring stabilization with no covalently bonded nucleophile (amidic group) is the most probable

intermediate. There are two possibilities of reactions of this pair. Recombination to the starting compound or external nucleophilic attack from the same side as the leaving group leaves. In this case the retention product is formed. Similar results to these were obtained using quantum chemistry calculations.[122-124]

3 Results and discussion

3.1 Transformations of isothiouronium salts derived from substituted 2-bromobutyrolactones

3.1.1 Preparation and structure of the salts and their transformation products

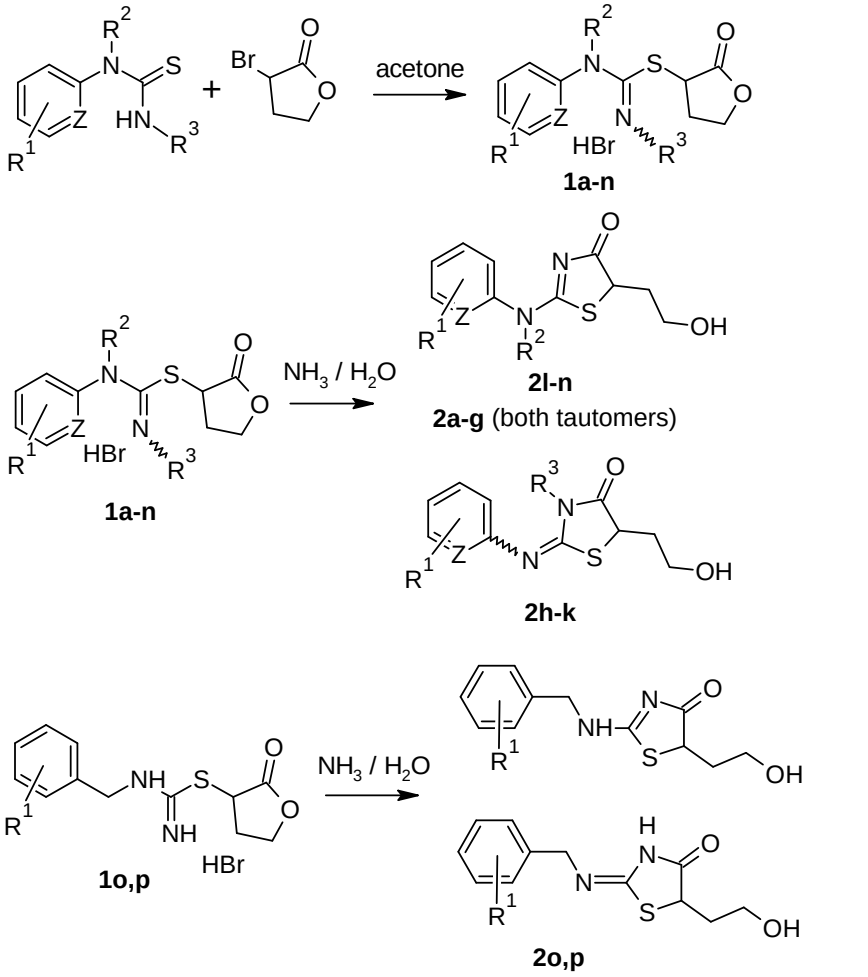

a:R^1=R^2=R^3=H;Z=CH
b:R^1=4-OCH_3;R^2=R^3=H;Z=CH
c:R^1=4-CH_3;R^2=R^3=H;Z=CH
d:R^1=4-Cl;R^2=R^3=H;Z=CH
e:R^1=4-Br;R^2=R^3=H;Z=CH
f:R^1=3-CF_3;R^2=R^3=H;Z=CH
g:R^1=R^2=R^3=H;Z=N
h:R^1=R^2=CH_3;R^3=H;Z=CH
i:R^1=R^2=C_2H_5;R^3=H;Z=CH
j:R^1=R^2=C_6H_5;R^3=H;Z=CH
k:R^1=4-OCH_3;R^2=CH_3;R^3=H;Z=CH
l:R^1=4-OCH_3;R^2=R^3=CH_3;Z=CH
m:R^1=R^2=R^3=C_2H_5;Z=CH
n:R^1=4-Cl;R^2=R^3=CH_3;Z=CH
o:R^1=H
p:R^1=4-OCH_3

Scheme 38 - Preparation and transformation of isothiouronium salts derived from 2-bromobutyrolactone.

S-(2-oxotetrahydrofuran-3-yl)-*N*-(subst. phenyl, benzyl) isothiouronium bromides (**1a-p**) were prepared by the reaction of 2-bromobutyrolactone with phenyl or benzyl substituted thioureas in acetone. These salts underwent rearrangement in basic medium to give desired 5-(2-hydroxyethyl)-2-phenylimino-1,3-thiazolidin-4-ones (**2a-g**, **2l-n**), 5-(2-hydroxyethyl)-2-phenylamino-4,5-dihydro-1,3-thiazol-4-ones (**2h-k**) or 2-(benzylamino)-5-(2-hydroxyethyl)-1,3-thiazol-4(5*H*)-ones (**2o**,**p**) (Scheme 38). In most cases it was impossible to characterize pure isothiouronium salts by NMR because of their spontaneous cyclization giving **2a-p** in DMSO-d_6 solution. The only exceptions were *S*-(2-oxotetrahydrofuran-3-yl)-*N*-(4-methoxyphenyl) isothiouronium bromide (**1b**) and benzyl substituted isothiouronium salts (**1o**,**p**) which were prepared in a pure form and characterized by ^{1}H, ^{13}C NMR and microanalysis. The reason for enhanced reactivity of the other derivatives lies in the presence of electron-withdrawing group in the benzene nucleus or methyl group on nitrogen(s). All of these substituents facilitate rearrangement involving bicyclic tetrahedral intermediate. Therefore, the kinetic of the transformation was studied for isothiouronium salts (**1b**,**p**).

Prepared 5-(2-hydroxyethyl)-2-phenylimino-1,3-thiazolidin-4-ones (**2a-g**), **(2l-n**) 5-(2-hydroxyethyl)-2-phenylamino-4,5-dihydro-1,3-thiazol-4-ones (**2h-k**) and 2-(benzylamino)-5-(2-hydroxyethyl)-1,3-thiazol-4(5*H*)-ones (**2o**,**p**) were characterized by ^{1}H, ^{13}C NMR and microanalyses and some of them (**2g**,**i**) also by X-ray diffraction (Figs. 9 and 10) and mass spectroscopy.

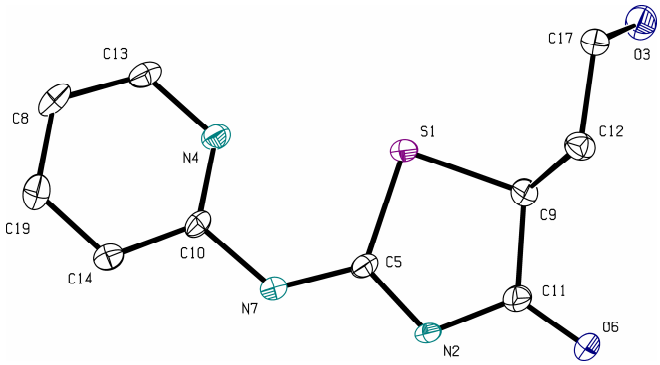

Figure 9 - ORTEP view of compound **2g** (thermal ellipsoids at 40 % probability).

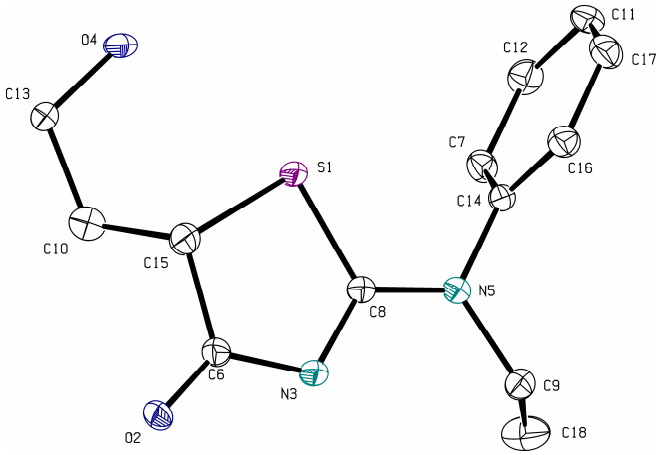

Figure 10 - ORTEP view of compound **2i** (thermal ellipsoids at 40 % probability).

Compounds **2a-f** carrying hydrogen atoms on both nitrogen atoms (R^2 = R^3 = H) exist in the form of two tautomers differing in the position of C=N double bond. Moreover the tautomer with exocyclic double bond exists as a mixture of *E*- and *Z*- stereoisomers in the proportion depending on substitution of the benzene nucleus and temperature. This tautomerism and stereoisomerism which can be seen in both ^{1}H and ^{13}C NMR spectra was previously studied for C-5 unsubstituted 2-phenyliminothiazolidin-4-ones by several authors.[125-127] In the case of compounds **2h-k** (R^2 = CH_3, C_2H_5, C_6H_5; R^3 = H) and **2l-n** (R^2 = H; R^3 = CH_3, C_2H_5) prototropic tautomerism is absent due to C=N double bond fixation and stereoisomerism is possible only for **2l-n**. In both ^{1}H and ^{13}C NMR spectra of **2g** there is only one set of signals. From this observation it can be deduced that compound **2g** exists only as *E*- stereoisomer stabilized in solution by intramolecular hydrogen bond (Fig. 11). On the other hand in crystal lattice two molecules of **2g** are connected by intermolecular hydrogen bonds (N_{ring}–H···N_{mino}) which constrains *Z*-configuration of C=N double bond (Fig. 9).

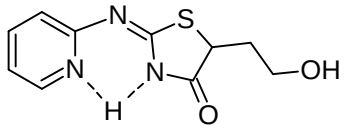

Figure 11 - Intramolecular hydrogen bond in solution of **2g** in DMSO-d_6.

3.1.2 Kinetic measurements

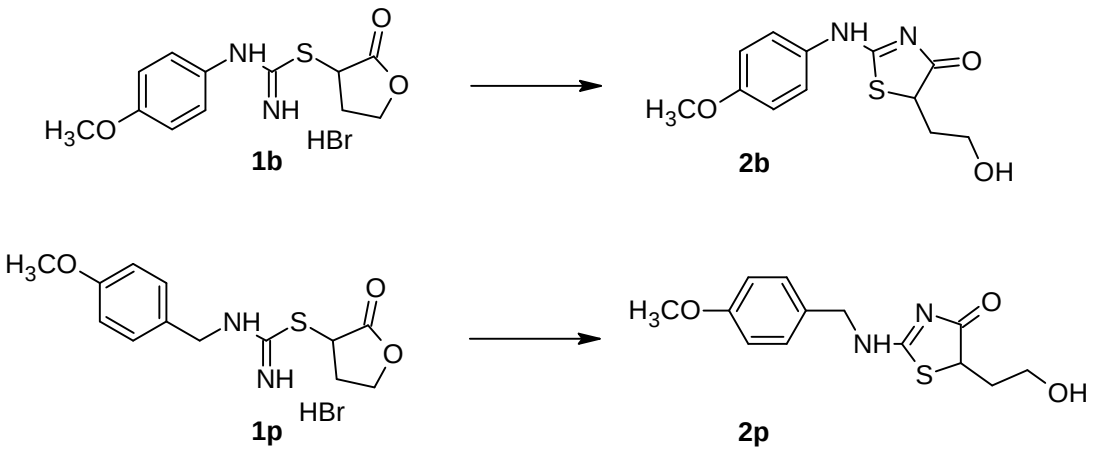

Scheme 39 – Transformation of *S*-(2-oxotetrahydrofuran-3-yl)-*N*-(4-methoxyphenyl) isothiouronium bromide (**1b**) and *S*-(2-oxotetrahydrofuran-3-yl)-*N*-(4-methoxybenzyl) isothiouronium bromide (**1p**) to 5-(2-hydroxyethyl)-2-[(4-methoxyphenyl)imino]-1,3-thiazolidin-4-one (**2b**) and 5-(2-hydroxyethyl)-2-[(4-methoxybenzyl)amino]-1,3-thiazol-4(5*H*)-one (**2p**) respectively.

The acid-base catalyzed transformations of isothiouronium salts **1b**,**p** giving thiazolidin-4-ones **2b**,**p** as the only products were studied spectrophotometrically under pseudo-first order conditions in aqueous hydrochloric acid solutions (c = 0.001-0.7 mol·Γ^{-1}), in aqueous buffers (pH = 2-9) and in sodium(potassium) hydroxide solutions (c = 0.0005-0.7 mol·Γ^{-1}) at constant ionic strength (I = 1 mol·Γ^{-1}) and at 25 °C. All spectra recorded during the rearrangement reaction showed sharp isosbestic points which prove[128-130] the existence of only two absorbing species, *i.e.* this result allows to reject consecutive reaction mechanisms. In other words, only short-living intermediates in negligible concentration can occur on the reaction coordinate. Only in sodium hydroxide solutions the reaction proceeds through different pathway and the different products of the reaction were isolated. The NMR spectra showed the complicated mixture of anilines, starting thioureas and 2-sulfanylbutyrolactone.

Observed rate constants, k_{obs}, were calculated in each buffer/acid/hydroxide solution from the absorbance *vs.* time dependence of the absorptions at 260 or 273 nm and k_{obs} for buffers were plotted against the total buffer concentration ($c_{Buff} = c_B + c_{BH}$). It was found that in dichloroacetate (DCA), chloroacetate (CA), methoxyacetate (MEA), acetate (AC),

hydroxylamine (HA), *N*-methylmorpholine (NMM), glycinamide (GA), tris(hydroxymethyl)aminomethane (TRIS) and morpholine (MP) buffers the observed rate constants (k_{obs}) increase with both the total buffer concentration (c_{Buff}) and the basicity (pH) of the medium (Figs. 12-14). From this observation it is clear that the transformation involves general buffer catalysis as well as specific acid-base catalysis.

The two different dependences of k_{obs} on the total buffer concentration (c_{Buff}) were observed: in DCA, CA, MEA, AC, and partially in HA buffers, k_{obs} increases linearly with c_{Buff} (Fig. 12 and 14) whereas in NMM, GA, TRIS and MP buffers the slopes of plots decreased with increasing c_{Buff} until at sufficiently high buffer concentration the lines appear to approach linearity (Figs. 13 and 14). With NMM, TRIS and MP buffers the linear portion, at high c_{Buff}, is easily discernable and, therefore, a more detailed analysis of those buffers was made (see below). Curved buffer dilution plots of k_{obs} reveal a change in the rate-limiting step with the change in the total buffer concentration at a constant pH which in turn implies the presence of a reactive intermediate on the reaction coordinate.[19,40,131-138] Another possible reason for the nonlinear plots in Fig. 13 is that the nitrogen buffers undergo some kind of complexation with **1b,p** (pre-equilibria with amine/ammonium or H-bonding) and the complex becomes more reactive than uncomplexed **1b,p**. However, this possibility seems to be unlikely because hydroxylamine buffers differ in their behaviour dependent on the ratios of both components (Fig. 12): a linear relationship is observed at a low fraction of free base (low pH) and a non-linear relationship at a high fraction of free base (high pH). Therefore it is clear that the non-linearity of the plots is simply a function of pH and similar observations have been reported for other reaction systems.[19,134]

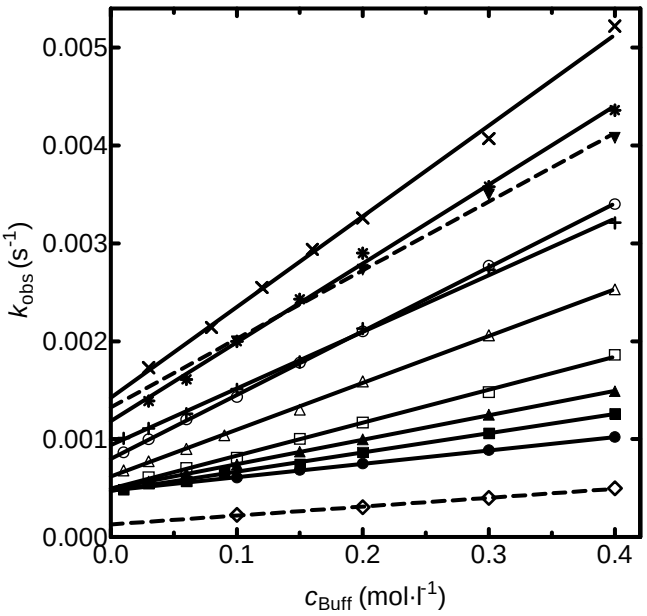

Figure 12 - Dependence of the observed rate constant (k_{obs}; s^{-1}) on the total buffer concentration (c_{Buff}; mol·l^{-1}) for **1b** measured at 25 °C in CA [(2:1a) pH 2.36 (●); (1:1) pH 2.68 (■); (1:1) pD 3.14 (◇); (1:2b) pH 2.94 (▲)], MEA [(2:1a) pH 3.04 (□); (1:1) pH 3.35 (△); (1:2b) pH 3.67 (○)] and AC buffers [(6:1a) pH 3.76 (+); (4:1a) pH 3.93 (✳); (3:1a) pH 4.04 (×); (1:1) pD 5.14 (▼)]. a-acidic; b-basic. Dashed lines correspond to measurements in D_2O.

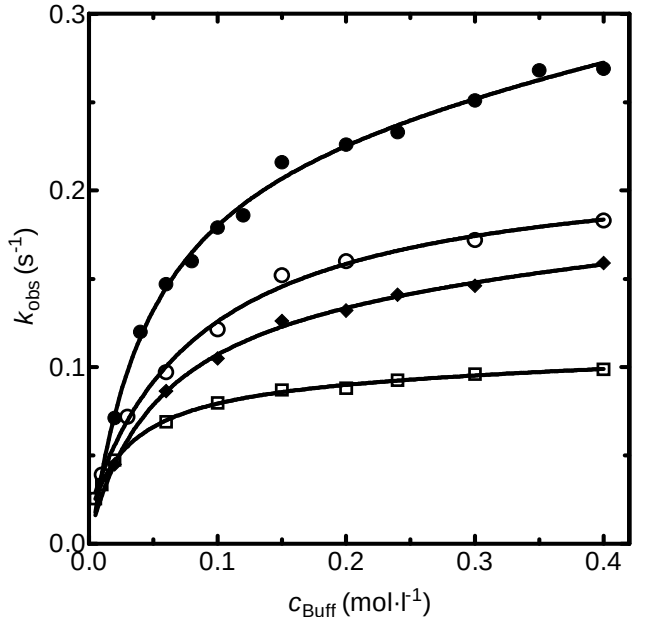

Figure 13 - Dependence of the observed rate constant (k_{obs}; s^{-1}) on the total buffer concentration (c_{Buff}; mol·l^{-1}) for **1b** measured at 25 °C in NMM [(1:1) pH 8.24 (□)]; TRIS [(1:1) pH 8.36 (◆)]; GA [(1:1) pH 8.65 (○)] and MP buffers [(1:1) pH 8.94 (●)].

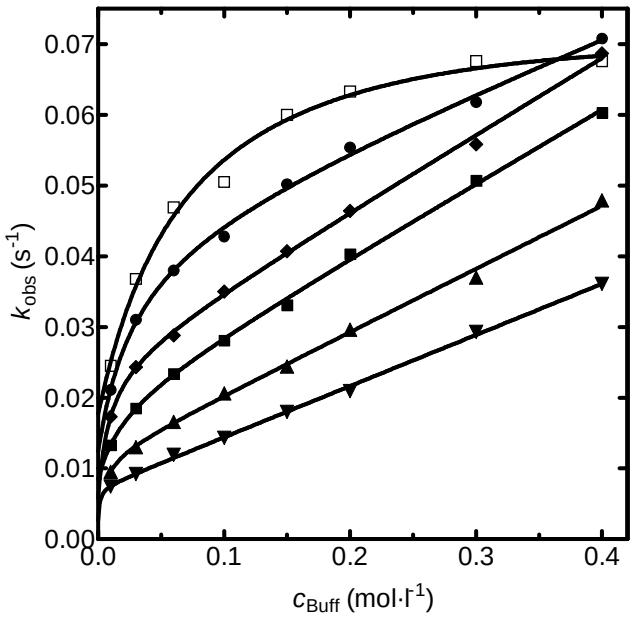

Figure 14 - Dependence of the observed rate constant (k_{obs}; s^{-1}) on the total buffer concentration (c_{Buff}; mol·l^{-1}) for **1b** measured at 25 °C in hydroxylamine (HA) buffers [(4:1a) pH 5.52 (▼); (2:1a) pH 5.85 (▲); (1:1) pH 6.15 (■); (1:2b) pH 6.42 (◆); (1:4b) pH 6.75 (●); (1:8b) pH 7.05 (□)]. a - acidic; b - basic.

Extrapolation of the plots of k_{obs} *vs.* c_{Buff} to zero buffer concentration provided, as intercepts the values of the catalytic constants (k_{ext}). In this case, the only catalytic species are the hydroxide anion and hydroxonium ion, whose concentrations are given by the ratio of both buffers components (c_B /c_{BH}) or by concentration of the hydrochloric acid. From this data the corresponding pH profile (Fig. 15) can be generated whose shape, in the pH region 0-3, is similar to that observed for cyclization of *S*-(ethoxycarbonylmethyl)isothiouronium chloride.**Chyba! Záložka není definována.**

There are six breaks in the pH profiles in Fig. 15. In hydrochloric acid solutions the log k_{obs} increases with pH up to *ca* 1.5. Between pH 1.5 and 3.0 the values of log k_{obs} (log k_{ext}) are pH-independent and then linearly increase again with exceptionally low slope (*ca* 0.45; a slope +1 has been observed for similar cyclization[139]). The third slight breaks downwards occur at pH ≈ 5 and then log k_{ext} gradually increases again with pH (slope *ca* 0.3) up to pH 7. The last downwards breaks to zero slope occur at pH ≈ 7. The values of log k_{ext} are somewhat scattered above pH 7 because the extrapolation from non-linear dependences (basic buffers) is less precise as compared with extrapolation from linear dependences found for substituted acetate buffers. Last upward break occurs at pH 11 and the slopes

approaches unit values. This last break is associated with the opening of a new reaction pathway.

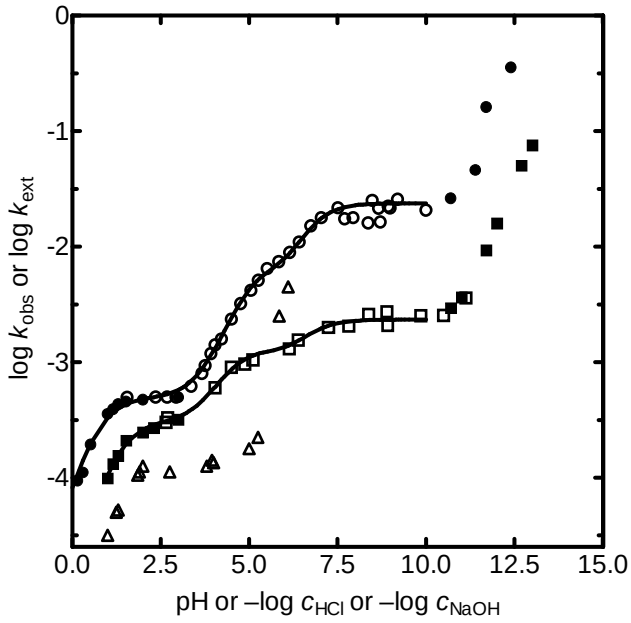

Figure 15 - pH profile (log k_{ext} *vs.* pH) for rearrangement of **1b,p** to **2b,p** in buffers (○ for **a**) (□ for **b**) and (log k_{obs} *vs.* –log c_{HCl}) in hydrochloric acid and sodium hydroxide (● for **a**) (■ for **b)**. The (Δ) corresponds to the transformation of *S*-(ethoxycarbonylmethyl) isothiouronium chloride.[139] The lines represent the best fits of all data points using Eq. 2 or Eq. 5 with parameters given in the text.

Since the isothiouronium salts **1b,p** (= $\mathbf{SH}^+$) ourselfs do not undergo rearrangement, it was necessary to relate k_{obs} to the concentration of free isothiourea (**S**). The corrected rate constants (k_{cor}) were calculated from the pK_a of the isothiouronium salt **1b,p** and pH of the buffer solution according to Eq. (13). A pK_a of 6.7 was adopted for this purpose (for details of the pK_a estimation see below) for both of the salts.

$$k_{cor} = k_{obs}\frac{K_a}{K_a + [H^+]} = k_{obs}(1 + 10^{(pK_a - pH)}) \qquad (13)$$

For buffers showing linear dependence of k_{cor} *vs.* c_{Buff} (substituted acetates, acidic HA buffers) the catalytic constants k_{Buff} were determined from the slopes of the plots. A second plot of k_{Buff} values against the ratio c_B/c_{Buff} then provides a linear dependence from which it is possible to determine the catalytic constants of both buffer components: extrapolation

to c_B/c_{Buff} = 0 and 1 gives the catalytic constants k_B^{cor} and k_{BH}^{cor}, respectively. For the reactions monitored here, no significant general base-catalyzed rearrangement (k_B^{cor}) was observed in all the substituted acetate buffers. Only the acid-buffer component catalyzes the reaction *i.e.* the reaction is general-acid catalyzed. The catalytic constant k_{BH}^{cor} for the individual general acids are given in Table 3. A Brønsted plot of log k_{BH}^{cor} *vs.* pK_a(BH) for **1a** is linear with the slope $\alpha = -0.47$ (Fig. 16). The point corresponding to catalysis by H_3O^+ can be calculated from the plateau at pH 2-3 and this point falls 0.5 log units below the extrapolated straight line in Fig. 16.

Table 3: Catalytic rate constants k_{BH}^{cor} and k_B' for individual buffer components for compound **1b**.

Base buffer component (B)	pK_a(BH)[31]	k_{BH}^{cor} ($l \cdot mol^{-1} \cdot s^{-1}$)	k_B'
H_2O	–1.74	2460[a]	–
Dichloroacetate (DCA)	1.29	175 ± 5	–
Chloroacetate (CA)	2.86	48.0 ± 3	–
Methoxyacetate (MEA)	3.53	22.6 ± 0.8	–
Acetate (AC)	4.76	6.3 ± 0.2	–
Hydroxylamine (HA)	5.96	1.6 ± 0.1[b]	–
N-Methylmorpholine (NMM)	7.41	–	0.12 ± 0.01[c]
TRIS	8.10	–	0.26 ± 0.02[c]
Glycinamide (GA)	8.00	–	0.24 ± 0.01[c]
Morpholine (MP)	8.39	–	0.48 ± 0.02[c]

[a]From the plateau at pH 2-3 (Fig. 15). $k_H = k_1k_2/k_{-1}$

[b]From buffer with c_B/c_{BH} 1:4.

[c]From buffers with c_B/c_{BH} 1:1.

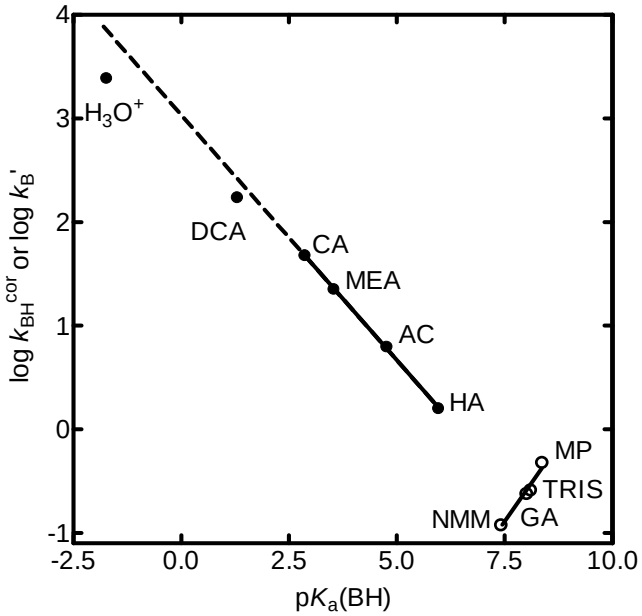

Figure 16 **-** Brønsted plot for **1b** of log k_{BH}^{cor} *vs.* pK_a(BH) (●) and log k_B' *vs.* pK_a(BH) (○).

For basic buffers (Fig. 17) when k_{cor} is plotted against concentration of the base-buffer component (c_B) the linear portions of non-linear dependences (at high c_{Buff}) are almost parallel. From this observation it can be concluded that the reaction in concentrated amine buffers involves general-base catalysis. In dilute buffers both acid as well as base-buffer component can catalyze the reaction.

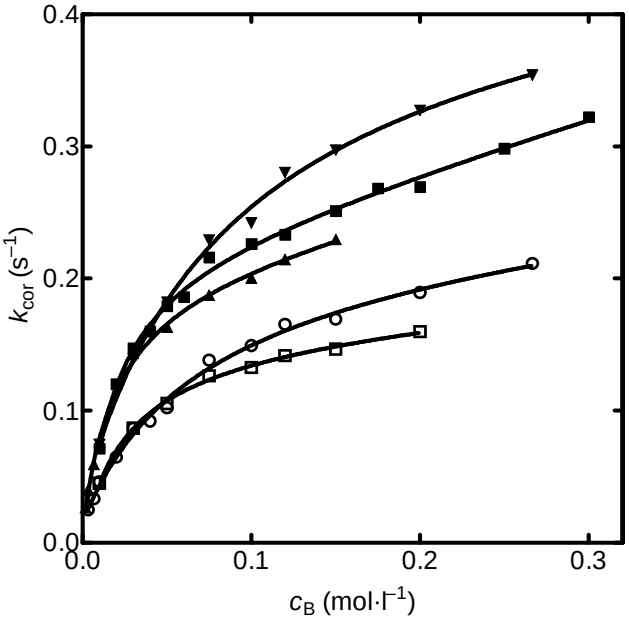

Figure 17 **-** Dependence of the corrected rate constant (k_{cor}; s^{-1}) on the concentration of base-buffer component (c_B; mol·l^{-1}) for **1b** measured at 25 °C in morpholine (MP) buffers

[(2:1a) pH 8.63 (▲); (1:1) pH 8.93 (■); (1:2b) pH 9.21 (▼)] and TRIS buffers [(1:1) pH 8.37 (□); (1:2b) pH 8.70 (○)]. a - acidic; b - basic.

A solvent kinetic isotope effect was also studied for **1b** in (1:1) chloroacetate and acetate buffer (Fig. 1). Both dependences of k_{obs} *vs.* c_{Buff} in D_2O were linear (like in water) and the values for chloroacetate k_{ext}^{H}/k_{ext}^{D} = 3.55, $k_{Buff}^{H}/k_{Buff}^{D}$ = 2.14 and for acetate k_{ext}^{H}/k_{ext}^{D} = 1.83, $k_{Buff}^{H}/k_{Buff}^{D}$ = 2.36 were obtained. For **1p** in acetate k_{ext}^{H}/k_{ext}^{D} = 2.05 and $k_{Buff}^{H}/k_{Buff}^{D}$ = 2.02 were obtained.

3.1.3 Estimation of the pK_a of isothiouronium salts (1b,p)

Knowledge of the pK_a value is essential for correct evaluation of all kinetic data. It was not possible to measure the thermodynamic pK_a value of **1b,p** because of the very high rates of cyclization at pH 6-8 but a pK_a(**1a,b**) around 7 would be reasonable for an *N*-phenylisothiouronium salt. The pK_a of *S*-methyl-*N*-phenylisothiouronium is 7.14.[140] The lactone group in **1b,p** will have an acidifying effect (through polar effects as well as due to intramolecular hydrogen bond) whereas methoxy group in *para*-position has an opposite effect. In our case the best fit of all data points in Fig. 15 using Eq. 2 or 5 with parameters given below was achieved for pK_a(**1b,p**) = 6.7.

We also verified this pK_a(**1**) value using SPARC program[141] which was successfully tested[142] by estimation of more than 4300 ionization pK_as. SPARC program gave pK_a(**1b**) 6.2 and 7.3, respectively, for both possible canonical structures. For the salt **1p** the calculated values are pK_a(**1p**) 7.9 and 7.8.

The same pK_a values resulting from the data-fitting are quite surprising. In accordance with the electronic effects the pK_a of the benzyl salt **1p** should be higher than pK_a of the phenyl salt **1b**. This could be explained by the fact that these kinetically estimated dissociation constants consider more effects (*e.g.* hydrogen bond, tautomeric equilibria, appearance of new kinetically detectable intermediate, *etc.*) and apparent pK_as instead of thermodynamical are estimated in this case.

3.1.4 Mechanism of the rearrangement and evaluation of the kinetic data

The bimolecular[143-149] and intramolecular aminolyses of esters that have been studied to date have shown large differences in the detailed mechanism. However, it is generally accepted that with most esters, the attack of amine to form the labile intermediate $T^{\pm}$ is rapid and reversible, and the rate determining step at high pH is the trapping of this

intermediate by proton removal with a general base giving T^-, a proton switch through water (T^0), or direct breakdown of $T^\pm$ to products. Only in very few cases when the intermediate $T^\pm$ or T^- is too unstable to permit proton transfer to take place in a discrete step before its breakdown, a concerted mechanism or enforced concerted mechanism of catalysis is possible in order to avoid this labile intermediate.[10,150,151] The existence of such labile tetrahedral intermediates has been proven indirectly on the basis of curved pH profiles[18,147,148], curved buffer dependence plots[19,39,131], curved Brønsted plots[146,148] , kinetic isotope effects[13,17] and quantum chemical calculations.[152-153] The intramolecular aminolysis of alkyl esters involves[17-19,21] either breakdown of T^- or its general base-catalyzed formation from T^0. However, for cyclization of *S*-(ethoxycarbonylmethyl) isothiouronium chloride, which best resemble the rearrangement of our lactone, the rate limiting formation and breakdown of $T^\pm$ was reported.[139] To the best of our knowledge, the coexistence of all three kinetically detectable intermediates $T^\pm$, T^0 and T^- during an aminolysis reaction has not yet been published.

In our case the transitions in the pH profile (Fig. 15) above pH 1 and 4.5 establish the formation of at least two different kinetically detectable intermediates, whose rate of formation and breakdown to product are pH dependent.[154] The break at pH ≈ 7 gives either the value of the apparent ionization constant pK_{app} for **1a** or is caused by appearance of another kinetically detectable intermediate (*cf.* behaviour in buffers where at pH > 6 linear dependences of k_{obs} *vs.* c_{Buff} change to non-linear). The combination of both the possibilities is also conceivable and can explain the observation of the similar pK_a values of phenyl **1b** and benzyl **1p** substituted isothiouronium salts (see chapter 3.1.3).

It is impossible to neglect break at pH 5, although it is very slight, because the slope of the straight line crossing the points between pH 3.2-6.0 would be only 0.45. It is well known that the slopes in pH profiles have mostly integral values giving whole number reaction orders.[155] Only in very rare systems, involving auto-catalysis or auto-inhibition, the ratios of small integers such as ½ are allowed (mostly in the gas phase). However, in a relatively narrow pH region (approximately two pH units), the slopes can change from one integral value to another, giving intermediate values as for example during hydrolysis of aspirin.[156,157]

According to the literature and kinetic measurements the following Scheme 40 can be suggested for rearrangement of **1b** to **2b**. (For structures of particular intermediates see Scheme 41).

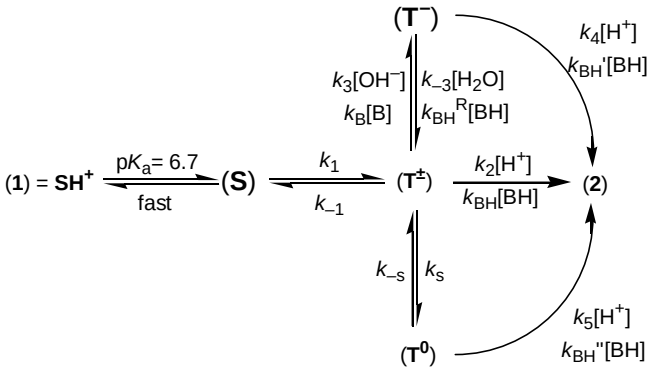

Scheme 40 – Possible reaction paths during the rearrangement.

Applying a steady state approximation to the tetrahedral intermediates $\mathbf{T}^{\pm}$, $\mathbf{T}^{0}$ and $\mathbf{T}^{-}$ we obtained Eq. (14) for the reaction at zero buffer concentration where K_a is the ionization constant of **1a** (= $\mathbf{SH}^+$) and $K_W = 10^{-14}$ (at 25 °C) is the ion product of water.

$$k_{ext} = \frac{k_1 \dfrac{K_a}{K_a + [H^+]}}{k_{-1} + k_2[H^+]} \left(k_2[H^+] + \frac{k_S k_5 [H^+]}{k_{-S} + k_5[H^+]} + \frac{k_3 k_4 K_W}{k_{-3}[H_2O] + k_4[H^+]} \right) \qquad (14)$$

The three terms in parentheses concern the acid-catalyzed breakdown of the intermediates $\mathbf{T}^{\pm}$, $\mathbf{T}^{0}$ and $\mathbf{T}^{-}$. Fitting the pH profile using Eq. (14) is not sufficient to determine all nine rate constants and only products or ratios of particular rate constants are accessible.

Table 4: Comparing of the fitted constants for both salts.

constant	**1a**	**1b**
k_S (s^{-1})	1260	3600
k_1 (s^{-1})	492	80
k_{-1} (s^{-1})	$1.42 \cdot 10^6$	$1.42 \cdot 10^6$
k_2 ($l \cdot mol^{-1} \cdot s^{-1}$)	$7.100 \cdot 10^6$	$2.698 \cdot 10^7$
k_3 ($l \cdot mol^{-1} \cdot s^{-1}$)	$1.0 \cdot 10^{10}$	$1.0 \cdot 10^{10}$
k_{-3} ($l \cdot mol^{-1} \cdot s^{-1}$)	0.04	0.04
k_4 ($l \cdot mol^{-1} \cdot s^{-1}$)	$1.52 \cdot 10^6$	$9.20 \cdot 10^5$
K_a	$2.0 \cdot 10^7$	$2.0 \cdot 10^7$
pK_a(SH)	6.7	6.7
$k_{(-S)}/k_5$ ($mol \cdot l^{-1}$)	$1.3 \cdot 10^{-5}$	$4.0 \cdot 10^{-5}$

At pH 0 - 3.2 the starting compound is present almost entirely as the protonated species $\mathbf{SH^+}$, since the pK_a is 6.7, and the last two terms in parentheses can be neglected. Simultaneously the ratio $K_a/(K_a + [H^+]) = K_a/[H^+]$, and Eq. (14) can be rewritten to Eq. (15) which is completely consistent with previously reported equation.[12]

$$k_{ext} = \frac{k_1 k_2 K_a}{k_{-1} + k_2[H^+]} \tag{15}$$

The values k_1 = 492 s^{-1} and k_2/k_{-1} = 5 $l \cdot mol^{-1}$ were obtained from the data (pH 0.5-3.2) using non-linear regression. The optimized k_1 value which is the rate constant for cyclization of **S** to $\mathbf{T^{\pm}}$ for **1b** is 40-fold less than the value found for cyclization of *S*-(ethoxycarbonylmethyl)isothiouronium chloride ($k_c = 2 \cdot 10^4$ s^{-1}).[139] The reason lies in the presence of 4-methoxyphenyl group which lowers the nucleophilicity of the distant nitrogen (polar as well as steric effects). The break at pH 1.5 indicates a change in the rate-limiting step. At pH < 1.5 the term $k_2[H^+] >> k_{-1}$ and Eq. (15) can be simplified as follows: $k_{ext} = k_1 K_a/[H^+]$ and the formation of $\mathbf{T^{\pm}}$ is rate-limiting. At pH > 1.5, $k_2[H^+] << k_{-1}$ and $k_{ext} = k_1 k_2 K_a/k_{-1}$ is pH independent. The acid-catalyzed breakdown of $\mathbf{T^{\pm}}$ is now the rate-limiting step of the rearrangement. The value of the solvent kinetic isotope effect k_{ext}^{H}/k_{ext}^{D} = 3.55 measured in chloroacetate buffer (c_B/c_{BH} = 1, pH 2.67) must be consistent with the simplified form of Eq. (15) at pH > 1.5 (plateau). It can be presumed that the solvent kinetic isotope effect for the formation and reverse breakdown of $\mathbf{T^{\pm}}$ will be negligible ($K_1^{H}/K_1^{D} \approx 1$). Solvent kinetic isotope effect for the ionization constant $K_a^{H}/K_a^{D} \approx 3$ can be estimated from fractionation factors. The value of k_2^{H}/k_2^{D} which corresponds to the H_3O^+-catalyzed breakdown of $\mathbf{T^{\pm}}$ is then 1.18. This value is substantially lesser than the value found for chloroacetic acid $k_{Buff}^{H}/k_{Buff}^{D}$ = 2.14 like in Ref.[**Chyba! Záložka není definována.**] This result can be explained by different transition-state geometry. In the case of weak acids (BH) the proton has almost a central position between $\mathbf{T^{\pm}}$ and acid in the transition state (as seen from α = – 0.47; *i.e.* $\mathbf{T^{\pm}}\cdots H\cdots B$) whereas in the case of much stronger H_3O^+ the transition state closely resembles reactants (early transition state $\mathbf{T^{\pm}}\cdots\cdots H\text{--}OH_2^+$ for which α should approach zero – as can be seen from point fallen below the straight line in Fig. 12).

At pH 3.2 a new reaction pathway through $\mathbf{T^0}$ gradually opens and the second term in Eq. 14 becomes kinetically significant. k_{ext} is given by Eq. (16).

$$k_{ext} = \frac{k_1 K_a}{k_{-1}} \left(k_2 + \frac{k_S k_5}{k_{-S} + k_5[H^+]} \right) \quad (16)$$

Using the parameters mentioned above the ratios $k_{-S}/k_5 = 1.3 \cdot 10^{-5}$ mol·l^{-1} and $k_S/k_{-1} = 8.8 \cdot 10^{-4}$ were obtained by optimization of the data for **1a** in pH profile. From the break at pH 4.9 it can be concluded that a change in the rate-limiting step occurs again. At pH < 4.9 the formation of $\mathbf{T^0}$ is rate-limiting whereas at pH > 4.9 its acid-catalyzed breakdown is involved. The value of solvent kinetic isotope effect $k_{ext}{}^H/k_{ext}{}^D = 1.83$ measured in acetate buffer ($c_B/c_{BH} = 1$, pH 4.61) is much less than observed in chloroacetate buffer. This observation is consistent with Eq. (16) under the following presumptions. Solvent kinetic isotope effect is still $K_a{}^H/K_a{}^D \approx 3$ but the ratio of fractions $(k_S{}^H k_5{}^H/(k_{-S}{}^H + k_5{}^H[H^+]))/(k_S{}^D k_5{}^D/(k_{-S}{}^D + k_5{}^D[D^+]))$ must be less than 1 because the concentration of D^+ is 3 times less than $[H^+]$ in buffer with the same c_B/c_{BH}. The value 1.83 refers to the rearrangement of $\mathbf{T^\pm}$ to $\mathbf{T^0}$ ($K_S{}^H/K_S{}^D$) as well as to acid-catalyzed decomposition of $\mathbf{T^0}$ ($k_5{}^H/k_5{}^D$).

The last reaction pathway (at pH > 5) involves the trapping of $\mathbf{T^\pm}$ by proton removal with a base giving $\mathbf{T^-}$. The non-linear regression of all experimental data points using previously optimized parameters with Eq. (14) gave the values of $k_{-3}/k_4 = 2.6 \cdot 10^{-8}$ s^{-1} and $k_3/k_{-1} = 7 \cdot 10^3$ l·mol^{-1}.

Although the values of individual rate constants are not directly accessible from optimization of the measured data they can be estimated as follows. Proton transfer from $\mathbf{T^\pm}$ to the strong base hydroxide ion will be thermodynamically favourable, so that the value of k_3 is taken as 10^{10} l·mol^{-1}·s^{-1} for hydroxide ion.[158] The rate constant for the reverse breakdown of $\mathbf{T^\pm}$ to **S** is then $k_{-1} = 1.4 \cdot 10^6$ s^{-1}. This value is approximately two orders of magnitude lesser than the estimated rate constant $k_{-1} = 6.6 \cdot 10^8$ s^{-1} for expulsion of amine from the related cyclic zwitterionic intermediate.[159] The value estimated by us is not totally unreasonable because our $\mathbf{T^\pm}$ is resonance-stabilized (Scheme 42) and, therefore, its reverse breakdown would be slower. If the value of k_{-1} is $1.4 \cdot 10^6$ s^{-1} then $k_2 = 7.0 \cdot 10^6$ l·mol^{-1}·s^{-1} and $k_S = 1260$ s^{-1}.

The two proton transfers that convert $\mathbf{T^\pm}$ to $\mathbf{T^0}$ could occur either in a stepwise mechanism through $\mathbf{T^+}$, with the rate constants k_{OH} and k_H (not shown in Schemes 40 and 41) or in a single concerted step, with the rate constant k_S which may include one to two water molecules. Water acts as a bifunctional catalyst for proton transfer through a five- or eight-membered ring. Experimental distinction between the two mechanisms can be done by

measuring a solvent isotope effect. Bifunctional concerted catalysis is in accord with a solvent isotope effect less than 2.[160] In our case the k_{ext}^{H}/k_{ext}^{D} obtained from linear dependences of k_{obs} *vs.* c_{Buff} measured in acetate buffer (1:1) in H_2O and D_2O is only 1.83 which supports the idea of water-mediated proton switch. The values of k_S are generally in the range[18,148,161-163] 10^5-10^8 s^{-1}. Our value k_S = 1260 s^{-1} is quite small (perhaps due to mentioned resonance stabilization of $\mathbf{T}^{\pm}$).

An alternative mechanism is proposed in Scheme 41 together with corresponding Eq. 17. The only difference between mechanisms in Scheme 40 and 41 is that the cleavage of a proton proceeds from $\mathbf{T}^{0}$ instead of $\mathbf{T}^{\pm}$ like in ref.[17]

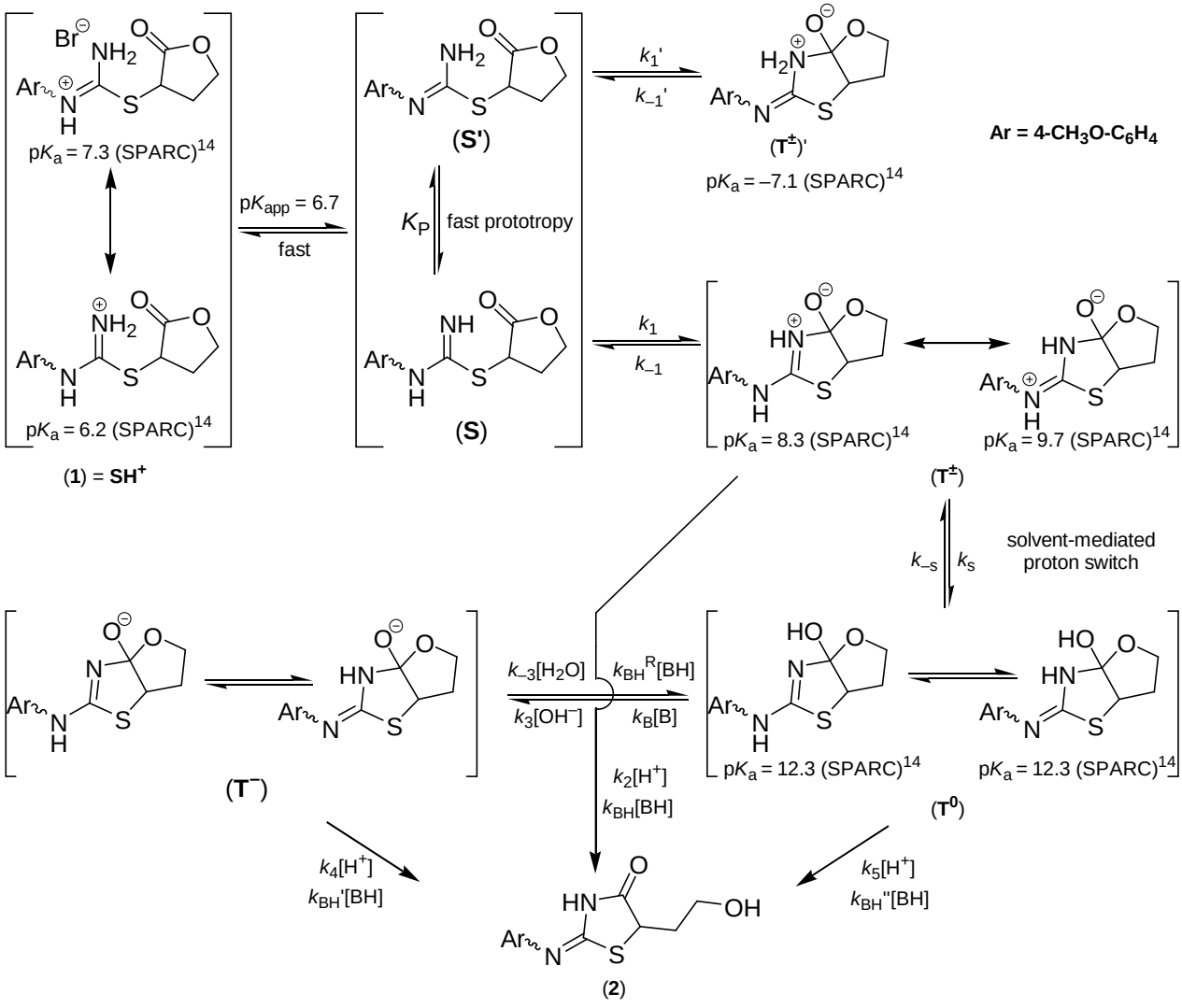

Scheme 41 – Possible reaction pathways and intermediates.

$$k_{ext} = \frac{k_1 \dfrac{K_a}{K_a + [H^+]}}{k_{-1} + k_2[H^+]} \left(k_2[H^+] + \frac{k_S k_5 [H^+]}{k_{-S} + k_5[H^+]} + \frac{k_S k_3 k_4 K_W}{(k_{-S} + k_5[H^+])(k_{-3}[H_2O] + k_4[H^+])} \right) \quad (17)$$

Optimized values of k_1, k_2/k_{-1} and k_{-S}/k_5 are the same as those obtained from Eq. (14). From the last two terms of Eq. (17) the ratios $k_S/k_{-1} = 8.0 \cdot 10^{-4}$, $k_{-3}/k_4 = 3.0 \cdot 10^{-7}$ s^{-1} and $k_3K_S/k_{-1} = 6 \cdot 10^4$ $l \cdot mol^{-1}$ were optimized. In order to calculate the rate constants k_{-1} and k_S the value of K_S is needed. K_S can be estimated from the values of pK_a(**T**$^{\pm}$) = 8.3 – 9.7 (*cf.* pK_a(**T**$^{\pm}$) = 9.8 determined for a similar intermediate[41]) and pK_a(**T**^{0}) = 12.3 which were calculated using SPARC.[14] From them, $K_S = k_S/k_{-S} = 4 \cdot 10^2 – 1 \cdot 10^4$.

If the value of k_3 is taken as 10^{10} $l \cdot mol^{-1} \cdot s^{-1}$ and K_S is in the range $4 \cdot 10^2 – 1 \cdot 10^4$ then $k_{-1} = 6.7 \cdot 10^7 – 1.7 \cdot 10^9$ s^{-1}, $k_2 = 3.4 \cdot 10^8 – 8.3 \cdot 10^9$ $l \cdot mol^{-1} \cdot s^{-1}$ and $k_S = 5.4 \cdot 10^5$ - $1.3 \cdot 10^6$ s^{-1} which conforms well to the literature mentioned above. The decision which mechanism is correct can be made from measurements in buffers.

In all buffer solutions the reaction involves general acid-base catalysis, therefore, at least one buffer component must also catalyze the rearrangement of **1** to **2** and extended kinetic Equations (18) and (19) derived from Schemes 2 and 3 can be written:

$$k_{obs} = k_{ext} + \frac{k_1 \dfrac{K_a}{K_a + [H^+]}}{k_{-1} + k_{BH}[BH]} \left(k_{BH}[BH] + \frac{k_S k_{BH}'[BH]}{k_{-S} + k_{BH}'[BH]} + \frac{k_B k_{BH}''[B]}{k_{BH}^{R} + k_{BH}''} \right) \quad (18)$$

$$k_{obs} = k_{ext} + \frac{k_1 \dfrac{K_a}{K_a + [H^+]}}{k_{-1} + k_{BH}[BH]} \left(k_{BH}[BH] + \frac{k_S k_{BH}'[BH]}{k_{-S} + k_{BH}'[BH]} + \frac{k_S k_B k_{BH}''[B]}{(k_{-S} + k_{BH}'[BH])(k_{BH}^{R} + k_{BH}'')} \right) \quad (19)$$

No significant general base-catalyzed reaction (k_B) was observed in substituted acetate buffers therefore the last term in parentheses in both Eq. (18) and (19) can be neglected. All dependences of k_{obs} *vs.* c_{Buff} are linear which means that $k_{BH}[BH] << k_{-1}$ (general acid BH is much weaker than H_3O^+) and $k_{BH}'[BH] >> k_{-S}$. Eq. (13) and (18) or (19) can be combined to Eq. (20) where $k_{BH}^{cor} = K_1k_{BH}$, $K_1 = k_1/k_{-1}$ and $k_0^{cor} = k_{ext}(K_a+[H^+])/K_a + K_1k_S$.

$$k_{cor} = k_0^{cor} + k_{BH}^{cor}[BH] \quad (20)$$

A Brønsted plot of log k_{BH}^{cor} *vs.* pK_a(BH) is linear and the slope α = –0.47 (Fig. 16) must reflect a rate-limiting step involving proton transfer from general acid to $\mathbf{T}^{\pm}$ which is concerted with C–O bond breaking (Scheme 42). The reaction may occur by a "one-encounter" mechanism in which the same molecule of catalyzing acid (BH) donates a proton to the poorly leaving alkoxide and removes it from the nitrogen[147] in order to avoid thermodynamically unfavourable protonated intermediate/product (p$K_a \approx -7$).

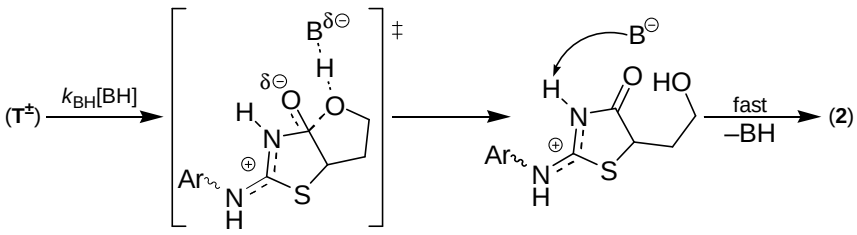

Scheme 42 – Transition state of general base catalyzed reaction.

In basic amine buffers the catalytic power of general acid BH decreases and the dependences of k_{obs} *vs.* c_{Buff} are no longer linear because the term k_{BH}[BH] is low and the term k_{BH}'[BH] becomes comparable with k_{-S}. Furthermore general-base catalyzed pathway gradually opens in those buffers (Eqs. (21) and (22)). Only Eq. (21) is consistent with the observation of linear increase of k_{cor} with c_B in concentrated buffers (Fig. 17) because the Eq. (22) predicts saturation kinetics. The mechanism in Scheme 40 is therefore more plausible.

$$k_{cor} = k_{ext}^{cor} + K_1\left(\frac{k_S k_{BH}'[BH]}{k_{-S} + k_{BH}'[BH]} + \frac{k_B k_{BH}''[B]}{k_{BH}^{R} + k_{BH}''}\right) \tag{21}$$

$$k_{cor} = k_{ext}^{cor} + K_1\left(\frac{k_S k_{BH}'[BH]}{k_{-S} + k_{BH}'[BH]} + \frac{k_S k_B k_{BH}''[B]}{(k_{-S} + k_{BH}'[BH])(k_{BH}^{R} + k_{BH}'')}\right) \tag{22}$$

From the linear portions of non-linear dependences (at high c_B) the slopes give $k_B' = K_1 k_{BH}'' k_B/(k_{BH}^{R} + k_{BH}'')$ for particular base-buffer components (Table 3). Brønsted plot of log k_B' *vs.* pK_a(BH) is linear and the slope β_{obs} = 0.6 (Fig. 16). This value cannot be interpreted in terms of simple proton transfer from $\mathbf{T}^{\pm}$ to the base (B) because k_B' is the composite constant. It can be presumed that the dependence of log k_B *vs.* pK_a(BH) should have a slope approaching unity[17,147] (Eigen-type Brønsted correlation) therefore the

difference between the predicted and observed slope $\Delta\beta = 0.4$ corresponds to two proton transfers (k_{BH}^{R} and k_{BH}") from general acid to $\mathbf{T}^{\pm}$.

3.1.5 Reaction in sodium hydroxide solution

The breaks upward at pH ≈ 11 are observed in the pH profiles (Fig. 15) for both of the salts **1b**,**p** and the slopes have almost unit value. This indicates opening of the new reaction pathway. The analysis of the reaction mixtures shows many different products. With the increasing hydroxide concentration the amount of the transformation product decreases and products of the decomposition appears. The formation of corresponding anilines, starting thioureas and thioles was observed. The strongly nucleophilic hydroxide anion attacks the ester group, the isothiourea carbon atom and the α-carbon atom of the lactone ring. In the last case, a nucleophilic substitution at aliphatic carbon atom occurs and starting thiourea is formed. The NMR spectra show all kinds of products present in the reaction mixture after evaporation of the solvent.

3.1.6 Influence of additional copper ions on the transformation rate

The influence of additional copper ions on the reaction rate of transformation **1b** to **2b** was followed spectrofotometrically in solutions of mineral acids at pH 2 without ionic strength correction ($CuCl_2$/HCl, $CuSO_4$/H_2SO_4, $Cu(ClO_4)_2$/$HClO_4$), but only a very negligible influence was observed.

Table 5: Table of observed rate constants measured in solutions of sulphuric, perchloric, hydrochloric and trichloroacetic acids with various concentrations of additional Cu(II) ions.

	$k_{obs} \cdot 10^4$ s^{-1}			
$c_{Cu(II)}$ mol·l^{-1}	H_2SO_4	$HClO_4$	HCl	Cl_3COOH
0	6.56	6.46	6.52	6.53
0.00025			6.52	6.40
0.001	6.71	6.25	6.61	6.44
0.002			6.66	6.45
0.005	6.63	6.28		
0.011	6.97	6.42		
0.02	7.16	6.41		
0.04	7.61	6.17		

Only in sulphuric acid, a small increase of the rate constant was observed. Similar behaviour was observed in the solution of Cu(II) ions in 0.01 mol·l^{-1} trichloroacetate buffers (Table 5).

The small acceleration in sulphuric acid solutions could be explained by the different ionic strength of the solutions which changes significantly in the uni-bivalent sulphuric acid system.

The different behaviour was observed in acetate, methoxyacetate, chloroacetate and dichloroacetate buffers with a constant buffer concentration of 0.1 mol·l^{-1} and with an increasing concentration of Cu(II) ions. The dependence of the observed rate constant plotted against Cu(II) concentration grows linearly at low Cu(II) concentration. With increasing Cu(II) concentration, the influence gradually diminishes and the slope of the dependence approaches zero (Fig. 18).

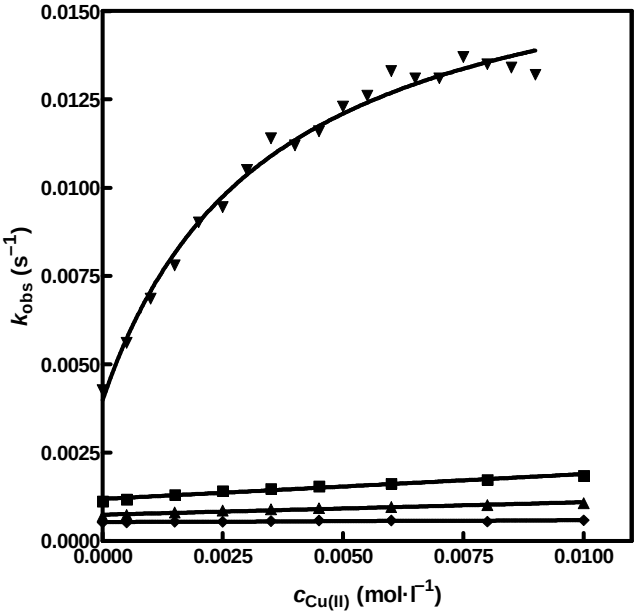

Figure 18 – Dependence of the observed rate constants (k_{obs}; s^{-1}) against copper(II) ions concentration. ($c_{Cu(II)}$; mol·l^{-1}) for **1b** measured at 25 °C in 0.1 mol·l^{-1} acetate, pH 4.53 (▼); 0.1 mol·l^{-1} chloroacetate, pH 2.65 (▲); 0.1 mol·l^{-1} methoxyacetate, pH 3.40 (■) and 0.1 mol·l^{-1} dichloroacetate, pH 1.50 (♦) buffer solutions. The fitted lines were calculated using Eq. (24).

The reaction was also studied in acetate buffers with changing the buffer concentration at a constant concentration of the Cu(II) ions (Fig. 19). In this case the ionic strength was adjusted to 1 mol·l^{-1} and the pH of the solutions was held constant.

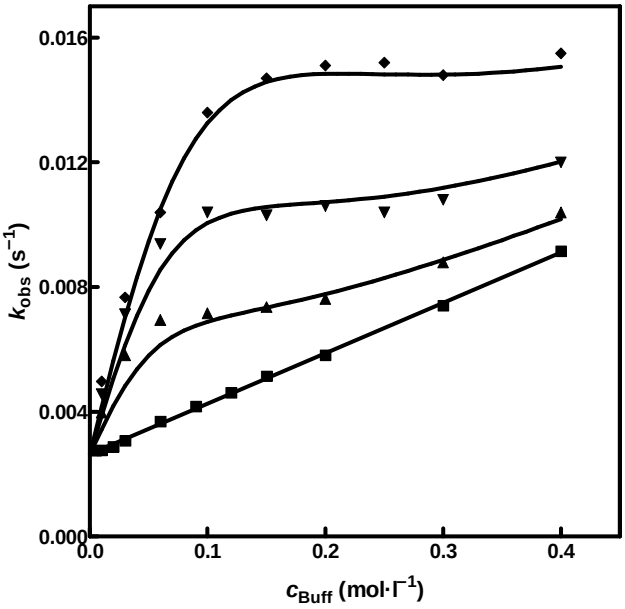

Figure 19 – Dependence of the observed rate constants (k_{obs}; s^{-1}) against buffer concentration (c_{Buff}; mol·l^{-1}) for **1b** measured at 25 °C in acetate buffer solutions with constant Cu(II) concentration: 0.001 mol·l^{-1} (▲); 0.003 mol·l^{-1} (▼); 0.006 mol·l^{-1} (♦) and without Cu(II) ions (■). The fitted lines were calculated using Eq. (23).

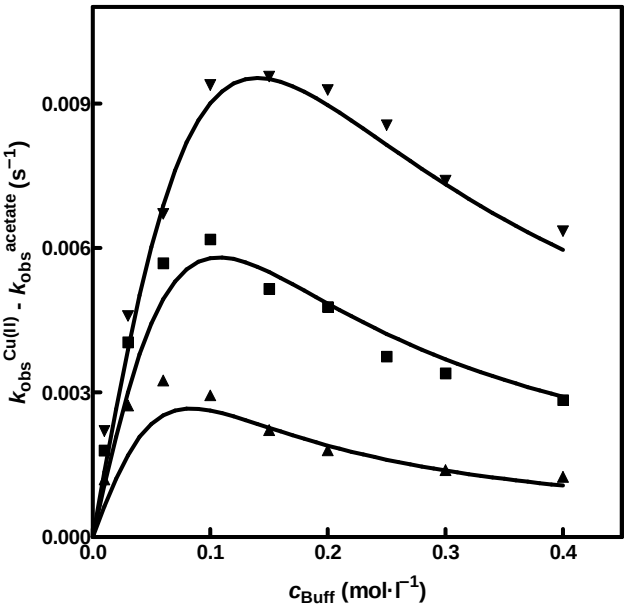

Figure 20 – Dependence of the difference between observed rate constants and observed rate constant measured without additional Cu(II) ions ($k_{obs}^{Cu(II)} - k_{obs}^{acetate}$; s^{-1}) on buffer concentration. (c_{Buff}; mol·l^{-1}) for **1a** measured at 25 °C in the constant concentration of Cu(II): 0.001 mol·l^{-1} (▲); 0.003 mol·l^{-1} (■); 0.006 mol·l^{-1} (▼). The fitted lines were calculated using Eq. (23) without the last term.

The steric demands of the catalyzing acid containing various aliphatic chains on the reaction course were studied in acetate, propionate and pivaloate buffers (Fig. 21). The concentration of 0.03 mol·l^{-1} was chosen because of the low solubility of pivalic acid in water and the ionic strength was adjusted to 1 mol·l^{-1} by the addition of KCl. All the dependences have the same character (Fig. 22) resembling saturation kinetics again. Correction of k_{obs} (Eq. 13) is necessary because of the differences in the pH of the buffers.

$$k_{cor} = k_{obs}\frac{K_a}{K_a + [H^+]} = k_{obs}(1 + 10^{(pK_a - pH)}) \tag{13}$$

This correction makes all dependences almost identical which indicates no influence of stericity demands of the catalyzing acid.

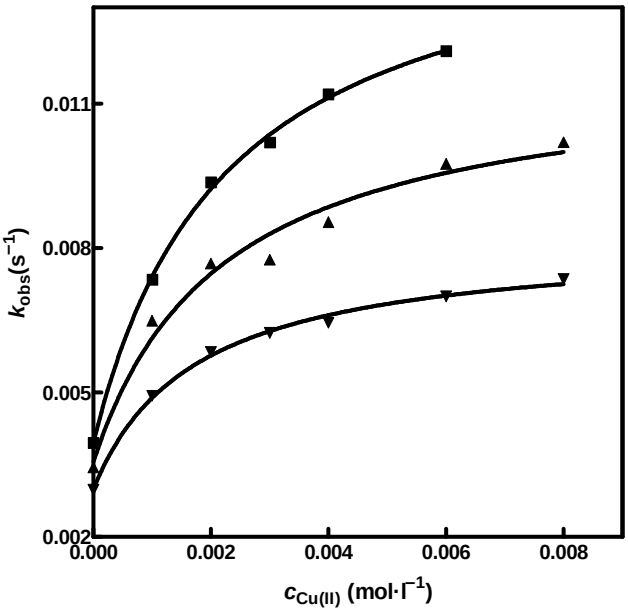

Figure 21 – Dependence of the observed rate constants (k_{obs}; s^{-1}) against copper(II) ions concentration. ($c_{Cu(II)}$; mol·l^{-1}) for **1b** measured at 25 °C in 0.03 mol·l^{-1} propionate, pH 4.80 (▲); 0.03 mol·l^{-1} pivaloate, pH 4.65 (■) and 0.03 mol·l^{-1} acetate, pH 4.53 (▼) buffer solutions. The fitted lines were calculated using Eq. (24).

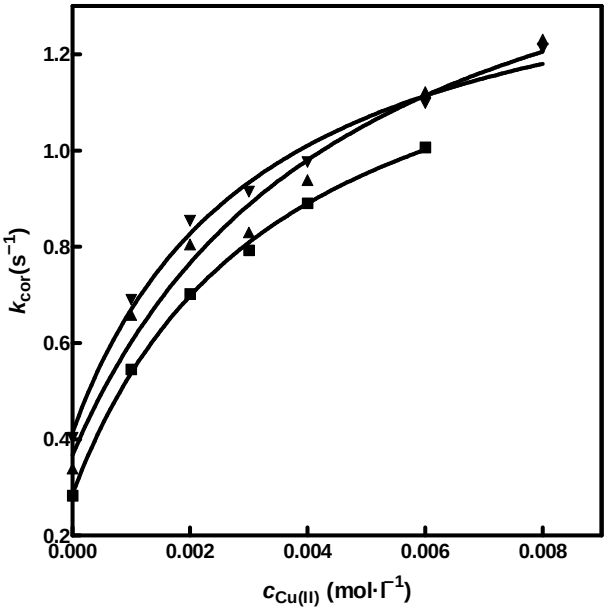

Figure 22 – Dependence of the corrected rate constants (k_{cor}; s^{-1}) against copper(II) ions concentration. ($c_{Cu(II)}$;mol·l^{-1}) for **1b** measured at 25 °C in 0.03 mol·l^{-1} propionate, pH 4.80 (▲); 0.03 mol·l^{-1} pivaloate, pH 4.65 (■) and 0.03 mol·l^{-1} acetate, pH 4.73 (▼) buffer solutions. The fitted lines were calculated using Eq. (24).

In accordance with the literature[44] a formation of a complex of the copper(II) acetate with the substrate was proposed in the first reaction step. It is obvious that only free base of the substrate **1b** is able to form such a complex.

The formation of the complex is rate limiting at low Cu(II) concentrations. From the dependence (Fig. 18) it is obvious that with increasing copper concentration the rate limiting step changes and the reaction starts to be independent of Cu(II) concentration. This is illustrated in Scheme 43. Taking measurements using buffers with a constant Cu(II) ions concentration and increasing buffer concentration shows unexpected dependences (Fig. 19). While the dependence of k_{obs} *vs.* c_{Buff} at $_{c}Cu(II)$ = 0 is linear the presence of Cu(II) ions causes nonlinearity in the buffer concentration range from 0.01 to 0.2 mol·l^{-1} (Fig. 20). Above this buffer concentration, the dependence linearly increases and its slope approaches to those obtained in acetate buffer in absence of Cu(II) ions. This behaviour can be explained as follows. The transformation of the substrate to the product takes place through two distinct parallel pathways. The first of them involves simple-general-acid catalysis (see chapter 3.1.4) and the second one involves the formation of relatively weak but a more reactive complex of the substrate with copper(II) acetate ([S-Cu$(OAc)_2$]). At

low buffer concentrations the general-acid-catalyzed transformation is much slower than the analogous transformation of the [S-Cu(OAc)$_2$] complex. As the concentration of the acid buffer component (*i.e.* AcOH as well) increases the rate of transformation increases too. However, when increasing buffer concentration, the concentration of the basic buffer component (acetate) increases too which causes rate retardation due to the formation of the more stable but unreactive $[Cu(OAc)_4]^{2-}$ complex.[164,168] In other words – there is competition between the acetate anion from the buffer and the substrate for complexation with the copper(II) acetate. Therefore, at high buffer concentrations where almost all the copper(II) acetate would be complexed to form unreactive $[Cu(OAc)_4]^{2-}$, simple general-acid-catalyzed transformation of the substrate becomes favourable again and the dependence k_{obs} *vs.* c_{Buff} linearly increases. Both of those observations are illustrated in Scheme 43 and the general equation (23) could be derived.

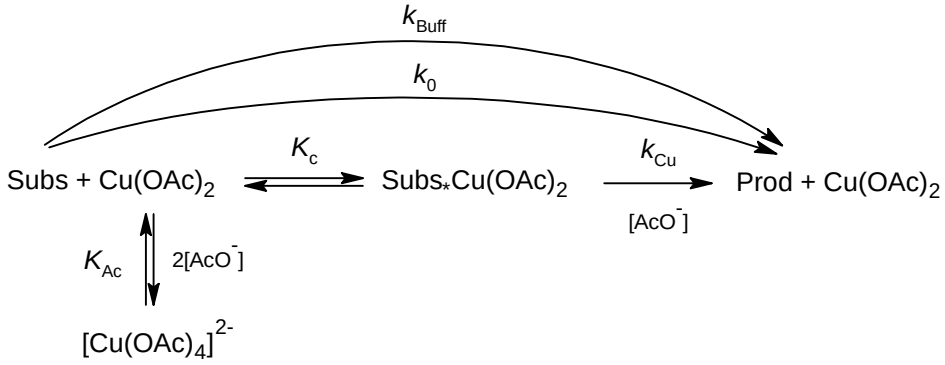

Scheme 43 - Reaction scheme of complex formation and its decomposition to product.

.

$$k_{obs} = k_0 + \frac{k_{Cu} \cdot \dfrac{K_c \cdot [Cu(II)]}{K_{Ac} \cdot [AcO^-]^2 + 1} \cdot [AcO^-]}{1 + \dfrac{K_c [Cu(II)]}{K_{Ac} \cdot [AcO^-]^2 + 1}} + k_{Buff} \cdot [AcOH] \qquad (23)$$

- k_0 is a rate constant for the buffer-catalyzed reaction, k_{Cu} is a rate constant for the copper(II) catalyzed reaction, K_c is a stability constant of the complex of copper(II)acetate with the substrate and K_{Ac} is the equilibrium constant for the formation of $[Cu(OAc)_4]^{2-}$.

The multiple regression of all the dependences measured in acetate buffers (Figs. 19 and 21) provides the values of all the parameters to be obtained, as follows: k_0 = 0.002644 s^{-1}; k_{Cu} = 0.345 s^{-1}; K_c = 600; K_{Ac} = 900 and k_{Buff} = 0.03232 $l \cdot mol^{-1} \cdot s^{-1}$.

In buffer solutions with an increasing Cu(II) ion concentration and constant buffer concentration some terms in eq. (23) become constant and therefore it can be simplified to form eq. (24). This enables for the corresponding constants for buffers other than acetate to be obtained. These are quoted in the Table 6 and are in good agreement with constants obtained from the multiple regression.

$$k_{obs} = k_0' + \frac{K'_c \cdot k'_{Cu}[Cu(II)]}{1 + K'_c[Cu(II)]} \qquad (24)$$

Table 6 – Calculated constants using equation (24).

buffer	pH	K'_c	$k'_0 \cdot 10^3$ (s^{-1})	$k'_{Cu} \cdot 10^2$ ($l \cdot mol^{-1} \cdot s^{-1}$)
Dichloroacetate	1.50	0.05305	0.5363[a]	9.59[a]
Chloroacetate	2.65	0.09285	0.7439[a]	38.32[a]
Methoxyacetate	3.40	0.1327	1.1910[a]	53.12[a]
Acetate	4.53	574 ± 68	0.300 ± 0.13	0.583 ± 0.037
Propanoate	4.65	455 ± 144	0.36 ± 0.40	0.821 ± 0.081
Pivaloate	4.80	444 ± 41	0.40 ± 0.11	1.121 ± 0.019

[a]Standard deviation for constants is higher than constants itself. It is caused by only small influence of additional copper(II) ions and insignificant curvature of the dependences.

The question is however: what is the structure of the catalyzing complex, and hence which atom(s) coordinate(s) to the copper(II)acetate. According to the HSAB theory[166] a Cu(II) ion as a soft acid prefers coordination to the sulphur or carbonyl oxygen instead of the nitrogen.[167] Moreover if the coordination on a nitrogen atom takes place, then decrease of electron density at this atom would cause the reaction retardation. From the comparison of moderate acceleration caused by Cu(II) ions during transformation from **1b** to **2b** with e.g. Cu(II) catalyzed hydrolysis of amino acid glycine esters[46] or other similar reactions[47] it can be concluded that the complex formed has only poor stability.[168] This conclusion is supported by the absence of any new absorbance band in the UV-VIS spectra during the reaction and the value of the previously mentioned complex stability constant K_c = 600. Coordination to a sulphur atom[49] could also create a more stable complex but its formation could not accelerate the reaction because of its unsuitable geometry. Therefore, the most probable is the coordination of the Cu(II) ion to the carbonyl oxygen[169] because of this

argument. In this case the Cu(II) ion acts as a Lewis acid catalyst and facilitates the attack of the imino group on the carbonyl by withdrawing electrons from the system.[170]

The complex stability constant calculated using equation (23) increases with increasing basicity of the coordinating substituted acids. For the dichloro, chloro and methoxyacetic acid, their values are less than 1; thus explaining the reason for only negligible rate acceleration in such buffers.

Coordination of the copper(II) to the carbonyl oxygen opens a new reaction pathway and there are several possibilities of its action (Scheme 44). The first one involves the participation of the coordinated acetate anion facilitating the hydrogen transfer from the zwitterionic intermediate through the six-membered ring (**$T^{\pm}$ - comp**)[43] and this shifts the equilibrium towards the anionic intermediate **T^{-}** in Scheme 41 resulting in Cu(II) stabilized **T^{-} - comp** being formed and readily decomposing to the product. This mechanism of action could be understood as a shift to the more basic area in the general scheme for transformation of **1b** to **2b** (Scheme 41). The second possibility, which is an alternative to the first one, proceeds in one reaction step. The formation of (**T^{-} - comp**) the intermediate can proceed by a concerted mechanism where acetate anion cleaves the proton at the same time when the imino group attacks the carbonyl group (**$T^{\pm}$ - conc**). The third possibility involves bond reorganization in the complex and coordination of the copper(II) to the oxygen of the leaving group (**$T^{\pm}$ - coord**). The leaving group ability of the oxygen atom is improved after this coordination and formation of the product is facilitated.[171] Combination of the first and the third mechanism of action of Cu(II) is possible and even the most probable.

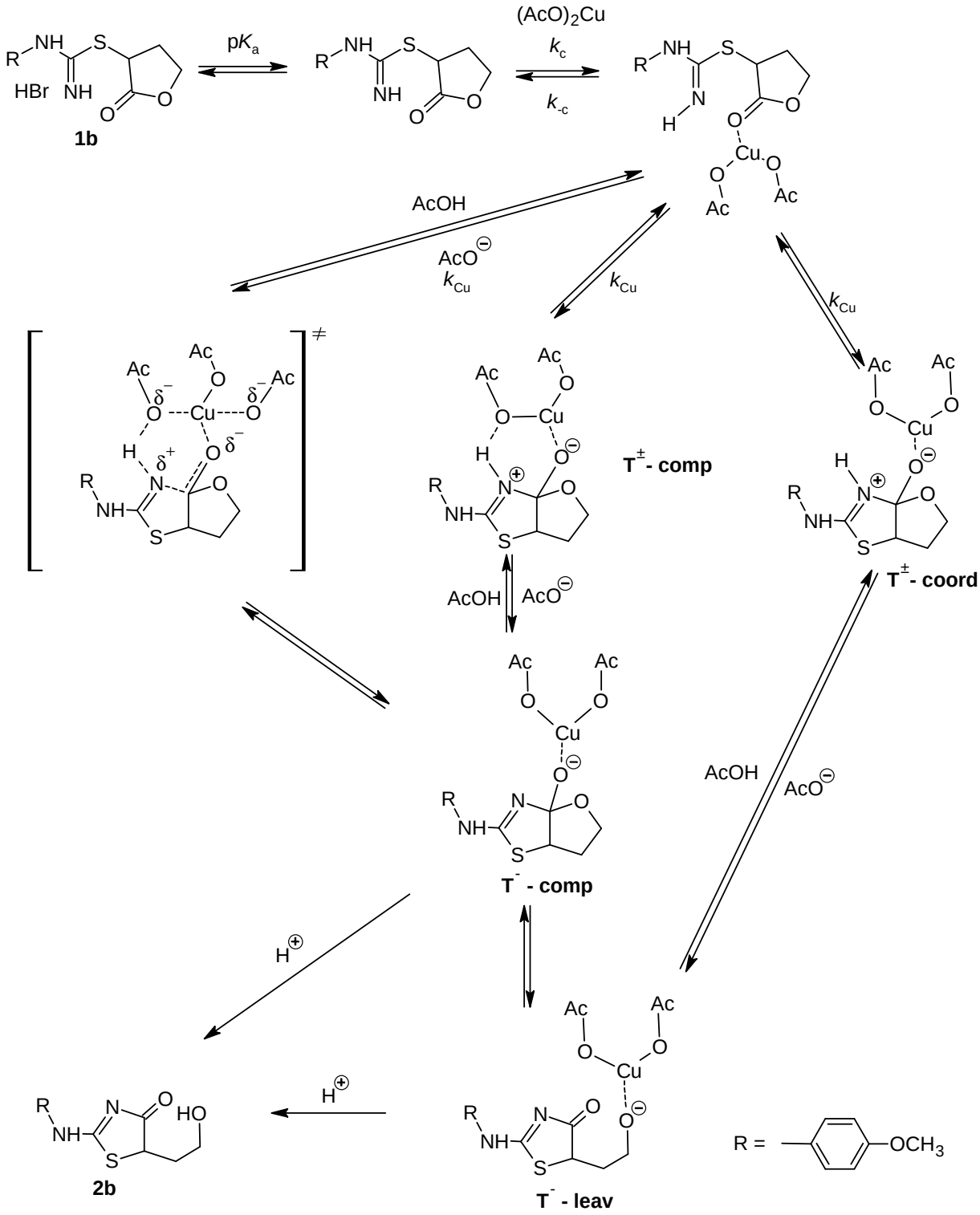

Scheme 44 – Possible reaction paths for the Cu(II) catalyzed rearrangement of **1b** to **2b**.

3.2 Transformations of isothiouronium salts derived from substituted 3-bromophthalides

3.2.1 Preparation and properties of the isothiouronium salts

6-Substituted-3-bromo-2-benzofuran-1-(3*H*)-ones were prepared by the radical bromination of the corresponding phthalides using *N*-bromosuccinimide in tetrachloromethane.[211] The bromination was carried out at the boiling point of the solvent, and azobisisobutyronitrile (AIBN), dibenzoylperoxide, or a 100 watt bulb light (or a combination of them) was used as the initiators. Only monobromination on the benzylic carbon atom was observed under such conditions. Prepared bromides are quite unstable and they decompose in a few days. For this reason, the bromides were used for the reaction with an appropriate thiourea immediately after the separation and recrystalization (Scheme 45).

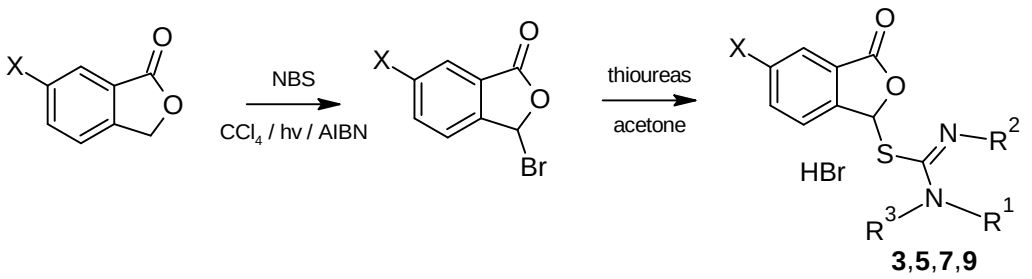

3,**5**,**7**,**9**

3a:R^1=H,R^2=H,R^3=H,X=H
3b:R^1=H,R^2=H,R^3=H,X=OCH_3
3c:R^1=H,R^2=H,R^3=H,X=Cl
3d:R^1=H,R^2=H,R^3=H,X=NO_2
5a:R^1=CH_3,R^2=H,R^3=H,X=H
5b:R^1=*i*-Pr,R^2=H,R^3=H,X=H

7a:R^1=Ph,R^2=H,R^3=H,X=H
7b:R^1=4-CH_3O-Ph,R^2=H,R^3=H,X=H
7c:R^1=2-pyridyl,R^2=H,R^3=H,X=H
7d:R^1=Ph,R^2=H,R^3=CH_3,X=H
7e:R^1=Ph,R^2=H,R^3=C_2H_5,X=H

9a:R^1=CH_3,R^2=CH_3,R^3=H,X=H
9b:R^1=CH_3,R^2=CH_3,R^3=H,X=OCH_3
9c:R^1=CH_3,R^2=CH_3,R^3=H,X=Cl
9d:R^1=CH_3,R^2=CH_3,R^3=H,X=NO_2
9h:R^1=4-Cl-Ph,R^2=CH_3,R^3=H,X=H
9j:R^1=CH_3,R^2=C_2H_5,R^3=H,X=H

Scheme 45 – Reaction scheme for preparation of isothiouronium salts **3**, **5**, **7**, **9**.

Substituted *S*-(3-oxo-1,3-dihydro-2-benzofuran-1-yl)isothiouronium bromides (**3**, **5**, **7**, **9)** were prepared by the mixing of a saturated hot acetone solution of bromides and thioureas. After 5 minutes of reflux and a few hours standing at room temperature, the precipitated crystals of isothiouronium salts were collected by filtration.[42] The yields were of about 80-90 %. The crystals of salts contain a variable amount of acetone, which can not be removed even under vacuum and makes elemental analysis problematic. Recrystalization from the

mixture of water/methanol/acetone can solve this problem in some cases, but it is accompanied by the partial transformation of the salts and lowering of the yields. Therefore, HRMS spectra were used for the characterization.

In the case of *N*-methyl-*N*-phenyl derivative **7d**, the single crystal was prepared and analyzed by X-ray analysis. The ORTEP diagram shows the presence of the acetone molecule in the molecular cell.

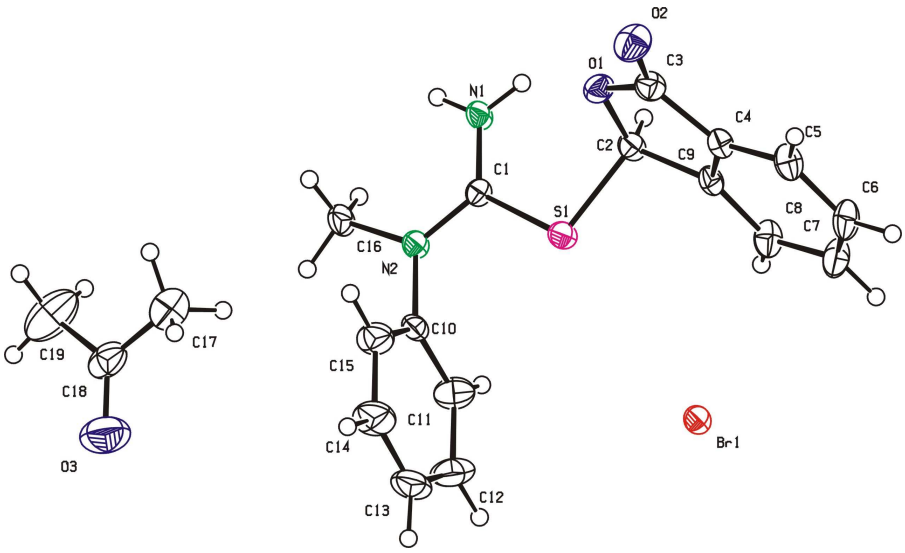

Figure 23 - ORTEP view of compound **7d** (thermal ellipsoids at 40 % probability).

The presence of the free isothiourea is necessary for the rearrangements to the products. Therefore, knowledge of pK_a of the salts is very important. The pK_as of the isothiouronium salts were determined by the rapid potentiometric titration using tetrabutylammonium hydroxide as a base and benzoic acid as a standard (Fig. 24). Each value is an average of at least four independent measurements. The values are shown in Fig. 25 and are consistent with the value of 6.7 which was estimated previously for isothiouronium salts **1b**,**p** (see chapter 3.1.3).

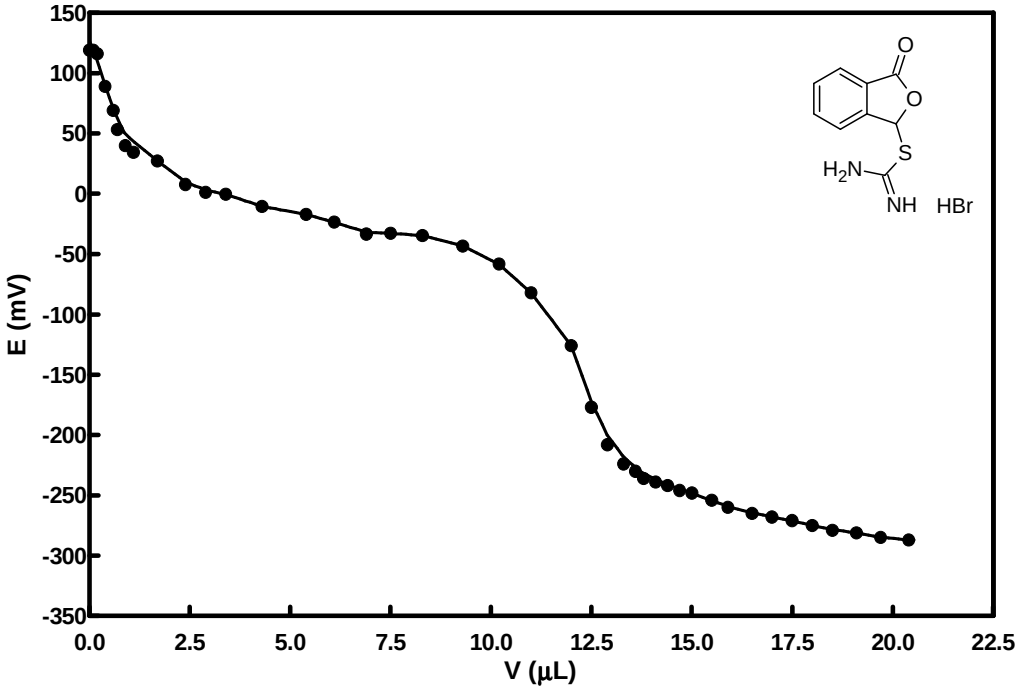

Figure 24 – Titration curve for the salt **3a** measured in water at 25 °C. Tetrabutylammonium hydroxide was used as a base.

The double sigmoidal shape of the titration curve was observed in some cases **5b**, **9b**, **9c** for which there may be two possible explanations. It is well-known that some salts can contain a non-stechiometrical amount of hydrogen bromide. Secondly, partial rearrangement occurs during the titration so the values are obtained with a larger variance than would normally occur with potentiometric titrations.

Usual trends for substitution were observed. Presence of a methyl group on the nitrogen atom of thiourea increases the pK_a value of about one order of magnitude and the second methyl group of next half order of magnitude. On the other hand substitution by phenyl group decreases the pK_a value of about one order of magnitude and the second phenyl group also lowers the pK_a a further order of magnitude. Similar differences were observed between *S*-methylisothiouronium iodide and *S*-methyl-*N*-phenylisothiouronium iodide with pK_a values of 9.83 and 7.14 respectively.[172] The presence of electron withdrawing chloro and nitro groups in position 6 of the phthalide aromatic ring increases the acidity of about 1 or 2 orders of magnitude. The SPARC program, which was successfully used for estimation of pK_as (**1b**,**p**), has been used to calculate pK_a values of selected salts (Fig. 25). In those cases a much smaller influence on all types of substitution has been found; with the best agreement being found for *N*-methyl substituted isothiouronium salt **5a** (Fig. 25).

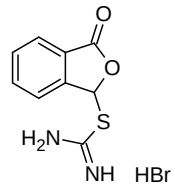

3a 6.5
SPARC 8.5

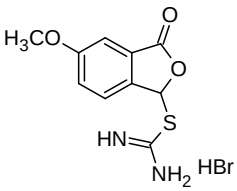

3b 6.4
SPARC 8.23

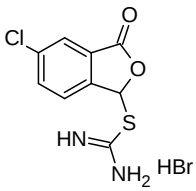

3c 5.6
SPARC 8.02

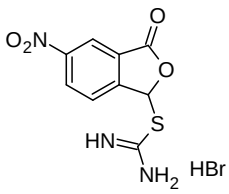

3d 4.4
SPARC 7.81

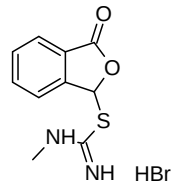

5a 7.6
SPARC 7.78

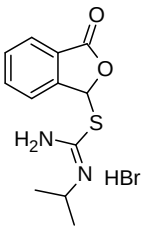

5b 7.5

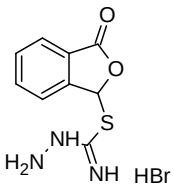

13a 5.8

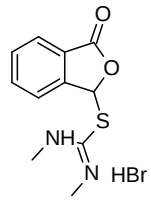

9a 8.1
SPARC 7.35

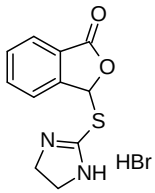

9e 4.6
SPARC 8.40

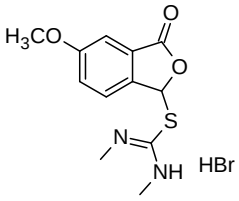

9b 7.9

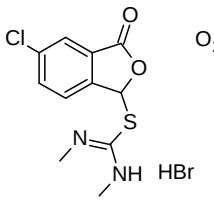

9c 3.4 and 10.7

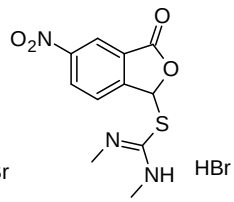

9d 6.0

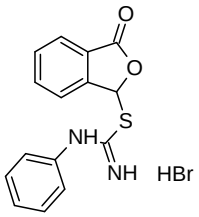

7a 5.4

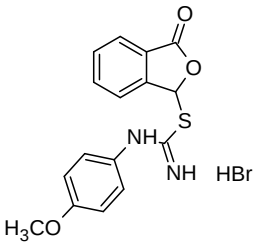

7b 5.3

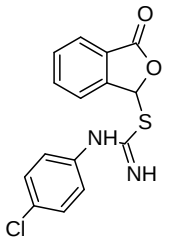

4.2

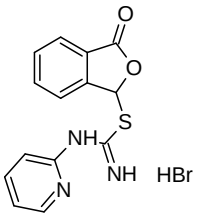

7c 4.7

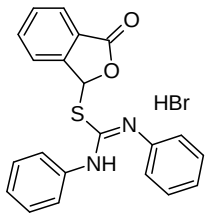

7f 4.0

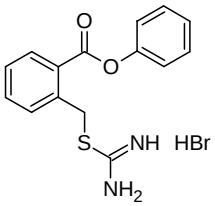

11b 7.9

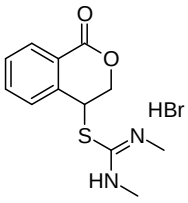

12c 8.6

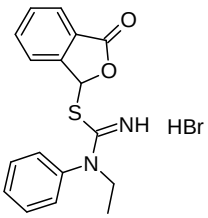

7e 6.0

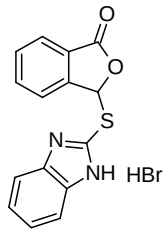

9g 3.1

Figure 25 – Measured and calculated pK_as for selected isothiouronium salts.

The value of the Hammett constant ρ = +2.5 was found for 6-substituted salts derived from un-substituted **3** and for *N*,*N*´-disubstituted thioureas **9** whereas for 4-substituted phenyl salts **7** the ρ value is around +5 (Fig. 26). These values are surprisingly high and the only possible explanation is the sulphur bridge effect.[173,174] There are several examples in the literature where transmission of electronic effect across the sulphur bridge is more effective than in related compounds without such a sulphur bridge. It is believed that *d*-orbitals of sulphur are responsible for this behaviour.

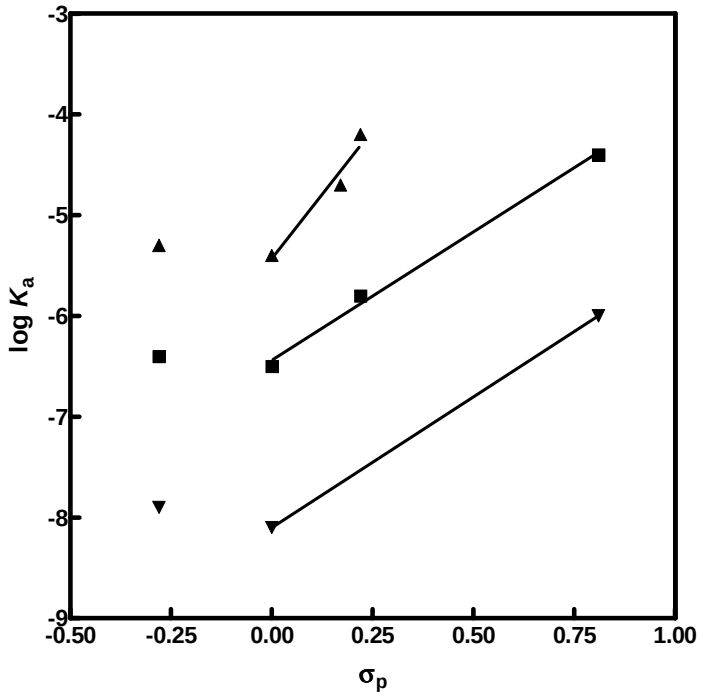

Figure 26 – Dependence of log K_a for non-substituted **3a-d** (■); *N*,*N*´-dimethylsubstituted **9a,b,d** (▼) and 4-substituted phenyl **7a-c** (▲) isothiouronium salts.

6-Methoxy substituted salts **3b**, **9b** deviates from the Hammett correlation. Their acidity is a little bit higher than for unsubstituted salts **3a**, **9a**, (Fig. 26) and the same situation was observed in the case of *N*-(4-methoxyphenyl) substituted salts **7b**.

S-Methyl-*N*-(4-subst. phenyl) isothioureas (Scheme 46) were used as theoretical models for explanation of the non-Hammett behaviour of 4-methoxy substituted isothiouronium salts.

Optimized geometries and proton affinities were calculated for 4-methoxyphenyl, 4-chlorophenyl, 4-nitrophenyl, 4-*N*,*N*-dimethylamino and phenyl isothioureas using B3LYP/6-31+G** level of theory in the gas phase.

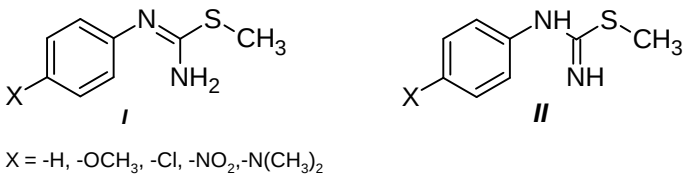

Scheme 46 - *S*-methyl-*N*-(4-substituted)phenyl isothioureas with internal (***I***) and terminal (***II***) double bonds.

The energy comparison of free bases of the salts shows that all compounds prefer configuration ***II*** with the double bond situated between unsubstituted nitrogen and carbon. The structure ***I*** where the conjugation is possible is less favourable and the energy difference between these two isomers is about 6 kJ·mol^{-1}. Geometries for all possible proton attachments for both isomers were also calculated, indicating that all the compounds prefer protonation on the unsubstituted nitrogen atom and it was found that the bond lengths of both carbon-nitrogen bonds after the protonation are almost identical. Plotting of calculated proton affinities against Hammett *σ*-constants shows a perfect linear trend for H, Cl and NO_2 substituents. The methoxy substituted compound is slightly deviated and the biggest difference was predicted for the *N*,*N*-dimethylamino substituent whose affinity is similar to the nitro derivative (Fig. 27).

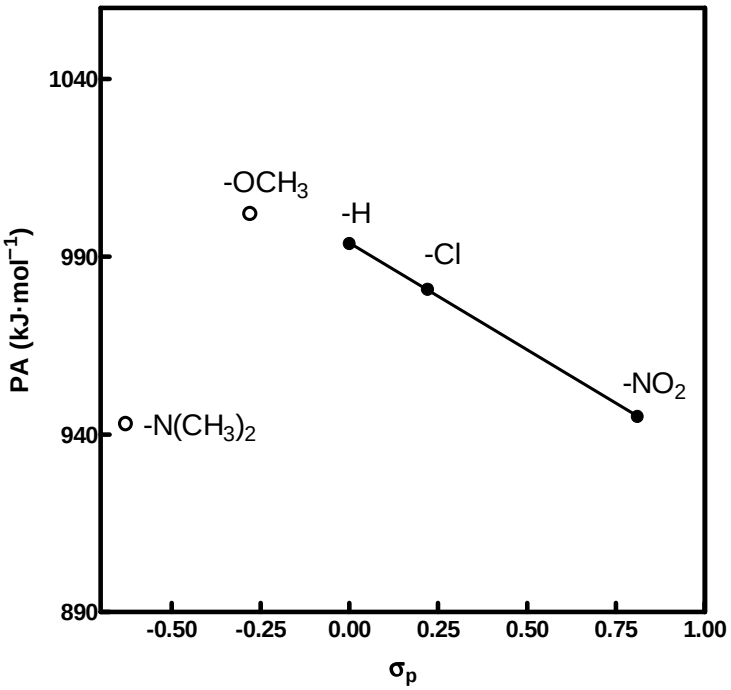

Figure 27 – Hammett plot of the calculated proton affinities (PA; kJ·mol^{-1}) plotted against Hammett σ_p constants.

The influence of solvent could be very important. Therefore, the calculation has been repeated using the COSMO solvation model with water as a solvent. Due to the solvent stabilization, the predicted proton affinities are approximately 100 $kJ \cdot mol^{-1}$ higher than in the gas phase. The trend in values and Hammett correlation remains the same with only a change in the value of the slope from –60 to –30. The decrease of the slope is in accordance with the well-known fact of decreasing the influence of substituents and the structure of compounds on acid-base properties when changing the medium to a more polar one. Results of these calculations unfortunately do not offer any reasonable explanation of deviations of the Hammett plots.

3.2.2 Transformation of unsubstituted and alkyl monosubstituted salts (3, 5)

The formation of various types of products comes into consideration during the transformation of unsubstituted salts (**3**) or monoalkylsubstituted isothiouronium salts (**5**) (Scheme 47). The seven membered benzothiazepine ring, isoindolone ring, phthalidyl thiourea, sulphanylphthalide or stable free base could be formed.

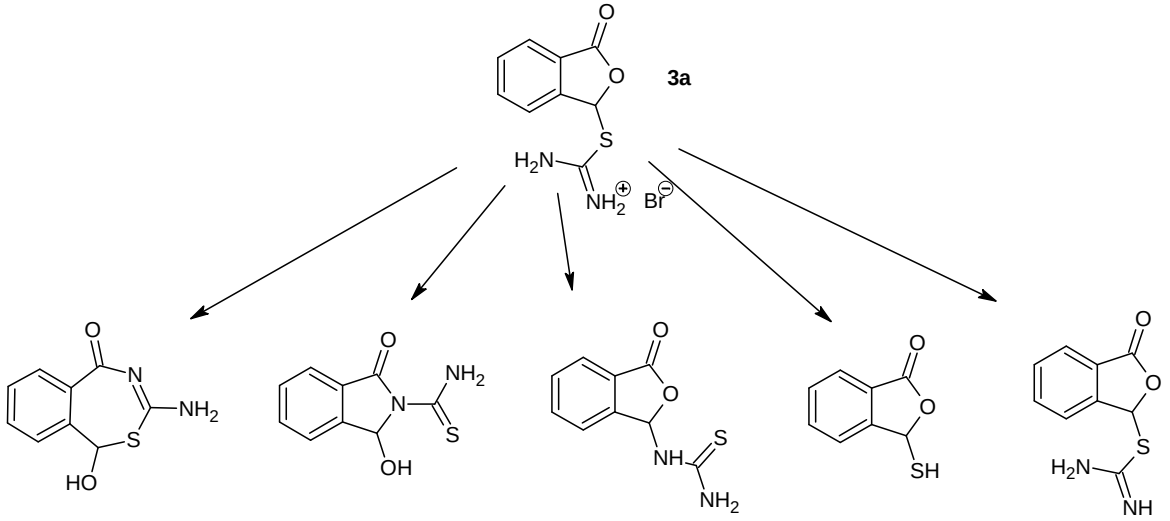

Scheme 47 – Possible products of transformations of *S*-(3-oxo-1,3-dihydro-2-benzofuran-1-yl)isothiouronium bromides (**3**).

Different reaction conditions were adopted (NH_3/H_2O, Na_2CO_3/acetone, aqueous 1:1 acetate buffer solution), but only one major product was isolated in all cases. The X-ray structure confirmed that corresponding *N*-substituted 1-hydroxy-3-oxo-1,3-dihydro-2*H*-isoindol-2-carbothioamides **4**, **6** are formed (Scheme 48). The yields of these transformations are almost quantitative and only in a few cases small amounts of undetermined impurities were detected.

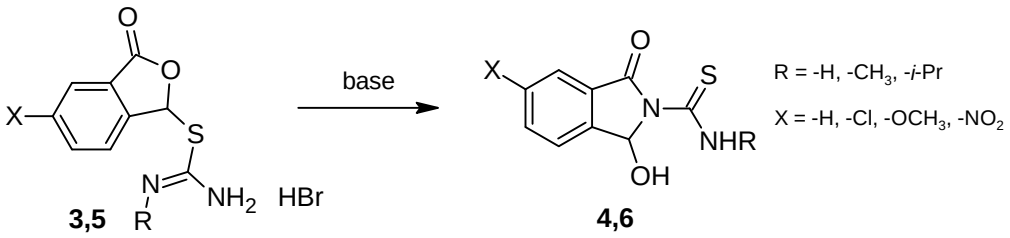

Scheme 48 – Transformation of unsubstituted **3** and monoalkylsubstituted **5** isothiouronium salts.

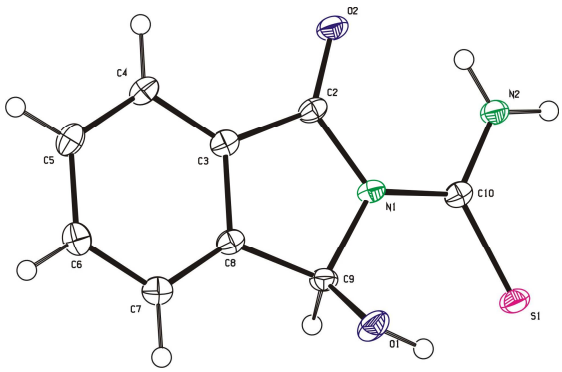

Figure 28 - ORTEP view of compound **4a** (thermal ellipsoids at 40 % probability).

In order to explain the formation of the only product based on the energies of the four possible products, their energies were calculated in the gas phase using B3LYP/AUG-cc-pVTZ // B3LYP/6-31+G(d,p) level of theory with the correction to the zero point energy. The results show (Fig. 29) that the isoindolone ring **4a** is most favoured energy-wise. The difference between the isoindolone product **4a** and the phthalidyl thiourea type product ***VI*** is 2.17 kJ·mol^{-1}. The seven membered rings ***IV***, ***V*** are disfavoured of ca. 100 kJ·mol^{-1}. The energy of transition states has not been calculated but they must be even higher so that the seven-membered ring could be the only unstable intermediate on the reaction coordinate.

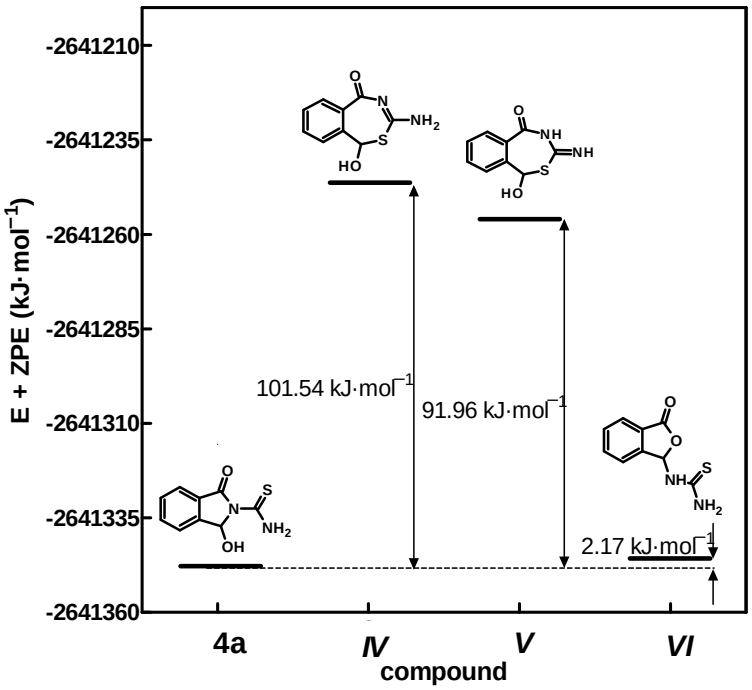

Figure 29 – Calculated energy for four possible structures **4a**, ***IV***, ***V***, ***VI*** using B3LYP/AUG-cc-pVTZ // B3LYP/6-31+G(d,p) level of theory.

The following mechanism can be proposed for the transformation (Scheme 49).

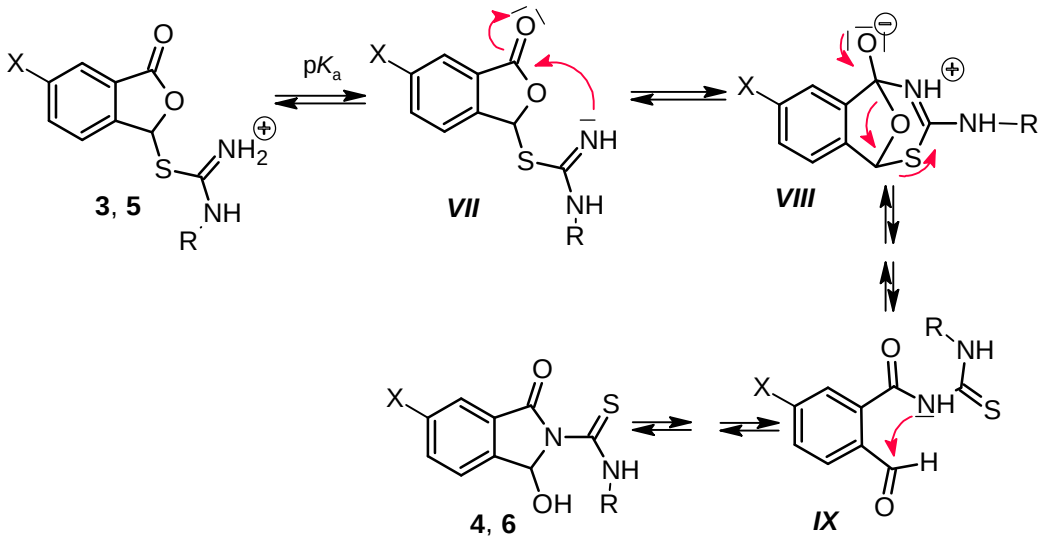

Scheme 49 – Possible mechanism of transformation **3**,**5** to **4**,**6**.

Free isothiourea ***VII*** is formed in the fast pre-equilibrium by deprotonation of the isothiouronium salts **3**, **5**. According to the previous observation,[175] the more nucleophilic imino group intramolecularly attacks the carbonyl group to form a bicyclic zwitterionic intermediate which quickly decomposes to the aldehyde ***IX***. The existence of zwitterionic intermediate is questionable because all attempts to calculate the geometry failed and the simulations always led to a non-cyclic structure. Calculations are in accordance with very high energetic demands for this intermediate. However, formation of the seven-membered ring cannot be excluded because similar rings are formed (Scheme 52). It appears that some type of concerted process is occurring, thus avoiding the intermediate where oxygen atom leaves simultaneously with the attack of the imino nitrogen on the carbonyl group.

The presence of the aldehyde ***IX*** as a reaction intermediate was confirmed by its trapping with *N*,*N*-dimethylhydrazine in the NMR tube (Scheme 50).

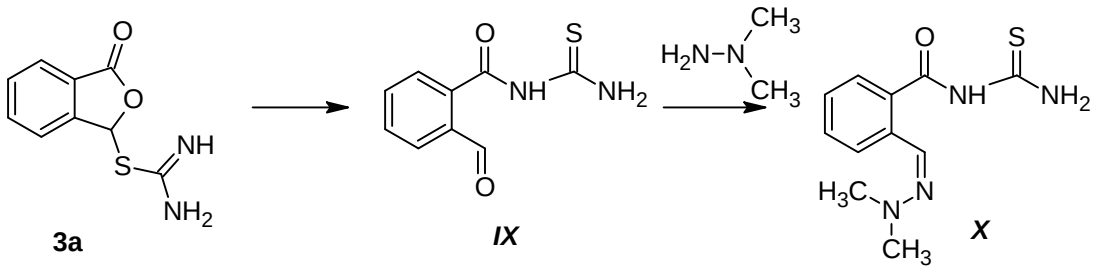

Scheme 50 – Trapping of the intermediate aldehyde ***IX*** using *N*,*N*-dimethylhydrazine.

The isothiouronium salt **3a** was dissolved in DMSO-d_6 and 1 ml of hydrazine was added. The solution turned green immediately and in the proton NMR a new singlet at 8.32 ppm appeared. The signal representing benzylic carbon in the ^{13}C NMR at 81.3 ppm for the starting salt **3a** also disappeared and a new signal at 134.6 ppm corresponding to hydrazone appeared. The HMQC spectrum shows a cross peak between these two signals (Fig. 30). In addition, the chemical shifts are very close to the chemical shifts of benzaldehyde *N*,*N*-dimethylhydrazone (7.21 and 138.0 ppm in deuteromethanol[176]). The formation of an aldehyde ***IX*** from product **4a** is also possible but the reverse reaction of the product **4a** with dimethylhydrazine occurs significantly slowly (ca. one day) giving the same spectra as in the measurement starting from **3a**. This observation confirms the reversibility of the reaction. All attempts to isolate pure hydrazone failed and only the transformation product was isolated in all cases. The instability of the hydrazone is confirmed by the change of colour inside the NMR-tube. After one day the green colour turns to brown and following a further day the mixture becomes colourless. The spectrum indicates the presence of a complex mixture of compounds.

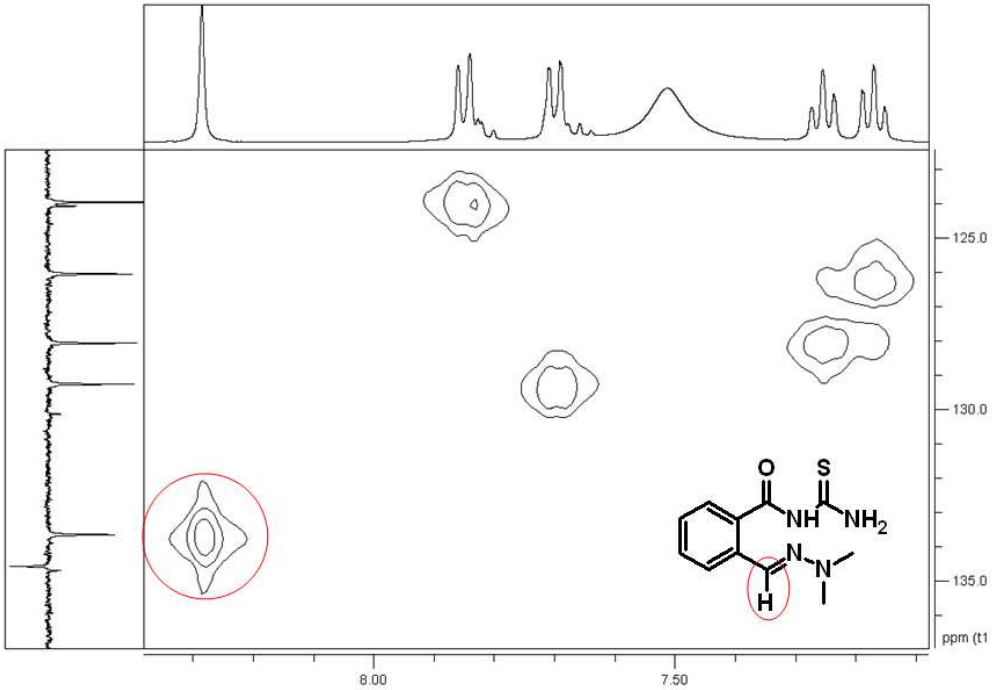

Figure 30 – HMQC NMR spectrum of hydrazone ***X***.

The lifetime and stability of the aldehyde ***IX*** were also probed in the NMR experiment using tetradeuteromethanol as the solvent, as it better resembles water. A solution of salt **3a** in CD_3OD was cooled to –50 °C, 0.2 ml of triethylamine was added and only the formation of free isothiourea was observed. The temperature was increased in 10 °C

increments and new spectra were recorded. The change in spectrum started at 0 °C when the signals of the transformation product **3b** started to appear and after 10 minutes, the reaction had finished. No signal for an aldehydic proton was observed which indicates only very low concentration of the aldehyde intermediate and its very fast transformation to the product. The stability of the aldehyde intermediate could be highly influenced by the properties of a solvent. The aldehyde ***IX*** is not the final product because it immediately undergoes intramolecular cyclization forming a stable five-membered isoindolone ring **4**, **6** (Scheme 49). Studying the reaction using a UV-VIS spectrophotometer in TEA solutions in various solvents shows different types of behaviour. A one-step reaction (single exponential kinetics) is observed in water and methanol and only in DCM does a two-step reaction (double-exponential-consecutive kinetics) occur.

An alternative reaction mechanism leading to the aldehyde intermediate ***IX*** can be drawn (Scheme 51). The first reaction step involves dissociation of **3a** to the ion pair ***XI***. The formed carbocation is resonance stabilized *i.e.* it is possible to draw two canonical structures ***XI***, ***XII***. The thioureide anion which is in close proximity can attack the carbonyl group. The attack by nitrogen instead of sulphur is due to the higher affinity of nitrogen to the carboxyl group.[177]

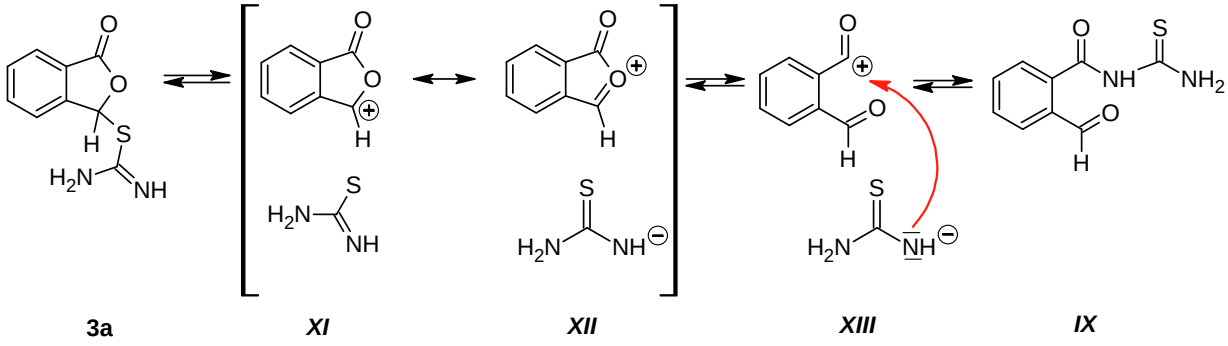

Scheme 51 – Possible reaction path for formation of ***IX*** via carbocation intermediate.

The final conclusion as to which mechanism occurs cannot be made. However, the support for the formation of a seven-membered intermediate give reactions of analogous methyl **11a** and phenyl **11b** esters of isothiouronium salts (Scheme 52). These esters were prepared under the same conditions. All attempts to transform the methyl ester **11a** under mild conditions failed and only free isothiourea ***XIV*** was obtained. Traces of a cyclic product ***XV*** were detected as far as after 7 hours of reflux in Na_2CO_3/acetone heterogeneous system. When the phenyl ester **11b,** containing a better leaving group was

used under the same conditions, the transformation occurred smoothly and the benzothiazepine product ***XV*** was isolated in a quantitative yield.

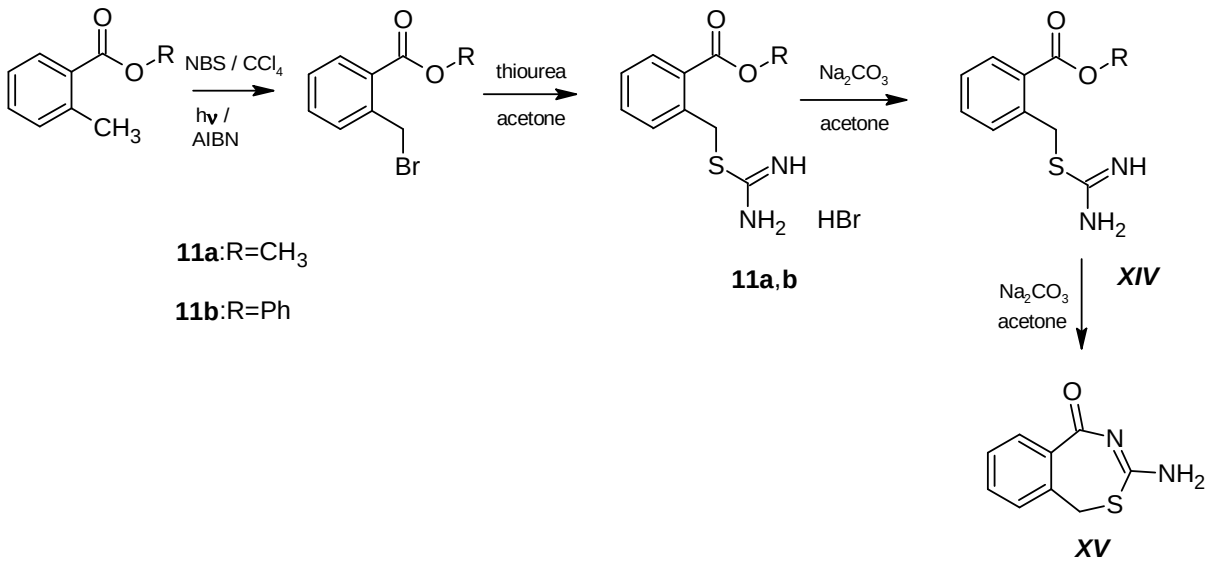

Scheme 52 – Preparation of methyl (**11a**) and phenyl (**11b**) esters isothiouronium salts and their cyclization to 3-amino-2,4-benzothiazepin-5(1*H*)-one ***XV***.

The formation of a benzothiazepine ring ***XV*** could be explained by a similar nucleophilic attack of imino nitrogen to the carbonyl group and the formation of a zwitterionic intermediate ***XVI*** (Scheme 53) with consecutive cleavage of phenoxide. In contrary to the previous mechanisms, this intermediate does not have a labile "thioacetal" group and is less rigid. The better leaving group ability of the phenoxide ion facilitates the reaction and the product is easily formed.

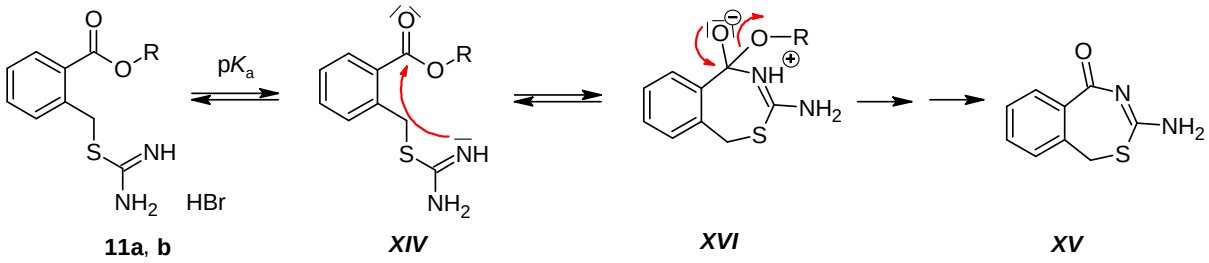

Scheme 53 – Mechanism of transformation of phenyl 2-[(carbamimidoylsulfanyl) methyl]benzoate hydrobromide (**11b**) to 3-amino-2,4-benzothiazepin-5(1*H*)-one ***XV***.

Additional evidence which supports the mechanism which involves a seven-membered intermediate ***VIII*** or transition state is the observation of no secondary kinetic isotopic effect in acetate and carbonate buffers for the substrate containing deuterium instead of hydrogen placed on the benzylic carbon atom. The rate of reaction proceeding through a carbocationic intermediate should be influenced by this substitution.[178]

Kinetics of the transformation of the unsubstituted salt **3a** to **4a** was followed (Figs. 31-33) in acetate (1:1) , hydroxylamine (1:1, 1:2b), 2-picoline (1:1), 4-picoline (1:1), imidazole (1:1) and TRIS (3:1a) buffers. The dependences of k_{obs} plotted against buffer concentrations are linear (acetate, picolines, imidazole, TRIS) or parabolical (HA). Logarithms of k_{ext}, obtained from these dependences by extrapolation to zero buffer concentration, plotted against pH of the buffers (pH-profile) gives liner dependence with a slope very close to 1 being observed (Fig. 37).

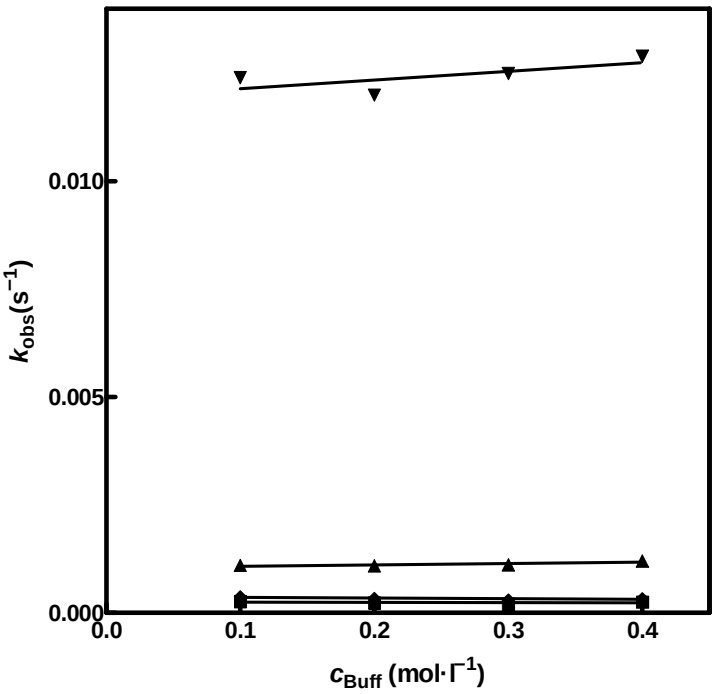

Figure 31 - Plot of the observed rate constant (k_{obs}; s^{-1}) against buffer concentration (c_{Buff}; mol·Γ^{-1}) measured in acetate buffer (1:1) pH 4.50 against buffer concentration for salts; **3a (■), 3b(♦), 3c(▲), 3d(▼)**.

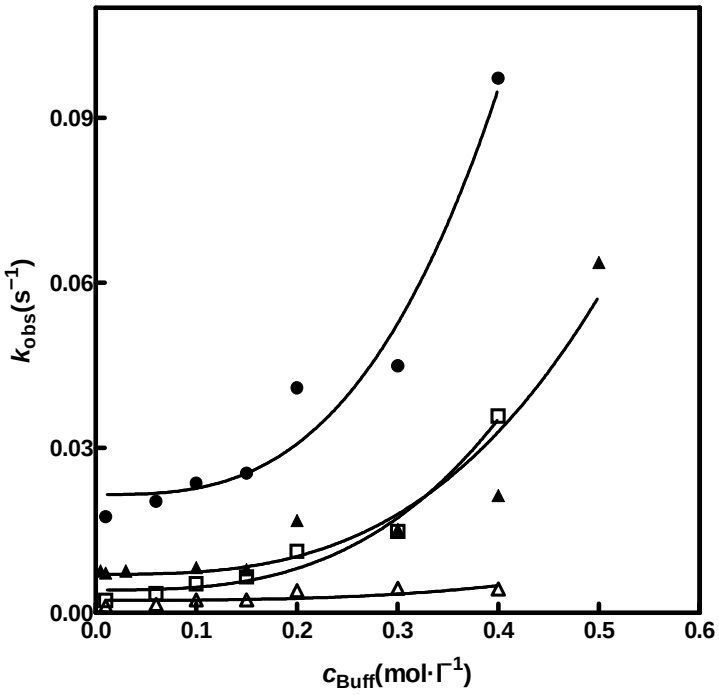

Figure 32 – Plot of the observed rate constants (k_{obs}; s^{-1}) against buffer concentration (c_{Buff}; $mol \cdot l^{-1}$) for compounds **3a**, **5a**, **5b** measured in hydroxylamine 1:1 pH 6.15 and 1:2b pH 6.42 buffers. **3a:** HA1:2b (●), **3a:** HA1:1 (▲), **5a:** HA1:2b (□), **5b:** HA 1:2b (Δ).

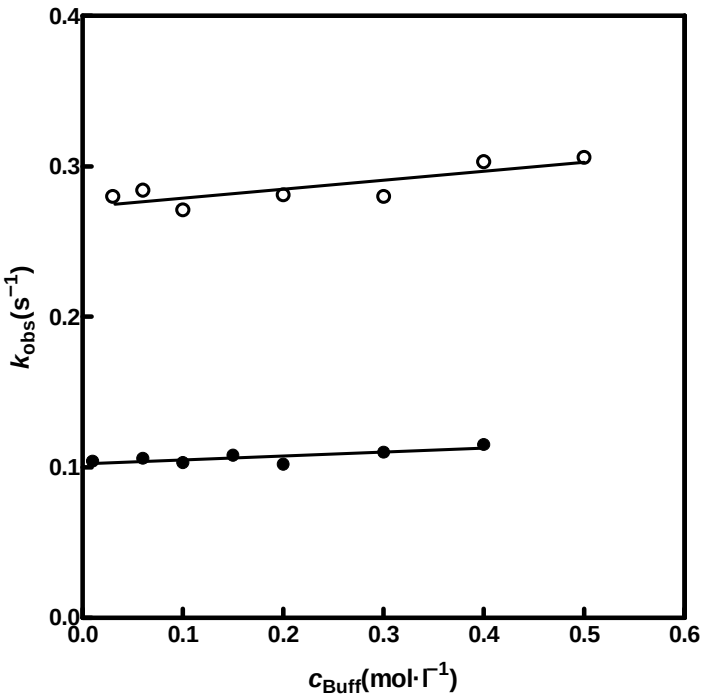

Figure 33 – Plot of the observed rate constants (k_{obs}; s^{-1}) plotted against buffer concentration (c_{Buff}; $mol \cdot l^{-1}$) for **3a** measured in TRIS 3:1a pH 8.02 (○) and imidazole 1:1 pH 7.28 (●) buffers.

Plots of the observed rate constants against buffer concentration in acetate buffers show a linear character with slopes close to zero (Fig. 31). It indicates specific catalysis with the proton transfer prior to the rate-limiting step. The extrapolated rate constant k_{ext} for the unsubstituted isothiouronium salt **3a** is about one order of magnitude higher than for the methyl substituted salt **5a** and another half an order of magnitude higher than for isopropyl substituted salt **5b**. The completely different behaviour was observed in HA 1:2b buffers. The dependences are not linear and grow with increasing buffer concentration (Fig. 32) in this case. Opening of a new reaction pathway is a reasonable explanation. The hydroxylamine acts both as a base deprotonating the isothiouronium salt as well as a nucleophile attacking the carbonyl group or benzylic carbon atom. The fitting of the dependences shows best agreement with equation (25).

$$k_{obs} = k_{ext} + k[HA]^3 \qquad (25)$$

That implies the presence of at least three hydroxylamine molecules during the course of the reaction. Formation of different products depending on hydroxylamine concentration is confirmed by the UV-VIS spectra (Fig. 32) of the reaction mixture after the reaction.

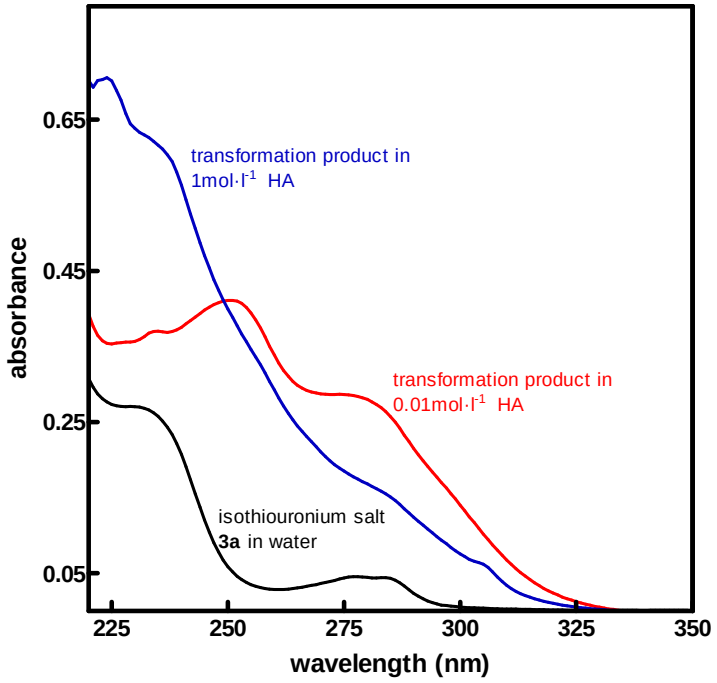

Figure 34 – UV-VIS spectra of the reaction mixture after transformation of **3a** in hydroxylamine 1:1 buffers with various concentrations. Black line – isothiouronium salt, Red line – product in 0.01 mol·l^{-1} hydroxylamine 1:1 (pH 6.14), Blue line – product in 1 mol·l^{-1} hydroxylamine 1:1 (pH 6.14).

The correlation of the extrapolated rate constants k_{ext} measured in acetate buffers (Fig. 31) on σ_p Hammett constants for **3a**, **3c** and **3d** derivates shows linear character with a slope of ≈ +2 (Fig. 35) and the methoxy derivative **3b** is found a little bit above this line again.

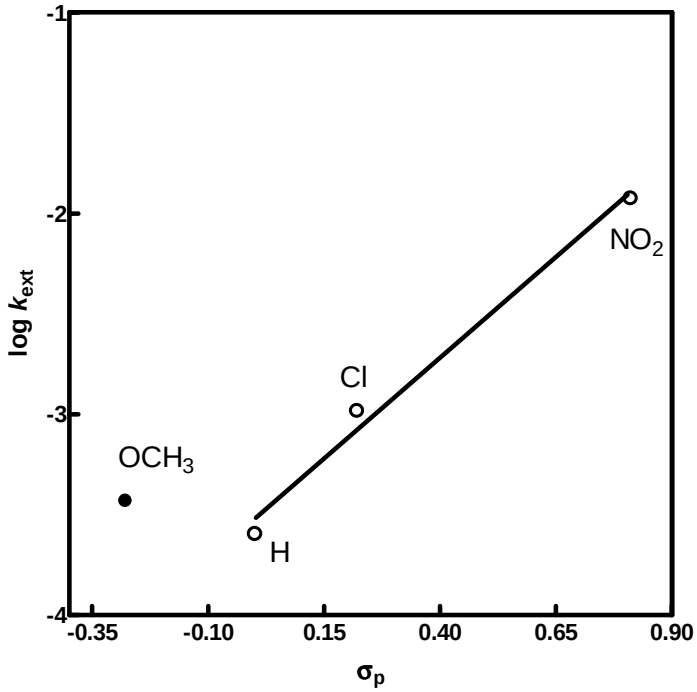

Figure 35 – Diagram of log k_{ext} for **3a-d** obtained from acetate buffer (Fig. 31) plotted against Hammett σ_p constants.

These observations are in agreement with the measured pK_a values of the salts. A comparison of the Hammett plots (Fig. 36) for **3a**, **3c** and **3d** show very close ρ values; exactly ρ_{Ka} = 2.5 for pK_as and ρ_{kext} = 2 for log k_{ext}. Together with the unit value in the pH profile (Fig. 37) it could be suggested that the reaction rate is pH controlled. It means that it depends mainly on the presence of free isothiourea in the reacting buffer solution. Subtraction of both of the dependences $\rho_{kext} - \rho_{Ka}$ (Fig. 36) gives the straight line with the slope –0.5 and the non-linearity of methoxy group is eliminated by this correction on pK_as. In other words – the deviation from the Hammett plot of log k_{ext} of salt **3a** is caused only by the different pK_a of this salt.

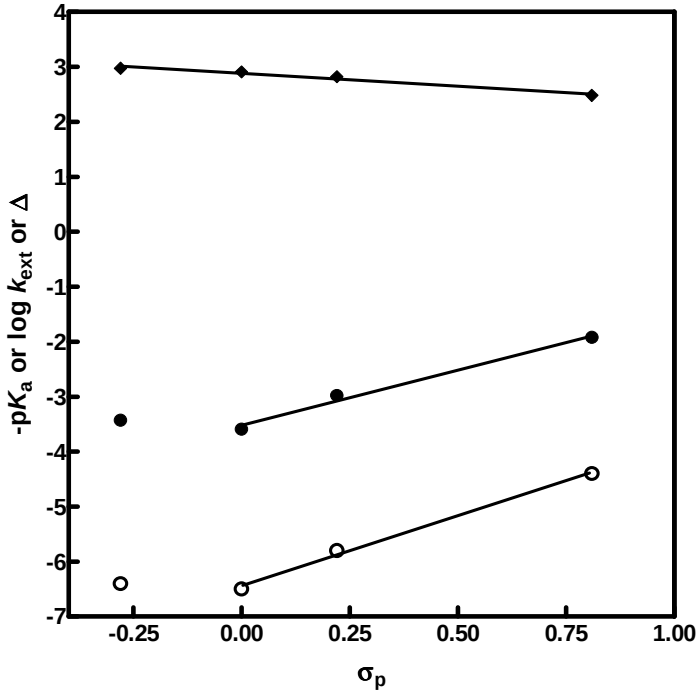

Figure 36 – Diagram of log K_a (○) of the isothiouronium salts **3a-d** and log k_{ext} (●) from acetate buffers and difference of those two values (♦) plotted against Hammett σ_p constants.

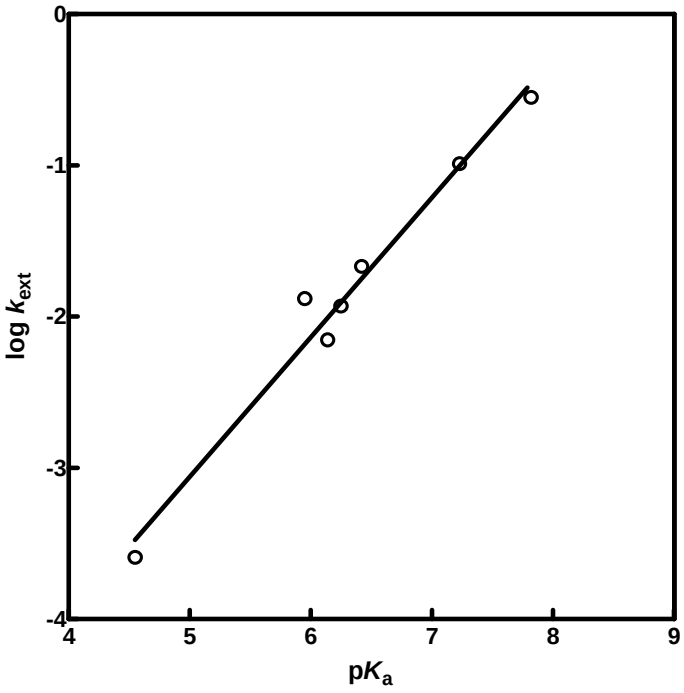

Figure 37 – pH Profile for the reaction of **3a**.

It is obvious that electron-withdrawing substituents decrease the reaction rate. This difference between both plots (Fig. 36) could be explained as the influence of the substitution on the benzene ring in the 6 position on the reaction rate. This allows a decision as to whether the nucleophilic attack of the imino nitrogen and the formation of the zwitterionic intermediate ***VIII*** or the consecutive cyclization of aldehyde ***IX*** is the rate-limiting step of the transformation of **3** to **4** in the aqueous solution (Scheme 49).

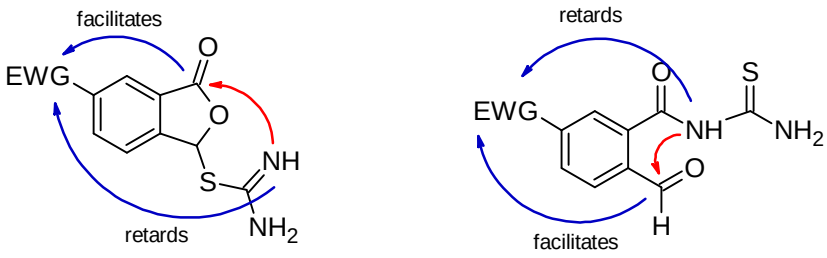

Figure 38 – Influence of electron withdrawing group on reaction rates of both the reaction steps of transformation of **3** to **4**.

It is obvious that the substituent in position 6 influences the reaction centre, the benzylic carbon and the carbonyl group. The nucleophilic attack on the carbonyl group is facilitated by the electron withdrawing substituents in the *meta* position towards the carbonyl and the electron donating group in the *para* position towards the isothiourea moiety. On the other hand, the cyclization of aldehyde ***IX*** is facilitated by an electron withdrawing group in the *para* position towards the aldehyde group and by an electron donating group in the *meta* position towards the amide group (Fig. 38).

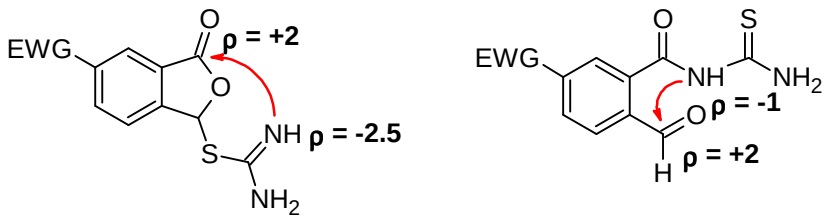

Figure 39 – Predicted Hammett ρ constants for the both reaction steps of transformation of **3** to **4**.

Hammett ρ constants could be predicted for every single effect (Fig. 39). The ρ constant for the nucleophilic attack on ester or lactone group in water should be of about +2.[179,180] It

is probable that effect on nucleophility of the isothiourea moiety should be of a similar size as the effect on the pK_as of the isothiouronium salts. Therefore, the value –2.5 is proposed for the attack of the imino group. These two effects act together and the resulting predicted value of Hammett ρ constant for the nucleophilic attack on the carbonyl group must be the sum of the two values i.e. $\rho = -0.5$.

If the cyclization of aldehyde ***IX*** is the rate-limiting step then the expected value would be about +2[181,182] for the nucleophilic attack to the aldehydic carbon and –1 for the nucleophilicity of the amidic nitrogen. The sum of these two effects is then +1. A comparison of the predicted values with an experimental value of –0.5 show that the nucleophilic attack of the imino group of the isothiourea and formation of the seven-membered intermediate is a rate-limiting step of the transformation. The observation of no kinetic isotopic effect for the substrate with deuterium instead of hydrogen on the benzylic carbon in acetate and carbonate buffers also supports this conclusion.

3.2.3 Transformation of *N,N´*-disubstituted salts

N,N´-Disubstituted isothiouronium salts **9** were prepared under the similar conditions as the monosubstituted salts. The first attempts on their transformation to the products were done in aqueous ammonia solution. After the extraction to dichloromethane, the mixture of two products was isolated and the structure of the major product was determined by the X-ray analysis. The results confirmed structure of 1,3-dimethyl-1-(3-oxo-1,3-dihydro-2-benzofuran-1-yl)thiourea (**10a**) to be the major product (Scheme 54). The structure of the minor product was identified by NMR to be 3-hydroxy-2,3-dihydro-1*H*-isoindol-1-one (**10k**).[183]

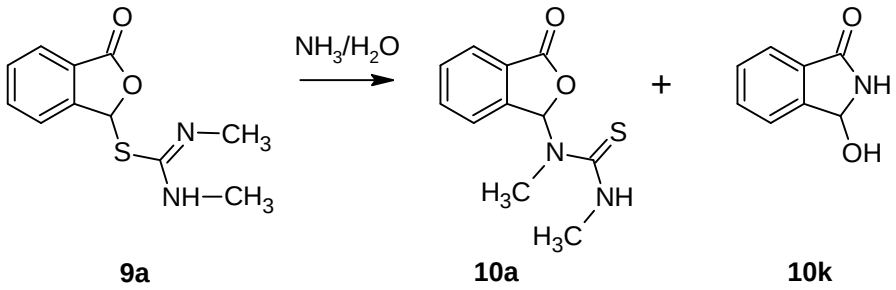

9a **10a** **10k**

Scheme 54 – Products of transformation of *N,N*-dimethylisothiouronium salt **9a**.

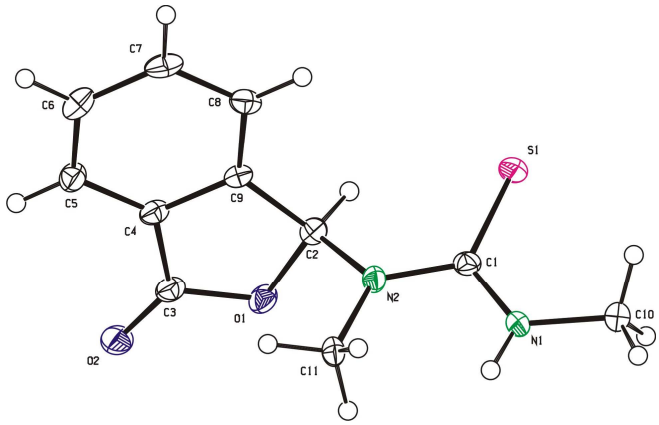

Figure 40 - ORTEP view of compound **10a** (thermal ellipsoids at 40 % probability).

The influence of ammonia concentration on the product distribution has been investigated. The dependence of the product ratio plotted against ammonia concentration shows linear character (Fig. 41). Increasing ammonia concentration increased the yield of 3-hydroxy-

2,3-dihydro-1*H*-isoindol-1-one (**10k**). This held for **9a** and **9c** derivates but it also depends which way is used for addition of the ammonia solution. The addition of ammonia solution to the pure salt in solid state gives higher ratio of transformation product as compared to the addition of aqueous ammonia to the aqueous solution of the isothiouronium salt **9a**.

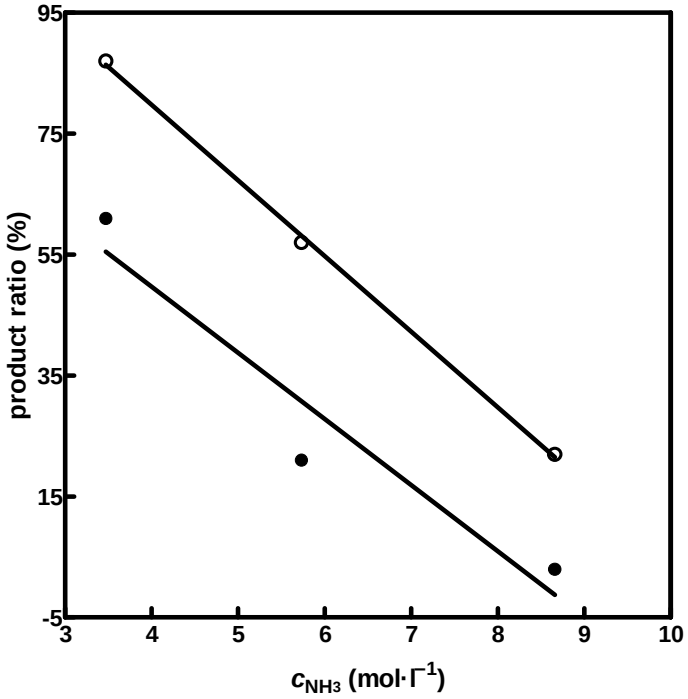

Figure 41 – Dependence of the product ratio (rearrangement:decomposition) on ammonia concentration for the isothiouronium salts **9a** (○), **9c**(●).

Under different conditions (Na_2CO_3/acetone, Na_2CO_3/H_2O, TEA/DCM) the 1,3-dimethyl-1-(3-oxo-1,3-dihydro-2-benzofuran-1-yl)thiourea (**10a**) is the only product of the transformation. There are two possible explanations for the formation of the products **10a** and **10k**:

3-Hydroxy-2,3-dihydro-1*H*-isoindol-1-one (**10k**) could be formed in two different ways (Scheme 55). The first one is an analogy to the transformation of the unsubstituted salts **3**. Molecule of the ammonia which is good external nucleophile intermolecularly attacks the carbonyl group of the free base ***XVII*** giving a zwitterionic tetrahedral intermediate ***XVIII.*** This intermediate then decomposes to an aldehyde ***IXX*** that undergoes ring closure to the product **10k**. The second possibility involves nucleophilic substitution of the isothiouronium moiety. An ammonia nitrogen atom acts as an external nucleophile again and it attacks benzylic carbon atom in this case. The isothiouronium part of the molecule acts as a leaving group. The so formed 3-aminophthalide ***XXI*** is unstable and

spontaneously rearranges to the 3-hydroxy-2,3-dihydro-1*H*-isoindol-1-one (**10k**). According to the literature[56,59] a molecule of ammonia as a stronger nucleophile should prefer attack on the carbonyl group. Also relatively poor leaving group as isothiourea is supports this mechanism. The reaction of **9a** with *N*,*N*-dimethylhydrazine gives analogous NMR spectra like unsubstituted salt **3a**. That also indicates the mechanism proceeding through the aldehyde intermediate ***IXX***.

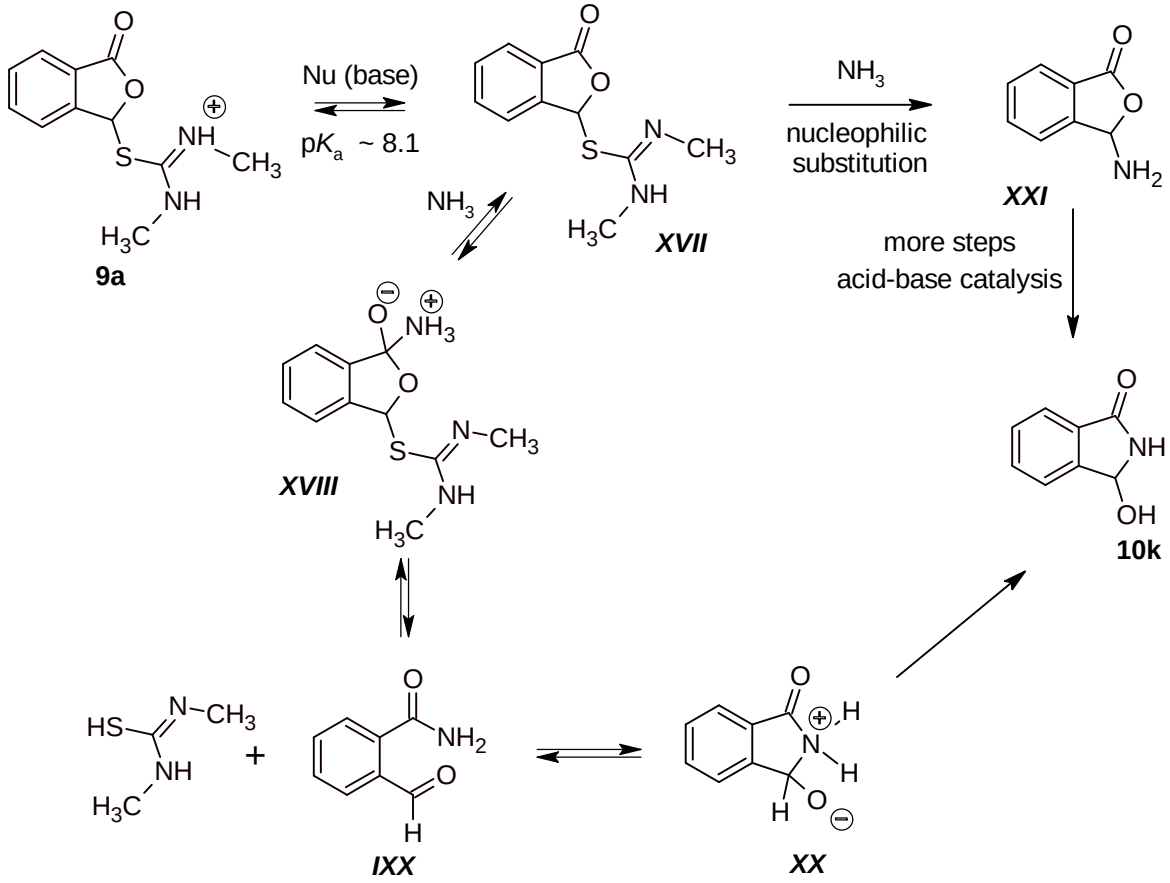

Scheme 55 – Possible reaction pathways leading to 3-hydroxy-2,3-dihydro-1*H*-isoindol-1-one **10k**.

The influence of the steric demands was observed for *N*-ethyl-*N´*-methyl isothiouronium salt **9j** (Scheme 56). The ratio of the two possible products after the transformation in acetone is 3:1 with the majority of the product carrying methyl group on the nitrogen atom next to the benzylic carbon atom. This indicates relatively high steric demands on the transition state of the reaction.

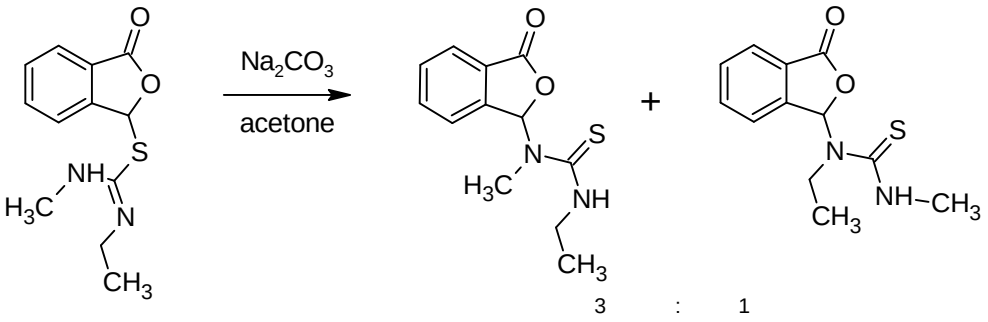

Scheme 56 – The product ratio of the transformation of **9j** in Na_2CO_3/acetone solution.

There exists several possible explanations of the formation of 1,3-dimethyl-1-(3-oxo-1,3-dihydro-2-benzofuran-1-yl)thiourea (**10a**). The reaction can be seen as an alkyl transfer from sulphur to the nitrogen atom involving any type of nucleophilic substitution reaction. The application of the classical Winstein scheme[63] (Scheme 25) leads to the proposal of the two limiting mechanisms (Scheme 57).

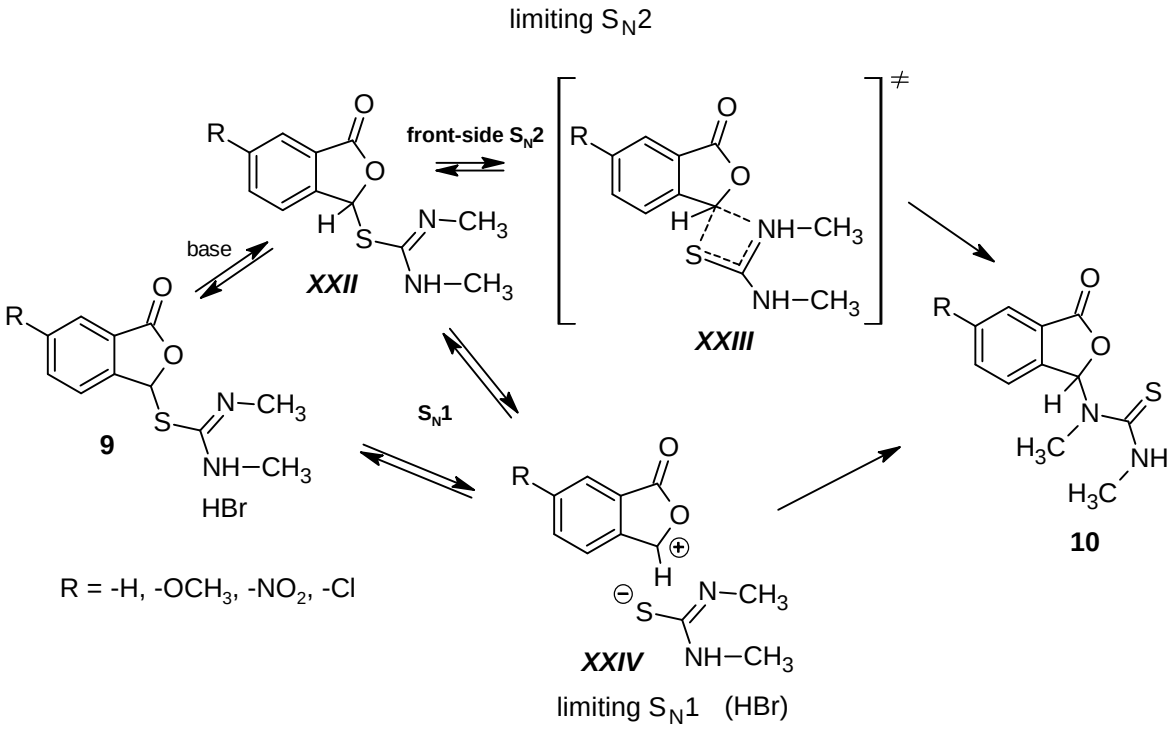

Scheme 57 – Limiting S_N1 and S_N2 mechanisms for transformation of **9** to **10**.

Firstly, a limiting S_N1 mechanism, where isothiourea acts as a leaving group and a carbocation ***XXIV*** is formed in the first reaction step can be suggested. This carbocation could be considered both of the benzyl type and of the oxocarbonium type. The

stabilization by the oxygen atom is weaker as compared to the acetals[185,184] because of the electron withdrawing effect of the neighbouring carbonyl group. In the second reaction step, a nitrogen atom of the thioureide anion attacks the carbocation and the final product **10** is formed. The transformation of the isothiouronium salt instead of its free base is also possible.

In the limiting S_N2 reaction the nitrogen atom attacks benzylic carbon and the product is formed *via* a four-membered transition state ***XXIII***. The insight on the stereochemistry enforces the nucleophilic frontside attack from the same side of the molecule as the leaving group leaves. Generally, the formation of the four-membered ring containing only carbon skeleton is unfavourable but the presence of a sulphur atom enables easier torsion deformation and the four-membered rings containing sulphur atom with bonding angle smaller than 90° have been observed.[186,187] Also rearrangements of acylthioureas or imides are proposed to occur *via* four-membered ring.[188-190] Further factor facilitating this kind of reaction is a longer length of the sulphur-carbon bond.

The reaction involving an intermolecular attack of the two molecules of free isothioureas is improbable because of high reaction rate of transformation. The mechanism operating through the same type of the bicyclic intermediate ***VIII*** as in the case of the unsubstituted salts **3** could be also written (Scheme 49) but is energetically and sterically disfavoured. As compared to previous unsubstituted **3** and monosubstituted **5** compounds those salts **9** are stable in acetate buffers that indicate a different type of the transformation mechanism.

Understanding of the stability and behaviour of the possibly formed carbocation is crucial for the understanding and decision which mechanism reaction involves. The most probable explanation is some kind of the borderline mechanism. Therefore, I have followed the kinetics of the reaction of simple 3-bromophthalide with the various nucleophiles in MeOH/H_2O (1:1) solutions with the ionic strength maintained at 0.2 mol·l^{-1} by the addition of sodium perchlorate (Scheme 58).

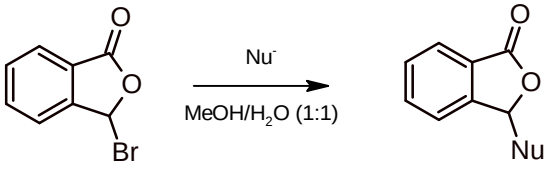

Nu = N_3^-, SCN^-, AcO^-, $S_2O_3^{2-}$

Scheme 58 – Reaction of 3-bromophthalide with various nucleophiles in methanol/water (1:1) solutions.

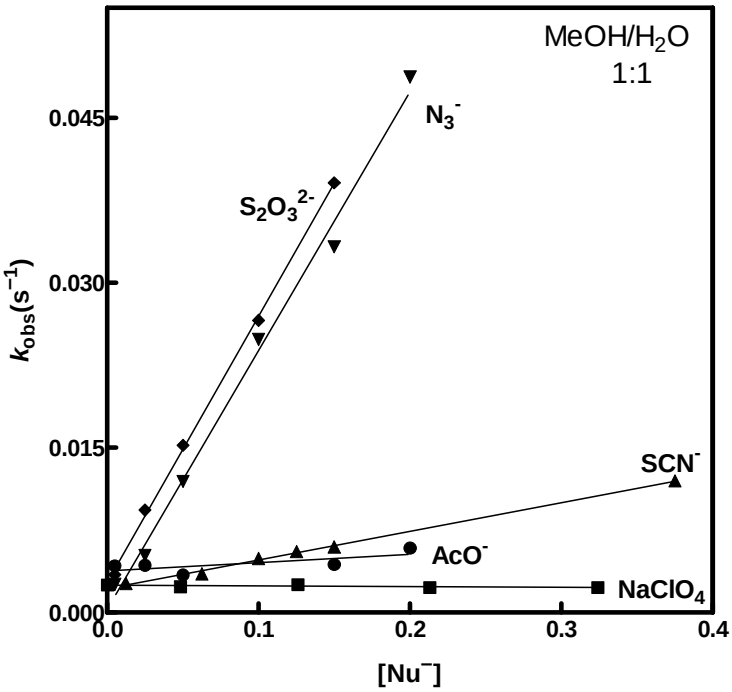

Figure 42 – Dependence of observed rate constants (k_{obs}; s^{-1}) on nucleophile concentration [Nu^-] for the reaction of 3-bromophthalide with various nucleophiles in methanol/water (1:1) solutions. Ionic strength was maintained at 0.2 $mol \cdot l^{-1}$ with $NaClO_4$.

Fig. 42 shows the dependence of the observed rate constants on nucleophile concentration. It is obvious that the slopes of the dependences change from values close to zero for weak nucleophiles as acetate, to higher values for thiocyanate and the highest values for the azide and thiosulphate ions. The reaction with $NaClO_4$ means the solvolysis without additional nucleophiles, and only the concentration of sodium perchlorate has been changed to observe the influence of the salt effect. The product of reaction in the presence of sodium perchlorate is a mixture of 3-hydroxy and 3-methoxyphthalides in the molar ratio 1:2. The analysis of the products of the reaction with other nucleophiles shows that all compounds react only at the benzylic carbon atom and the carbonyl group is not attacked. All of the dependences have a small y-intercept with the value corresponding approximately to k_{ext} = 0.003 $l \cdot mol^{-1} \cdot s^{-1}$ which corresponds to the rate of solvolysis. Using the equation (26) which is identical to (10), it is possible to calculate the rate constants for both the concurrent reactions. (Table 7)

$$k_{obs} = k_{Sol} + k_{Nu} \cdot [\mathrm{Nu}] \qquad (26)$$

Table 7 - Calculated rate constants for the reaction of 3-bromophthalide with various nucleophiles.

Nucleophile	$k_{sol} \cdot 10^3$ (s^{-1})	$k_{Nu} \cdot 10^2$ ($l \cdot mol^{-1} \cdot s^{-1}$)
ClO_4^-	2.49 ± 0.08	≈ 0
AcO^-	3.79 ± 0.47	0.76 ± 0.41
SCN^-	2.18 ± 0.12	2.61 ± 0.69
N_3^-	0.32 ± 1.07	23.5 ± 0.95
$S_2O_3^{2-}$	2.78 ± 0.37	24.1 ± 0.44

These results indicate a mechanism very close to S_N2 because this could be influenced by the nucleophility of the attacking nucleophile.[69] The stronger the nucleophile, the higher the reaction rate is. In the case of S_N1 mechanism with the carbocation formation in the rate limiting step the reaction rate would not depend on the nucleophilicity of the nucleophile.

There is another possible explanation of the observed results. According to the Kim[191], concurrent S_N1 and S_N2 reactions proceed. The intercepts on the y-axis determine the rate constants for S_N1 mechanism, independent on nucleophility of the nucleophile and the slopes determine the rate constants for S_N2 reaction in this case.

The second portion of experiments was made using directly the *N,N´*-disubstituted salts **9a-d**. The dependence of the observed rate constant on azide concentration are linear with the zero slope for unsubstituted salt **9a** and with the slope higher than zero for 6-chlorosalt **9c** (Fig. 43). Unfortunately the reaction of 6-nitrosalt **9d** is too fast to be measured. The comparison of the UV-VIS spectra for an unsubstituted **9a** and 6-chloro **9c** salts shows similar behaviour and the same character, also similar to the spectra after the reaction of 3-bromophthalide with azide. The absorption band at 260 nm is increasing during the reaction which indicates the attack on the same reaction centre and only a change in the mechanism for both of the compounds. The explanation could be the shift on the potential energy surface (PES) where the reaction pathway for unsubstituted salt **9a** is closer to the limiting S_N1 mechanism. On the other hand, the reaction of 6-chloro salt **9c,** whose carbocation is destabilized, proceeds through the reaction path closer to the limiting S_N2 reaction where the presence of the nucleophile in the transition state in necessary.

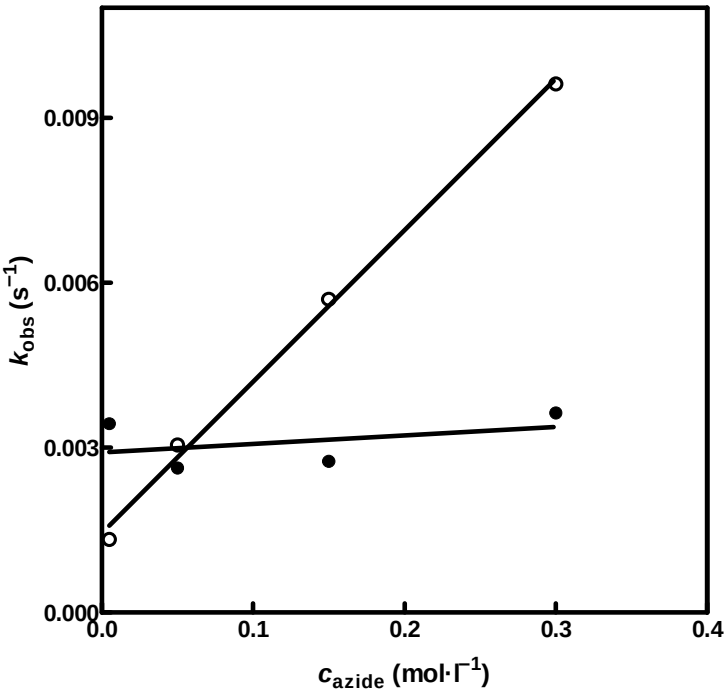

Figure 43 – Plot of the observed rate constants (k_{obs}; s^{-1}) plotted on azide concentration (c_{azide}; mol·l^{-1}) for reaction of **9a** (●) and **9c** (○) in sodium azide solutions.

The new insight into the reaction mechanism brings an analysis of the initial salt **9a** and product **10a** in a gas phase. The reaction was probed using the Ion spectroscopy and the Infrared multiphoton dissociation spectroscopy (IRMPD).[192] The IRMPD spectra of the isothiouronium salt **9a** (Fig. 44) in combination with the theoretical models (predicted using quantum chemistry calculations) give the structure identical to the solid state **9a**. During the measurement of the transformation product **10a** the hydrochloric acid had to be added to make the sufficient amount of positively charged ions. The IRMPD spectrum (Fig. 44) shows the presence of compound different to the classical transformation product **10a**. The signal at 1720 cm^{-1} corresponds to C=O vibration in carboxylic acids.

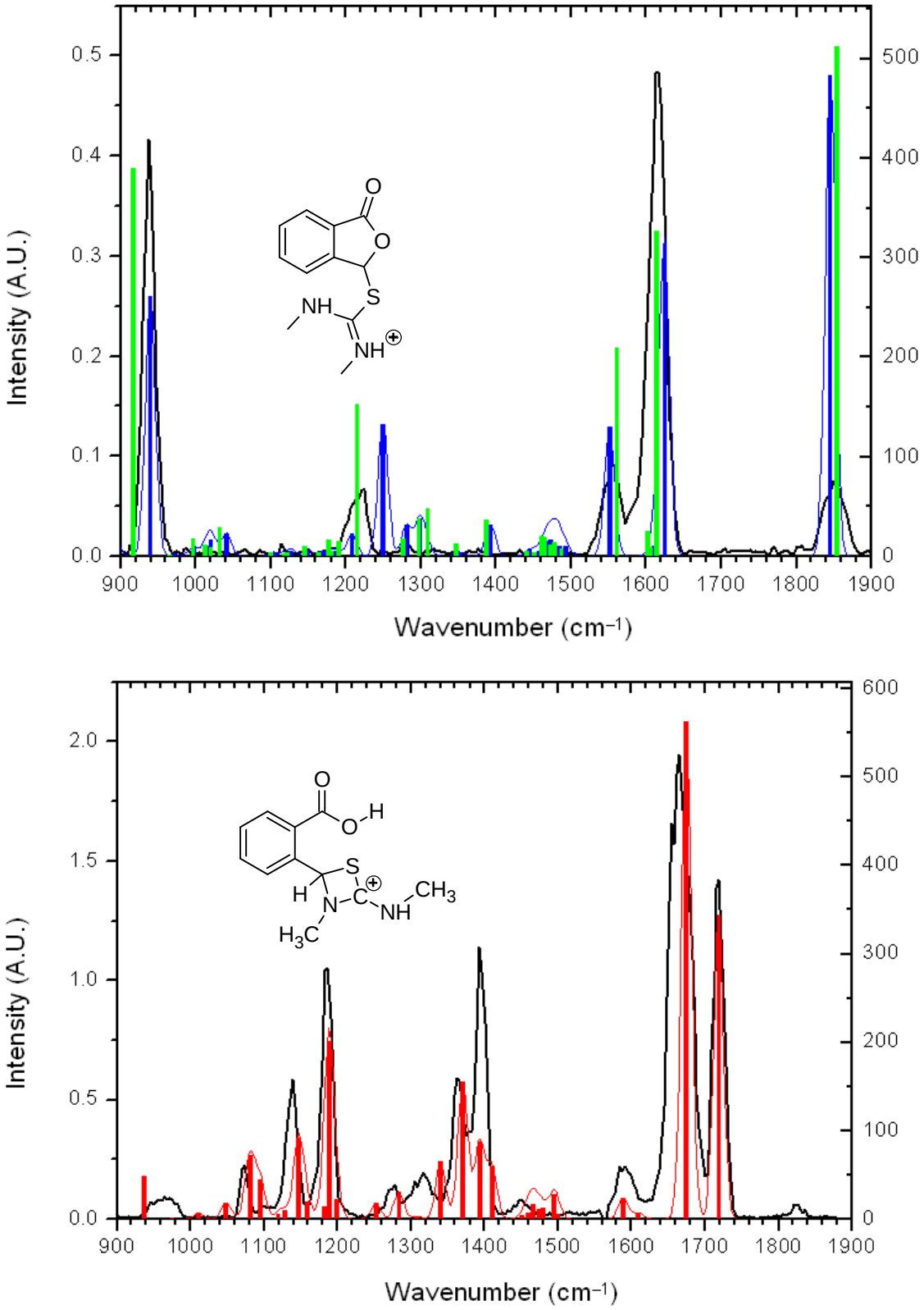

Figure 44 - The IRMPD spectra (black) for compounds **9a** and **10a**. Theoretical absorption frequencies are depicted as coloured lines. For illustration, spectra for two different calculated conformers are depicted. Predicted spectra were calculated using B3LYP/6-311+G(2d,p) level of theory and scaling factor 0.985 were used for the frequencies.

Calculation of the possible structures and comparing of the predicted and measured spectra determines the ***XXVI*** as the most probable compound formed in the gas phase. The proton catalyzed equilibrium reaction (Scheme 59) could be proposed for the formation of this intermediate ***XXVI***.

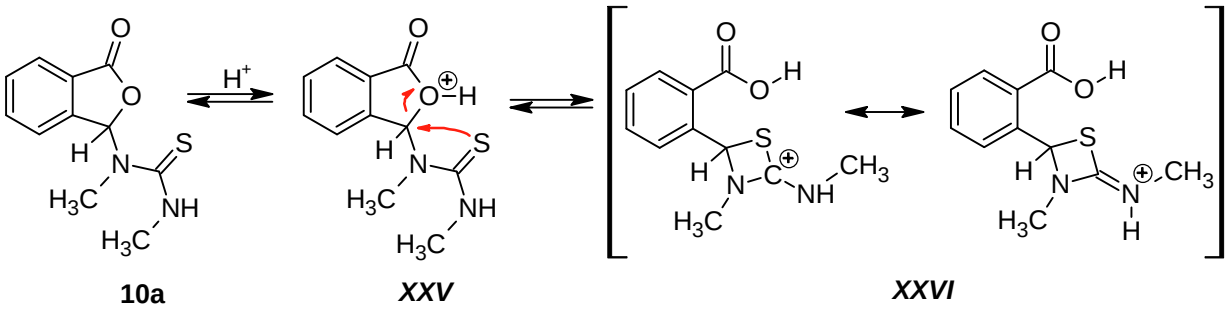

Scheme 59 – Proposed mechanism for the formation of ***XXVI*** from **10a** in the gas phase.

The presence of this intermediate ***XXVI*** offers more explanations for the reaction mechanism of the transformation. The first one considers acid ***XXVI*** as a product of the independent reaction of the cyclizate **10a** with proton and no occurrence of this intermediate during the rearrangement of **9a** to **10a**. The second explanation takes the reversibility of the rearrangement into account with the acid ***XXVI*** as an intermediate. The remaining question is a transfer of this mechanism to the liquid phase and to the basic reaction conditions.

The reaction proceeding *via* the above mentioned intermediate in the base solutions requires two steps (Scheme 60). Imino nitrogen attacks the carbon atom through the above proposed four-membered transition state but an oxygen instead of a sulphur atom acts as a leaving group now (the classical backside attack). The so formed zwitterionic intermediate ***XXVII*** undergoes rotation around the single bond C–C allowing the sulphur atom to get opposite to the oxygen atom ***XXVIII***. This rotation could be facilitated by the electrostatic interaction of the positively charged nitrogen atom with the negatively charged carboxylate oxygen. In the second step, the oxygen atom attacks the benzylic carbon atom again and the sulphur atom leaves to form the final product **10a** now. Both the steps could proceed as a classical S_N2 reaction with a backside attack with the Walden inversion. This could be seen as a double-displacement mechanism in the enzymatic reactions.[110,193,194]

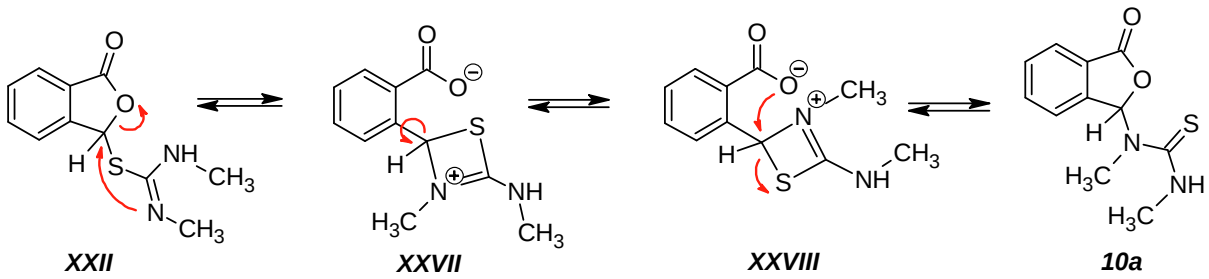

Scheme 60 – Proposed mechanism of transformation of **9a** to **10a** *via* double-displacement S_N2 reaction.

It is obvious from the kinetic measurements that the reaction occurs only in the presence of a base in the solution of the pH higher than 6. This shows that only a free base of isothiourea ***XXII*** undergoes the cyclization and an intermediate should exist as carboxylate and not as an acid under these conditions. The study of the reaction of **9a** in carbonate/D_2O buffers shows no influence of the solvent kinetic isotopic effect on the reaction rate (KIE = 0). It indicates that there is no necessity of the water molecule participation during the reaction course and the transformation could be considered as a monomolecular process.[195] The second reaction step is analogous to the base catalyzed ring-closure of 2-carbomethoxybenzaldehyde methyl 3,5-dichlorophenyl acetal.[195] In this reaction the carboxylate anion electrostatically stabilizes the formed carbocation and facilitates the leaving of the phenoxide leaving group. These observations indicate that there is not complete dissociation of the reaction intermediate ***XXVII*** and the reaction occurs in the form of an ionic pair.

The support for this mechanism in the liquid phase give reaction of the isothiouronium salts **12c** containing the six-membered lactone ring (Scheme 61). An absence of the oxygen atom next to the benzylic carbon could help to decide if the rearrangement occurs either *via* some type of the frontside substitution or *via* the double-displacement mechanism. If the reaction occurs *via* some type of the frontside mechanism – the only effect of oxygen is the stabilization of the developing positive charge on the benzylic carbon. Substitution of the oxygen could reduce the reaction rate, but the reaction should still occur. On the other hand, the presence of the oxygen atom is crucial for the double-displacement mechanism where the oxygen atom acts as both, the leaving group and the internal nucleophile. Five hours reflux of **12c** in acetone Na_2CO_3 mixture gave only the 1*H*-isochromen-1-one **12d** as a reaction product which is formed by elimination and product of the sulphur to nitrogen migration have not been observed (Scheme 61). This shows that the presence of the

oxygen atom next to the benzylic carbon is crucial for the *S* to *N* migration and the double-displacement is more probable than the frontside S_N2 mechanism.

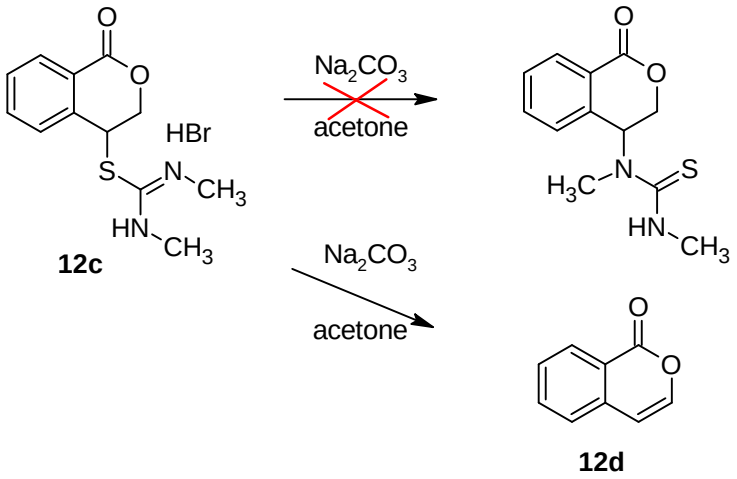

Scheme 61 – Transformation of **12c** in the Na_2CO_3/acetone solution.

The question if the reaction of **9a** proceeds through mechanism close to the S_N1 or the double-displacement mechanism, could help answer the reaction of **11c** with Na_2CO_3 in acetone (Scheme 62).

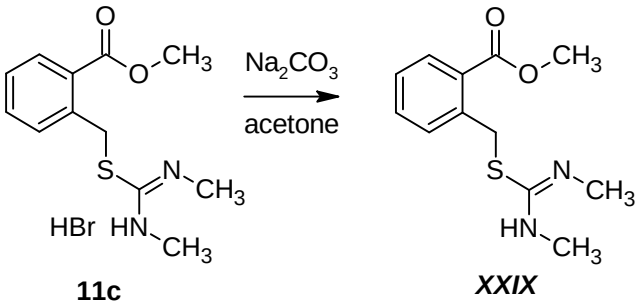

Scheme 62 – Reaction of **11c** in the Na_2CO_3/acetone solution.

This substrate enables the *S* to *N* migration *via* the benzyl type carbocation ***XXX*** that can be stabilized both the neighbouring benzene ring and the electrostatic effect of the oxygen atoms of ester group ***XXXa,b*** (Scheme 63). This make this carbocation very similar to the carbocation ***XXIV*** proposed for the transformation of the salt **9a**. The double-displacement mechanism cannot occur in this case because of the absence of the oxygen atom acting as the leaving group. The 5 hours reflux of **11c** gives only free base of the isothiouronium salt

XXIX as product and sulphur to nitrogen migration have not been observed. This supports the double-displacement mechanism.

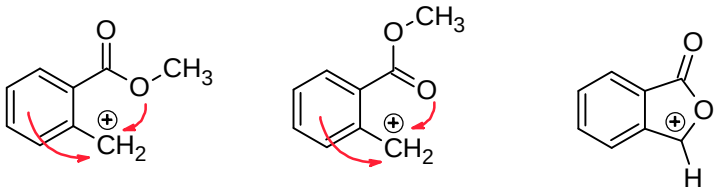

XXXa ***XXXb*** ***XXIV***

Scheme 63 – Possible carbocationic intermediates for the S_N1 reaction pathways for the transformation of **9a** and **11c**. The arrows show stabilization effects.

The important argument for the double-displacement mechanism in the solutions would be the trapping of the carboxylic acid type intermediate ***XXVII***. The 20 fold excess of the methyl iodide was added to the mixture of the isothiouronium salt **9a** and sodium carbonate in acetone. The solvent was evaporated after 3 hours of reflux and the reaction residue was analyzed by the NMR spectroscopy. The spectra show complicated mixture of compounds but a signal at 3.79 ppm in the ^1H spectrum appears. The HMBC spectrum (Fig. 45) shows the correlation of this signal with the signal of a carbon atom at 166.9 ppm. These signals are in a very good agreement with the signals of a methyl ester group in compound ***XXIX*** (3.86 and 167.0 ppm). This observation confirms the presence of the methyl ester group ***XXXI*** in the reaction mixture. The only reasonable explanation of its formation is the partial trapping of the formed carboxylic acid intermediate ***XXVII*** by the methyl iodide (Scheme 64).

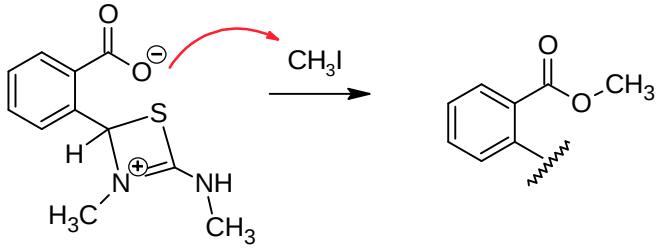

XXVII ***XXXI***

Scheme 64 – Trapping of the carboxylic acid intermediate by methyl iodide.

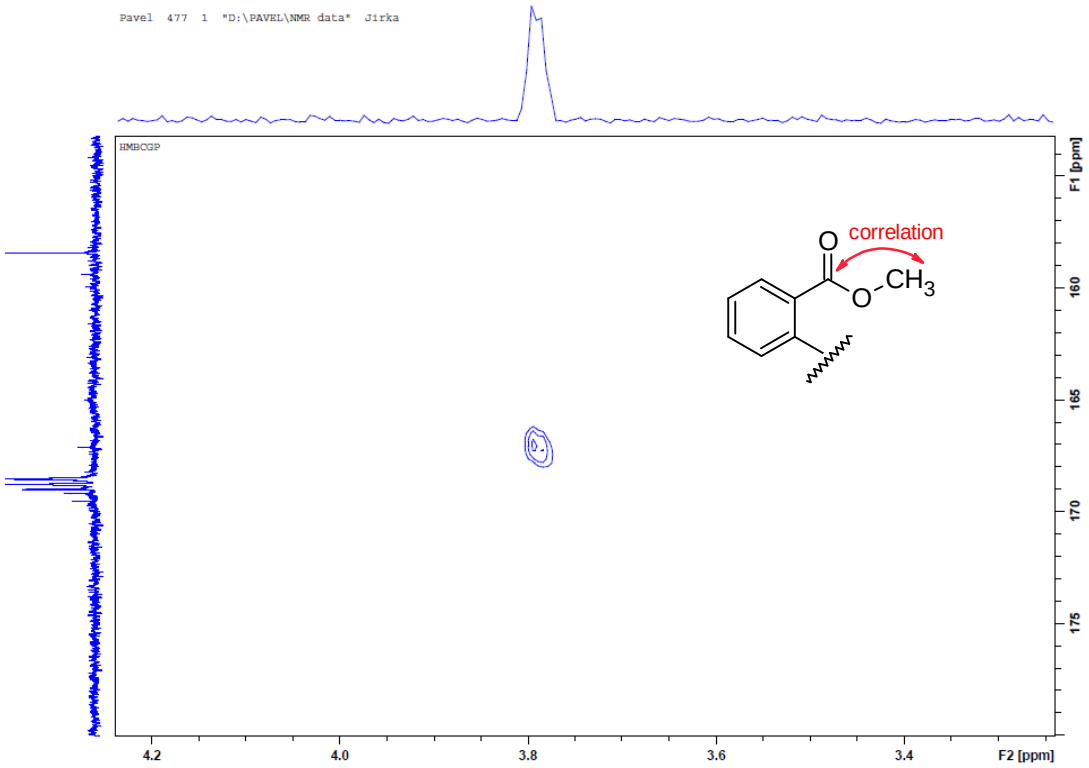

Figure 45 – HMBC Spectrum showing long-range correlation in ester function of trapped intermediate ***XXXI***.

The very important information about the reaction course could provide the preparation of the enantiomerically pure isothiouronium salt of **9a** and studying, if a racemisation occurs during the transformation. I have done many experiments to prepare the chiral salt but all of them were unsuccessful. In addition, the separation on the chiral column did not succeed. It was probably caused by the low stability of isothiouronium salts.

It is possible to conclude that there are three limiting mechanisms for the transformation of the isothiouronium salts **9** to thioureas **10**. The classical two step S_N1 mechanism, the frontside S_N2 mechanism and the double-displacement mechanism. The most of the previously mentioned observations are in accordance with the double displacement mechanism for the transformation of **9a** to **10a**.

4 Experimental section

4.1 Experimental equipment

4.1.1 Used chemicals

All chemicals were purchased from commercial suppliers (Sigma-Aldrich, Acros Organics, Merck) and used without further purification. The solvents were dried and distilled before the use.

4.1.2 Elemental analysis

The microanalyses were performed on an apparatus of Fisons Instruments EA 1108 CHN.

4.1.3 NMR spectroscopy

^{1}H and ^{13}C NMR spectra were recorded on a Bruker Avance 500 (400) MHz instrument in DMSO-d_6 solution. Chemical shifts are referenced to solvent residual peak δ(DMSO-d_6) = 2.50 (^{1}H) and 39.6 ppm (^{13}C). Coupling constants J are quoted in Hz. ^{13}C NMR spectra were measured in a standard way and by means of the APT (attached proton test) pulse sequence to distinguish CH, CH_3 and CH_2, C_{quart}. Proton–proton connectivities were found by *gs*-COSY. Protonated carbon atoms were assigned by *gs*-HSQC spectra. All NMR experiments were performed with the aid of the manufacturer's software.

4.1.4 Mass spectrometry

HRMS spectra were recorded on a Bruker MicrOTOF-Q Mass Spectrometer using Electrospray Ionisation (ESI) in positive mode. Accurate masses were done on either the (M+H) ion or the (M+Na) ion.

The mass spectra (EI) were recorded on an Agilent Technologies Co. gas chromatograph 6890N with a mass detector 5973 Network for samples dissolved on either dichloromethane or acetone.

4.1.5 IRMPD-spectroscopy

The gas-phase infrared (IR) spectra of mass-selected ions were recorded using a Bruker Esquire 3000 ion trap mounted to a free electron laser at CLIO (Centre Laser Infrarouge Orsay, France). The free electron laser (FEL) was operated in the 44 MeV electron-energy range and it provided light in a 1000 – 1800 cm^{-1} range. The relative spectral line width of

the FEL is of about 1% and the precision of the measurement of the wave numbers with a monochromator is about 1 cm^{-1}. Each point in a raw spectrum is an average of 20 measurements. The ions were generated by electrospray ionization as described above. The ions were mass-selected and stored in the ion trap. The fragmentation was induced by 5 to 10 laser macropulses of 8 μs admitted to the ion trap and the dependence of the fragmentation intensities on the wavelength of the IR light gives the infrared multiphoton dissociation (IRMPD) spectra. The reported IRMPD spectra are averages of 2 raw spectra and are not corrected for the power of the free-electron laser, which slightly changes in dependence of the wavenumbers.[196]

4.1.6 Buffer solution preparation

The stock solutions of imidazole, *N*-methylmorphline, tris(hydroxymethyl)aminomethane (TRIS), glycinamide and morpholine buffers were prepared by partial neutralization of appropriate amines by hydrochloric acid. The solutions of dichloroacetate, chloroacetate, methoxyacetate, acetate, propanoate and pivaloate buffers were prepared by partial neutralization of acid by NaOH or KOH. Hydroxylamine and aminoacetonitrile buffers were prepared by partial neutralization of hydrochlorides of amines. Appropriate amount of this solutions was pipetted do 25 ml volumetric flasks and filled in with calculated amount of 2 $mol \cdot l^{-1}$ KCl and redistilled water to ionic strength I = 1 $mol \cdot l^{-1}$. The solvent kinetic isotope effect was measured in chloroacetate and acetate buffers (c_B/c_{BH} = 1:1) of the same composition and ionic strength, which were prepared from potassium chloride, sodium hydroxide, chloroacetic anhydride/acetic anhydride and H_2O or D_2O (99.8% D).

4.1.7 pH Measurements

The pH of individual buffers was measured using PHM 93 Radiometer Copenhagen apparatus equipped with glass electrode. The electrode was calibrated using two buffers Radiometer IUPAC series.

4.1.8 Kinetic measurements

Kinetic measurements were carried out in 1 cm closable cell using a Hewlett Packard 8453 Diode Array Spectrophotometer at 25 ± 0.1 °C. The observed pseudo-first order rate constants k_{obs} were calculated from absorbance-time dependences at the wavelengths of 260 and 273 nm using OPKIN software. In typical procedure, 2 ml of buffer were pipetted to the cell and after 5 minutes 15 μL substrate in methanol was added.

The measurements of reactions with half-lives below 2 s were carried out using a Diode Array Stopped-Flow SX.18 MV-R (Applied Photophysics) apparatus. The observed pseudo-first-order rate constants k_{obs} were calculated from the measured time dependence of absorbance with the help of an optimisation program.

4.1.9 Calculations

All calculations were performed using Gaussian 03 software package[197] using MetaCentrum computing facilities. B3LYP[198-201] functional with appropriate basis sets were used for the geometry optimalization. Local minima and transition states were verified by establishing that Hessians have zero and one negative eigenvalues. The total energies were corrected by addition of the zero point energies calculated at the same level of theory. To estimate the effect of the solvent on the energies the COSMO[202] solvation model implemented in Gaussian were used.

The access to the MetaCentrum computing facilities provided under the programme "Projects of Large Infrastructure for Research, Development, and Innovations" LM2010005 funded by the Ministry of Education, Youth, and Sports of the Czech Republic is highly acknowledged.

4.1.10 X-ray Crystallography

The colorless single crystals were grown from DMSO solution. The X-ray diffraction data were collected at 150(2)K on a Nonius KappaCCD diffractometer with graphite-monochromated MoKα radiation (λ = 0.71073 Å). The structures were solved by direct methods (SIR92).[203] All reflections were used in the structure refinement based on F2 by full-matrix least-squares technique (SHELXL97).[204]

4.2 Preparation and characterization of the compounds

_S_-(2-Oxotetrahydrofuran-3-yl)-_N_-substituted isothiouronium bromides (1)[42]

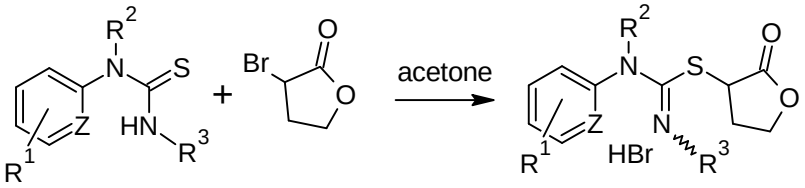

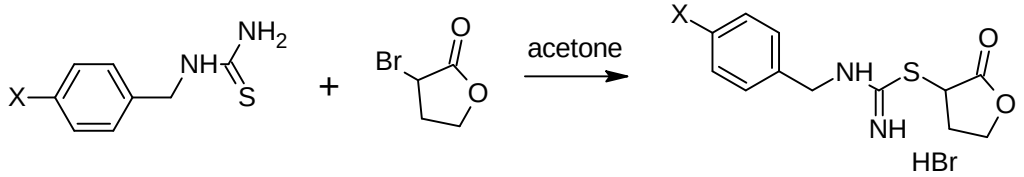

To a hot solution of *N*-arylthioureas (5 mmol) in dry acetone 5 mmol (0.83 g) of 3-bromotetrahydrofuran-2-one was injected. Reaction mixture was refluxed for 5 min and left to stand at room temperature for 2 days. Then precipitated crystals were collected by filtration.

_S_-(2-Oxotetrahydrofuran-3-yl)-_N_-phenyl isothiouronium bromide (1a)

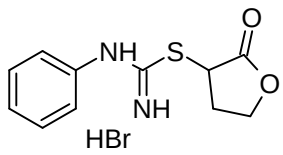

yield: 78 %

m.p.: 153-155 °C

Elemental analysis for $C_{11}H_{13}BrN_2O_2S$: Calculated 41.65 % C; 4.13 % H; 25.19 Br; 8.83 % N; 10.11 % S. Found 41.74 % C; 4.13 % H; 25.05 % Br; 9.01 % N; 10.16 % S

_S_-(2-Oxotetrahydrofuran-3-yl)-_N_-(4-methoxyphenyl) isothiouronium bromide (1b)

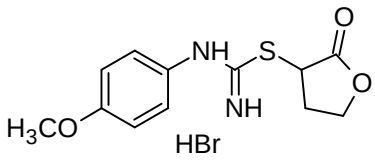

yield: 44 %

m.p.: 154-156 °C

^{1}H-NMR (500 MHz, DMSO) δ 10.79 (bs, 3H), 7.37 (d, 2H, J = 9.0 Hz), 7.16 (d, 2H, J = 9 Hz), 4.72 (dd, 1H, J = 7.5, 4.5 Hz) 3.82 (s, 3H), 3.65 (m, 2H), 2.29 (m, 2H)

^{13}C-NMR (125 MHz, DMSO) δ 175.0, 174.1, 160.7, 129.6, 123.6, 115.3, 57.8, 55.7 47.5, 33.6

Elemental analysis for $C_{12}H_{15}BrN_2O_3S$: Calculated 41.51 % C; 4.35 % H; 23.01 Br; 8.07 % N; 9.23 % S. Found 41.56 % C; 4.29 % H; 22.99 % Br; 8.07 % N; 9.08 % S

_S_-(2-Oxotetrahydrofuran-3-yl)-_N_-(4-methylphenyl) isothiouronium bromide (1c)

yield: 50 %

m.p.: 160-164 °C

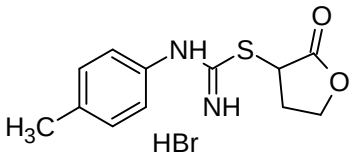

Elemental analysis for $C_{12}H_{15}BrN_2O_2S$: Calculated 43.51 % C; 4.56 % H; 24.12 Br; 8.46 % N; 9.68 % S. Found 43.71 % C; 4.60 % H; 24.32 % Br; 8.26 % N; 9.45 % S

_S_-(2-Oxotetrahydrofuran-3-yl)-_N_-phenyl-_N_-methyl isothiouronium bromide (1h)

yield: 78 %

m.p.: 155-159 °C

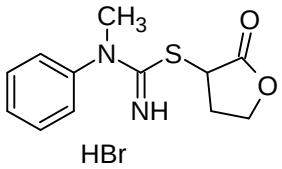

Elemental analysis for $C_{12}H_{15}BrN_2O_2S$: Calculated 41.51 % C; 4.56 % H; 24.12 Br; 8.46 % N; 9.68 % S. Found 43.51 % C; 4.86 % H; 24.03 % Br; 8.35 % N; 9.90 % S

_S_-(2-Oxotetrahydrofuran-3-yl)-_N_-phenyl-_N_-ethyl isothiouronium bromide (1i)

yield: 92 %

m.p.: 155-157 °C

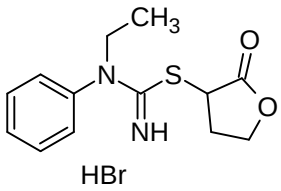

Elemental analysis for $C_{13}H_{17}BrN_2O_2S$: Calculated 45.23 % C; 4.96 % H; 23.14 Br; 8.11 % N; 9.29 % S. Found 45.14 % C; 5.11 % H; 23.20 % Br; 8.08 % N; 9.03 % S

_S_-(2-Oxotetrahydrofuran-3-yl)-_N_-(4-methoxyphenyl)-_N_-methyl isothiouronium bromide (1k)

yield: 53 %

m.p.: 164-167 °C

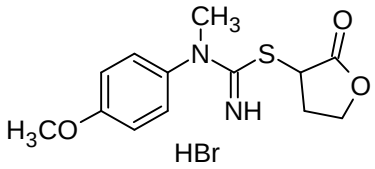

Elemental analysis for $C_{13}H_{17}BrN_2O_3S$: Calculated 43.22 % C; 4.74 % H; 22.12 Br; 7.75 % N; 8.87 % S. Found 43.06 % C; 4.80 % H; 22.03 % Br; 7.66 % N; 8.68 % S

_S_-(2-Oxotetrahydrofuran-3-yl)-_N_-phenyl-_N'_-ethyl isothiouronium bromide (1m)

yield: 75 %

m.p.: 144-146 °C

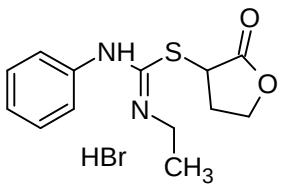

Elemental analysis for $C_{13}H_{17}BrN_2O_2S$: Calculated 45.23 % C;

4.96 % H; 23.14 Br; 8.11 % N; 9.29 % S. Found 45.43 % C; 5.08 % H; 23.14 % Br; 7.96 % N; 9.10 % S

_S_-(2-Oxotetrahydrofuran-3-yl)-_N_-(4-methoxybenzyl) isothiouronium bromide (1p)

yield: 72 %

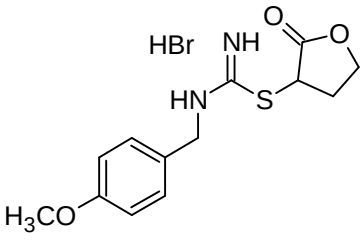

m.p.: 173-175 °C

^{1}H-NMR (400 MHz, DMSO) δ 11.48 (bs, 2H), 7.33 (d, 2H, J = 8.8 Hz), 6.95 (d, 2H, J = 8.8 Hz), 4.98 (m, 2H), 4.80 (q, 1H, J = 4.4 Hz), 3.77 (s, 3H), 3.64-3.60 (m, 2H), 2.36-2.32 (m, 1H), 2.21-2.12 (m, 1H)

^{13}C-NMR (100 MHz, DMSO) δ 174.9, 174.0, 159.3, 129.3, 125.7, 114.2, 58.2, 55.3, 47.5, 45.8, 33.9

Elemental analysis for $C_{13}H_{17}BrN_2O_3S$: Calculated 43.22 % C; 4.74 % H; 22.12 Br; 7.75 % N; 8.88 % S. Found 43.48 % C; 5.01 % H; 22.22 % Br; 7.71 % N; 9.07 % S

_S_-(2-Oxotetrahydrofuran-3-yl)-_N_-benzyl isothiouronium bromide (1o)

yield: 50 %

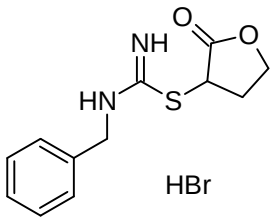

m.p.: 160-163 °C

^{1}H-NMR (400 MHz, DMSO) δ 11.31 (s, 2H), 7.39-7.31 (m, 5H), 5.06-4.97 (m, 2H), 4.81 (q, 1H, J = 4 Hz), 3.63-3.56 (m, 2H), 2.35-2.28 (m, 1H), 2.18-2.10 (m, 1H)

^{13}C-NMR (100 MHz, DMSO) δ 174.7, 174.0, 133.5, 128.7, 128.0, 127.1, 58.0, 47.4, 45.9, 33.8

Elemental analysis for $C_{12}H_{15}BrN_2O_2S$: Calculated 43.51 % C; 4.56 % H; 24.12 Br; 8.46 % N; 9.68 % S. Found 43.74 % C; 4.77 % H; 23.92 % Br; 8.30 % N; 9.44 S %

2-(Subst. phenylamino)-5-(2-hydroxyethyl)-1,3-thiazol-4(5*H*)-ones (2)

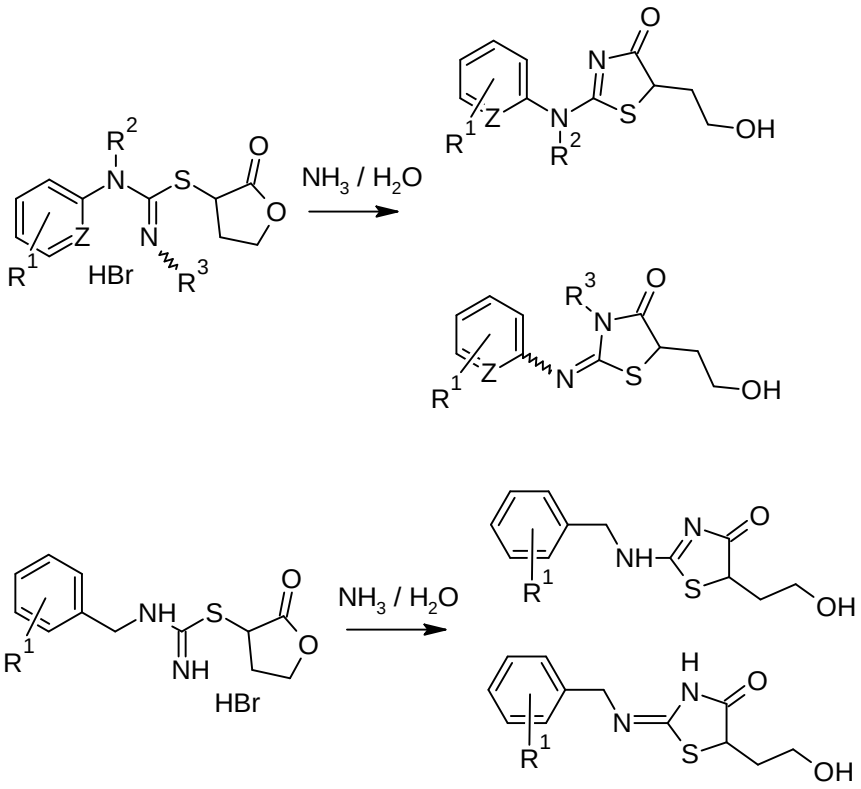

Isothiouronium salts (2 mmol) were dissolved in a minimum amount of aqueous ammonia (25 %) and solution was stirred until precipitation of products. Crude products (yields 80–90 %) were filtered off and recrystallized from water.

5-(2-Hydroxyethyl)-2-(phenylimino)-1,3-thiazolidin-4-one (2a)

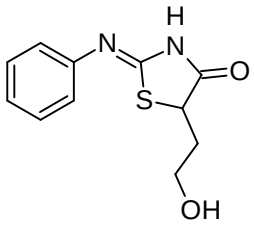

yield: 94 %

m.p.: 123-124 °C

^{1}H-NMR (500 MHz, DMSO) δ 11.71 (bs, 1H), 11.14 (bs, 1H), 7.36 (m, 2H), 7.12 (m, 1H), 7.72 (m, 1H), 7.00 (m, 1H), 4.74 (m, 1H), 4.29 (m, 1H), 3.45 (m, 2H), 2.26 (m, 1H), 1.79 (m, 1H)

^{13}C-NMR (125 MHz, DMSO) δ 178.5 and 177.5, 146.8 and 138.9, 129.4 and 129.1, 124.8 and 124.7, 121.6 and 120.5, 59.6 and 58.8, 52.1 and 47.7, 36.6 and 36.0

Elemental analysis for $C_{11}H_{12}N_2O_2S$: Calculated 55.91 % C; 5.12 % H; 11.86 % N; 13.57 % S. Found 56.13 % C; 5.32 % H; 11.62 % N; 13.35 % S

EI-MS: m/z 236, 218, 205, 192, 160, 151, 145, 135, 118 (100 %), 109, 101, 91, 77, 71, 65, 59, 51.

5-(2-Hydroxyethyl)-2-[(4-methoxyphenyl)imino]-1,3-thiazolidin-4-one (2b)

yield: 91 %

m.p.: 124-126 °C

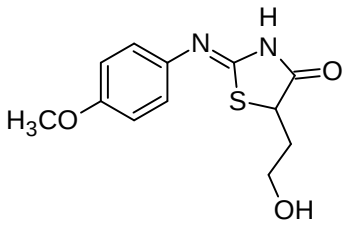

^{1}H-NMR (500 MHz, DMSO) δ 11.56 (bs, 1H), 11.02 (bs, 1H), 7.60 (m, 1H), 6.99 (m, 1H), 6.94 (m, 2H), 4.73 (m, 1H), 4.26 (dt, 1H, J = 11.8, 3.5 Hz), 3.74 (s, 3H), 3.52 (m, 2H), 2.27 (m, 1H), 1.76 (m, 1H)

^{13}C-NMR (125 MHz, DMSO) δ 190.3, 176.6, 156.7 and 156.2, 131.9, 123.3 and 121.9, 114.4 and 114.0, 59.5 and 58.8, 55.2, 52.0 and 48.4, 36.5 and 36.0

Elemental analysis for $C_{12}H_{14}N_2O_3S$: Calculated 55.12 % C; 5.30 % H; 10.52 % N; 12.04 % S. Found 55.24 % C; 5.26 % H; 10.64 % N; 12.01 % S

EI-MS: m/z 266, 248, 235, 222, 207, 191, 175, 165, 148, 133 (100 %), 118, 105, 90, 78, 63, 55, 41

5-(2-Hydroxyethyl)-2-[(4-methylphenyl)imino]-1,3- thiazolidin-4-one (2c)

yield: 87 %

m.p.: 124-126 °C

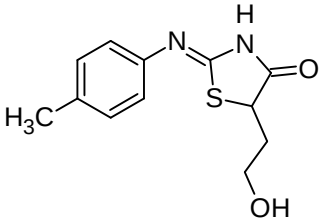

^{1}H-NMR (500 MHz, DMSO) δ 11.64 and 11.08 (vbd, 1H), 7.59 (d, 1H, J = 7.7 Hz), 7.15 (m, 2H), 6.91 (d, 1H, J = 7.4 Hz), 4.75 (m, 1H), 4.27 (m, 1H), 3.52 (m, 2H), 2.30 (m, 1H), 2.27 (s, 3H) 1.79 (m, 1H)

^{13}C-NMR (125 MHz, DMSO) δ 190.6, 179.4 and 177.1, 143.3 and 136.5, 134.0, 129.8 and 129.5, 121.7 and 120.4, 59.7 and 58.9, 52.1 and 48.1, 36.7 and 36.1, 20.3

Elemental analysis for $C_{12}H_{14}N_2O_2S$: Calculated 57.58 % C; 5.64 % H; 11.19 % N; 12.81 % S. Found 57.59 % C; 5.69 % H; 10.93 % N; 12.74 % S

5-(2-Hydroxyethyl)-2-[(4-chlorophenyl)imino]-1,3-thiazolidin-4-one (2d)

yield: 97 %

m.p.: 136-137 °C

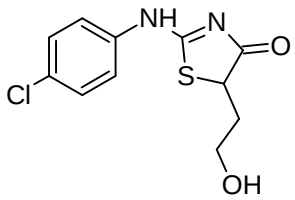

^{1}H-NMR (500 MHz, DMSO) δ 11.80 and 11.26 (vbd, 1H), 7.77 (d, 1H, J = 7.3 Hz), 7.42 (d, 1H, J = 8.5 Hz), 7.37 (d, 1H, J = 7.7 Hz), 6.96 (d, 1H, J = 7.5 Hz), 4.75 (bs, 1H), 4.31 (m, 1H), 3.52 (m, 2H), 2.25 (m, 1H), 1.79 (m, 1H)

^{13}C-NMR (125 MHz, DMSO) δ 190.5, 177.7 and 177.4, 146.7 and 137.1, 129.3 and 129.1, 128.6, 123.3 and 122.0, 59.6 and 58.7, 52.2 and 47.5, 36.5 and 35.8

Elemental analysis for $C_{11}H_{11}ClN_2O_2S$: Calculated 48.80 % C; 4.10 % H; 13.10 % Cl; 10.35 % N; 11.84 % S. Found 49.01 % C; 4.27 % H; 12.94 % Cl; 10.08 % N; 11.60 % S

5-(2-Hydroxyethyl)-2-[(4-bromophenyl)imino]-1,3-thiazolidin-4-one (2e)

yield: 61 %

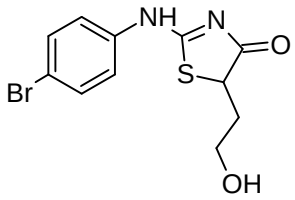

m.p.: 140-141 °C

^{1}H-NMR (500 MHz, DMSO) δ 11.70 and 11.37 (vbd, 1H), 7.67 (d, 1H, J = 7.5 Hz), 7.56 (d, 1H, J = 9.5 Hz), 7.51 (d, 1H, J = 8.5 Hz), 6.91 (d, 1H, J = 8.5 Hz), 4.77 (bs, 1H), 4.31 (m, 1H), 3.50 (m, 2H), 2.26 (m, 1H), 1.81 (m, 1H)

^{13}C-NMR (125 MHz, DMSO) δ 190.6, 177.6, 147.1 and 138.3, 132.3 and 132.0, 123.7 and 122.4, 116.7, 59.6 and 58.7, 52.1 and 47.5, 36.5 and 35.8

Elemental analysis for $C_{11}H_{11}BrN_2O_2S$: Calculated 41.92 % C; 3.52 % H; 25.35 % Cl; 8.89 % N; 10.17 % S. Found 41.93 % C; 3.71 % H; 24.98 % Cl; 8.78 % N; 10.40 % S

5-(2-Hydroxyethyl)-2-[(3-trifluormethylphenyl)-imino]-1,3-thiazolidin-4-one (2f)

yield: 53 %

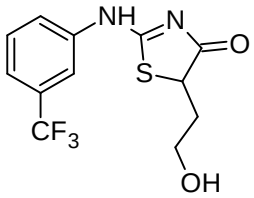

m.p.: 130-131 °C

^{1}H-NMR (500 MHz, DMSO) δ 11.56 and 11.02 (vbd, 1H), 8.22-7.79 (m, 1H), 7.60 (m, 1H), 7.48 (m, 1H), 7.24 (m, 1H), 4.78 (m, 1H), 4.3 (d, 1H, J = 6.0 Hz), 3.52 (m, 2H), 2.26 (m, 1H), 1.83 (m, 1H)

^{13}C-NMR (125 MHz, DMSO) δ 190.6, 178.3 and 176.9, 149.1 and 139.6, 130.6 and 125.2, 130.5 and 124.0, 120.8 and 117.8, 121.1 and 116.6, 130.1, 124.1, 59.6 and 58.6, 52.2 and 47.4, 36.4 and 35.6

Elemental analysis for $C_{12}H_{11}F_3N_2O_2S$: Calculated 47.37 % C; 3.46 % H; 9.21 % N; 10.54 % S. Found 47.56 % C; 3.67 % H; 9.42 % N; 10.31 % S

5-(2-Hydroxyethyl)-2-[(2-pyridyl)imino]-1,3-thiazolidin-4-one (2g)

yield: 84 %

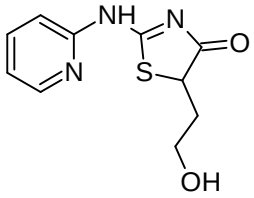

m.p.: 187-188 °C

^{1}H-NMR (500 MHz, DMSO) δ 11.93 (bs, 1H), 8.42 (m, 1H), 7.82 (m, 1H), 7.11 (m, 2H), 4.78 (bs, 1H), 4.10 (d, 1H, J = 7.0 Hz), 3.58 (m, 2H), 2.22 (m, 1H), 1.82 (m, 1H)

^{13}C-NMR (125 MHz, DMSO) δ 180.7, 165.3, 156.2, 146.9, 138.7, 119.8, 118.2, 58.9, 47.2, 39.5

Elemental analysis for $C_{10}H_{11}N_3O_2S$: Calculated 50.62 % C; 4.67 % H; 17.71 % N; 13.41 % S. Found 50.52 % C; 4.44 % H; 17.76 % N; 13.64 % S

EI-MS: m/z 237, 206, 119 (100 %), 78, 55, 44

5-(2-Hydroxyethyl)-2-[(*N*-phenyl-*N*-methyl)amino]-4,5-dihydro-1,3-thiazol-4-one (2h)

yield: 80 %

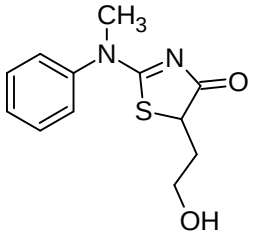

m.p.: 112-115 °C

^{1}H-NMR (500 MHz, DMSO) δ 7.47 (m, 5H), 4.69 (bs, 1H), 4.21 (d, 1H, J = 10.9 Hz), 3.50 (s, 3H), 3.44 (m, 2H), 2.24 (m, 1H), 1.67 (m, 1H)

^{13}C-NMR (125 MHz, DMSO) δ 189.3, 181.9, 142.2, 130.0, 129.3, 127.1, 59.6, 54.7, 41.8, 36.5

Elemental analysis for $C_{12}H_{14}N_2O_2S$: Calculated 57.58 % C; 5.64 % H; 11.19 % N; 12.81 % S. Found 57.53 % C; 5.56 % H; 10.90 % N; 12.76 % S

5-(2-Hydroxyethyl)-2-[(*N*-phenyl-*N*-ethyl)amino]- 4,5-dihydro-1,3-thiazol-4-one (2i)

yield: 90 %

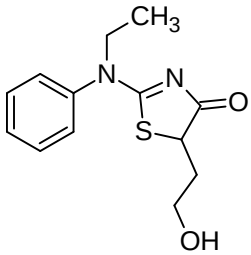

m.p.: 158-160 °C

^{1}H-NMR (500 MHz, DMSO) δ 7.52 (m, 3H), 7.45 (m, 2H), 4.68 (t, 1H, J = 4.8 Hz), 4.23 (dd, 1H, J = 10.6, 3.1 Hz), 4.01 (m, 2H), 3.46 (m, 2H), 2.26 (m, 1H), 1.67 (m, 1H), 1.12 (t, 3H, J = 7.1 Hz)

^{13}C-NMR (125 MHz, DMSO) δ 189.5, 181.7, 140.4, 130.0, 129.6, 128.2, 59.6, 54.3, 49.0, 36.5, 12.6

Elemental analysis for $C_{13}H_{16}N_2O_2S$: Calculated 59.07 % C; 6.10 % H; 10.60 % N; 12.13 % S. Found 58.84 % C; 5.92 % H; 10.76 % N; 12.31 % S

5-(2-Hydroxyethyl)-2-diphenylamino-4,5-dihydro-1,3-thiazol-4-one (2j)

yield: 60 %

m.p.: 153-155 °C

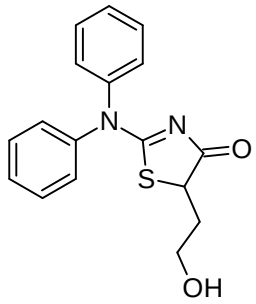

^{1}H-NMR (500 MHz, DMSO) δ 7.63-7.33 (m, 10H), 4.73 (t, 1H, J = 5.0 Hz), 4.26 (dd, 1H, J = 7.5, 3.0 Hz), 3.47 (m, 2H), 2.27 (m, 1H), 1.74 (m, 1H)

^{13}C-NMR (125 MHz, DMSO) δ 189.7, 183.2, 129.9, 129.1, 128.5, 126.5, 59.4, 54.5, 36.1

Elemental analysis for $C_{17}H_{16}N_2O_2S$: Calculated 65.36 % C; 5.16 % H; 8.97 % N; 10.26 % S. Found 65.12 % C; 5.27 % H; 8.79 % N; 10.44 % S

5-(2-Hydroxyethyl)-2-[(*N*-(4-methoxyphenyl)-*N*-methyl)amino]-4,5-dihydro-1,3-thiazol-4-one (2k)

yield: 79 %

m.p.: 119-120 °C

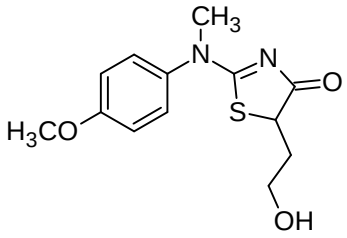

^{1}H-NMR (500 MHz, DMSO) δ 7.41 (d, 2H, J = 8.5 Hz), 7.05 (d, 2H, J = 8.5 Hz), 4.76 (t, 1H, J = 5.5 Hz), 4.18 (dd, 1H, J = 10.5, 3.0 Hz), 3.80 (s, 3H), 3.45 (m, 2H), 3.36 (s, 3H), 2.23 (m, 1H), 1.66 (m, 1H)

^{13}C-NMR (125 MHz, DMSO) δ 189.2, 182.1, 159.4, 134.8, 128.3, 114.8, 59.5, 55.4, 54.6, 41.7, 35.4

Elemental analysis for $C_{13}H_{16}N_2O_3S$: Calculated 55.70 % C; 5.75 % H; 9.99 % N; 11.44 % S. Found 56.03 % C; 5.96 % H; 10.32 % N; 11.76 % S

5-(2-Hydroxyethyl)-2-[(4-methoxyphenyl)imino]-3-methyl-1,3-thiazolidin-4-one (2l)

yield: 57 %

m.p.: 101-103 °C

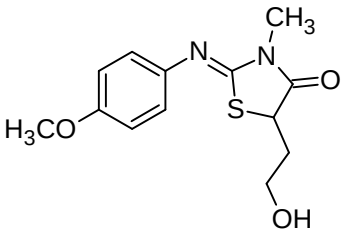

^{1}H-NMR (500 MHz, DMSO) δ 6.91 (m, 4H), 4.76 (bs, 1H), 4.33 (dd, 1H, J = 9.7, 3.5 Hz), 3.73 (s, 3H), 3.51-3-43 (m, 2H), 3.16 (s, 3H), 2.28 (m, 1H), 1.83 (m, 1H)

^{13}C-NMR (125 MHz, DMSO) δ 174.6, 156.0, 154.4, 141.2, 122.0, 114.3, 58.4, 55.1, 45.2, 35.8, 29.2

Elemental analysis for $C_{13}H_{16}N_2O_3S$: Calculated 55.70 % C; 5.75 % H; 9.99 % N; 11.44 % S. Found 55.81 % C; 5.54 % H; 10.37 % N; 11.21 % S

EI-MS: m/z 264 (100 %), 233, 221, 205, 192, 177, 163, 146, 131, 118, 104, 91, 77, 65, 55, 45, 35

5-(2-Hydroxyethyl)-2-(4-phenylimino)-3-ethyl-1,3-thiazolidin-4-one (2m)

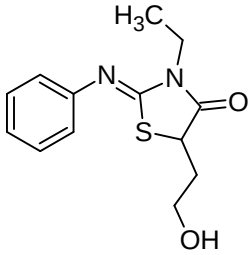

yield: 33 %

m.p.: oil

^{1}H-NMR (500 MHz, DMSO) δ 7.35 (t, 2H, J = 7.4 Hz), 7.11 (t, 1H, J = 7.3 Hz), 6.96 (d, 2H, J = 7.3 Hz), 4.75 (bs, 1H), 4.34 (dd, 1H, J = 9.6, 3.7 Hz), 3.77 (q, 2H, J = 7.0 Hz), 3.58-3.43 (m, 2H), 2.24 (m, 1H), 1.84 (m, 1H), 1.18 (t, 3H, J = 7.0 Hz)

^{13}C-NMR (125 MHz, DMSO) δ 174.4, 154.0, 148.3, 129.2, 124.2, 121.0, 58.3, 45.3, 37.4, 35.7, 12.3

Elemental analysis for $C_{13}H_{16}N_2O_2S$: Calculated 59.07 % C; 6.10 % H; 10.60 % N; 12.13 % S. Found 58.71 % C; 5.96 % H; 10.86 % N; 11.88 % S

EI-MS: m/z 264 (100 %), 233, 221, 205, 192, 177, 163, 146, 131, 118, 104, 91, 77, 65, 55, 45, 35

5-(2-Hydroxyethyl)-2-[(4-chlorophenyl)imino]-3-methyl-1,3-thiazolidin-4-one (2n)

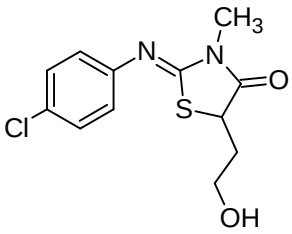

yield: 63 %

m.p.: 87-89 °C

^{1}H-NMR (500 MHz, DMSO) δ 7.40 (d, 2H, J = 8.5 Hz), 6.96 (d, 2H, J = 8.5 Hz), 4.75 (t, 1H, J = 5.0 Hz), 4.36 (dd, 1H, J = 9.8, 3.6 Hz), 3.54-3.45 (m, 2H), 3.16 (s, 3H), 2.27 (m, 1H), 1.86 (m, 1H)

^{13}C-NMR (125 MHz, DMSO) δ 174.3, 155.6, 147.0, 128.9, 128.0, 122.6, 58.1, 45.3, 35.3, 29.0

Elemental analysis for $C_{12}H_{13}ClN_2O_2S$: Calculated 50.61 % C; 4.60 % H; 9.84 % N; 11.26 % S. Found 50.35 % C; 4.63 % H; 10.15 % N; 11.02 % S

2-(Benzylamino)-5-(2-hydroxyethyl)-1,3-thiazol-4(5*H*)-one (2o)

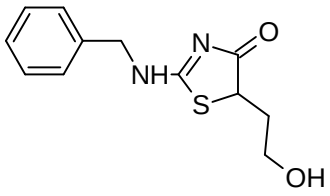

yield: 67 %

m.p.: 120-122 °C

^{1}H-NMR (400 MHz, DMSO) δ 10.20-9.66 (bd, 1H), 7.40-

7,33 (m, 5H), 4.82 (s, 1H), 4.71-4.45 (m, 2H), 4.31-4.25 (m, 1H), 3.60 (s, 2H), 2.33 (s, 1H), 1.77 (s, 1H)

^{13}C-NMR (100 MHz, DMSO) δ 189.5, 179.8, 137.5 and 137.0, 128.6 and 128.5, 127.6 and 127.5, 127.4 and 127.3, 59.6 and 59.5, 53.0 and 52.6, 48.0 and 47.7, 36.7 and 36.4

Elemental analysis for $C_{12}H_{14}N_2O_2S$: Calculated 57.58 % C; 5.64 % H; 11.19 % N; 12.81 % S. Found 57.78 % C; 5.71 % H; 11.02 % N; 12.62 % S

5-(2-Hydroxyethyl)-2-[(4-methoxybenzyl)amino]-1,3-thiazol-4(5*H*)-one (2p)

yield: 81 %

m.p.: 92-95 °C

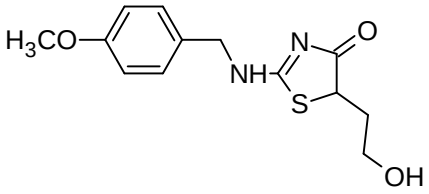

^{1}H-NMR (400 MHz, DMSO) δ 9.55 (bs, 1H), 7.23 (d, 2H, J = 8.8 Hz), 6.91 (d, 2H, J = 8.8 Hz) , 4.75 (s, 1H), 4.60-4.40 (m, 2H), 4.27-4.20 (m, 1H), 3.78 (s, 3H), 3.58-3.50 (m, 2H), 2.35-2.27 (m, 1H), 1.72-1.66 (s, 1H)

^{13}C-NMR (100 MHz, DMSO) δ 189.2, 179.3, 158.5, 129.3, 127.6, 129.0, 128.7, 59.5, 55.0, 52.8, 47.1, 36.7, 36.4

Elemental analysis for $C_{13}H_{16}N_2O_3S$: Calculated 55.70 % C; 5.75 % H; 9.99 % N; 11.44 % S. Found 55,51 % C; 5.59 % H; 10.17 % N; 11.68 % S

6-Nitrophthalide[205]

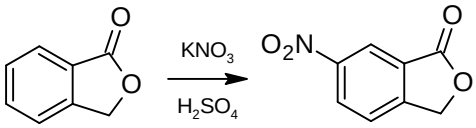

The solution of phthalide (0.22 mol; 30 g) in conc. H_2SO_4 (38 ml) was cooled to 0 °C. After cooling, solution of KNO_3 (0.28 mol; 28 g) in conc. H_2SO_4 (60 ml) was added dropwise during 45 minutes. After mixing for 1 h at 20 °C the mixture was poured on to ice and filtered off. Recrystalization from ethanol gives 24 g (60 %) with m. p. 135-137 °C (lit.[205] 140-142 °C).

6-Aminophthalide

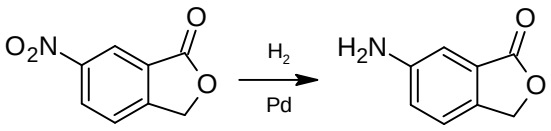

6-Nitrophtalide (55 mmol; 10 g) was suspended with 1.2 g Pd/C in 500 ml of EtOAc. The hydrogen gas was bubbled through this mixture for 3 days. After filtration, evaporation of solvent and recrystalization from EtOH, 7.1 g (8.6 %) of the product with m. p. 175-178 °C (lit.[206] 182-183 °C) was obtained.

6-Chlorophthalide[207]

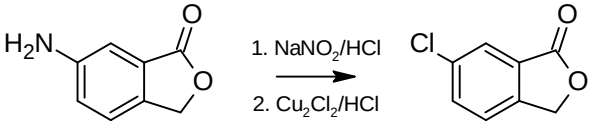

6-Aminophthalide (52 mmol; 7.75 g) was dissolved in conc. HCl (20 ml) and cooled to 0 °C. This solution was slowly diazotizated with saturated $NaNO_2$ (50 mmol; 3.44 g) water solution. Prepared solution was added to the solution of Cu_2Cl_2 (50 mmol; 5 g) in conc. HCl (10 ml). The precipitate was filtered off and recrystalized from EtOH/H_2O giving 4.76 g (55 %) with m. p. 106-109 °C (lit.[207] 107-108 °C).

6-Methoxyphthalide[208]

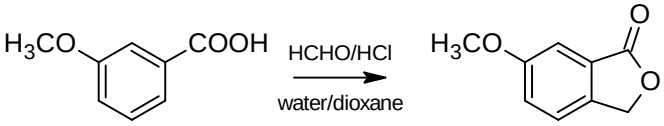

Into the 500 ml flask was added 3-methoxybenoic acid (79 mmol; 12 g), dioxane (70 ml), conc. HCl (80 ml) and 40 % formaldehyde water solution (50 ml). The mixture was heated to 70 °C for 5 days. After cooling 200 ml of water and 400 ml of DCM were added and organic layer was separated. Water residue was extracted by of DCM (2 x 250 ml). Combined extracts were washed with brine, dried over Na_2SO_4 and evaporated. Crude product was purified by flash chromatography (hexane/ethyl acetate 3:1). Overal yield 4.3 g (34 %) with m. p. 122-125 °C (lit[208] 124-126 °C) was obtained.

Isochromanone[209]

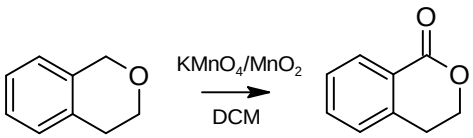

In 500 ml flask were dissolved isochromane (22 mmol; 3 g) in dichloromethane (250 ml). During next 15 minutes was added carefully spreaded mixture of $KMnO_4$ (70 mmol; 11 g)

with activated MnO_2 (380 mmol; 33 g). After 20 hours of reflux the reaction mixture was filtered through blue filter paper and evaporated giving 2.7 g (82 %) of oily product.

3,3-Dideuterophthalide[210]

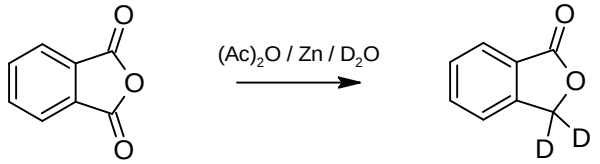

In to 250 ml round bottom flask were added phthalic acid anhydride (68 mmol; 10 g), Zn powder (30 g), dry acetananhydride (80 ml) and D_2O (16 ml). The reaction mixture was refluxed for 24 hours and after cooling filtered and washed by 100 ml of acetone. After the evaporation of the filtrate, crude phthalide was obtained. Recrystalization from water gives 30 % of pure compound.

3-Bromophthalide[211]

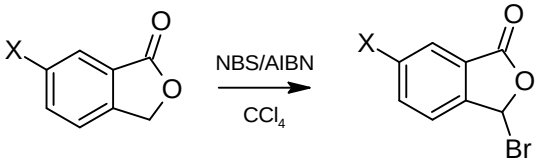

In to the 500 ml round bottom flask were added isochromanone (75 mmol; 10 g), NBS (75 mmol; 13.3 g), tetrachloromethane (100 ml), AIBN (0.05 g). Reaction mixture was refluxed 60 min under the 100 watt bulb irradiation. The end of the reaction was signalized by the presence of *N*-succinimide on the top of the solution. The reaction mixture was filtered and filtrate concentrated to the volume of ca. 10 ml. Cooling the residue and its filtration gives 13 g of crude product that could be recrystalized from cyclohexanone with overall yield of 70 % m. p. 77-79 °C (lit.[211] 78–80 °C).

4-Bromo-3,4-dihydro-1*H*-isochromen-1-one (12d)

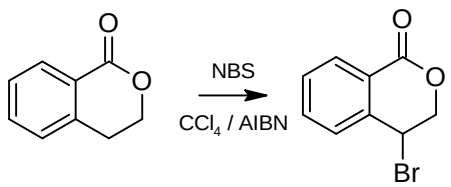

In to the 100 ml round bottom flask were added phthalide (17 mmol; 2.5 g), NBS (17 mmol 3.1 g), tetrachloromethane (40 ml) and AIBN (0.03 g). Reaction mixture was refluxed 30 min under the 100 watt bulb irradiation. The end of the reaction was signalized

by the presence of *N*-succinimide on the top of the solution. The reaction mixture was filtered and filtrate concentrated to the volume of ca. 5 ml. Cooling the residue and its filtration gives 3 g of crude product (m. p. 90-95 °C) that could be recrystalized from chloroform with overall yield of 52 % m. p. 201-203 °C.

4-Bromo-3,4-dihydro-1*H*-isochromen-1-one (12d)

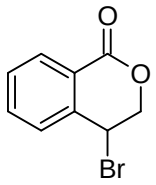

yield: 52 %

m.p.: 201-203 °C

^{1}H-NMR (400 MHz, $CDCl_3$) δ 8.14-8.12 (m, 1H), 7.64 (dt, 1H, *J* = 7.6, 1.6 Hz), 7.54-7.47 (m, 2H), 5.36 (t, 1H, *J* = 3.2 Hz), 4.75 (dq, 2H, *J* = 12.4, 2.8 Hz)

^{13}C-NMR (100 MHz, $CDCl_3$) δ 163.2, 139.4, 134.4, 130.7, 129.9, 127.3, 123.8, 71.9, 41.0

Elemental analysis for $C_9H_7BrO_2$: Calculated 47.61 % C; 3.11 % H; 35.19 Br. Found 47.82 % C; 3.17 % H; 35.26 % Br

EI-MS: m/z 228, 226, 170, 168, 147 (100 %), 141, 130, 119, 102, 91, 85, 77, 63, 51, 39

General procedure for bromination of other substrates (11, 12)

Bromo derivates of other substrates were prepared using the same protocol. Reaction time depends on the structure of substrate, but the end of reaction is still signalized by disappearance on NBS from the bottom of the flask and occurrence of precipitate of succinimide near the surface. Only oily product was obtained in some cases after cooling (**11**) the concentrated solution. This could be used to the next reactions without further purification.

General procedure for preparation of isothiouronium salts (3,5,7,9)[212]

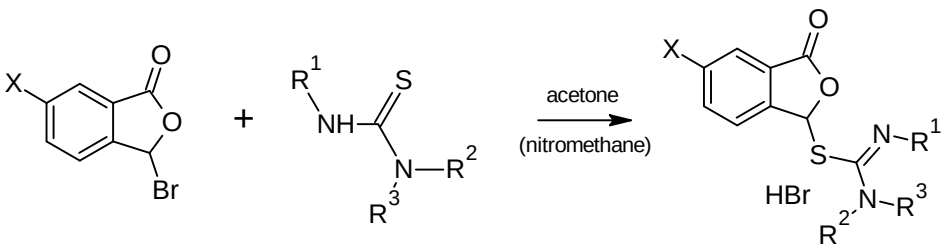

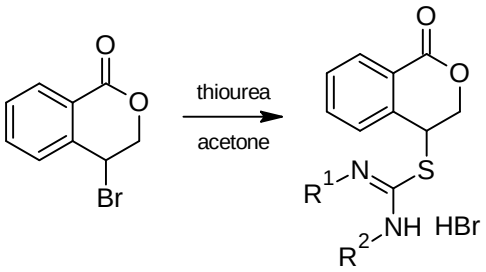

To the hot solution of bromo compound in acetone the saturated solution of equimolar amount of appropriate thiourea in acetone was added. The mixture was refluxed for 5 minutes and let stand overnight. Precipitated crystals were collected by filtration. The recrystalization from the mixture of acetone, methanol and water is possible in some cases. Overall yields strongly depend on the purity and structure of both reaction compounds. In case of **13a** nitromethane was used instead of the acetone as the solvent.

***S*-(3-Oxo-1,3-dihydro-2-benzofuran-1-yl) isothiouronium bromide (3a)**

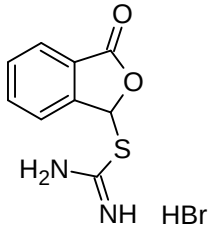

yield: 84 %

m.p.: 206-210 °C

^{1}H-NMR (400 MHz, DMSO) δ 9.62 (bd, 4H, J = 92.4 Hz), 7.99-7.91 (m, 2H), 7.84-7.75 (m, 3H)

^{13}C-NMR (100 MHz, DMSO) δ 167.8, 165.4, 143.3, 135.6, 131.5, 125.8, 124.9, 123.9, 81.3

Elemental analysis for $C_9H_9BrN_2O_2S$: Calculated 37.38 % C; 3.14 % H; 27.63 Br; 9.69 % N; 11.09 % S. Found 37.54 % C; 3.25 % H; 27.41 % Br; 9.85 % N; 10.89 % S

HRMS: Calculated for **$C_9H_9N_2O_2S$** 209.037925 Found 209.037941

***S*-(5-Methoxy-3-oxo-1,3-dihydro-2-benzofuran-1-yl) isothiouronium bromide (3b)**

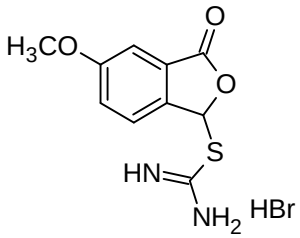

yield: 69 %

m.p.: 213-215 °C

^{1}H-NMR (400 MHz, DMSO) δ 9.76 (s, 2H), 9.49 (s, 2H), 7.81 (s, 1H), 7.71 (d, 1H, J = 8.4 Hz), 7.46 (dd, 1H, J = 8.4, 2.4 Hz), 7.40 (d, 1H, J = 2.0 Hz), 3.86 (s, 3H)

^{13}C-NMR (100 MHz, DMSO) δ 167.8, 165.8, 161.9, 135.4, 126.8, 125.1, 123.7, 108.6, 81.5, 56.3

Elemental analysis for $C_{10}H_{11}BrN_2O_3S$: Calculated 37.63 % C; 3.47 % H; 25.03 Br; 8.78 % N; 10.05 % S. Found 37.75 % C; 3.66 % H; 24.75 % Br; 8.98 % N; 10.32 % S

HRMS: Calculated for **$C_{10}H_{11}BrN_2O_3S$** 239.048489 Found 239.048607

***S*-(5-Chloro-3-oxo-1,3-dihydro-2-benzofuran-1-yl) isothiouronium bromide (3c)**

yield: 81 %

m.p.: 213-215 °C

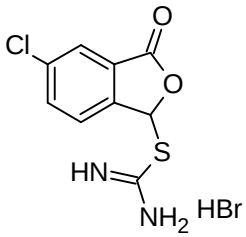

^{1}H-NMR (400 MHz, DMSO) δ 9.83 (s, 2H), 9.57 (s, 2H), 8.07 (d, 1H, *J* = 1.6 Hz), 8.02 (dd, 1H, *J* = 8.4, 2.0 Hz), 7.92-7.89 (m, 2H)

^{13}C-NMR (100 MHz, DMSO) δ 166.7, 165.4, 142.2, 136.3, 135.7, 127.3,
126.0, 125.6, 81.7,

Elemental analysis for $C_9H_8BrClN_2O_2S$: Calculated 33.40 % C; 2.49 % H; 24.69 Br; 10.96 % Cl; 8.66 % N; 9.91 % S. Found 33.54 % C; 2.57 % H; 8.93 % N; 9.73 % S

HRMS: Calculated for **$C_9H_8ClN_2O_2S$** 242.998952 Found 242.999334

***S*-(5-Nitro-3-oxo-1,3-dihydro-2-benzofuran-1-yl) isothiouronium bromide (3d)**

yield: 78 %

m.p: 207-210 °C

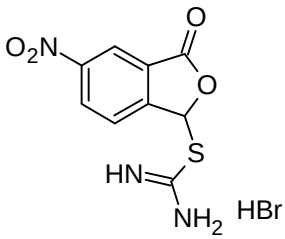

^{1}H-NMR (400 MHz, DMSO) δ 9.84 (s, 2H,), 9.55 (s, 2H), 8.70 (dd, 1H, J = 8.4, 2 Hz), 8.59 (d, 1H, 1.6 Hz), 8.12 (d, 1H, J = 8.4 Hz), 8.00 (s, 1H)

^{13}C-NMR (100 MHz, DMSO) δ 166.1, 165.1, 149.7, 148.9, 130.2, 126.9, 126.0, 120.8, 81.8

Elemental analysis for $C_9H_8BrN_3O_4S$: Calculated 32.35 % C; 2.41 % H; 23.91 Br; 12.58 % N; 9.60 % S. Found 32.65 % C; 2.66 % H; 23.71 % Br; 12.73 % N; 9.74 % S

HRMS: Calculated for **$C_9H_8N_3O_4S$** 254.023003 Found 254.023088

***S*-(3-Oxo-1,3-dihydro-2-benzofuran-1-yl)-*N*-methyl isothiouronium bromide (5a)**

yield: 82 %

m.p.: 203-205 °C

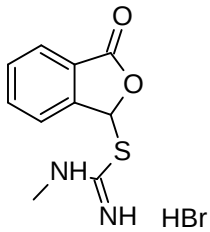

^{1}H-NMR (400 MHz, DMSO) δ 10.35 (bs, 1H), 10.02 (bs, 1H), 9.59 (bs, 1H), 7.41 (d, 1H, *J* = 7.6 Hz), 7.91-7.89 (m, 2H), 7.81 (d, 1H, *J* = 7.6 Hz), 7.74 (t, 1H, *J* = 7.6 Hz), 2.95 (s, 3H)

^{13}C-NMR (100 MHz, DMSO) δ 167.8, 161.4, 143.5, 135.5, 131.4, 125.7, 124.8, 123.8, 82.4, 31.1

Elemental analysis for $C_{10}H_{11}BrN_2O_2S$: Calculated 39.62 % C; 3.66 % H; 26.36 Br; 9.24 % N; 10.58 % S. Found 39.91 % C; 4.08 % H; 26.12 % Br; 9.54 % N; 10.29 % S

HRMS: Calculated for **$C_{10}H_{11}N_2O_2S$** 223.053575 Found 223.054257

***S*-(3-Oxo-1,3-dihydro-2-benzofuran-1-yl)-*N*-propan-2-yl isothiouronium bromide (5b)**

yield: 86 %

m.p.: 55-60 °C

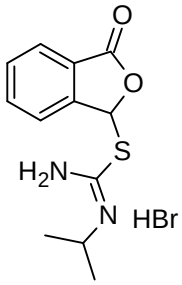

^{1}H-NMR (400 MHz, DMSO) δ 10.25 (d, 1H, *J* = 4 Hz), 9.94 (bs, 1H), 9.60 (bs, 1H), 8.01-7.95 (m, 2H), 7.88-7.8 (m, 2H), 7.83-7.77 (t, 1H, *J* = 7.6 Hz), 4.03-3.94 (m, 1H), 1.60 (dd, 6H, *J* = 14.8, 6.4 Hz)

^{13}C-NMR (100 MHz, DMSO) δ 168.1, 159.0, 143.9, 135.6, 131.4, 125.7, 125.2, 124.1, 83.0, 47.1, 21.1

Elemental analysis for $C_{10}H_{11}BrN_2O_2S$: Calculated 43.51 % C; 4.56 % H; 24.12 Br; 8.46 % N; 9.68 % S. Found 43.78 % C; 4.72 % H; 23.82 % Br; 8.54 % N; 10.13 % S

HRMS: Calculated for **$C_{10}H_{11}N_2O_2S$** 251.084875 Found 251.084861

***S*-(3-Oxo-1,3-dihydro-2-benzofuran-1-yl)-*N*-phenyl isothiouronium bromide (7a)**

yield: 60 %

m.p.: 190-195 °C

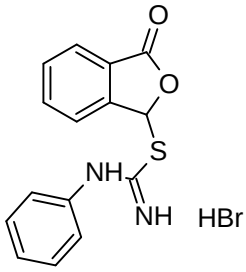

^{1}H-NMR (400 MHz, DMSO) δ 10.31 (bs, 3H), 8.01-7.94 (m, 3H), 7.89 (d, 1H, *J* = 7.6 Hz), 7.76 (t, 1H, *J* = 7.6 Hz), 7.51 (t, 2H, *J* = 7.6 Hz), 7.41 (t, 1H, *J* = 7.2Hz), 7.29 (d, 2H, *J* = 7.6 Hz)

^{13}C-NMR (100 MHz, DMSO) δ 167.8, 161.9, 143.6, 135.51, 134.7, 131.4, 129., 128.4, 125.6, 124.9, 124.8, 124.0, 82.6

Elemental analysis for $C_{15}H_{13}BrN_2O_2S$: Calculated 49.33 % C; 3.59 % H; 21.88 Br; 7.67 % N; 8.78 % S. Found 49.44 % C; 3.79 % H; 21.59 % Br; 7.40 % N; 9.05 % S

HRMS: Calculated for **$C_{15}H_{13}N_2O_2S$** 285.069225 Found 285.069284

***S*-(3-Oxo-1,3-dihydro-2-benzofuran-1-yl)-*N*-(4-methoxyphenyl) isothiouronium bromide (7b)**

yield: 95 %

m.p.: 110-115 °C

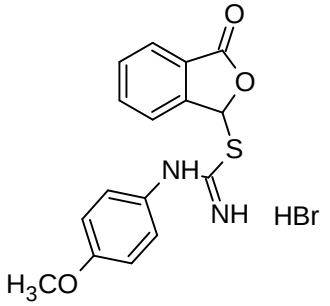

^{1}H-NMR (400 MHz, DMSO) δ 11.81 (bs, 1H), 10.07 (bs, 2H), 8.06 (s, 1H), 7.98-7.89 (m, 3H), 7.77 (t, 1H, *J* = 7.6 Hz), 7.22 (d, 2H, *J* = 8.4 Hz), 7.05 (d, 2H, *J* = 8.4 Hz), 3.77 (s, 3H)

^{13}C-NMR (100 MHz, DMSO) δ 167.8, 159.0, 143.6, 135.5, 121.4, 127.0, 126.6, 125.6, 124.9, 124.0, 115.1, 82.6, 55.5

Elemental analysis for $C_{16}H_{15}BrN_2O_3S$: Calculated 48,62 % C; 3.82 % H; 20.21 Br; 7.09 % N; 8.11 % S. Found 48.79 % C; 3.68 % H; 20.09 % Br; 6.97 % N; 8.17 % S

HRMS: Calculated for **$C_{16}H_{15}N_2O_3S$** 315.079787 Found 315.080348

_S_-(3-Oxo-1,3-dihydro-2-benzofuran-1-yl)-_N_-(pyridin-2-yl) isothiouronium bromide (7c)

yield: 81 %

m.p.: 192-194 °C

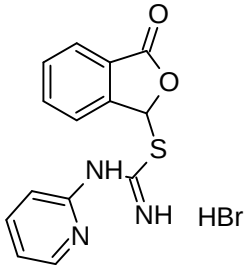

^{1}H-NMR (400 MHz, DMSO) δ 9.91 (bs, 3H), 8.44 (dd, 1H, *J* = 5.6 Hz, 1.2), 8.18 (t, 1H, *J* = 6 Hz), 7.94-7.90 (m, 2H), 7.84 (d, 1H, *J* = 7.6 Hz), 7.78 (s, 1H), 7.72 (t, 1H, *J* = 7.6 Hz)

^{13}C-NMR (100 MHz, DMSO) δ 168.1, 161.1, 144.0, 135.3, 131.0, 125.4, 125.1, 123.7, 82.7

Elemental analysis for $C_{14}H_{12}BrN_3O_2S$: Calculated 45.91 % C; 3.30 % H; 21.82 Br; 11.47 % N; 8.76 % S. Found 46.10 % C; 3.57 % H; 21.76 % Br; 11.61 % N; 9.00 % S

HRMS: Calculated for **$C_{14}H_{12}N_3O_2S$** 286.064474 Found 286.064712

_S_-(3-Oxo-1,3-dihydro-2-benzofuran-1-yl)- _N_-methyl-_N_-phenyl isothiouronium bromide (7d)

yield: 80 %

m.p.: 181-183 °C

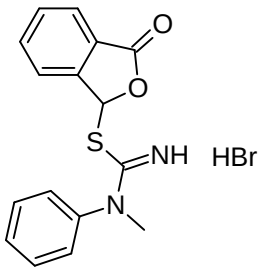

^{1}H-NMR (400 MHz, DMSO) δ 10.20 (bs, 2H), 7.98 (d, 1H, J = 7.6 Hz), 7.92-7.88 (m, 2H), 7.78-7.703 (m, 2H), 7.56-7.35 (m, 5H), 3.64 (s, 3H)

^{13}C-NMR (100 MHz, DMSO) δ 167.57, 164.1, 142.9, 141.6, 135.5, 131.4, 130.0, 129.9, 126.9, 125.7, 124.7, 123.7, 82.1, 43.4

Elementární analýza pro $C_{16}H_{15}BrN_2O_2S$: Vypočteno 50,67 % C; 3,99 % H; 21,07 % Br, 7,39 % N; 8,45 % S. Nalezeno 50,96 % C; 4,24 % H; % Br, 7,58 % N; 8,60 % S

HRMS: Calculated for **$C_{16}H_{15}BrN_2O_2S$** 299.084875 Found 299.085096

S-(3-Oxo-1,3-dihydro-2-benzofuran-1-yl)-*N*-ethyl-*N*-phenyl isothiouronium bromide (7e)

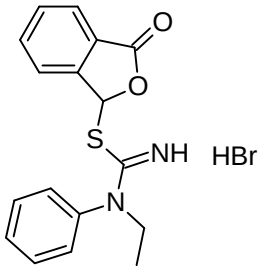

yield: 89 %

m.p.: 199-202 °C

^{1}H-NMR (400 MHz, DMSO) δ 10.32 (bs, 2H), 8.01 (s, 1H), 7.98 (d, 1H, J = 7.6 Hz), 7.92 (t, 1H, J = 7.2 Hz), 7.79-7.40 (m, 2H), 7.60-7.50 (m, 5H), 4.18-4.00 (m, 2H), 1.22 (t, 3H)

^{13}C-NMR (100 MHz, DMSO) δ 167.8, 164.0, 143.1, 139.6, 135.7, 131.6, 130.3, 128.0, 125.9, 124.9, 123.9, 82.1, 50.1, 11.9

Elemental analysis for $C_{17}H_{17}BrN_2O_2S$: Calculated 51.92 % C; 4.36 % H; 20.32 % Br, 7.12 % N; 8.15 % S. Found 51.86 % C; 4.46 % H; 20.25 % Br, 7.37 % N; 8.20 % S

HRMS: Calculated for **$C_{17}H_{17}N_2O_2S$** 313.100525 Found 313.101052

***S*-(3-Oxo-1,3-dihydro-2-benzofuran-1-yl)- *N*,*N*'-dimethyl isothiouronium bromide (9a)**

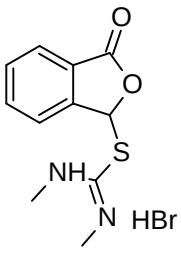

yield: 92 %

m.p.: 191-193 °C

^{1}H-NMR (400 MHz, DMSO) δ 10.20 (bs, 1H), 9.71 (bs, 1H), 7.95-7.87 (m, 3H), 7.81 (s, 1H), 7.75 (t, 1H, J = 7.2 Hz), 3.07 (s, 3H), 2.98 (s, 3H)

^{13}C-NMR (100 MHz, DMSO) δ 167.7, 161.7, 143.8, 135.4, 131.3, 125.5, 124.6, 123.9, 83.0, 32.2, 31.4

Elemental analysis $C_{11}H_{13}BrN_2O_2S$: Calculated 41.65 % C; 4.13 % H; 25.19 % Br, 8.83 % N; 10.11 % S. Found 41.85 % C; 4.37 % H; 25.40 % Br, 9.12 % N; 10.42 % S

HRMS: Calculated for $C_{11}H_{13}N_2O_2S$ 237.069225 Found 237.068726

S-(5-Methoxy-3-oxo-1,3-dihydro-2-benzofuran-1-yl)-*N*,*N*'-dimethyl isothiouronium bromide (9b)

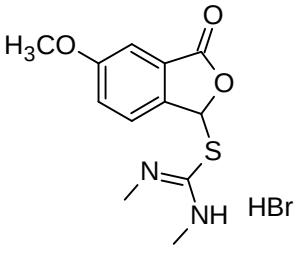

yield: 83 %

m.p.: 112-115 °C

^{1}H-NMR (400 MHz, DMSO) δ 10.12 (bs, 1H), 9.66 (bs, 1H), 7.78 (d, 1H, J = 8.4 Hz), 7.64 (s, 1H), 7.47 (dd, 1H, J = 8.8, 2.4 Hz), 7.42 (d, 1H, J = 2.0 Hz), 3.88 (s, 3H), 3.07 (s, 3H), 2.97 (s, 3H)

^{13}C-NMR (100 MHz, DMSO) δ 167.8, 162.3, 162.1, 136.3, 126.9, 125.5, 123.9, 108.6, 83.3, 56.6, 32.5, 31.7

Elemental analysis for $C_{12}H_{15}BrN_2O_3S$: Calculated 41.51 % C; 4.35 % H; 23.01 Br; 8.02 % N; 9.23 % S. Found 41.81 % C; 4.54 % H; 22.74 % Br; 7.81 % N; 9.52 % S

HRMS: Calculated for **$C_{12}H_{15}N_2O_3S$** 267.079789 Found 267.079655

_S_-(5-Chloro-3-oxo-1,3-dihydro-2-benzofuran-1-yl)-_N_,_N_'-dimethyl isothiouronium bromide (9c)

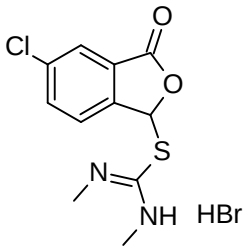

yield: 65 %

m.p.: 183-185 °C

^{1}H-NMR (400 MHz, DMSO) δ 10.19 (s, 1H), 9.71 (s, 1H), 8.09 (s, 1H), 8.03 (d, 1H, J = 8.0 Hz), 7.96 (d, 1H, J = 8.4 Hz), 7.69 (s, 1H), 3.13 (s, 3H), 2.99 (s, 3H)

^{13}C-NMR (100 MHz, DMSO) δ 166.7, 161.8, 143.0, 136.2, 135.5, 127.1, 126.0, 125.3, 83.2, 32.5, 31.4

Elemental analysis for $C_{11}H_{12}BrClN_2O_2S$: Calculated 37.57 % C; 3.44 % H; 22.72 Br; 10.08 % Cl; 7.97 % N; 9.12 % S. Found 37.86 % C; 3.34 % H; 7.88 % N; 9.31 % S

HRMS: Calculated for **$C_{11}H_{12}ClN_2O_2S$** 271.030252 Found 271.030084

_S_-(5-Nitro-3-oxo-1,3-dihydro-2-benzofuran-1-yl)-_N_,_N_'-dimethyl isothiouronium bromide (9d)

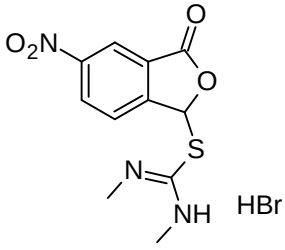

yield: 78 %

m.p: 220-225 °C

^{1}H-NMR (400 MHz, DMSO) δ 10.29 (d, 1H, J = 4 Hz), 9.76 (s, 1H), 7.75 (dd, 1H, J = 7.6, 2.0 Hz), 8.61 (d, 1H, J = 2 Hz), 8.23 (d, 1H, J = 3.6 Hz), 7.77 (s, 1H), 3.14 (d, 3H, J = 13.6 Hz), 3.00 (d, 3H, J = 3.6 Hz)

^{13}C-NMR (100 MHz, DMSO) δ 166.2, 161.6, 149.8, 149.7, 130.2, 126.9, 126.2, 120.7, 83.7, 32.6, 31.5

Elemental analysis for $C_{11}H_{12}BrN_3O_4S$: Calculated 36.48 % C; 3.34 % H; 22.06 Br; 11.60 % N; 8.85 % S. Found 36.75 % C; 3.61 % H; 22.15 % Br; 11.75 % N; 9.08 % S

HRMS: Calculated for **$C_{11}H_{12}N_3O_4S$** 282.054303 Found 282.054050

3-(4,5-Dihydro-1*H*-imidazol-2-ylsulfanyl)-2-benzofuran-1(3*H*)-one hydrobromide (9e)

yield: 59 %

m.p.: 210-213 °C

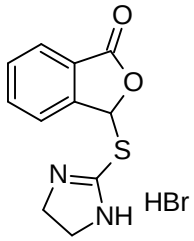

^{1}H-NMR (400 MHz, DMSO) δ 10.78 (s, 2H), 7.98-7.91 (m, 3H), 7.83 (d, 1H, J = 8.0 Hz), 7.77 (t, 1H, J = 7.6 Hz), 3.99 (m, 4H)

^{13}C-NMR (100 MHz, DMSO) δ 167.6, 164.8, 143.3, 135.7, 131.6, 125.8, 124.7, 123.9, 81.0, 45.4

Elemental analysis for $C_{11}H_{11}BrN_2O_2S$: Calculated 41.92 % C; 3.52 % H; 25.35 % Br, 8.89 % N; 10.17 % S. Found 41.93 % C; 3.82 % H; 25.12 % Br, 9.15 % N; 10.36 % S

HRMS: Calculated for **$C_{11}H_{10}N_2NaO_2S$** 257.035519 Found 257.035572

3-(4,5-Dihydro-1*H*-imidazol-2-ylsulfanyl)-6-methoxy-2-benzofuran-1(3*H*)-one hydrobromide (9f)

yield: 76 %

m.p.: 270-275 °C

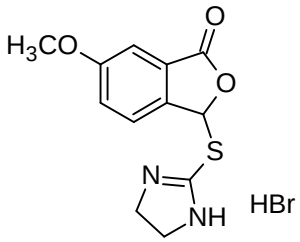

^{1}H-NMR (400 MHz, DMSO) δ 10.54 (bs, 2H), 7.77-7.72 (m, 2H), 7.49-7.44 (m, 2H), 3.96 (d, 4H, J = 1.6 Hz), 3.87 (s, 3H)

^{13}C-NMR (100 MHz, DMSO) δ 164.9, 161.8, 135.2, 126.5, 125.0, 123.6, 108.4, 81.0, 56.1, 45.4

Elemental analysis $C_{12}H_{13}BrN_2O_3S$: Calculated 41.75 % C; 3.80 % H; 23.15 Br; 8.11 % N; 9.29 % S. Found 42.00 % C; 4.02 % H; 23.26 % Br; 8.06 % N; 9.08 % S

3-(1*H*-Benzimidazol-2-ylsulfanyl)-2-benzofuran-1(3*H*)-one hydrobromide (9g)

yield: 62 %

m.p.: 215-220 °C

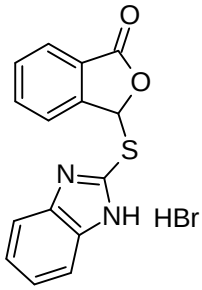

^{1}H-NMR (400 MHz, DMSO) δ 14.40 (bs, 2H), 7.91-6.70 (m, 9H)

^{13}C-NMR (100 MHz, DMSO) δ 168.0, 144.7, 143.1, 135.7, 133.3, 131.3, 126.1, 125.5, 124.8, 124.2, 114.1, 84.4

Elemental analysis for $C_{15}H_{11}BrN_2O_2S$: Calculated 49.60 % C; 3.05 % H; 7.71 % N; 8.83 % S. Found 49.72 % C; 3.20 % H; 7.93 % N; 9.09 % S

_S_-(3-Oxo-1,3-dihydro-2-benzofuran-1-yl)-_N_-(4-chlorophenyl)-_N'_-methyl isothiouronium bromide (9h)

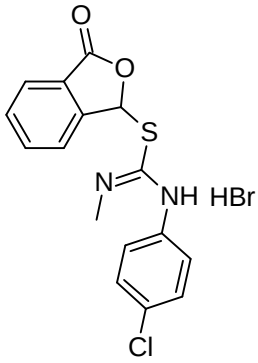

yield: 63 %

m.p.: 175-178 °C

^{1}H-NMR (400 MHz, DMSO) δ 10.62 (bs, 2H), 7.98 (d, 1H, J = 8 Hz), 7.94 (t, 1H, J = 7.6 Hz), 7.87 (s, 1H), 7.78 (t, 2H, J = 7.2 Hz), 7.58 (d, 2H, J = 8.8 Hz), 7.46 (bd, 2H, J = 8 Hz), 3.23 (s, 3H)

^{13}C-NMR (100 MHz, DMSO) δ 167.9, 143.9, 135.6, 132.7, 131.5, 129.6, 128.4, 125.8, 124.9, 124.0, 82.8, 32.8

Elemental analysis for $C_{16}H_{14}BrClN_2O_2S$: Calculated 46.45 % C; 3.41% H; 6.77 % N; 7.75 % S. Found 46.35 % C; 3.58 % H; 6.65 % N; 7.81 % S

_S_-(3-Oxo-1,3-dihydro-2-benzofuran-1-yl)-_N_,_N'_-diphenyl isothiouronium bromide (9i)

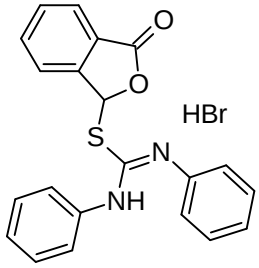

yield: 92 %

m.p.: 198-200 °C

^{1}H-NMR (400 MHz, DMSO) δ 10.32 (bs, 2H), 7.94-7.72 (m, 5H), 7.32-7.17 (m, 10H)

^{13}C-NMR (100 MHz, DMSO) δ 168.2, 144.6, 135.5, 131.3, 129.1, 126.2, 125.7, 125.1, 123.9, 123.2, 83.7

Elemental analysis for $C_{21}H_{17}BrN_2O_2S$: Calculated 57.15 % C; 3.88 % H; 18.10 % Br, 6.35 % N; 7.27 % S. Found 56.87 % C; 4.13 % H; 4.34 % Br, 6.56 % N; 7.37 % S

HRMS: Calculated for **$C_{21}H_{17}N_2O_2S$** 361.100525 Found 361.100617

_S_-(3-Oxo-1,3-dihydro-2-benzofuran-1-yl)-_N_-ethyl-_N'_-methyl isothiouronium bromide (9j)

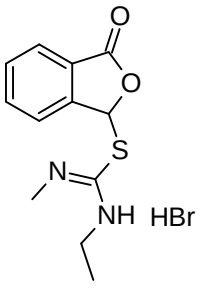

yield: 73 %

m.p.: 175-177 °C

^{1}H-NMR (400 MHz, DMSO) δ 10.27-9.79 (m, 2H), 8.01-7.93 (m, 3H), 7.82-7.79 (m, 2H), 3.60-3.40 (m, 2H), 3.10 (d, 3H, J = 28.0 Hz), 1.23-1.10 (m, 3H)

^{13}C-NMR (100 MHz, DMSO) δ 167.9, 160.9 and 160.5, 144.2 and 144.0, 135.7, 131.6 and 131.5, 125.8 and 125.7, 124.9, 124.2, 83.6 and 83.4, 41.2 and 39.4, 32.6 and 31.5, 15.1 and 12.9

Elemental analysis $C_{12}H_{15}BrN_2O_2S$: Calculated 43.51 % C; 4.56 % H; 24.12 % Br, 8.46 % N; 9.68 % S. Found 43.49 % C; 4.51 % H; 23.98 % Br, 8.68 % N; 9.54 % S

Methyl 2-[(carbamimidoylsulfanyl)methyl]benzoate hydrobromide (11a)

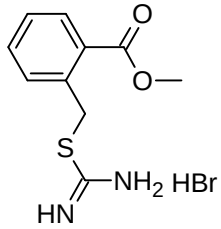

yield: 69 %

m.p.: 170-171 °C

^{1}H-NMR (400 MHz, DMSO) δ 9.31 (bs, 2H), 9.09 (bs, 2H), 7.93-7.91 (m, 1H), 7.63-7.58 (m, 2H), 7.50-7.45 (m, 1H), 4.78 (s, 2H), 3.83 (s, 3H)

^{13}C-NMR (100 MHz, DMSO) δ 169.3, 166.5, 136.5, 132.9, 131.3, 131.1, 128.7, 128.5, 52.4, 33.2

Elemental analysis for $C_{10}H_{13}BrN_2O_2S$: Calculated 39.35 % C; 4.72 % H; 26.18 Br; 9.18 % N; 10.51 % S. Found 39.57 % C; 4.72 % H; 26.43 % Br; 8.93 % N; 10.27 % S

HRMS: Calculated for **$C_{10}H_{13}N_2O_2S$** 225.069225 Found 225.069069

Phenyl 2-[(carbamimidoylsulfanyl)methyl]benzoate hydrobromide (11b)

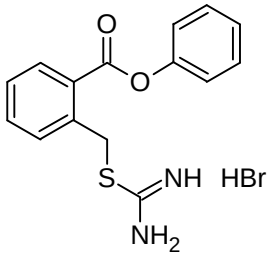

yield: 76 %

m.p.: 180-182 °C

^{1}H-NMR (400 MHz, DMSO) δ 9.20 (bd, 4H), 8.25 (d, 1H, J = 7.2 Hz), 7.80-7.75 (m, 2H), 7.66-7.62 (m, 1H), 7.56-7.52 (m, 2H), 7.39-7.36 (m, 3H), 4.89 (s, 2H)

^{13}C-NMR (100 MHz, DMSO) δ 169.3, 164.9, 150.5, 137.3, 133.8, 131.9, 131.6, 129.8, 129.1, 128.1, 126.4, 122.1, 33.4

Elemental analysis for $C_{15}H_{15}BrN_2O_2S$: Calculated 49.06 % C; 4.12 % H; 21.76 Br; 7.63 % N; 8.73 % S. Found 49.27 % C; 4.22 % H; 21.83 % Br; 7.93 % N; 8.57 % S

HRMS: Calculated for **$C_{15}H_{15}N_2O_2S$** 287.084875 Found 287.084120

Methyl 2-{[(*N*,*N*'-dimethylcarbamimidoyl)sulfanyl]methyl}benzoate hydrobromide (11c)

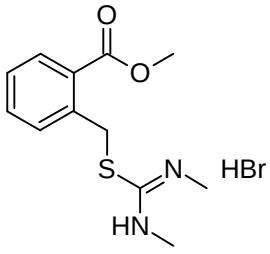

yield: 84 %

m.p.: 103-104 °C

^{1}H-NMR (400 MHz, DMSO) δ 9.50 (bd, 2H), 7.96 (dd, 1H, J = 7.6, 1.2 Hz), 7.71 (d, 1H, J = 7.2 Hz), 7.66 (dt, 1H, J = 7.6, 1.2 Hz), 7.54 (dt, 1H, J = 7.6, 1.2 Hz), 4.95 (s, 2H), 3.91 (s, 3H), 3.04 (d, 3H, J = 2.4

Hz), 2.92 (s, 3H)

^{13}C-NMR (100 MHz, DMSO) δ 166.4, 165.7, 135.8, 132.8, 131.5, 130.9, 128.8, 52.4, 34.3, 31.2, 30.9

Elemental analysis for $C_{12}H_{17}BrN_2O_2S$: Calculated 43.25 % C; 5.14 % H; 23.98 % Br; 8.41 % N; 9.62 % S. Found 43.20 % C; 4.92 % H; 23.83 % Br; 8.63 % N; 9.37 % S

HRMS: Calculated for **$C_{12}H_{17}N_2O_2S$** 253.100525 Found 253.099305

3-Oxo-1,3-dihydro-2-benzofuran-1-yl hydrazinecarbimidothioate hydrobromide (13a)

výtěžek: 95 %

b.t: 175-180°C

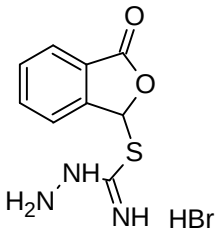

^{1}H-NMR (400 MHz, DMSO) δ 9.85 (bs, 5H), 7.96 (d, 1H, *J* = 7.6 Hz), 7.92 (t, 1H, *J* = 7.6 Hz), 7.80 (d, 1H, *J* = 7.6 Hz), 7.75 (t, 1H, *J* = 7.6 Hz), 7.60 (s, 1H)

^{13}C-NMR (100 MHz, DMSO) δ 168.1, 160.2, 135.4, 131.1, 125.6, 125.3, 123.8, 81.9

Elemental analysis for $C_9H_{10}BrN_3O_2S$: Calculated 35.54 % C; 3.31 % H; 26.27 % Br, 13.81 % N; 10.54 % S. Found 35.63 % C; 3.60 % H; 26.41 % Br, 14.11 % N; 10.72 % S

HRMS: Calculated for **$C_9H_{10}N_3O_2S$** 224.048824 Found 224.048605

***S*-(1-Oxo-3,4-dihydro-1*H*-isochromen-4-yl) isothiouronium bromide (12b)**

yield: 25 %

m.p: 201-203 °C

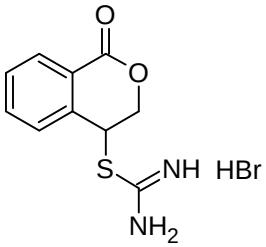

^{1}H-NMR (400 MHz, DMSO) δ 9.48 (bs, 4H), 8.05 (d, 1H, *J* = 7.6 Hz), 7.83 (t, 1H, *J* = 7.6 Hz), 7.75 (d, 1H, *J* = 7.6 Hz), 7.67 (t, 1H, *J* = 7.6 Hz), 5.78 (s, 1H), 4.99 (dd, 1H, *J* = 12.8, 2.4 Hz), 4.66 (dd, 1H, *J* = 12.8, 1.6 Hz)

^{13}C-NMR (100 MHz, DMSO) δ 166.7, 163.1, 136.1, 134.9, 130.3, 130.2, 128.3, 124.8, 69.2, 41.3

Elemental analysis for $C_{10}H_{11}BrN_2O_2S$: Calculated 39.62 % C; 3.66 % H; 26.36 Br; 9.24 % N; 10.58 % S. Found 39.51 % C; 3.89 % H; 26.14 % Br; 9.37 % N; 10.60 % S

HRMS: Calculated for **$C_{10}H_{11}N_2O_2S$** 223.053575 Found 223.053493

_S_-(1-Oxo-3,4-dihydro-1_H_-isochromen-4-yl)-_N_,_N_'-dimethyl isothiouronium bromide (12c)

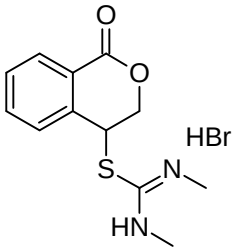

yield: 57 %

m.p: 200-202 °C

^{1}H-NMR (400 MHz, DMSO) δ 9.83 (bs, 1H), 9.40 (bs, 1H), 7.76 (dt, 1H, J = 7.6, 1.2 Hz), 7.67-7.59 (m, 2H), 5.61 (s, 1H), 4.91 (dd, 1H, J = 12.8, 2.4 Hz), 4.62 (dd, 1H, J = 12.8, 1.6 Hz), 2.96-2-92 (m, 6H)

^{13}C-NMR (100 MHz, DMSO) δ 163.1, 162.9, 136.0, 134.7, 130.2, 130.0, 128.2, 124.7, 68.9, 42.5, 31,5, 31.0

Elemental anylysis for $C_{12}H_{15}BrN_2O_2S$: Calculated 43.51 % C; 4.56 % H; 24.12 Br; 8.46 % N; 9.68 % S. Found 43.38 % C; 4.67 % H; 24.15 % Br; 8.26 % N; 9.84 % S

HRMS: Calculated for **$C_{12}H_{15}N_2O_2S$** 251.084875 Found 251.084123

Cyclization of the isothiouronium salts (4,6,8,10)

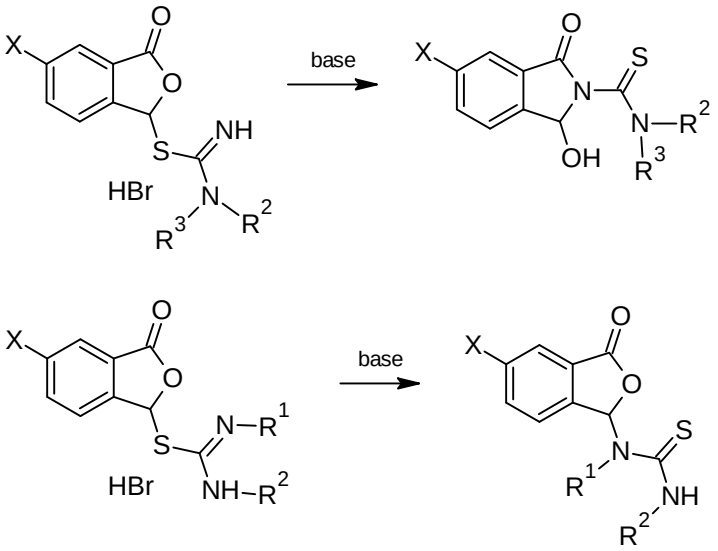

A - Diluted (1:1) ammonia solution was added to the salt. After 1 hour of standing, the precipitate was filtered off followed by recrystalization from the water-methanol solution.

B - To the 100 ml Erlenmeyer flask was added 0.5 g of salt, 1 g of sodium carbonate and 50 ml of acetone. After refluxing for 5 hours the reaction mixture was filtered and filtrate evaporated. The crude product was recrystalized from water-methanol solution.

C - Sodium carbonate water solution (15 ml of 1 mol·l^{-3}) was added to the 0.5 g of the salt and let stand for 1 hour. After this time, the mixture was extracted to 2 x 20 ml DCM.

Combined DCM extracts were washed with water and brine, dried over Na_2SO_4, filtered and evaporated.

1-Hydroxy-3-oxo-1,3-dihydro-2*H*-isoindole-2-carbothioamide (4a)

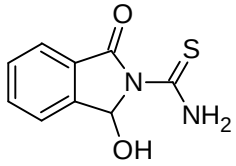

yield: 70 %

m.p.: 145-150 °C

^{1}H-NMR (400 MHz, DMSO) δ 9.63 (d, 2H, J = 32.8 Hz), 7.81-7,76 (m, 2H), 7.67-7.60 (m, 2H), 6.77-6.71 (m, 2H)

^{13}C-NMR (100 MHz, DMSO) δ 180.3, 166.8, 144.0, 134.7, 130.2, 128.86, 124.2, 124.1, 83.2

Elemental analysis for $C_9H_8N_2O_2S$: Calculated 51.91 % C; 3.87 % H; 13.45 % N; 15.40 % S. Found 51.99 % C; 4.05 % H; 13.72 % N; 15.22 % S

EI-MS: m/z 208, 191, 174, 149, 130, 105 (100 %), 77, 66, 51, 44

1-Hydroxy-5-methoxy-3-oxo-1,3-dihydro-2*H*-isoindole-2-carbothioamide (4b)

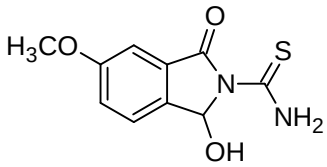

yield: 99 %

m.p.: 231-233 °C

^{1}H-NMR (400 MHz, DMSO) δ 9.59 (s, 2H), 7.57 (d, 1H, J = 8.4 Hz), 7.34 (dd, 1H, J = 8.4, 2.0 Hz), 7.27 (d, 1H. J = 2.4 Hz), 6.70 (s, 1H), 3.87 (s, 3H)

^{13}C-NMR (100 MHz, DMSO) δ 180.4, 166.9, 161.0, 136.6, 130.6, 125.4, 122.6, 107.0, 83.0, 55.9

Elemental analysis for $C_{10}H_{10}N_2O_3S$: Calculated 50.41 % C; 4.23 % H; 11.76 % N; 13.46 % S. Found 50.67 % C; 4.30 % H; 11.93 % N; 13.21 % S

5-Chloro-1-hydroxy-3-oxo-1,3-dihydro-2*H*-isoindole-2-carbothioamide (4c)

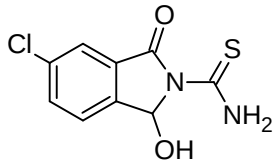

yield: 92 %

m.p.: 245-250 °C

^{1}H-NMR (400 MHz, DMSO) δ 9.76 (s, 1H), 9.54 (s, 1H), 7.87-7.85 (m, 2H), 7.73-7.70 (m, 1H), 6.86 (d, 1H, J = 7.2 Hz), 6.79(d, 1H, J = 7.2 Hz)

^{13}C-NMR (100 MHz, DMSO) δ 180.2, 165.5, 142.9, 135.0, 134.7, 131.0, 126.3, 123.9, 83.1,

Elemental analysis for $C_9H_7ClN_2O_2S$: Calculated 44.54 % C; 2.91 % H; 14.61 % Cl; 11.54 % N; 13.21 % S. Found 44.72 % C; 2.87 % H; 14.35 % Cl; 11.78 % N; 12.99 % S

1-Hydroxy-5-nitro-3-oxo-1,3-dihydro-2*H*-isoindole-2-carbothioamide (4d)

yield: 90 %

m.p.: 223-226 °C

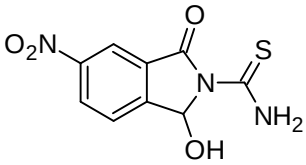

^{1}H-NMR (400 MHz, DMSO) δ 9.86 (bs, 1H), 9.56 (bs, 1H), 8.65 (dd, 1H, J = 8.3, 2.2 Hz), 8.51 (d, 1H, J = 2,2 Hz), 7.98 (d, 1H, J = 8.3 Hz), 7.15 (d, 1H, J = 7.5 Hz), 6.95 (d, 1H, J = 7.5 Hz)

^{13}C-NMR (100 MHz, DMSO) δ 180.0, 164.8, 149.9, 149.3, 130.6, 129.6, 126.2, 119.4, 83.2

Elemental analysis for $C_9H_7N_3O_4S$: Calculated 42.69 % C; 2.79 % H; 16.59 % N; 12.66 % S. Found 42.73 % C; 2.85 % H; 16.73 % N; 12.51 % S

1-Hydroxy-*N*-methyl-3-oxo-1,3-dihydro-2*H*-isoindole-2-carbothioamide (6a)

yield: 55 %

m.p.: 133-135 °C

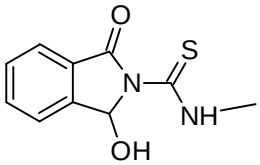

^{1}H-NMR (400 MHz, DMSO) δ 10.35 (s, 1H), 7.80-7.75 (m, 2H), 7.65-7.60 (m, 2H), 6.81-6.78 (m, 2H), 3.11 (d, 3H, J = 2.4 Hz)

^{13}C-NMR (100 MHz, DMSO) δ 179.1, 166.6, 144.1, 134.5, 130.1, 128.9, 124.1, 124.0, 83.3, 32.0

Elemental analysis for $C_{10}H_{10}N_2O_2S$: Calculated 54.04 % C; 4.53 % H; 12.60 % N; 14.43 % S. Found 53.94 % C; 4.61 % H; 12.68 % N; 14.13 % S

EI-MS: m/z 222, 189, 175, 161, 149 (100 %), 137, 130, 105, 77, 51, 42

1-Hydroxy-3-oxo-*N*-(propan-2-yl)-1,3-dihydro-2*H*-isoindole-2-carbothioamide (6b)

yield: 69 %

m.p.: 95-96 °C

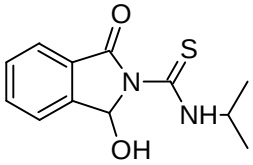

^{1}H-NMR (400 MHz, DMSO) δ 10.36 (d, 1H, J = 7.6 Hz), 7.81-7.77 (m, 2H), 7.67-7.61 (m, 2H), 6.87-6.77 (m, 2H), 4.50-4.45 (m, 1H), 1.28 (d, 6H, J = 6.4 Hz)

^{13}C-NMR (100 MHz, DMSO) δ 177.2, 167.1, 144.1, 134.6, 130.2, 128.8, 124.1, 123.9, 83.3, 46.5, 21.2, 21.1

Elemental analysis for $C_{12}H_{14}N_2O_2S$: Calculated 57.58 % C; 5.64 % H; 11.19 % N; 12.81 % S. Found 57.79 % C; 5.74 % H; 11.33 % N; 12.84 % S

EI-MS: m/z 250, 231, 218, 207 (100 %), 190, 175, 160, 149, 133, 120, 105, 90, 77, 58, 43

1-Hydroxy-3-oxo-*N*-phenyl-1,3-dihydro-2*H*-isoindole-2-carbothioamide (8a)

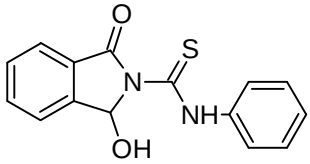

yield: 48 %

m.p: 207-209 °C

^{1}H-NMR (400 MHz, DMSO) δ 12.1 (s, 1H), 7.91-7.85 (m, 2H), 7.75-7.69 (m, 4H), 7.48 (t, 2H, J = 7.6 Hz), 7.33 (t, 1H, J = 7.6 Hz), 7.11-7.09 (m, 1H), 6.98 (d, 1H, J = 7.2 Hz)

^{13}C-NMR (100 MHz, DMSO) δ 177.4, 166.9, 144.5, 138.2, 134.9, 130.5, 128.9, 128.8, 126.4, 124.5, 124.3, 124.2, 83.5

Elemental analysis for $C_{15}H_{12}N_2O_2S$: Calculated 63.36 % C; 4.25 % H; 9.85 % N; 11.28 % S. Found 63.13 % C; 4.50 % H; 10.06 % N; 11.24 % S

EI-MS: m/z 222, 189, 175, 161, 149 (100 %), 137, 130, 105, 77, 51, 42

***N*-ethyl-1-hydroxy-3-oxo-*N*-phenyl-1,3-dihydro-2*H*-isoindole-2-carbothioamide (8e)**

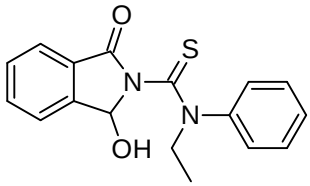

yield: 91 %

m.p.: 199-202 °C

^{1}H-NMR (400 MHz, DMSO) δ 7.65-7.2 (m, 10H), 8.83 (d, 1H, J = 5.2 Hz), 4.67-4.64 (m, 1H), 4.07-4.01 (m, 1H), 1.18 (m, 3H)

^{13}C-NMR (100 MHz, DMSO) δ 179.8, 159.8, 144.3, 142.8, 133.4, 129.9, 128.8, 128.3, 127.1, 126.3, 123.9, 123.2, 83.7, 51.2, 11.3

Elemental analysis for $C_{17}H_{16}N_2O_2S$: Calculated 65.36 % C; 5.16 % H; 8.97 % N; 10.26 % S. Found 65.38 % C; 5.15 % H; 9.18 % N; 10.49 % S

1,3-Dimethyl-1-(3-oxo-1,3-dihydro-2-benzofuran-1-yl)thiourea (10a)

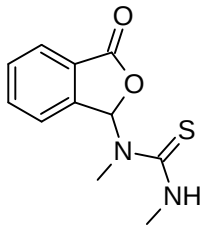

yield: 95 %

m.p.: 155-156 °C

^{1}H-NMR (400 MHz, DMSO) δ 8.66 (s, 1H), 8.33 (bs, 1H), 7.92 (d, 1H, J = 7.6 Hz), 7.83 (dt, 1H, J = 7.6, 1.2 Hz), 7.69 (t, 1H, J = 7.6 Hz), 7.55 (dd, 1H, J = 7.6, 0.8 Hz), 3.03 (d, 3H, J = 2 Hz), 2.53 (s, 3H)

^{13}C-NMR (100 MHz, DMSO) δ 184.0, 168.2, 144.8, 135.0, 130.6, 127.0, 125.2, 123.0, 89.4, 33.1, 30.4

Elemental analysis for $C_{11}H_{12}N_2O_2S$: Calculated 55.91 % C; 5.12 % H; 11.86 % N; 13.57 % S. Found 55.84 % C; 4.90 % H; 11.86 % N; 13.65 % S

1-(5-Methoxy-3-oxo-1,3-dihydro-2-benzofuran-1-yl)-1,3-dimethylthiourea (10b)

yield: 70 %

m.p.: 112-115 °C

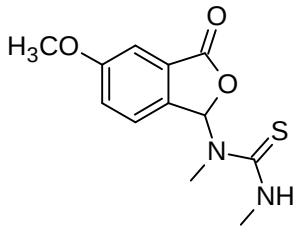

^{1}H-NMR (400 MHz, DMSO) δ 8.60 (s, 1H), 8.33 (d, 1H, *J* = 4.4 Hz), 7.81 (s, 1H), 7.48-7.46 (m, 1H), 7.39-7.37 (m, 2H), 3.89 (s, 3H), 3.05 (d, 3H, *J* = 4.4 Hz), 2.56 (s, 3H)

^{13}C-NMR (100 MHz, DMSO) δ 184.0, 168.2, 161.3, 137.0, 128.9, 124.2, 123.0, 107.0, 89.4, 56.0, 32.2, 30.5

Elemental analysis for $C_{12}H_{14}N_2O_3S$: Calculated 54.12 % C; 5.30 % H; 10.52 % N; 12.04 % S. Found 54. 36 % C; 5.22 % H; 10.63 % N; 12.23 % S

1-(5-Chloro-3-oxo-1,3-dihydro-2-benzofuran-1-yl)-1,3-dimethylthiourea (10c)

yield: 87 %

m.p.: 183-185 °C

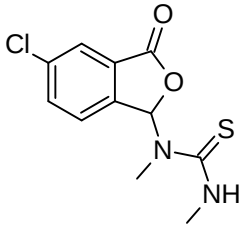

^{1}H-NMR (400 MHz, DMSO) δ 8.68 (s, 1H), 8.36 (d, 1H, *J* = 4.4 Hz), 7.98 (d, 1H, *J* = 1.6 Hz), 7.87 (dd, 1H, *J* = 8.4, 2 Hz), 7.60 (d, 1H, *J* = 8.4 Hz), 3.04 (d, 3H, *J* = 4.0 Hz), 2.57 (s, 1H)

^{13}C-NMR (100 MHz, DMSO) δ 184.1, 167.0, 143.6, 135.4, 135.0, 129.4, 125.0, 89.6, 33.2, 30.7

Elemental analysis for $C_{11}H_{11}ClN_2O_2S$: Calculated 48.80 % C; 4.10 % H; 10.35 % N; 11.84 % S. Found 49.07 % C; 4.37 % H; 10.55 % N; 12.11 % S

1,3-Dimethyl-1-(5-nitro-3-oxo-1,3-dihydro-2-benzofuran-1-yl)thiourea (10d)

yield: 87 %

m.p: 212-213 °C

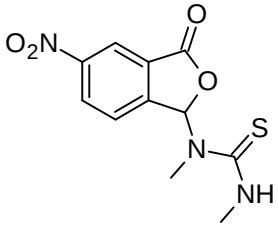

^{1}H-NMR (400 MHz, DMSO) δ 8.82 (s, 1H), 8.62 (dd, 1H, *J* = 8.4, 2.0 Hz), 8.57 (d, 1H, *J* = 1.6 Hz), 8.43 (d, 1H, *J* = 4 Hz), 7.86 (d, 1H, *J* = 8.4 Hz), 3.05 (d, 3H, *J* = 4 Hz), 2.61 (s, 3H)

^{13}C-NMR (100 MHz, DMSO) δ 183.9, 166.3, 150.4, 149.4, 129.6, 129.0, 124.8, 120.3, 89.8, 33.2, 30.9

Elemental analysis for $C_{11}H_{11}N_3O_4S$: Calculated 46.97 % C; 3.94 % H; 14.94 % N; 11.40 % S. Found 46.74 % C; 4.21 % H; 14.79 % N; 11.26 % S

3-(2-Thioxoimidazolidin-1-yl)-2-benzofuran-1(3*H*)-one (10e)

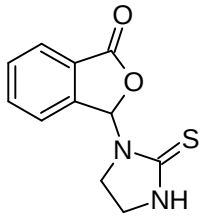

yield: 40 %

m.p: 213-215 °C

^{1}H-NMR (400 MHz, DMSO) δ 9.30 (bs, 1H), 7.97-7.96 (m, 1H), 7.92-7.89 (m, 1H), 7.84-7.40 (m, 2H), 7.70-7.68 (m, 1H), 3.55-3.40 (m, 2H), 3.30-3.24 (m, 1H), 3.11-3.09 (m, 1H) more tautomeric forms

^{13}C-NMR (100 MHz, DMSO) δ 183.3, 168.1, 144.1, 134.9, 131.0, 126.8, 125.2, 123.4, 85.7, 44.0, 41.9, 41.1 more tautomeric forms – only major signals

Elemental analysis for $C_{11}H_{10}N_2O_2S$: Calculated 56.39 % C; 4.30 % H; 11.96 % N; 13.69 % S. Found 56.55 % C; 4.26 % H; 11.81 % N; 13.48 % S

EI-MS: m/z 234, 221, 201(100%), 191, 173, 160, 147, 133, 117, 105, 87, 77, 63, 51, 39

3-(2-Thioxo-2,3-dihydro-1*H*-benzimidazol-1-yl)-2-benzofuran-1(3*H*)-one (10g)

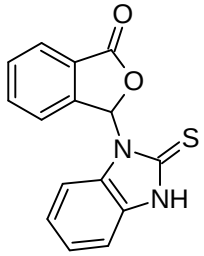

yield: 53 %

m.p.: 235-240 °C

^{1}H-NMR (400 MHz, DMSO) δ 8.09 (d, 1H, J = 8 Hz), 7.96-7,94 (m, 2H), 7.90-7.83 (m, 2H), 7.79 (s, 1H), 7.71 (t, 1H, J = 7.2 Hz), 7.53 (t, 1H, J = 7.2 Hz), 7.45 (t, 1H, J = 7.2 Hz)

^{13}C-NMR (100 MHz, DMSO) δ 168.4, 152.3, 145.1, 135.5, 135.2, 130.9, 126.8, 125.7, 125.5, 125.3, 123.8, 122.1, 122.0, 83.8

Elemental analysis for $C_{15}H_{10}N_2O_2$: Calculated 63.81 % C; 3.57 % H; 9.92 % N; 11.36 % S. Found 63.56 % C; 3.78 % H; 9.87 % N; 11.06 % S

References

1. Page M., Williams A., In *Organic & Bio-organic Mechanisms*; Addison Wesley Longman Ltd.: Singapore, **1997**.
2. Jencks W. P., In *Catalysis in Chemistry and Enzymology*; General Publishing Comp. Ltd.: Toronto, **1987**.
3. Bruice T. C., In *Enzymes*; Boyer P. D. (Ed.) Vol. 2, pp. 217–279; Academic Press: New York, **1970**.
4. Anslyn E. V., Dougherty D. A., In *Modern Physical Organic Chemistry*; University Science Books: Sausalito, **2006**.
5. Lightstone F. C., Bruice T. C., *J. Am. Chem. Soc.*, **1996**, *118*, *8*, 2595–2605.
6. Bruice T. C., Lightstone F. C., *Acc. Chem. Res.*, **1999**, *32*, *2*, 127–136.
7. Schultz P. G., *Acc. Chem. Res.*, **1989**, *22*, 287–294.
8. Bender M. L., *Chem. Rev.*, **1960**, *60*, 53–113.
9. Johnson S. L., *Adv. Phys. Org. Chem.*, **1967**, *5*, 237–330.
10. Jencks W. P., *Chem. Rev.*, **1972**, *72*, 705–718.
11. Williams A., *Acc. Chem. Res.*, **1989**, *22*, 387–392.
12. Faber K., Riva S., *Synthesis*, **1992**, 895–910.
13. Marlier J. F., *Acc. Chem. Res.*, **2001**, *34*, 283–290.
14. Lee I., Sung D. D., *Curr. Org.. Chem.*, **2004**, *8*, 557–567.
15. Martin R. B., Parcell A., Hedrick R. I., *J. Am. Chem. Soc.*, **1964**, *86*, 2406–2413.
16. Hay R. W., Morris P. J., *J. Chem. Soc., Perkin Trans. 2*, **1972**, 1021–1029.
17. Fife T. H., DeMark B. R., *J. Am. Chem. Soc.*, **1976**, *98*, 6978–6982.
18. Caswell M., Chaturvedi R. K., Lane S. M., Zvilichovsky B., Schmir G. L., *J. Org. Chem.*, **1981**, *46*, 1585–1593.
19. Fife T. H., Duddy N. W., *J. Am. Chem. Soc.*, **1983**, *105*, 74–79.
20. Buur A., Bundgaard H., Lee V. H. L., *Int. J. Pharm.*, **1988**, *42*, 51–60.
21. Patterson K. H., Depree G. J., Zender J. A., Morris P. J., *Tetrahedron Lett.*, **1994**, *35*, 281–284.
22. Fife T. H., Chauffe L., *J. Org. Chem.*, **2000**, *65*, 3579–3586.
23. Larsen S. W., Ankersen M., Larsen C., *Eur. J. Pharm. Sci.*, **2004**, *22*, 399–408.
24. Barroso S., Blay G., Cardona L., Fernandez I., Garcia B., Pedro J. R., *J. Org. Chem.*, **2004**, *69*, 6821–6829.

25. Skwarczynski M., Kiso Y., *Curr. Med. Chem.*, **2007**, *14*, 2813–2823.

26. Vivona N., Buscemi S., Frenna V., Cusmano G., *Adv. Heterocycl. Chem.*, **1993**, *56*, 49–154.

27. van der Plas H. C., *Adv. Heterocycl. Chem.*, **1999**, *74*, 153–221.

28. van der Plas H. C., *J. Heterocycl. Chem.*, **2000**, *37*, 427–438.

29. Hajós G., Riedl Z., Kollenz G., *Eur. J. Org. Chem.*, **2001**, 3405–3414.

30. Dejaegher Y., Mangelinckx S., De Kimpe N., *J. Org. Chem.*, **2002**, *67*, 2075–2081.

31. Buscemi S., Pace A., Piccionello A. P., Pibiri I., Vivona N., Giorgi G., Mazzanti A., Spinelli D., *J. Org. Chem.*, **2006**, *71*, 8106–8113.

32. Van Brabandt W., De Kimpe N., *J. Org. Chem.*, **2005**, *70*, 8717–8722.

33. D'hooghe M., De Kimpe N., *Tetrahedron*, **2006**, *62*, 513–535.

34. Duggan P. J., Liepa A. J., O'Dea L. K., Tranberg C. E., *Org. Biomol. Chem.*, **2007**, *5*, 472–477.

35. Karikomi M., D'hooghe M., Verniest G., De Kimpe N., *Org. Biomol. Chem.*, **2008**, *6*, 1902–1904.

36. Pozgan F., Kočevar M., *Heterocycles*, **2009**, *77*, 657–678.

37. Hanusek J., Sedlák M., Drabina P., Růžička A., *Acta Crystallogr., Sect. E*, **2009**, *65*, 411–o412.

38. Hanusek J., Sedlák M., Drabina P., Růžička A., *Acta Crystallogr., Sect. E* **2009**, *65*, o413.

39. Sedlák M., Hejtmánková L., Hanusek J., Macháček V., *J. Heterocycl. Chem.*, **2002**, *39*, 1105–1107.

40. Sedlák M., Hanusek J., Hejtmánková L., Kašparová P., *Org. Biomol. Chem.*, **2003**, *1*, 1204–1209.

41. Hanusek J., Hejtmánková L., Štěrba V., Sedlák M., *Org. Biomol. Chem.*, **2004**, *2*, 1756–1763.

42. Váňa J., Thesis, University of Pardubice, **2008**.

43. D´Anna F., Frenna V., Guernelli S., Macaluso G., Marullo S., Spinelli D., *J. Phys. Org. Chem*, **2008**, *21*, 306-314.

44. Buscemi S., Frenna V., Vivona N., Spinelli D., J. *Chem. Soc. Perkin Trans. I.*, **1993**, 2491-2493.

45. D´Anna, Frenna V., Marullo S., Noto R., Spinelli D., *Tetrahedron*, **2008**, *64*, 11209-11217.

46. Kroll H., *J. Am. Chem Soc*., **1952**, *74*, 2036-2039.

47. Bender M. L., Turnquest B. W., *J. Am. Chem. Soc*., **1957**, *79*, 1889-1893.

48. Westheimer F. H., Shookhoff M. W., *J. Am. Chem. Soc*., **1940**, *62*, 269-275.

49. White J. M., Manning R. A., Li N. C., *J. Am. Chem. Soc*., **1956**, *78*, 2367-2370.

50. Fujita H., Sato Y., *Chem. Pharm. Bull*., **1975**, *23*, *8*, 1764-1774.

51. Wan J., Wu B., Pan Y., *Tetrahedron*, **2007**, *63*, 9338 - 9344.

52. Khattab S. N., Hassan Y. S., El-Faham A. E., Monaim A., El Massry M., Amer A., *J. Heterocyclic Chem.*, **2007**, *44*, 617-626.

53. Amer A., Zimmer H., *J. Heterocycl. Chem.*, **1981**, *18*, 1625-1628.

54. Bowden K., Misic-Vukovic M. M., Ranson R. J., *Collect. Czech. Chem. Commun*., **1999**, *64*, 1601-1604.

55. Kubota Y., Tatsuno T., *Chem. Pharm. Bull*., **1971,** *19*, *6*, 1226-1233.

56. Sloan K. B., Koch S. A. M., *J. Org. Chem*., **1983**, *48*, 635-640.

57. Bodor N., Woods R., Raper C., Kearney P., Kaminski J. J., *J. Med. Chem.*, **1980**, *23*, 474-480.

58. Westaway K. Ch., Ali S. F., *Can. J. Chem*., **1979**, *57*, 1354-1367.

59. Sloan K. B., Koch S. A. M., *J. Org. Chem*., **1983**, *48*, 3777-3783.

60. Singh S. N., George M. V., *J. Org. Chem*., **1972**, *37*, *9*, 1375-1382.

61. Bender M. L., Reinstein J. A., Silver M. S., Mikulak R., *J. Am. Chem. Soc.*, **1965**, *87*, *20*, 4545-4553.

62. Guthrie E. D., *Pure & Appl. Chem.*, **1989**, *61*, 1, 23-56.

63. Raber D. J., Harris J. M., Hall R. E., Schleyer R. P., *J. Am. Chem. Soc*., **1971**, *93*, 4821-4828.

64. Hartshorn S. R., *Aliphatic Nucleophilic Substitution***, 1973**, Cambridge University Press, London, ISBN 0-521-09801-7.

65. Sneen R. A., Larsen J. W., *J. Am. Chem. Soc.*, **1969**, *91*, 362-366.

66. Sneen R. A., *Acc. Chem. Res.*, **1973**, *6*, 46-53.

67. Amyes T. L., Toteva M. A., Richard J. P., Crossing the Borderline between S_N1 and S_N2 Nucleophilic Substitution at Aliphatic Carbon, *Contemporary Reactive Intermediates*, **2004**, R. A. Moss, M. S. Platz, and M. Jones, Jr. ed. John Wiley and Sons: New York, 41–68.

68. Katritzky A. R., Brycki B. E., *Chem. Soc. Rev.*, **1990**, *19*, 83-105.

69. Richard J. P., Jencks W. P., *J. Am. Chem. Soc.*, **1984**, *106*, 1383-1396.

70. Carey F. A., Sundberg R. J.,*Advanced Organic Chemistry 5th Edition*, **2007**, Springer Science+Business Media. Virginia, ISBN- 13: 978-0-387-44897-8.

71. Bordwell F. G., Mecca T. G., *J. Am. Chem. Soc*., **1975**, *97*, 123-127.

72. Bordwell F. G., Mecca T. G., *J. Am. Chem. Soc*., **1975**, *97*, 127-131.

73. Bordwell F. G., Wiley P. F., Mecca T. G., *J. Am. Chem. Soc*., **1975**, *97*, 132-136.

74. Bordwell F. G., *Acc. Chem. Res.*, **1970**, *3*, 281-290.

75. McLennan D. J., *Acc. Chem. Res*., **1976**, *9*, 281-287.

76. Richard J. P., Tsuji Y., *J. Am. Chem. Soc*., **2000**, *122*, 3963-3964.

77. Richard J. P., Amyes T. L., Toteva M. M., *Acc. Chem. Res*., **2001**, *34*, 981-988.

78. Lawlor D. A., More O'Ferrall R. A., Rao S. N., *J. Am. Chem. Soc***., 2008**, *130*, 17997–18007.

79. Amyes T. L., Richard J. P., *J. Am. Chem. Soc.*, **1990,** *112*, 9507-9512.

80. Sneen R. A., Carter J. V., Kay P. S., *J. Am. Chem. Soc*., **1966**, *88*, 2594-2595.

81. Ta-Shma R., Rappaport Z., *J. Am. Chem. Soc*., **1983**, *105*, 6082-6095.

82. Dietze P. E., Jencks W. P., *J. Am. Chem. Soc.*, **1986**, *108*, 4549-4555.

83. Dietze P. E., Wojciechowski M., *J. Am. Chem. Soc*., **1990**, *112*, 5240-5244.

84. Tsuji Y., Richard J. P., *J. Am. Chem. Soc*., **2006**, *128*, 17139-17145.

85. Stein A. R., Tencer M., Moffatt E. A., Dave R., Sweet J., *J. Org. Chem.* **1980,** *45***,** 3540-3543.

86. Streitwieser A., *Chem. Rev*., **1956,** *56*, 571-752**.**

87. Ballistreri F. P., Maccarone E., Mamo A., *J. Org. Chem.*, **1976**, *41*, 3364-3367.

88. Young P. R., Jencks W. P., *J. Am. Chem. Soc.*, **1979**, *101***,** 3288-3294.

89. Bento A. P., Bickelhaupt F. M., *J. Org. Chem*., **2008**, *73*, 7290-7299.

90. Uggerud E., *J. Phys. Org. Chem*, **2006**, 19, 461-466.

91. Glukhovtsev M. N., Pross A., Schlegel H. B., Bach R. D., Radom L., *J. Am. Chem. Soc*,. **1996,** *118*, 11258-11264.

92. Glukhovtsev M. N., Pross A., Radom L., *J. Am. Chem. Soc.* **1996,** *118*, 6273-6284.

93. Uggerud E., *Chem. Eur. J.*, **2006**, *12*, 1127– 1136.

94. Parthiban S., Oliveira g., Martin J. M. L., *J. Phys. Chem. A,* **2001**, *105*, 895-904.

95. Laerdahl J. K., Uggerud E., *Org. Biomol. Chem.*, **2003**, *1*, 2935-2942.

96. Laerdahl J. K., Bache-Andreassen L., Uggerud E., *Org. Biomol. Chem.*, **2003**, *1*, 2943–2950.

97. Laerdahl J. K., Civcir P. U., Bache-Andreassen L., Uggerud E., *Org. Biomol. Chem.*, **2006**, *4*, 135-141.

98. Schreiner P. R., Schleyer P. R, Hill R. K., *J. Org. Chem*., **1994,** *59*, 1849-1854.

99. Hughes E. D., Ingold C. K., Whitfield I. C., *Nature***, 1941,** *147*, 206.

100. Kice J. L., Hanson G. C., *J. Org. Chem*., **1973**, *38*, 1410-1415.

101. Schreiner P. R., Schleyer P. R, Hill R. K, *J. Org. Chem***., 1993,** *58***,** 2822-2829.

102. Koch H. J., Lee H. W., Lee I., *J. Chem. Soc. Perkin Trans. 2*, **1994**, 125-129.

103. Lee I., *Chem. Soc. Rev***., 1990**, *19*, 317-333.

104. Oh H. K., Yang J. H., Lee H. W., Lee I., *New J. Chem.*, **2000**, 24, 213-219.

105. Hoque M. E. U., Guha A. K., Kim Ch. K., Lee B., Lee H. W., *Org. Biomol. Chem***.,** **2009**, *7*, 2919–2925.

106. Dey N. K., Kim Ch. K., Lee H. W., *Org. Biomol. Chem.*, **2011**, *9*, 717–724.

107. Bickelhaupt F. M., Ziegler T., Schleyer P. R., *Organometallics*, **1995**, *14*, 2288-2296.

108. Lairson L.L., Henrissat B., Davies G.J., Withers S. G., *Annu. Rev. Biochem*., **2008**, *77*, 521-555.

109. Henrissat B., Sulzenbacher G., Bourne Y., *Curr. Opin. Struct. Biol.*, **2008**, *18*, 527-533.

110. Kirby J., Hollenfelder F., *From enzyme models to model enzyme*, **2009,** Royal Society of Chemistry; First Edition, London, ISBN 978-0854041756.

111. Errey J.C., Lee S.S., Gibson R.P., Fleites C. M., Barry S. S., Jung P. M. J., O'Sullivan A. C., Davis B. G., Davies G. J., *Angew. Chem. Int. Ed.*, **2010,** *49*, *7*, 1234-1237.

112. Gibson R.P., Turkenburg J.P., Charnock S.J., Lloyd R., Davies G. J., *Chem. Biol*., **2002,** *9*, *12*, 1337-1346.

113. Goncalves S., Borges N., Esteves A. M., Victor B: L., Soares C. M., Santos H., Matias P. M., *J. Biol. Chem*., **2010**, *285*, *23*, 17857-17867.

114. Withers S.G., Wakarchuk W.W., Strynadka N.C.J., *Chem. Biol*., **2002**, *9*, *12*, 1270-1273.

115. Batt S. M., Jabeen T., Mishra A. K., Veerapen N., Krumbach K., Eggeling L., Besra G. S., Futterer K., *J. Biol. Chem.*, **2010**, *285*, 37741–37752.

116. Nidetzky B., Eis C., *Biochem. J*., **2001,** *360*, 727-736.

117. Sinnott M. L., Jencks W. P., *J. Am . Chem. Soc*., **1980,** *102*, *6*, 2026-2032.

118. Banait N. S., Jencks W. P., *J. Am. Chem. Soc*, **1991**, *113*, 7951-7958.

119. Banait N. S., Jencks W. P., *J. Am. Chem. Soc*, **1991**, *113*, 7958-7963.

120. Goedl Ch., Nidetzky B., *ChemBioChem*, **2009**, *10*, 2333-2337.

121. O´Hagan D., Schmidberger J. W., *Nat. Prod. Rep.*, **2010**, *27*, 900-918.

122. Tvaroska I., *ACS Symposium Series*, **2006,** 285-301.

123. Andre I., Tvaroska I., Carver J. P., *Carbohydr. Res.*, **2003,** *338*, 865–877.

124. Botoni A., Miscione G. P., Vivo M., *Proteins*, **2005**, *59*, 118-130.

125. Najer H., Giudicelli R., Menin J., Morel C., *Bull. Soc. Chim. Fr.*, **1963**, *5*, 1022.

126. Ramsh S. M., V'yunov K. A., Ginak A. I., Sochilin E. G., *Zh. Org. Khim.*, **1973**, *9*, 412-414.

127. Engoyan A. P., Peresleni E. M., Vlasova T. F., Chizhevskaya I. I., Sheinker Yu. N., *Khim. Geterosikl. Soedin.*, **1978**, *2*, 190.

128. Chylewski C., *Angew. Chem., Int. Ed.* **1979**, *10*, 195–196.

129. Cornard J. P., Dangleterre L., Lapouge C., *Chem. Phys. Lett.*, **2006**, *419*, 304–308.

130. Croce A. E., *Can. J. Chem.*, **2008**, *86*, 918–924.

131. Jencks W. P., *Progr. Phys. Org. Chem.*, **1964**, *2*, 63–128.

132. Jencks W. P., Gilchrist M., *J. Am. Chem. Soc.*, **1964**, *86*, 5616–5620.

133. Johnson S. L., *Adv. Phys. Org. Chem.*, **1967**, *5*, 237–330.

134. McDonald R. S., Patterson P., Stevens–Whalley A., *Can. J. Chem.*, **1983**, *61*, 1846–1852.

135. Bruice P. Y., Bruice T. C., *J. Am. Chem. Soc.*, **1978**, *100*, 4793–4801.

136. Alborz M., Douglas K. T., Rullo G. R., Yaggi N. F., *J. Chem. Soc., Perkin Trans. 2*, **1982**, 1681–1687.

137. Khan M. N., *J. Chem. Soc., Perkin Trans. 2*, **1988**, 1129–1134.

138. Sedlák M., Kaválek J., Macháček V., Štěrba V., *Molecules*, **1996**, *1*, 170–174.

139. Macháček V., El-Bahai S., Štěrba V., *Collect. Czech. Chem. Commun.*, **1979**, *44*, 912–917.

140. Pant R., *Z. Physiol. Chem.*, **1964**; *335*, 272–274.

141. http://ibmlc2.chem.uga.edu/sparc/.

142. Hilal S. H., Karickhoff S. W., Carreira L. A., *Quant. Struc. Act. Rel.*, **1995**, *14*, 348–355.

143. Bunnett J. F., Davis G. T., *J. Am. Chem. Soc.*, **1960**, *82*, 665–674.

144. Jencks W. P., Carriuolo J., *J. Am. Chem. Soc.*, **1960**, *82*, 675–681.

145. Bruice T. C., Mayahi M. F., *J. Am. Chem. Soc.*, **1960**, 82, 3067–3071.

146. Jencks W. P., Gilchrist M., *J. Am. Chem. Soc.*, **1968**, *90*, 2622–2637.

147. Blackburn G. M., Jencks W. P., *J. Am. Chem. Soc.*, **1968**, *90*, 2638–2645.

148. Satterthwait A. C., Jencks W. P., *J. Am. Chem. Soc.*, **1974**, *96*, 7018–7031.

149. Kovach I. M., Belz M., Larson M., Rousy S., Schowen R. L., *J. Am. Chem. Soc.*, **1985**, *107*, 7360–7365.

150. Jencks W. P., *Acc. Chem. Res.*, **1976**, *9*, 425–432.

151. Williams A., In *Concerted Organic and Bio-organic Mechanisms*; CRC Press: Boca Raton, 2000.

152. Ilieva S., Galabov B., Musaev D. G., Morokuma K., Schaefer III H. F., *J. Org. Chem.,* **2003**, *68*, 1496–1502.

153. Sung D. D., Koo I. S., Yang K., Lee I., *Chem. Phys. Lett.,* **2006**, *426*, 280–284.

154. Holmquist B., Bruice T. C., *J. Am. Chem. Soc.,* **1969**, *91*, 2993–3002.

155. Birk J. P., *J. Chem. Educ.,* **1976**; *53*, 704–707.

156. Edwards L. J., *Trans. Faraday Soc.,* **1950,** *46*, 723–735.

157. Garrett E. R., *J. Am. Chem. Soc.,* **1957**, *79*, 3401–3408.

158. Eigen M., *Angew. Chem., Int. Ed. Engl.,* **1964**, *3*, 1–19.

159. Barnett R. E., Jencks W. P., *J. Am. Chem. Soc.,* **1969**, *91*, 2358–2369.

160. Cox M. M., Jencks W. P., *J. Am. Chem. Soc.,* **1981**, *103*, 580–587.

161. Chang K. C., Grunwald E., *J. Phys. Chem.,* **1976**, *80*, 1422–1425.

162. Grunwald E., Chang K. C., Skipper P. L., Anderson V. K., *J. Phys. Chem.,* **1976**, *80*, 1425–1431.

163. Bensaude O., Dreyfus M., Dodin G., Dubois J. E., *J. Am. Chem. Soc.,* **1977**, *99*, 4438–4446.

164. Warden A. C., Hearn M. T. W., Spiccia L., *Inorg. Chem.*, **2003**, *42*, 7037-7040.

165. Pedersen K. J., *Kgl. Dan. Vidensk. Selsk. Mat. Fys. Medd.*, **1945**, *22*, *12*, 1-25.

166. Pearson R. G., *J.Am. Chem. Soc.*, **1963**, *85*, 3533-3539.

167. Concepts in transition metal chemistry, Edited by Crabb E., Moore E., Smart L., RSC Publishing, Cambridge, ISBN 9781849730600, **2010.**

168. Przystaz T. J, Fife T. H., Fife T. H., *J. Am . Chem. Soc.*, **1980**, *102*, *13*, 4391-4396.

169. Buckingham D.A., Harrowfield J. MacB., Sargeson A.M., *J. Am. Chem. Soc*., **1974**, *96*, *6*, 1726-1729.

170. Suh J., *Acc. Chem. Res*., **1992**, *25*, *7*, 273-279.

171. Fife T. H., Przystaz T. J., *J. Am. Chem. Soc.,* **1982**, *104*, 2251-2257.

172. Albert A., Goldacre R., Phillips J., *J. Chem. Soc*., **1948**, 2240-2249.

173. Hyne J. B., Greidanus J. W., *Can. J. Chem*., **1968**, *47*, 803-812.

174. Hogeveen H., *Rec. Trav. Chim.*, **1964**, *83*, 813-828.

175. Váňa J., Sedlák M., Hanusek J., *J. Org. Chem.*, **2010**, *75*, *11*, 3729-3736.

176. Larina L. I., Karnaukhova R. V., Nakhmanovich A. S., Shagun V. A., Ushakov P. E., Lopyrev V. A., *J. Mol. Structure*, **2002**, *604*, 165-176.

177. Andreae S., Schmitz E., *J. Prakt. Chem*. (Leipzig), **1987**, *329*, *6*, 1008-14.

178. Fife T. H., De N. C., *J. Am. Chem. Soc.*, **1974**, *96*, *19*, 6158-6165.

179. Tasman A., *Rec. Trav. Chim*, **1927**, *46*, 653-698.

180. Jaffe H. H., *Chem. Rev.*, **1953**, *53*, *2*, 191–261.

181. Baker J. W., Holdsworth H. B., *J. Chem. Soc.*, **1947**, 713-726.

182. Bright W . L., Briscoe H. T., *J. Phys. Chem.*, **1933**, *37*, *6*, 787–796.

183. Orzeszko A., MAurin J. K., Niedzwiecka-Kornas A., Kazimierczuk Z, *Tetrahedron*, **1998**, *54*, 7517-7524.

184. Fife T. H., De N.C., *J. Am. Chem. Soc*., **1974**, *96*, *19*, 6158-6165.

185. Fife T. H., Bembi R., Natarajan R., *J. Am. Chem. Soc*., **1996**, *118*, 12956-12963.

186. Gattow G., Klaeser J., *Z. Anorg. Allg. Chem.*, **1977**, *434*, *1*, 110-114.

187. Dabholkar V. V., Parab S. D., *Indian J. Chem. B.***,** , **2007** , *46*, *1*, 195 – 200.

188. Kaválek J., Macháček V., Sedlák M., Štěrba V., *Collect. Czech. Chem. Commun.*,**1993**, *58*, 1122-1132.

189. Pratt R. F., Bruice T. C., *J. Am. Chem. Soc.*, **1972**, *94*, *8*, 2823-2837.

190. Miller L. L., Curtin D.Y., *J. Am. Chem. Soc.*, **1967**, *89*, *3*, 637-645.

191. Kim S. H., Yoh S. D., Lim C., Mishima M., Fujio M., Tsuno Y., *J. Phys. Org. Chem.*, **1998**, *11*, 254-260.

192. Roithová J., *Chem. Soc. Rew.*, **2012**, DOI: 10.1039/c1cs15133a.

193. Withers S. G., *Carbohydr. Polym.*, **2001**, *44*, 325-337.

194. Monegal A., Planas A., *J. Am. Chem. Soc.*, **2006**, *128*, 16030-16031.

195. Fife T. H., Przystas T. J., *J. Am. Chem. Soc.*, **1977**, *99*, *20*, 6693-6699.

196. Ortega J. M., Glotin F., Prazeres R., *Infrared Phys. Technol.*, **2006**, *49*, 133-138.

197. Gaussian 03, Revision C.02, Frisch M. J., Trucks G. W., Schlegel H. B., Scuseria G. E., Robb M. A., Cheeseman J. R., Montgomery Jr. J. A., Vreven T., Kudin K. N., Burant J. C., Millam J. M., Iyengar S. S., Tomasi J., Barone V., Mennucci B., Cossi M., Scalmani G., Rega N., Petersson G. A., Nakatsuji H., Hada M., Ehara M., Toyota K., Fukuda R., Hasegawa J., Ishida M., Nakajima T., Honda Y., Kitao O., Nakai H., Klene M., Li X., Knox J. E., Hratchian H. P., Cross J. B., Bakken V., Adamo C., Jaramillo J., Gomperts R., Stratmann R. E., Yazyev O., Austin A. J., Cammi R., Pomelli C., Ochterski J. W., Ayala P. Y., Morokuma K., Voth G. A., Salvador P., Dannenberg J. J., Zakrzewski V. G., Dapprich S., Daniels A. D., Strain M. C., Farkas O., Malick D. K., Rabuck A. D., Raghavachari K., Foresman J. B., Ortiz J. V., Cui Q., Baboul A. G., Clifford S., Cioslowski J., Stefanov B. B., Liu G., Liashenko A., Piskorz P., Komaromi I., Martin R. L., Fox D. J., Keith T., Al-Laham M. A., Peng C. Y., Nanayakkara A., Challacombe M.,

Gill P. M. W., Johnson B., Chen W., Wong M. W., Gonzalez C., and Pople J. A., Gaussian, Inc., Wallingford CT, **2004**.

198. Vosko S. H., Wilk L., Nusair M., *Can. J. Phys.*, **1980**, *58*, 1200-1211.
199. Lee C., Yang W., Parr R. G., *Phys. Rev. B*, **1988**, 37, 785-789.
200. Becke A. D., *Phys. Rev. A*, **1988**, *38*, 3098-3100.
201. Becke A. D., *J. Chem. Phys.*, **1993**, *98*, 5648-5652.
202. Klamt A., Schüürmann G., *J. Chem. Soc., Perkin Trans. 2*, **1993**, 799-805.
203. Altomare A., Cascarone G., Giacovazzo C., Guagliardi A., Burla M. C., Polidori G., Camalli M., *J. Appl. Crystallogr.*, **1994**, *27*, 1045.
204. Sheldrick G. M., SHELXL-97, A Program for Crystal Structure Refinement; University of Göttingen: Germany, **1997**.
205. Katritzky A. R., Ji F. B., Fan W. Q., Beretta P., Bertoldi M., *J. Heterocycl. Chem.*, **1992**, *29*, 1519-1523.
206. Austin P. R., Bousquet E. W., Lazier W. A., *J. Am. Chem. Soc.*, **1937**, *59*, *5*, 864–866.
207. Pokhodylo N. T., Matiychuk V. S., Obushak M. D., *Chem. Heterocycl. Comp.*, **2010**, *46*, *2*, 140-145.
208. Sperry J., Gibsson J. S., Sejberg J. J. P., Brimble M. A., *Org. Biomol. Chem.*, **2008**, *6*, 4261–4270.
209. Shaabani A., Mirzaei P., Naderi S., Lee D. G., *Tetrahedron*, **2004**, *60*, 11415–11420.
210. Nelsen N. F., *J. Org. Chem.*, **1973**, *38*, *15*, 2693-2697.
211. Kotten I. A., Sauer R. J., *Org. Syntheses*, **1973**, *Coll. Vol. 5*, 145-146; **1962**, *Vol. 42*, 26.
212. Kammel R., Bachelor work, Preparation and reactions of isothiouronium salts derived from 3-bromo-3*H*-isobenzofuran-1-one, University of Pardubice, **2010**.

Appendix

Efficient Synthesis of 5-(2-Hydroxyethyl)-2-phenylimino-1,3-thiazolidin-4-ones and 5-(2-Hydroxyethyl)-2-phenylamino-4,5-dihydro-1,3-thiazol-4-ones

Jiří Váňa,[a] Jiří Hanusek,[a]* Aleš Růžička,[b] and Miloš Sedlák[a]

[a]Institute of Organic Chemistry and Technology, Faculty of Chemical Technology, University of Pardubice, Pardubice, The Czech Republic
[b]Department of General and Inorganic Chemistry, Faculty of Chemical Technology, University of Pardubice, Pardubice, The Czech Republic
*E-mail: Jiri.Hanusek@upce.cz

Received January 9, 2009
DOI 10.1002/jhet.118
Published online 7 July 2009 in Wiley InterScience (www.interscience.wiley.com).

Dedicated to Professor Vladimír Macháček on the occasion of his 65th birthday.

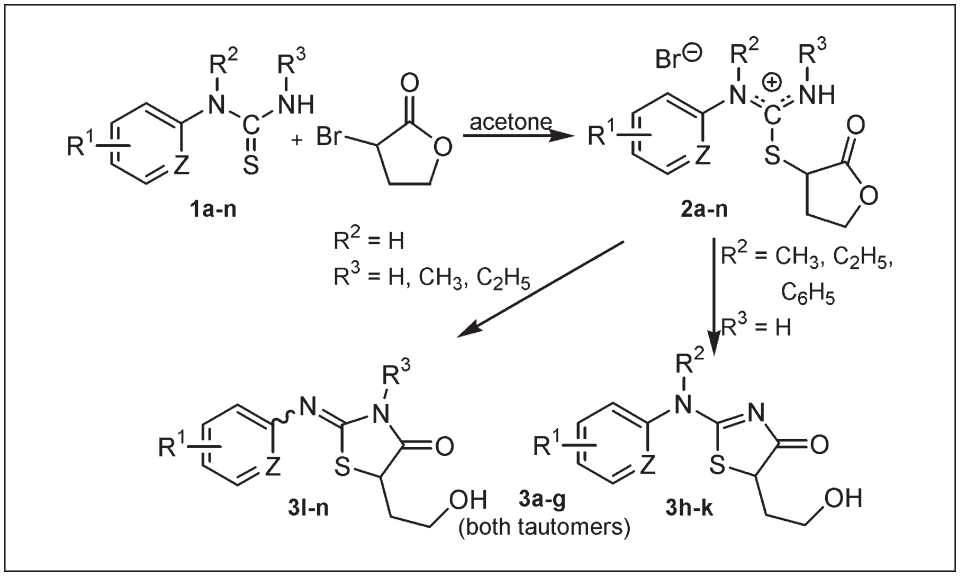

A new method for the synthesis of substituted 5-(2-hydroxyethyl)-2-phenylimino-1,3-thiazolidin-4-ones and 5-(2-hydroxyethyl)-2-phenylamino-4,5-dihydro-1,3-thiazol-4-ones is described, starting from phenylthioureas and 3-bromotetrahydrofuran-2-one. The reaction proceeds under mild conditions, is very simple to perform, and is applicable to a relatively wide range of substituents in benzene nucleus. Some 1,3-thiazolidin-4-ones show dynamic NMR behavior in solution because of prototropy tautomerism and *E*-/*Z*-stereoisomerism.

J. Heterocyclic Chem., **46**, 635 (2009).

INTRODUCTION

Natural [1] as well as synthetic heterocyclic compounds, containing a thiazole ring system often exhibit good antifungal [2], antibacterial [3], and anti-inflammatory [4] activity and are widely used in new pharmaceutical and agrochemical compounds. Also thiazolidine cycle belongs among pharmaceutically significant heterocycles representing an important group of per oral antidiabetics [5]. Thiazole skeleton is also present in many dyes and pigments [6].

There exist a lot of synthetic methods leading to thiazole or thiazolidine skeleton [7] from which those involving rearrangements of another heterocyclic rings represent new interesting alternative. Such rearrangements may provide fascinating routes to derivatives that can be obtained only with great difficulties—or not at all—by other procedures.

RESULTS AND DISCUSSION

Recently, we have found [8] that substituted *S*-(1-phenylpyrrolidin-2-on-3-yl) isothiuronium salts in weakly basic medium undergo an intramolecular transformation reaction. In this particular case, the γ-lactam ring is cleaved and a thiazolidine ring is formed, i.e. substituted 2-imino-5-[2-(phenylamino)ethyl]-1,3-thiazolidin-4-ones are obtained in very good yields. In this work, we extended the scope of this transformation replacing γ-lactam cycle by γ-lacton cycle. In the first step, we have prepared corresponding *S*-(2-oxotetrahydrofuran-3-yl)-*N*-(subst. phenyl) isothiuronium

Scheme 1

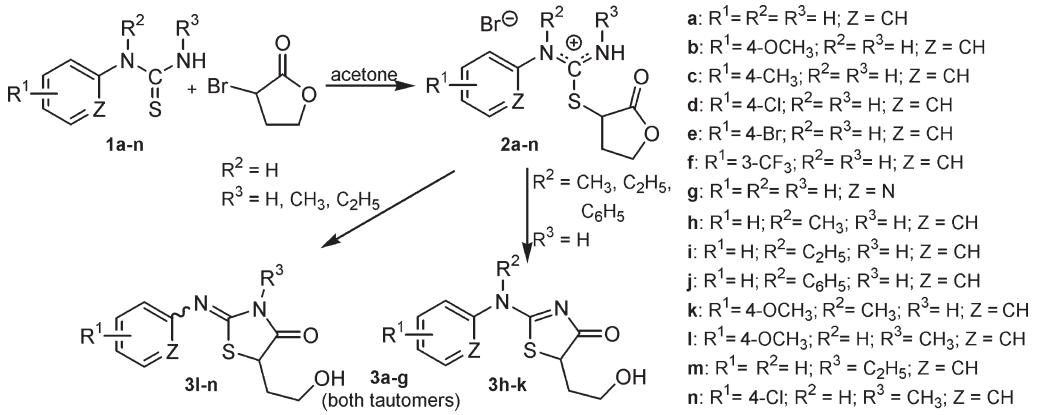

bromides (**2a–n**) from substituted phenylthioureas (**1a–n**) and 3-bromotetrahydrofuran-2-one (α-bromo-γ-butyrolactone), which then underwent rearrangement in basic medium to give desired 5-(2-hydroxyethyl)-2-phenylimino-1,3-thiazolidin-4-ones (**3a–g**, **3l–n**) or 5-(2-hydroxyethyl)-2-phenylamino-4,5-dihydro-1,3-thiazol-4-ones (**3h–k**) (Scheme 1). In most cases, it was impossible to characterize pure isothiuronium salts by NMR because of their spontaneous cyclization giving **3a–n** in DMSO-d_6 solution.

The only exception was *S*-(2-oxotetrahydrofuran-3-yl)-*N*-(4-methoxyphenyl)isothiuronium bromide (**2b**) which was prepared in a pure form and characterized by ^{1}H, ^{13}C NMR, and microanalysis. The reason for enhanced reactivity of the other derivatives lies in the presence of electron-withdrawing group in the benzene nucleus or methyl group on nitrogen(s). All of these substituents facilitate rearrangement involving bicyclic tetrahedral intermediate.

Similar method [9] starting from substituted phenylthioureas and ethyl 3-bromo-5-methyl-2-oxo-tetrahydrofuran-3-carboxylate, ethyl 3-bromo-5,5-dimethyl-2-oxotetrahydrofuran-3-carboxylate, and ethyl 3-bromo-5-isobutoxymethyl-2-oxotetrahydrofuran-3-carboxylate giving spirocyclic 2-aza-3-amino or substituted amino-4-thia-7-oxa-8-methyl-8-substituted spiro[4.4]-2-nonene-1,6-diones was recently published. In this case, nitrogen atom of isothiuronium salt attacks ethoxycarbonyl group in position 3 instead of lactone carbonyl group.

Prepared 5-(2-hydroxyethyl)-2-phenylimino-1,3-thiazolidin-4-ones (**3a–g**, **3l–n**) 5-(2-hydroxyethyl)-2-phenylamino-4,5-dihydro-1,3-thiazol-4-ones (**3h–k**) were characterized by ^{1}H, ^{13}C NMR, and microanalyses and some of them also by X-ray diffraction (Figs. 1, 2) and mass spectroscopy.

Compounds **3a–f** carrying hydrogen atoms on both nitrogen atoms ($R^2 = R^3 = H$) exist in the form of two tautomers differing in the position of C=N double bond. Moreover, the tautomer with exocyclic double bond exists as a mixture of *E*- and *Z*-stereoisomers in the proportion depending on substitution of the benzene nucleus and temperature. This tautomerism and stereoisomerism, which can be seen in both ^{1}H and ^{13}C NMR spectra was previously studied for C-5 unsubstituted 2-phenyliminothiazolidin-4-ones by several authors [10].

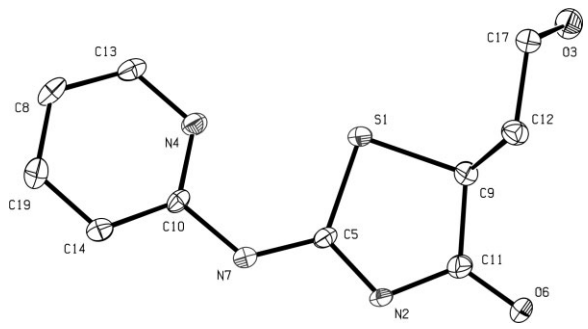

Figure 1. ORTEP view of compound **3g** (thermal ellipsoids at 40% probability).

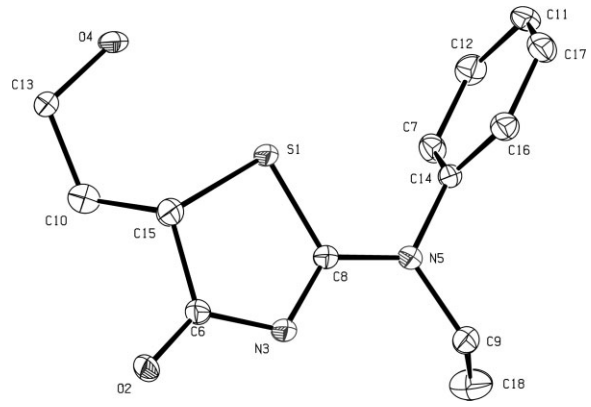

Figure 2. ORTEP view of compound **3i** (thermal ellipsoids at 40% probability).

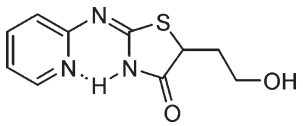

Figure 3. Intramolecular hydrogen bond in solution of **3g** in DMSO-d_6.

In the case of compounds **3h–k** (R^2 = CH_3, C_2H_5, C_6H_5; R^3 = H) and **3l–n** (R^2 = H; R^3 = CH_3, C_2H_5), prototropic tautomerism is absent due to C=N double bond fixation and stereoisomerism is possible only for **3l–n**. In both ^{1}H and ^{13}C NMR spectra of **3g**, there is only one set of signals. From this observation, it can be deduced that compound **3g** exists only as *E*-stereoisomer stabilized in solution by intramolecular hydrogen bond (Fig. 3). On the other hand, in crystal lattice two molecules of **3g** are connected by intermolecular hydrogen bonds (N_{ring}—H···N_{imino}), which constrains *Z*-configuration of C=N double bond (Fig. 1).

EXPERIMENTAL

Starting arylthioureas **1a–n** were prepared and purified by known methods [11]. All other chemicals were purchased from commercial suppliers and used as received. Before use, solvents were dried and distilled. ^{1}H and ^{13}C NMR spectra were recorded on a Bruker Avance 500 MHz instrument in DMSO-d_6 solution. Chemical shifts δ are referenced to solvent residual peak δ(DMSO-d_6) = 2.50 (^{1}H) and 39.6 ppm (^{13}C). Coupling constants *J* are quoted in Hz. ^{13}C NMR spectra were measured in a standard way and by means of the APT (attached proton test) pulse sequence to distinguish CH, CH_3, and CH_2, C_{quart}. Proton–proton connectivities were found by gs-COSY. Protonated carbon atoms were assigned by gs-HSQC spectra. All NMR experiments were performed with the aid of the manufacturer's software. The microanalyses were performed on an apparatus of Fisons Instruments, EA 1108 CHN. The mass spectra (EI) were recorded on an Agilent Technologies Co. gas chromatograph 6890N with a mass detector 5973 Network for samples dissolved in either ether or acetone.

X-ray Crystallography of 3g and 3i. The colorless single crystals of **3g** and **3i** were grown from DMSO solution. The X-ray diffraction data were collected at 150(2)K on a Nonius KappaCCD diffractometer with graphite-monochromated Mo Kα radiation (λ = 0.71073 Å). The structures were solved by direct methods (SIR92) [12]. All reflections were used in the structure refinement based on F2 by full-matrix least-squares technique (SHELXL97) [13].

Compound 3g. $C_{10}H_{11}N_3O_2S$; triclinic, space group P-1, *a* = 5.7500(3), *b* = 8.7980(3), *c* = 10.9290(6) (Å), α = 90.703(4)°, β = 95.787(4)°, γ = 107.550(4)°, *Z* = 2, *V* = 523.93(4) Å^3, Dc = 1.504 g·cm^{-3}. Intensity data collected with 3.0 ≤ θ ≤ 27.5°; 2404 independent reflections measured; 2000 observed [$I > 2\sigma(I)$]. Final *R* index = 0.0589 (observed reflections), Rw = 0.1329 (all reflections), *S* = 1.112. CCDC 704421.

Compound 3i. $C_{13}H_{16}N_2O_2S$; monoclinic, space group P-21/c, *a* = 9.3440(7), *b* = 18.8800(1), *c* = 7.5690(5) (Å), α = 90.000(5)°, β = 105.913(6)°, γ = 90.000(5)°, *Z* = 4, *V* = 1284.11(15) Å^3, Dc = 1.367 g·cm^{-3}. Intensity data collected with 3.0 ≤ θ ≤ 27.5°; 2849 independent reflections measured; 2406 observed [$I > 2\sigma(I)$]. Final *R* index = 0.0608 (observed reflections), Rw = 0.1481 (all reflections), *S* = 1.062. CCDC 704422.

Isothiuronium salts 2; General Procedure. To a hot solution of *N*-arylthiourea **1a–n** (5 mmol) in dry acetone 5 mmol (0.83 g) of 3-bromotetrahydrofuran-2-one was injected. Reaction mixture was refluxed for 5 min and left to stand at room temperature for 2 days. Then precipitated crystals were collected by filtration and submitted to cyclization. In the case of compounds **2d–g**, **2j**, **2l**, and **2n**, no crystals precipitated so that the solution was evaporated and resulting oil was submitted to cyclization without any further purification (yields are given only for **3d–g**, **3j**, **3l**, and **3n**). Crystalline isothiuronium salts **1a–c**, **1h**, **1i**, **1k**, and **1m** were characterized by melting point and by microanalysis. Only in the case of salt **1b**, it was possible to measure ^{1}H and ^{13}C NMR spectra immediately after its dissolution in DMSO-d_6. For all the other salts quick transformation to **3a–n** was observed during the measurement.

S-(2-Oxotetrahydrofuran-3-yl)-N-phenyl isothiuronium bromide (2a). Yield: 1.24g (78%); m.p. 153–155°C. *Anal*. Calcd. for $C_{11}H_{13}BrN_2O_2S$: C, 41.65; H, 4.13; N, 8.83; S, 10.11; Br, 25.19. Found: C, 41.74; H, 4.13; N, 9.01; S, 10.16; Br, 25.05.

S-(2-Oxotetrahydrofuran-3-yl)-N-(4-methoxyphenyl) isothiuronium bromide (2b). Yield: 0.77g (44%); m.p. 154–156°C; ^{1}H NMR (500 MHz): δ = 2.29 (m, 2H, CH_2), 3.65 (m, 2H, OCH_2), 3.82 (s, 3H, OCH_3), 4.72 (dd, *J* = 7.5 and 4.5 Hz, 1H, SCH), 7.16 (AA′XX′, *J* = 9 Hz, 2H, ArH), 7.37 (AA′XX′, *J* = 9 Hz, 2H, ArH), 10.79 (vbs, 3H, NH and NH_2).

^{13}C NMR (125 MHz): δ = 33.6 (CH_2), 47.5 (S—CH), 55.7 (OCH_3), 57.8 (O—CH_2), 115.3 (Ar C-3), 123.6 (Ar C-1), 129.6 (Ar C-2), 160.7 (Ar C-4), 174.1 (C=N), 175.0 (C=O). *Anal*. Calcd. for $C_{12}H_{15}BrN_2O_3S$: C, 41.51; H, 4.35; N, 8.07; S, 9.23; Br, 23.01. Found: C, 41.56; H, 4.29; N, 8.07; S, 9.08; Br, 22.99.

S-(2-Oxotetrahydrofuran-3-yl)-N-(4-methylphenyl) isothiuronium bromide (2c). Yield: 0.83g (50%); m.p. 160–164°C. *Anal*. Calcd. for $C_{12}H_{15}BrN_2O_2S$: C, 43.51; H, 4.56; N, 8.46; S, 9.68; Br, 24.12. Found: C, 43.71; H, 4.60; N, 8.26; S, 9.45; Br, 24.32.

S-(2-Oxotetrahydrofuran-3-yl)-N-phenyl-N-methyl isothiuronium bromide (2h). Yield: 1.3g (78%); m.p. 155–159°C. *Anal*. Calcd. for $C_{12}H_{15}BrN_2O_2S$: C, 43.51; H, 4.56; N, 8.46; S, 9.68; Br, 24.12. Found: C, 43.51; H, 4.86; N, 8.35; S, 9.90; Br, 24.03.

S-(2-Oxotetrahydrofuran-3-yl)-N-phenyl-N-ethyl isothiuronium bromide (2i). Yield: 1.59g (92%); m.p. 155–157°C. *Anal*. Calcd. for $C_{13}H_{17}BrN_2O_2S$: C, 45.23; H, 4.96; N, 8.11; S, 9.29; Br, 23.14. Found: C, 45.14; H, 5.11; N, 8.08; S, 9.03; Br, 23.20.

S-(2-Oxotetrahydrofuran-3-yl)-N-(4-methoxyphenyl)-N-methyl isothiuronium bromide (2k). Yield: 0.96g (53%); m.p. 164–167°C. *Anal*. Calcd. for $C_{13}H_{17}BrN_2O_3S$: C, 43.22; H, 4.74; N, 7.75; S, 8.87; Br, 22.12. Found: C, 43.06; H, 4.80; N, 7.66; S, 8.68; Br, 22.03.

S-(2-Oxotetrahydrofuran-3-yl)-N-phenyl-N′-ethyl isothiuronium bromide (2m). Yield: 1.3g (75%); m.p. 144–146°C. *Anal*. Calcd. for $C_{13}H_{17}BrN_2O_2S$: C, 45.23; H, 4.96; N, 8.11; S, 9.29; Br, 23.14. Found: C, 45.43; H, 5.08; N, 7.96; S, 9.10; Br, 23.14.

5-(2-Hydroxyethyl)-2-phenyliminothiazolidin-4-ones (3a-n); General Procedure. Isothiuronium salts (2 mmol) were dissolved in a minimum amount of aqueous ammonia (25%) and solution was stirred until precipitation of products. Crude products (yields 80–90%) were filtered off and recrystallized from water. Isothiuronium salts **2k–m** were quite insoluble in aqueous ammonia and stirring of suspension gave an oil which was extracted by dichloromethane. Extract was dried and evaporated to give oil solid which was characterized.

5-(2-Hydroxyethyl)-2-(phenylimino)-1,3-thiazolidin-4-one (3a). Yield: 0.44g (94%); m.p. 123–124°C; ^{1}H NMR (500 MHz): δ = 1.79 and 2.26 (2 × m, 2H, CH_2), 3.45 (m, 2H, OCH_2), 4.29 (m, 1H, S—CH), 4.74 (m, 1H, OH), 7.00 and 7.72 (2 × m, 2H, Ar H-2,6), 7.12 (m, 1H, Ar H-4), 7.36 (m, 2H, Ar H-3,5), 11.14, and 11.71 (2 × bs, 1H, NH); ^{13}C NMR (125 MHz): δ = 36.0 and 36.6 (CH_2), 47.7 and 52.1 (S—CH), 58.8 and 59.6 (O—CH_2), 120.5 and 121.6 (Ar C-2,6), 124.7 and 124.8 (Ar C-4), 129.1 and 129.4 (Ar C-3,5), 138.9 and 146.8 (Ar C-1), 177.5 and 178.5 (C=N), 190.6 (C=O). *Anal*. Calcd. for $C_{11}H_{12}N_2O_2S$: C, 55.91; H, 5.12; N, 11.86; S, 13.57. Found: C, 56.13; H, 5.32; N, 11.62; S, 13.35. EI-MS: *m/z* 236 [M^+], 218 [M^+—H_2O], 205, 192, 160, 151, 145, 135, 118 (100 %), 109, 101, 91, 77, 71, 65, 59, 51.

5-(2-Hydroxyethyl)-2-[(4-methoxyphenyl)imino]-1,3-thiazolidin-4-one (3b). Yield: 0.48g (91%); m.p. 124–126°C; ^{1}H NMR (500 MHz): δ = 1.76 and 2.27 (2 × m, 2H, CH_2), 3.52 (m, 2H, OCH_2), 3.74 (s, 3H, OCH_3), 4.26 (dt, *J* = 11.8 and 3.5 Hz, 1H, S—CH), 4.73 (m, 1H, OH), 6.94 (m, 2H, Ar H-3,5), 6.99 and 7.60 (2 × m, 2H, Ar H-2,6), 11.02 and 11.56 (2 × bs, 1H, NH); ^{13}C NMR (125 MHz): δ = 36.0 and 36.5 (CH_2), 48.4 and 52.0 (S—CH), 55.2 (OCH_3), 58.8 and 59.5 (O—CH_2), 114.0 and 114.4 (Ar C-3,5), 121.9 and 123.3 (Ar C-2,6), 131.9 (Ar C-1), 156.2 and 156.7 (Ar C-4), 176.6 (C=N), 190.3 (C=O). *Anal*. Calcd. for $C_{12}H_{14}N_2O_3S$: C, 55.12; H, 5.30; N, 10.52; S, 12.04. Found: C, 55.24; H, 5.26; N, 10.64; S, 12.01. EI-MS: *m/z* 266 [M^+], 248 [M—H_2O], 235, 222, 207, 191, 175, 165, 148, 133 (100%), 118, 105, 90, 78, 63, 55, 41.

5-(2-Hydroxyethyl)-2-[(4-methylphenyl)imino]-1,3-thiazolidin-4-one (3c). Yield: 0.43g (87%); m.p. 124–126°C; ^{1}H NMR (500 MHz): δ = 1.79 and 2.30 (2 × m, 2H, CH_2), 2.27 (s, 3H, CH_3), 3.52 (m, 2H, OCH_2), 4.27 (m, 1H, S—CH), 4.75 (m, 1H, OH), 6.91 and 7.14 (2 × AA′XX′, 2H, Ar H-2,6), 7.15 and 7.59 (2 × AA′XX′, 2H, Ar H-3,5), 11.08 and 11.64 (2 × bs, 1H, NH); ^{13}C NMR (125 MHz): δ = 20.3 (CH_3), 36.1 and 36.7 (CH_2), 48.1 and 52.1 (S—CH), 58.9 and 59.7 (O—CH_2), 120.4 and 121.7 (Ar C-2,6), 129.5 and 129.8 (Ar C-3,5), 134.0 (Ar C-4), 136.5 and 143.3 (Ar C-1), 177.1 and 179.4 (C=N), 190.6 (C=O). *Anal*. Calcd. for $C_{12}H_{14}N_2O_2S$: C, 57.58; H, 5.64; N, 11.19; S, 12.81. Found: C, 57.59; H, 5.69; N, 10.93; S, 12.74.

5-(2-Hydroxyethyl)-2-[(4-chlorophenyl)imino]-1,3-thiazolidin-4-one (3d). Overall yield: 1.7g (97%); m.p. 136–137°C; ^{1}H NMR (500 MHz): δ = 1.79 and 2.25 (2 × m, 2H, CH_2), 3.52 (m, 2H, OCH_2), 4.31 (m, 1H, S—CH), 4.75 (bs, 1H, OH), 6.96 and 7.37 (2 × AA′XX′, 2H, Ar H-2,6), 7.42 and 7.77 (2 × AA′XX′, 2H, Ar H-3,5), 11.26 and 11.80 (2 × bs, 1H, NH); ^{13}C NMR (125 MHz): δ = 35.8 and 36.5 (CH_2), 47.5 and 52.2 (S—CH), 58.7 and 59.6 (O—CH_2), 122.0 and 123.3 (Ar C-2,6), 128.6 (Ar C-4), 129.1 and 129.3 (Ar C-3,5), 137.1 and 146.7 (Ar C-1), 177.4 and 177.7 (C=N), 190.5 (C=O). *Anal*. Calcd. for $C_{11}H_{11}ClN_2O_2S$: C, 48.80; H, 4.10; N, 10.35; S, 11.84; Cl, 13.10. Found: C, 49.01; H, 4.27; N, 10.08; S, 11.60; Cl, 12.94.

5-(2-Hydroxyethyl)-2-[(4-bromophenyl)imino]-1,3-thiazolidin-4-one (3e). Overall yield: 1.21g; (61%) m.p. 140–141°C; ^{1}H NMR (500 MHz): δ = 1.81 and 2.26 (2 × m, 2H, CH_2), 3.50 (m, 2H, OCH_2), 4.31 (m, 1H, S—CH), 4.77 (bs, 1H, OH), 6.91 and 7.51 (2 × AA′XX′, 2H, Ar H-2,6), 7.56 and 7.67 (2 × AA′XX′, 2H, Ar H-3,5), 11.37 and 11.70 (2 × bs, 1H, NH); ^{13}C NMR (125 MHz): δ = 35.8 and 36.5 (CH_2), 47.5 and 52.1 (S—CH), 58.7 and 59.6 (O—CH_2), 116.7 (Ar C-4), 122.4 and 123.7 (Ar C-2,6), 132.0 and 132.3 (Ar C-3,5), 138.3 and 147.1 (Ar C-1), 176.6 (C=N), 190.6 (C=O). *Anal*. Calcd. for $C_{11}H_{11}BrN_2O_2S$: C, 41.92; H, 3.52; N, 8.89; S, 10.17; Br, 25.35. Found: C, 41.93; H, 3.71; N, 8.78; S, 10.40; Br, 24.98.

5-(2-Hydroxyethyl)-2-[(3-trifluoromethylphenyl)-imino]-1,3-thiazolidin-4-one (3f). Overall yield: 1.02g (53%); m.p. 130–131°C; ^{1}H NMR (500 MHz): δ = 1.83 and 2.26 (2 × m, 2H, CH_2), 3.52 (m, 2H, OCH_2), 4.34 (d, *J* = 6.0 Hz, 1H, S—CH), 4.78 (m, 1H, OH), 7.24 (m, 1H, Ar H-6), 7.48 (m, 1H, Ar H-4), 7.60 (m, 1H, Ar H-5), 7.89 and 8.22 (2 × m, 1H, Ar H-2), 11.02 and 11.56 (2 × bs, 1H, NH); ^{13}C NMR (125 MHz): δ = 35.6 and 36.4 (CH_2), 47.4 and 52.2 (S—CH), 58.6 and 59.6 (O—CH_2), 124.1 (q, *J* = 272 Hz, CF_3), 130.1 (q, *J* = 31.6 Hz, Ar C-3), 116.6 and 121.1 (Ar C-2), 117.8 and 120.8 (Ar C-5), 124.0 and 130.5 (Ar C-4), 125.2 and 130.6 (Ar C-6), 139.6 and 149.1 (Ar C-1), 176.9 and 178.3 (C=N), 190.6 (C=O). *Anal*. Calcd. for $C_{12}H_{11}F_3N_2O_2S$: C, 47.37; H, 3.64; N, 9.21; S, 10.54. Found: C, 47.56; H, 3.67; N, 9.42; S, 10.31.

5-(2-Hydroxyethyl)-2-[(2-pyridyl)imino]-1,3-thiazolidin-4-one (3g). Overall yield: 1.34g (84%); m.p. 187–188°C; ^{1}H NMR (500 MHz): δ = 1.82 and 2.22 (2 × m, 2H, CH_2), 3.58 (m, 2H, OCH_2), 4.10 (d, *J* = 7.0 Hz, 1H, S—CH), 4.78 (bs, 1H, OH), 7.11 (m, 2H, Ar H-4,6), 7.82 (m, 1H, Ar H-5), 8.42 (m, 1H, Ar H-3), 11.93 (bs, 1H, NH); ^{13}C NMR (125 MHz): δ = 35.9 (CH_2), 47.2 (S—CH), 58.9 (O—CH_2), 118.2 (Ar C-6), 119.8 (Ar C-4), 138.7 (Ar C-5), 146.9 (Ar C-3), 156.2 (Ar C-1), 165.3 (C=N), 180.7 (C=O). *Anal*. Calcd. for $C_{10}H_{11}N_3O_2S$: C, 50.62; H, 4.67; N, 17.71; S, 13.41. Found: C, 50.52; H, 4.44; N, 17.76; S, 13.64. EI-MS: *m/z* 237 [M^+], 206, 119 (100%), 78, 55, 44.

5-(2-Hydroxyethyl)-2-[(N-phenyl-N-methyl)amino]-4,5-dihydro-1,3-thiazol-4-one (3h). Yield: 0.40g (80%); m.p. 112–115°C; ^{1}H NMR (500 MHz): δ = 1.67 and 2.24 (2 × m, 2H, CH_2), 3.44 (m, 2H, OCH_2), 3.50 (s, 3H, NCH_3), 4.21 (d, *J* = 10.9 Hz, 1H, S—CH), 4.69 (bs, 1H, OH), 7.47 (m, 5H, Ar H-2,3,4,5,6); ^{13}C NMR (125 MHz): δ = 36.5 (CH_2), 41.8 (S—CH), 54.7 (NCH_3), 59.6 (O—CH_2), 127.1 (Ar C-2,6), 129.3 (Ar C-4), 130.0 (Ar C-3,5), 142.2 (Ar C-1), 181.9 (C=N), 189.3 (C=O). *Anal*. Calcd. for $C_{12}H_{14}N_2O_2S$: C, 57.58; H, 5.64; N, 11.19; S, 12.81. Found: C, 57.53; H, 5.56; N, 10.90; S, 12.76.

5-(2-Hydroxyethyl)-2-[(N-phenyl-N-ethyl)amino]-4,5-dihydro-1,3-thiazol-4-one (3i). Yield: 0.47g (90%); m.p. 158–160°C; ^{1}H NMR (500 MHz): δ = 1.12 (t, *J* = 7.1 Hz, 3H, CH_3), 1.67 and 2.26 (2 × m, 2H, CH_2), 3.46 (m, 2H, OCH_2), 4.01 (m, 2H, NCH_2), 4.23 (dd, *J* = 10.6 and 3.1 Hz, 1H, S—CH), 4.68 (t, *J* = 4.8 Hz, 1H, OH), 7.45 (m, 2H, Ar H-2,6), 7.52 (m, 3H, Ar H-3,4,5); ^{13}C NMR (125 MHz): δ =

12.6 (CH_3), 36.5 (CH_2), 49.0 (S—CH), 54.3 (NCH_3), 59.6 (O—CH_2), 128.2 (Ar C-2,6), 129.6 (Ar C-4), 130.0 (Ar C-3,5), 140.4 (Ar C-1), 181.7 (C=N), 189.5 (C=O). *Anal*. Calcd. for $C_{13}H_{16}N_2O_2S$: C, 59.07; H, 6.10; N, 10.60; S, 12.13. Found: C, 58.84; H, 5.92; N, 10.76; S, 12.31.

5-(2-Hydroxyethyl)-2-diphenylamino-4,5-dihydro-1,3-thiazol-4-one (3j). Overall yield: 1.66g (60%); m.p. 153–155°C; ^{1}H NMR (500 MHz): δ = 1.74 and 2.27 (2 × m, 2H, CH_2), 3.47 (m, 2H, OCH_2), 4.26 (dd, J = 7.5 and 3.0 Hz, 1H, S—CH), 4.73 (t, J = 5.0 Hz, 1H, OH), 7.33-7.63 (m, 10H, Ar H); ^{13}C NMR (125 MHz): δ = 36.1 (CH_2), 54.5 (S—CH), 59.4 (O—CH_2), 126.5 (Ar C-2,6), 128.5 (Ar C-4), 129.1 (Ar C-3,5), 129.9 (Ar C-1), 183.2 (C=N), 189.7 (C=O). *Anal*. Calcd. for $C_{17}H_{16}N_2O_2$: C, 65.36; H, 5.16; N, 8.97; S, 10.26. Found: C, 65.12; H, 5.27; N, 8.79; S, 10.44.

5-(2-Hydroxyethyl)-2-[(N-(4-methoxyphenyl)-N-methyl) amino]-4,5-dihydro-1,3-thiazol-4-one (3k). Yield: 0.44g (79%); m.p. 119–120°C; ^{1}H NMR (500 MHz): δ = 1.66 and 2.23 (2 × m, 2H, CH_2), 3.36 (s, 3H, NCH_3), 3.45 (m, 2H, OCH_2), 3.80 (s, 3H, OCH_3), 4.18 (dd, J = 10.5 and 3.0 Hz, 1H, S—CH), 4.76 (t, J = 5.5 Hz, 1H, OH), 7.05 (AA′XX′, J = 8.5 Hz, 2H, Ar H-2,6), 7.41 (AA′XX′, J = 8.5 Hz, 2H, Ar H-3,5); ^{13}C NMR (125 MHz): δ = 35.4 (CH_2), 41.7 (S—CH), 54.6 (NCH_3), 55.4 (OCH_3), 59.5 (O—CH_2), 114.8 (Ar C-2,6), 128.3 (Ar C-3,5), 134.8 (Ar C-1), 159.4 (Ar C-4), 182.1 (C=N), 189.2 (C=O). *Anal*. Calcd. for $C_{13}H_{16}N_2O_3S$: C, 55.70; H, 5.75; N, 9.99; S, 11.44. Found: C, 56.03; H, 5.96; N, 10.32; S, 11.76.

5-(2-Hydroxyethyl)-2-[(4-methoxyphenyl)imino]-3-methyl-1,3-thiazolidin-4-one (3l). Overall yield: 1.03g (57%); m.p. 101–103°C; ^{1}H NMR (500 MHz): δ = 1.83 and 2.28 (2 × m, 2H, CH_2), 3.16 (s, 3H, NCH_3), 3.43 and 3.51 (2 × m, 2H, OCH_2), 3.73 (s, 3H, OCH_3), 4.33 (dd, J = 9.7 and 3.5 Hz, 1H, S—CH), 4.76 (bs, 1H, OH), 6.91 (m, 4H, Ar H-2,3,5,6); ^{13}C NMR (125 MHz): δ = 29.2 (NCH_3), 35.8 (CH_2), 45.2 (S—CH), 55.1 (OCH_3), 58.4 (O—CH_2), 114.3 (Ar C-2,6), 122.0 (Ar C-3,5), 141.2 (Ar C-1), 154.4 (C=N), 156.0 (Ar C-4), 174.6 (C=O). *Anal*. Calcd. for $C_{13}H_{16}N_2O_3S$: C, 55.70; H, 5.75; N, 9.99; S, 11.44. Found: C, 55.81; H, 5.54; N, 10.37; S, 11.21. EI-MS: *m/z* 280 [M^+] (100 %), 265, 249, 236, 221, 207, 194, 179, 162, 147, 133, 119, 106, 90, 78, 64, 55, 45, 35.

5-(2-Hydroxyethyl)-2-(4-phenylimino)-3-ethyl-1,3-thiazolidin-4-one (3m). Yield: 0.17g (33%); oil; ^{1}H NMR (500 MHz): δ = 1.18 (t, J = 7.0 Hz, 3H, CH_3), 1.84 and 2.24 (2 × m, 2H, CH_2), 3.43-3.58 (m, 2H, OCH_2), 3.77 (q, J = 7.0 Hz, 2H, NCH_2), 4.34 (dd, J = 9.6 and 3.7 Hz, 1H, S—CH), 4.75 (bs, 1H, OH), 6.96 (d, J = 7.3 Hz, 2H, Ar H-2,6), 7.11 (t, J = 7.3 Hz, 1H, Ar H-4), 7.35 (t, J = 7.4 Hz, 2H, Ar H-3,5); ^{13}C NMR (125 MHz): δ = 12.3 (CH_3), 35.7 (CH_2), 37.4 (NCH_2), 45.3 (S—CH), 58.3 (O—CH_2), 121.0 (Ar C-2,6), 124.2 (Ar C-4), 129.2 (Ar C-3,5), 148.3 (Ar C-1), 154.0 (C=N), 174.4 (C=O). *Anal*. Calcd. for $C_{13}H_{16}N_2O_2S$: C, 59.07; H, 6.10; N, 10.60; S, 12.13. Found: C, 58.71; H, 5.96; N, 10.86; S, 11.88. EI-MS: *m/z* 264 [M^+] (100 %), 233, 221, 205, 192, 177, 163, 146, 131, 118, 104, 91, 77, 65, 55, 45, 35.

5-(2-Hydroxyethyl)-2-[(4-chlorophenyl)imino]-3-methyl-1,3-thiazolidin-4-one (3n). Overall yield: 1.15g (63%); m.p. 87–89°C; ^{1}H NMR (500 MHz): δ = 1.86 and 2.27 (2 × m, 2H, CH_2), 3.16 (s, 3H, NCH_3), 3.45 and 3.54 (2 × m, 2H, OCH_2), 4.36 (dd, J = 9.8 and 3.6 Hz, 1H, S—CH), 4.75 (t, J = 5.0 Hz, 1H, OH), 6.96 (AA′XX′, J = 8.5 Hz, 2H, Ar H-2,6) 7.40 (AA′XX′, J = 8.5 Hz, 2H, Ar H-3,5); ^{13}C NMR (125 MHz): δ = 29.0 (NCH_3), 35.3 (CH_2), 45.3 (S—CH), 58.1 (O—CH_2), 122.6 (Ar C-2,6), 128.0 (Ar C-4), 128.9 (Ar C-3,5), 147.0 (C-1), 155.6 (C=N), 174.3 (C=O). *Anal*. Calcd. for $C_{12}H_{13}ClN_2O_2S$: C, 50.61; H, 4.60; N, 9.84; S, 11.26. Found: C, 50.35; H, 4.63; N, 10.15; S, 11.02.

Acknowledgments. The authors thank to Ministry of Education, Youth and Sports of the Czech Republic for financial support (Project MSM 002 162 7501).

REFERENCES AND NOTES

[1] (a) Lewis, J. R. Nat Prod Rep 2002, 19, 223; (b) Jin, Z.; Li, Z. G.; Huang, R. Q. Nat Prod Rep 2002, 19, 454; (c) Jin, Z. Nat Prod Rep 2006, 23, 464.

[2] Vicini, P.; Geronikaki, A.; Incerti, M.; Zani, F.; Dearden, J.; Hewitt, M. Bioorg Med Chem 2008, 16, 3714.

[3] (a) Sattigeri, V. J.; Soni, A.; Singhal, S.; Khan, S.; Pandya, M.; Bhateja, P.; Mathur, T.; Rattan, A.; Khanna, J. M.; Mehta, A. Arkivoc 2005, 46; (b) Bondock, S.; Khalifa, W.; Fadda, A. A. Eur J Med Chem 2007, 42, 948; (c) Karegoudar, P.; Karthikeyan, M. S.; Prasad, D. J.; Mahalinga, M.; Holla, B. S.; Kumari, N. S. Eur J Med Chem 2008, 43, 261.

[4] Johnson, A. R.; Marletta, M. A.; Dyer, R. D. Biochemistry 2001, 40, 7736.

[5] (a) Cantello, B. C. C.; Cawthorne, M. A.; Cottam, G. P.; Duff, P. T.; Haigh, D.; Kindley, R. M.; Lister, C. A.; Smith, S. A.; Thurlby, P. L. J Med Chem 1994, 37, 3977; (b) Lehmann, J. M.; Moore, L. B.; Smitholiver, T. A.; Wilkinson, W. O.; Willson, T. M.; Kliewer, S. A. J Biol Chem 1995, 270, 12953; (c) Gale, E. Lancet 2001, 357, 1870.

[6] (a) Farris, R. E. In Kirk-Othmer Encyclopedia of Chemical Technology, 3rd ed.; Wiley: New York, 1983; Vol. 22, p 918; (b) Fisher, J. G.; Clark, G. T. In Kirk-Othmer Encyclopedia of Chemical Technology, 3rd ed.; Wiley: New York, 1983; Vol. 22, p 927.

[7] (a) Metzger, J. V., Ed. The Chemistry of Heterocyclic Compounds. In Thiazole and Its Derivatives; Weissberger, A.; Taylor, E. C., Eds.; Wiley: New York, 1979; Vol. 34, Parts 1–3; (b) Kabashima, S.; Okawara, T.; Yamasaki, T.; Furukawa, M. Heterocycles 1990, 31, 1129; (c) Hamama, W. S.; Ismail, M. A.; Shaaban, S.; Zoorob, H. J Heterocycl Chem 2008, 45, 939.

[8] (a) Sedlák, M.; Hejtmánková, L.; Hanusek, J.; Macháček, V. J Heterocycl Chem 2002, 39, 1105; (b) Sedlák, M.; Hanusek, J.; Hejtmánková, L.; Kašparová, P. Org Biomol Chem 2003, 1, 1204; (c) Hanusek, J.; Hejtmánková, L.; Štěrba, V.; Sedlák, M. Org Biomol Chem 2004, 2, 1756.

[9] (a) Kochikyan, T. V. Synth Commun 2004, 34, 4219; (b) Kochikyan, T. V. Russ J Org Chem 2005, 41, 580; (c) Kochikyan, T. V.; Samvelyan, M. A.; Harutyunyan, V. S.; Avetisyan, A. A. Chem Heterocycl Compd 2006, 42, 446.

[10] (a) Najer, H.; Giudicelli, R., Menin, J.; Morel, C. Bull Soc Chim Fr 1963, 1022; (b) Ramsh, S. M.; V'yunov, K. A.; Ginak, A. I.; Sochilin, E. G. Zh Org Khim 1973, 9, 412; (c) Engoyan, A. P.; Peresleni, E. M.; Vlasova, T. F.; Chizhevskaya, I. I.; Sheinker, Yu. N. Khim Geterosikl Soedin 1978, 2, 190.

[11] (a) King, H.; Tonkin, I. M. J Chem Soc 1946, 1063; (b) Frank, R. L.; Smith, P. V. In Organic Synthesis, Coll. Vol. 3, 1955, 3, 735; (c) Narayana, B; Raj, K. K. V.; Ashalatha, B. V.; Kumari, N. S.; Sarojini, B. K. Eur J Med Chem 2004, 39, 867.

[12] Altomare, A.; Cascarone, G.; Giacovazzo, C.; Guagliardi, A.; Burla, M. C.; Polidori, G.; Camalli, M. J Appl Crystallogr 1994, 27, 1045.

[13] Sheldrick, G. M. SHELXL-97, A Program for Crystal Structure Refinement; University of Göttingen: Germany, 1997.

JOC Article
pubs.acs.org/joc

Kinetic Evidence for the Coexistence of Zwitterionic ($T^{\pm}$), Neutral (T^{0}) and Anionic (T^{-}) Intermediates during Rearrangement of *S*-(2-Oxotetrahydrofuran-3-yl)-*N*-(4-methoxyphenyl)isothiuronium Bromide to 5-(2-Hydroxyethyl)-2-(4-methoxyphenylimino)-1,3-thiazolidin-4-one

Jiří Váňa, Miloš Sedlák, and Jiří Hanusek*

Faculty of Chemical Technology, Institute of Organic Chemistry and Technology, University of Pardubice, Studentská 573, CZ-532 10 Pardubice, The Czech Republic

jiri.hanusek@upce.cz

Received March 16, 2010

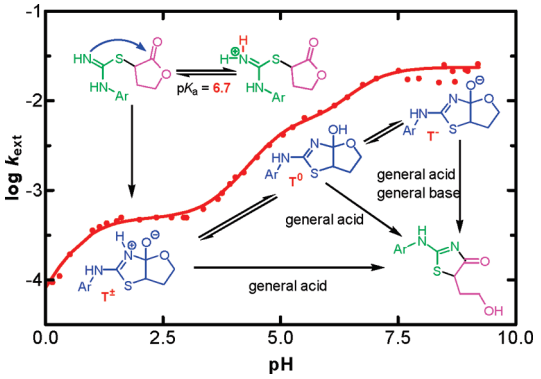

The kinetics and mechanism of rearrangement of *S*-(2-oxotetrahydrofuran-3-yl)-*N*-(4-methoxyphenyl)-isothiuronium bromide (**1**) into 5-(2-hydroxyethyl)-2-[(4-methoxyphenyl)imino]-1,3-thiazolidin-4-one have been studied under pseudo-first-order reaction conditions in aqueous buffer solutions and in diluted HCl at 25 °C. Multiple breaks in the pH profile establish the formation of three different kinetically detectable intermediates $\mathbf{T}^{\pm}$, $\mathbf{T}^{0}$, and $\mathbf{T}^{-}$. Treatment of **1** (pK_a = 6.7) with base produces reactive isothiourea, which undergoes cyclization to give $\mathbf{T}^{\pm}$ (rate limiting step at pH < 0.5). Intermediate $\mathbf{T}^{\pm}$ then undergoes either general acid-catalyzed, concerted ($\alpha = -0.47$) breakdown to **2** (rls at pH 2−3) or a water-mediated proton switch to $\mathbf{T}^{0}$ which is followed by its general acid-catalyzed breakdown (pH 3−6). The last reaction pathway involves the formation of $\mathbf{T}^{-}$ either from $\mathbf{T}^{\pm}$ or from $\mathbf{T}^{0}$ (pH > 6). The first possibility seems to be more likely because it is in accordance with kinetics observed in basic amine buffers, where the nonlinear increase of the k_{obs} with the c_{Buffer} changes to a linear increase as a general base-catalyzed pathway is introduced. Coexistence of all three kinetically detectable intermediates is very rare and is possibly due to relatively enhanced stability of these intermediates necessitating participation of an acid for progression to products.

Introduction

It is well-known that intramolecular reactions bear a striking resemblance to the reactions of enzymes and can give insight into the analogous enzymatic process.[1] Small molecules undergoing intramolecular cyclization reactions frequently have been used as models for understanding the nature of preorganizational effects and their relative contributions to the enhanced rates observed in enzymatic reactions.[1,2] Acyl groups have a prominent position in biochemistry and biology, and just their biochemical relevance has made acyl

(1) (a) Page, M.; Williams, A. In *Organic & Bio-organic Mechanisms*; Addison Wesley Longman Ltd.: Singapore, 1997. (b) Jencks, W. P. In *Catalysis in Chemistry and Enzymology*; General Publishing Comp. Ltd.: Toronto, 1987. (c) Bruice, T. C. In *Enzymes*; Boyer, P. D., Ed.; Academic Press: New York, 1970; Vol. 2, pp 217−279. (d) Anslyn, E. V.; Dougherty, D. A. In *Modern Physical Organic Chemistry*; University Science Books: Sausalito, 2006.

(2) (a) Lightstone, F. C.; Bruice, T. C. *J. Am. Chem. Soc.* **1996**, *118* (11), 2595–2605. (b) Bruice, T. C.; Lightstone, F. C. *Acc. Chem. Res.* **1999**, *32* (2), 127–136. (c) Schultz, P. G. *Acc. Chem. Res.* **1989**, *22*, 287–294.

DOI: 10.1021/jo1004873 Published on Web 04/29/2010

group transfer one of the most studied reactions in all of organic chemistry.[3] Intramolecular aminolysis are an specially important class of acyl-transfer reactions and are of great importance in biochemistry and medicinal chemistry, and a large amount of research has been devoted in this area.[4]

Rearrangements of heterocyclic compounds are also of great significance toward providing new routes to otherwise difficult to prepare biologically active compounds. This new approach to the synthesis of heterocycles has rapidly grown in the past several years.[5] In many cases, such transformations are subject to general acid−base catalysis and proceed under very mild conditions, even at physiological pH. This finding has great importance, not only for the synthesis of these compounds but also for their potential application in medicine (pro-drug approach[4k]). For example, the thiazolidine ring, which is the product formed in the present study, is an important pharmacophore.[6]

Recently, we have studied the structure[7] and reactivity[8] of substituted *S*-(1-phenylpyrrolidin-2-on-3-yl)isothiuronium salts which, in weakly basic medium, undergo an intramolecular rearrangement to give substituted 2-imino-5-[2-(phenylamino)-ethyl]-1,3-thiazolidin-4-ones. More recently, we have extended the scope of this transformation: replacing the γ-lactam ring with a γ-lactone ring.[9] The *S*-(2-oxotetrahydrofuran-3-yl)-*N*-(substituted phenyl)isothiuronium bromides underwent[9]

SCHEME 1

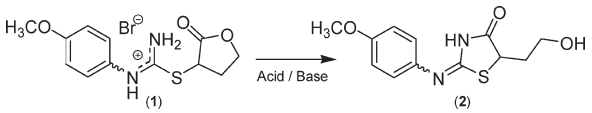

rearrangement in acidic and basic medium to give 5-(2-hydroxyethyl)-2-phenylimino-1,3-thiazolidin-4-ones or 5-(2-hydroxyethyl)-2-phenylamino-4,5-dihydro-1,3-thiazol-4-ones in very good yields. This transformation proceeds readily under mild conditions in aqueous buffer solutions and is able to accept a relatively wide range of substituents in the benzene nucleus.

The aim of the work reported here was to carry out a detailed study of the mechanism of acid−base-catalyzed intramolecular rearrangement of *S*-(2-oxotetrahydrofuran-3-yl)-*N*-(4-methoxyphenyl)isothiuronium bromide (**1**) to 5-(2-hydroxyethyl)-2-[(4-methoxyphenyl)imino]-1,3-thiazolidin-4-one (**2**) (Scheme 1).

Results and Discussion

Kinetic Measurements. The acid−base-catalyzed transformation of isothiuronium salt **1** giving thiazolidin-4-one **2** as the only product was studied spectrophotometrically under pseudo-first-order conditions in aqueous hydrochloric acid solutions (c = 0.001−0.7 mol·L^{-1}) and in aqueous buffers (pH = 2−9) at constant ionic strength (I = 1 mol·L^{-1}) and at 25 °C. All spectra recorded during the rearrangement reaction showed sharp isosbestic points which prove[10] the existence of only two absorbing species; i.e., this result allows us to reject consecutive reaction mechanisms. In other words, only short-living intermediates in negligible concentration can occur on the reaction coordinate.

Observed rate constants, k_{obs}, were calculated in each buffer/acid solution from the absorbance vs time dependence of the absorptions at 260 or 273 nm and were plotted against the total buffer concentration ($c_{Buff} = c_B + c_{BH}$). It was found that in dichloroacetate (DCA), chloroacetate (CA), methoxyacetate (MEA), acetate (AC), hydroxylamine (HA), *N*-methylmorpholine (NMM), glycinamide (GA), tris-(hydroxymethyl)aminomethane (TRIS), and morpholine (MP) buffers the observed rate constant (k_{obs}) increases with both the total buffer concentration (c_{Buff}) and the basicity (pH) of the medium (Figures 1−3). From this observation, it is clear that the transformation involves general buffer catalysis as well as specific acid−base catalysis.

Two different dependences of k_{obs} on the total buffer concentration (c_{Buff}) were observed: in DCA, CA, MEA, AC, and partially in HA buffers, k_{obs} increases linearly with c_{Buff} (Figures 1 and 3), whereas in NMM, GA, TRIS, and MP buffers the slopes of plots decreased with increasing c_{Buff} until at sufficiently high buffer concentration the lines appear to approach linearity (Figures 2 and 3). With NMM, TRIS, and MP buffers, the linear portion, at high c_{Buff}, is easily discernible, and therefore, a more detailed analysis of those buffers was made (see below). Curved buffer dilution plots of k_{obs} reveal a change in the rate-limiting step with the change in the total buffer concentration at a constant pH, which in turn implies the presence of a reactive intermediate

(3) (a) Bender, M. L. *Chem. Rev.* **1960**, *60*, 53–113. (b) Johnson, S. L. *Adv. Phys. Org. Chem.* **1967**, *5*, 237–330. (c) Jencks, W. P. *Chem. Rev.* **1972**, *72*, 705–718. (d) Williams, A. *Acc. Chem. Res.* **1989**, *22*, 387–392. (e) Faber, K.; Riva, S. *Synthesis* **1992**, 895–910. (f) Marlier, J. F. *Acc. Chem. Res.* **2001**, *34*, 283–290. (g) Lee, I.; Sung, D. D. *Curr. Org.. Chem.* **2004**, *8*, 557–567.

(4) (a) Martin, R. B.; Parcell, A.; Hedrick, R. I. *J. Am. Chem. Soc.* **1964**, *86*, 2406–2413. (b) Hay, R. W.; Morris, P. J. *J. Chem. Soc., Perkin Trans. 2* **1972**, 1021–1029. (c) Fife, T. H.; DeMark, B. R. *J. Am. Chem. Soc.* **1976**, *98*, 6978–6982. (d) Caswell, M.; Chaturvedi, R. K.; Lane, S. M.; Zvilichovsky, B.; Schmir, G. L. *J. Org. Chem.* **1981**, *46*, 1585–1593. (e) Fife, T. H.; Duddy, N. W. *J. Am. Chem. Soc.* **1983**, *105*, 74–79. (f) Buur, A.; Bundgaard, H.; Lee, V. H. L. *Int. J. Pharm.* **1988**, *42*, 51–60. (g) Patterson, K. H.; Depree, G. J.; Zender, J. A.; Morris, P. J. *Tetrahedron Lett.* **1994**, *35*, 281–284. (h) Fife, T. H.; Chauffe, L. *J. Org. Chem.* **2000**, *65*, 3579–3586. (i) Larsen, S. W.; Ankersen, M.; Larsen, C. *Eur. J. Pharm. Sci.* **2004**, *22*, 399–408. (j) Barroso, S.; Blay, G.; Cardona, L.; Fernandez, I.; Garcia, B.; Pedro, J. R. *J. Org. Chem.* **2004**, *69*, 6821–6829. (k) Skwarczynski, M.; Kiso, Y. *Curr. Med. Chem.* **2007**, *14*, 2813–2823.

(5) (a) Vivona, N.; Buscemi, S.; Frenna, V.; Cusmano, G. *Adv. Heterocycl. Chem.* **1993**, *56*, 49–154. (b) van der Plas, H. C. *Adv. Heterocycl. Chem.* **1999**, *74*, 153–221. (c) van der Plas, H. C. *J. Heterocycl. Chem.* **2000**, *37*, 427–438. (d) Hajós, G.; Riedl, Z.; Kollenz, G. *Eur. J. Org. Chem.* **2001**, 3405–3414. (e) Dejaegher, Y.; Mangelinckx, S.; De Kimpe, N. *J. Org. Chem.* **2002**, *67*, 2075–2081. (f) Van Brabandt, W.; De Kimpe, N. *J. Org. Chem.* **2005**, *70*, 8717–8722. (g) Buscemi, S.; Pace, A.; Piccionello, A. P.; Pibiri, I.; Vivona, N.; Giorgi, G.; Mazzanti, A.; Spinelli, D. *J. Org. Chem.* **2006**, *71*, 8106–8113. (h) D'hooghe, M.; De Kimpe, N. *Tetrahedron* **2006**, *62*, 513–535. (i) Duggan, P. J.; Liepa, A. J.; O'Dea, L. K.; Tranberg, C. E. *Org. Biomol. Chem.* **2007**, *5*, 472–477. (j) Karikomi, M.; D'hooghe, M.; Verniest, G.; De Kimpe, N. *Org. Biomol. Chem.* **2008**, *6*, 1902–1904. (k) Pozgan, F.; Kočevar, M. *Heterocycles* **2009**, *77*, 657–678.

(6) (a) Cantello, B. C. C.; Cawthorne, M. A.; Cottam, G. P.; Duff, P. T.; Haigh, D.; Kindley, R. M.; Lister, C. A.; Smith, S. A.; Thurlby, P. L. *J. Med. Chem.* **1994**, *37*, 3977–3985. (b) Zarghi, A.; Najafnia, L.; Daraee, B.; Dadrass, O. G.; Hedayati, M. *Bioorg. Med. Chem. Lett.* **2007**, *17*, 5634–5637. (c) Xia, Z.; Knaak, C.; Ma, J.; Beharry, Z. M.; McInnes, C.; Wang, W.; Kraft, A. S.; Smith, C. D. *J. Med. Chem.* **2009**, *52*, 74–86. (d) Li, Q.; Al-Ayoubi, A.; Guo, T.; Zheng, H.; Sarkar, A.; Nguyen, T.; Eblen, S. T.; Grant, S.; Kellogg, G. E.; Zhang, S. *Bioorg. Med. Chem. Lett.* **2009**, *19*, 6042–6046.

(7) (a) Hanusek, J.; Sedlák, M.; Drabina, P.; Ružička, A. *Acta Crystallogr., Sect. E* **2009**, *65*, o411–412. (b) Hanusek, J.; Sedlák, M.; Drabina, P.; Ružička, A. *Acta Crystallogr., Sect. E* **2009**, *65*, o413.

(8) (a) Sedlák, M.; Hejtmánková, L.; Hanusek, J.; Macháček, V. *J. Heterocycl. Chem.* **2002**, *39*, 1105–1107. (b) Sedlák, M.; Hanusek, J.; Hejtmánková, L.; Kašparová, P. *Org. Biomol. Chem.* **2003**, *1*, 1204–1209. (c) Hanusek, J.; Hejtmánková, L.; Štěrba, V.; Sedlák, M. *Org. Biomol. Chem.* **2004**, *2*, 1756–1763.

(9) Váňa, J.; Hanusek, J.; Ružička, A.; Sedlák, M. *J. Heterocycl. Chem.* **2009**, *46*, 635–639.

(10) (a) Chylewski, C. *Angew. Chem., Int. Ed.* **1971**, *10*, 195–196. (b) Cornard, J. P.; Dangleterre, L.; Lapouge, C. *Chem. Phys. Lett.* **2006**, *419*, 304–308. (c) Croce, A. E. *Can. J. Chem.* **2008**, *86*, 918–924.

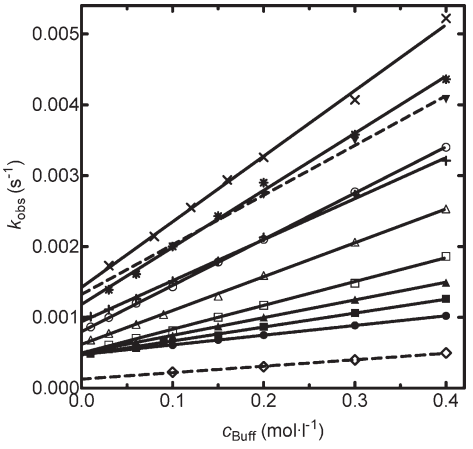

FIGURE 1. Dependence of the observed rate constant (k_{obs}, s^{-1}) on the total buffer concentration (c_{Buff}, mol·L^{-1}) measured at 25 °C in CA [(2:1a) pH 2.36 (●); (1:1) pH 2.68 (■); (1:1) pD 3.14 (◊); (1:2b) pH 2.94 (▲)], MEA [(2:1a) pH 3.04 (□); (1:1) pH 3.35 (△); (1:2b) pH 3.67 (○)] and AC buffers [(6:1a) pH 3.76 (+); (4:1a) pH 3.93 (∗); (3:1a) pH 4.04 (×); (1:1) pD 5.14 (▼)]: (a) acidic; (b) basic. Dashed lines correspond to measurements in D_2O. Note: Data for DCA (1:2b) and AC buffer ratios (2:1a, 1:1; 1:2b, 1:4b) are not depicted here for better clarity of the Figure but they are in the Supporting Information.

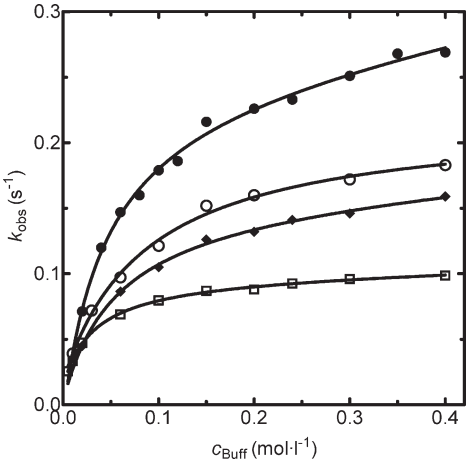

FIGURE 2. Dependence of the observed rate constant (k_{obs}, s^{-1}) on the total buffer concentration (c_{Buff}, mol·L^{-1}) measured at 25 °C in NMM [(1:1) pH 8.24 (□)]; TRIS [(1:1) pH 8.36 (♦)]; GA [(1:1) pH 8.65 (○)] and MP buffers [(1:1) pH 8.94 (●)]. Data for other buffer ratios are not depicted here for better clarity of the Figure but they are in the Supporting Information.

on the reaction coordinate.[4e,8b,11] Another possible reason for the nonlinear plots in Figure 2 is that the nitrogen buffers undergo some kind of complexation with **1** (pre-equilibria with amine/ammonium or H-bonding) and the complex becomes more reactive than uncomplexed **1**. However, this possibility seems to be unlikely because hydroxylamine buffers differ in their behavior dependent on the ratios of both components (Figure 3): a linear relationship is observed at a low fraction of free base (low pH) and a nonlinear relationship at a high fraction of free base (high pH). Therefore, it is clear that the nonlinearity of the plots is simply a function of pH, and similar observations have been reported for other reaction systems.[4e,11d]

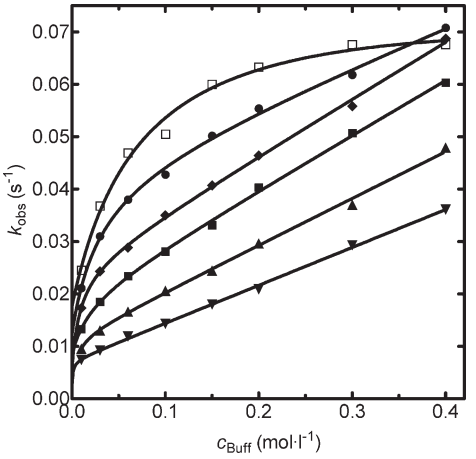

FIGURE 3. Dependence of the observed rate constant (k_{obs}, s^{-1}) on the total buffer concentration (c_{Buff}, mol·L^{-1}) measured at 25 °C in hydroxylamine (HA) buffers [(4:1a) pH 5.52 (▼); (2:1a) pH 5.85 (▲); (1:1) pH 6.15 (■); (1:2b) pH 6.42 (♦); (1:4b) pH 6.75 (●); (1:8b) pH 7.05 (□)]: (a) acidic; (b) basic.

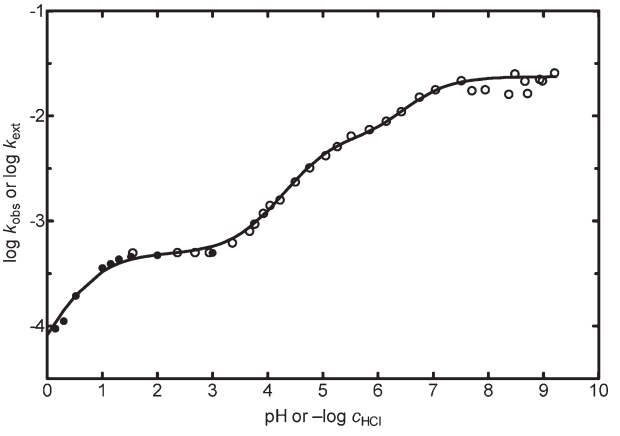

FIGURE 4. pH profile (log k_{ext} vs pH) for rearrangement of **1** to **2** in buffers (○) and (log k_{obs} vs −log c_{HCl}) in hydrochloric acid (●). The line represents the best fit of all data points using eq 2 or eq 5 with parameters given in the text.

Extrapolation of the plots of k_{obs} vs c_{Buff} to zero buffer concentration provided, as intercepts, the values of the catalytic constants (k_{ext}). In this case, the only catalytic species are the hydroxide anion and hydroxonium ion, whose concentrations are given by the ratio of both buffers components (c_B / c_{BH}) or by concentration of the hydrochloric acid. From this data the corresponding pH profile (Figure 4) can be generated whose shape, in the pH region 0−3, is similar to that observed for cyclization of *S*-(ethoxycarbonylmethyl)isothiuronium chloride.[12]

(11) (a) Jencks, W. P. *Prog. Phys. Org. Chem.* **1964**, *2*, 63–128. (b) Jencks, W. P; Gilchrist, M. *J. Am. Chem. Soc.* **1964**, *86*, 5616–5620. (c) Johnson, S. L. *Adv. Phys. Org. Chem.* **1967**, *5*, 237–330. (d) McDonald, R. S.; Patterson, P.; Stevens-Whalley, A. *Can. J. Chem.* **1983**, *61*, 1846–1852. (e) Bruice, P. Y.; Bruice, T. C. *J. Am. Chem. Soc.* **1978**, *100*, 4793–4801. (f) Alborz, M.; Douglas, K. T.; Rullo, G. R.; Yaggi, N. F. *J. Chem. Soc., Perkin Trans. 2* **1982**, 1681–1687. (g) Khan, M. N. *J. Chem. Soc., Perkin Trans. 2* **1988**, 1129–1134. (h) Sedlák, M.; Kaválek, J.; Macháček, V.; Štěrba, V. *Molecules* **1996**, *1*, 170–174.

(12) Macháček, V.; El-Bahai, S.; Štěrba, V. *Collect. Czech. Chem. Commun.* **1979**, *44*, 912–917.

TABLE 1. Catalytic Rate Constants k_{BH}^{cor} and k_B' for Individual Buffer Components

base buffer component (B)	pK_a(BH)[29]	k_{BH}^{cor} ($L \cdot mol^{-1} \cdot s^{-1}$)	k_B'
H_2O	−1.74	2460[a]	
dichloroacetate (DCA)	1.29	175 ± 5	
chloroacetate (CA)	2.86	48.0 ± 3	
methoxyacetate (MEA)	3.53	22.6 ± 0.8	
acetate (AC)	4.76	6.3 ± 0.2	
hydroxylamine (HA)	5.96	1.6 ± 0.1[b]	
N-methylmorpholine (NMM)	7.41		0.12 ± 0.01[c]
TRIS	8.10		0.26 ± 0.02[c]
glycinamide (GA)	8.00		0.24 ± 0.01[c]
morpholine (MP)	8.39		0.48 ± 0.02[c]

[a]From the plateau at pH 2−3 (Figure 4). $k_H = k_1k_2/k_{-1}$. [b]From buffer with c_B/c_{BH} 1:4. [c]From buffers with c_B/c_{BH} 1:1.

There are five breaks in the pH profile in Figure 4. In hydrochloric acid solutions, the log k_{obs} increases with pH up to ca. 1.5. Between pH 1.5 and 3.0, the values of log k_{obs} (log k_{ext}) are pH-independent and then linearly increase again with exceptionally low slope (ca. 0.45; a slope +1 has been observed for similar cyclization[12]). The third slight break downward occurs at pH ~5, and then log k_{ext} gradually increases again with pH (slope ca. 0.3) up to pH 7. The last break downward to zero slope occurs at pH ~7. The values of log k_{ext} are somewhat scattered above pH 7 because the extrapolation from nonlinear dependences (basic buffers) is less precise as compared with extrapolation from linear dependences found for substituted acetate buffers.

Since the isothiuronium salt **1** (= $\mathbf{SH}^+$) itself does not undergo rearrangement, it was necessary to relate k_{obs} to the concentration of free isothiourea (**S**). The corrected rate constants (k_{cor}) were calculated from the pK_a of the isothiuronium salt **1** and pH of the buffer solution according to eq 1. A pK_a of 6.7 was adopted for this purpose (for details of the pK_a estimation, see below)

$$k_{cor} = k_{obs}\frac{K_a}{K_a + [H^+]} = k_{obs}(1 + 10^{(pK_a - pH)}) \qquad (1)$$

For buffers showing linear dependence of k_{cor} vs c_{Buff} (substituted acetates, acidic HA buffers), the catalytic constants k_{Buff} were determined from the slopes of the plots. A second plot of k_{Buff} values against the ratio c_B/c_{Buff} then provides a linear dependence from which it is possible to determine the catalytic constants of both buffer components: extrapolation to $c_B/c_{Buff} = 0$ and 1 gives the catalytic constants k_B^{cor} and k_{BH}^{cor}, respectively. For the reactions monitored here, no significant general base-catalyzed rearrangement (k_B^{cor}) was observed in all the substituted acetate buffers. Only the acid−buffer component catalyzes the reaction, i.e., the reaction is general acid catalyzed. The catalytic constant k_{BH}^{cor} for the individual general acids is given in Table 1. A Brønsted plot of log k_{BH}^{cor} vs pK_a(BH) is linear with the slope $\alpha = -0.47$ (Figure 5). The point corresponding to catalysis by H_3O^+ can be calculated from the plateau at pH 2−3, and this point falls 0.5 log units below the extrapolated straight line in Figure 5.

For basic buffers (Figure 6) when k_{cor} is plotted against concentration of the base−buffer component (c_B), the linear portions of nonlinear dependences (at high c_{Buff}) are almost parallel. From this observation it can be concluded that the reaction in concentrated amine buffers involves general-base catalysis. In dilute buffers, both acid as well as base−buffer component can catalyze the reaction.

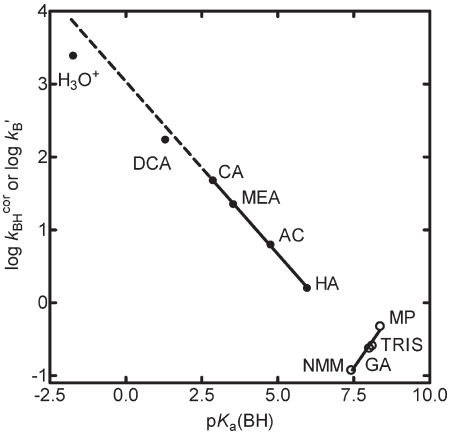

FIGURE 5. Brønsted plot of log k_{BH}^{cor} vs pK_a(BH) (●) and log k_B' vs pK_a(BH) (○).

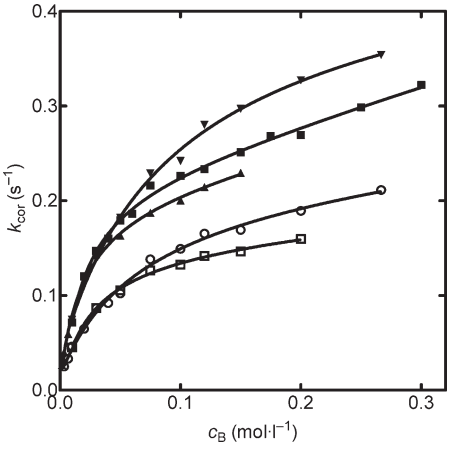

FIGURE 6. Dependence of the corrected rate constant (k_{cor}, s^{-1}) on the concentration of base-buffer component (c_B, $mol \cdot L^{-1}$) measured at 25 °C in morpholine (MP) buffers [(2:1a) pH 8.63 (▲); (1:1) pH 8.93 (■); (1:2b) pH 9.21 (▼)] and TRIS buffers [(1:1) pH 8.37 (□); (1:2b) pH 8.70 (○)]: (a) acidic; (b) basic.

A solvent kinetic isotope effect was also studied in (1:1) chloroacetate and acetate buffer (Figure 1). Both dependences of k_{obs} *vs* c_{Buff} in D_2O were linear (like in water), and the values for chloroacetate $k_{ext}^H/k_{ext}^D = 3.55$, $k_{Buff}^H/k_{Buff}^D = 2.14$ and for acetate $k_{ext}^H/k_{ext}^D = 1.83$, $k_{Buff}^H/k_{Buff}^D = 2.36$ were obtained.

Estimation of the pK_a of Isothiuronium Salt 1. Knowledge of the pK_a value is essential for correct evaluation of all kinetic data. It was not possible to measure the thermodynamic pK_a value of **1** because of the very high rates of cyclization at pH 6−8, but a pK_a(**1**) around 7 would be reasonable for an *N*-phenylisothiuronium salt. The pK_a of *S*-methyl-*N*-phenylisothiuronium is 7.14.[13] The lactone group in **1** will have an acidifying effect (through polar effects as well as due to intramolecular hydrogen bond), whereas a methoxy group in the *para*-position will have an opposite effect. In our case, the best fit of all data points in

(13) Pant, R. *Z. Physiol. Chem.* **1964**, *335*, 272–274.

Figure 4 using eq 2 or 5 with parameters given below was achieved for $pK_a(\mathbf{1}) = 6.7$.

We also verified this $pK_a(\mathbf{1})$ value using the SPARC program,[14a] which was successfully tested[14b] by estimation of more than 4300 ionization pK_a's. The SPARC program gave $pK_a(\mathbf{1})$ 6.2 and 7.3, respectively, for both possible canonical structures.

Mechanism of the Rearrangement and Evaluation of the Kinetic Data. The bimolecular[15] and intramolecular[4] aminolyses of esters that have been studied to date have shown large differences in the detailed mechanism. However, it is generally accepted that, with most esters, the attack of amine to form the labile intermediate $\mathbf{T}^{\pm}$ is rapid and reversible, and the rate-determining step at high pH is the trapping of this intermediate by proton removal with a general base giving $\mathbf{T}^{-}$, a proton switch through water ($\mathbf{T}^{\mathbf{0}}$), or direct breakdown of $\mathbf{T}^{\pm}$ to products. Only in very few cases when the intermediate $\mathbf{T}^{\pm}$ or $\mathbf{T}^{-}$ is too unstable to permit proton transfer to take place in a discrete step before its breakdown, a concerted mechanism or enforced concerted mechanism of catalysis is possible in order to avoid this labile intermediate.[3c,16,17] The existence of such labile tetrahedral intermediates has been proven indirectly on the basis of curved pH profiles,[4d,15e,f] curved buffer dependence plots,[4e,8b,11] curved Brønsted plots,[15d,f] kinetic isotope effects,[3f,4c] and quantum chemical calculations.[18] The intramolecular aminolysis of alkyl esters involves[4c−e,h] either breakdown of $\mathbf{T}^{-}$ or its general base-catalyzed formation from $\mathbf{T}^{\mathbf{0}}$. However, for cyclization of *S*-(ethoxycarbonylmethyl)isothiuronium chloride, which best resembles the rearrangement of our lactone, the rate-limiting formation and breakdown of $\mathbf{T}^{\pm}$ was reported.[12] To the best of our knowledge, the coexistence of all three kinetically detectable intermediates $\mathbf{T}^{\pm}$, $\mathbf{T}^{\mathbf{0}}$, and $\mathbf{T}^{-}$ during an aminolysis reaction has not yet been published.

In our case, the transitions in the pH profile (Figure 4) above pH 1 and 4.5 establish the formation of at least two different kinetically detectable intermediates, whose rate of formation and breakdown to product are pH dependent.[19] The break at pH ~7 gives either the value of the apparent ionization constant pK_{app} for **1** or is caused by appearance of another kinetically detectable intermediate (cf. behavior in buffers where at pH >6 linear dependences of k_{obs} vs c_{Buff} change to nonlinear). The combination of both possibilities is also conceivable.

It is impossible to neglect break at pH 5, although it is very slight, because the slope of the straight line crossing the points between pH 3.2−6.0 would be only 0.45. It is well-known that the slopes in pH profiles have mostly integral values giving whole number reaction orders.[20] Only in very rare systems, involving autocatalysis or autoinhibition, are the ratios of small integers such as 1/2 allowed (mostly in the gas phase). However, in a relatively narrow pH region (approximately two pH units), the slopes can change from one integral value to another, giving intermediate values as, for example, during hydrolysis of aspirin.[21]

SCHEME 2

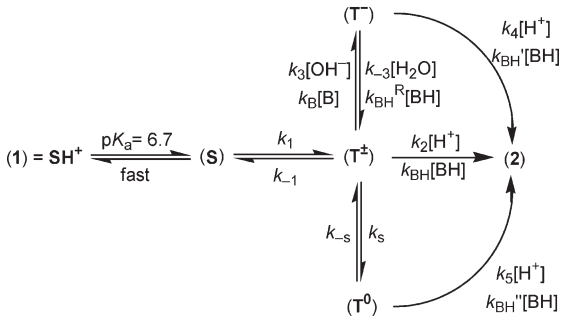

According to the literature and kinetic measurements, the following Scheme 2 can be suggested for rearrangement of **1** to **2**. (For structures of particular intermediates, see Scheme 3.)

Applying a steady-state approximation to the tetrahedral intermediates $\mathbf{T}^{\pm}$, $\mathbf{T}^{\mathbf{0}}$, and $\mathbf{T}^{-}$, we obtained eq 2 for the reaction at zero buffer concentration where K_a is the ionization constant of **1** (= $\mathbf{SH}^{+}$) and $K_W = 10^{-14}$ (at 25 °C) is the ion product of water.

$$k_{ext} = \frac{k_1 \frac{K_a}{K_a + [H^+]}}{k_{-1} + k_2[H^+]}\left(k_2[H^+] + \frac{k_S k_5 [H^+]}{k_{-S} + k_5[H^+]} + \frac{k_3 k_4 K_W}{k_{-3}[H_2O] + k_4[H^+]}\right) \quad (2)$$

The three terms in parentheses concern the acid-catalyzed breakdown of the intermediates $\mathbf{T}^{\pm}$, $\mathbf{T}^{\mathbf{0}}$, and $\mathbf{T}^{-}$. Fitting the pH profile using eq 2 is not sufficient to determine all nine rate constants, and only products or ratios of particular rate constants are accessible.

At pH 0−2.5, the starting compound is present almost entirely as the protonated species $\mathbf{SH}^{+}$, since the pK_a is 6.7, and the last two terms in parentheses can be neglected. Simultaneously, the ratio $K_a/(K_a + [H^+]) = K_a/[H^+]$ and eq 2 can be rewritten to eq 3, which is completely consistent with the previously reported equation.[12]

$$k_{ext} = \frac{k_1 k_2 K_a}{k_{-1} + k_2[H^+]} \quad (3)$$

The values $k_1 = 492\ s^{-1}$ and $k_2/k_{-1} = 5\ L \cdot mol^{-1}$ were obtained from the data (pH 0.5−2.5) using nonlinear regression. The optimized k_1 value which is the rate constant for cyclization of **S** to $\mathbf{T}^{\pm}$ is 40-fold less than the value found for cyclization of *S*-(ethoxycarbonylmethyl)isothiuronium chloride ($k_c = 2 \times 10^4\ L \cdot mol^{-1} \cdot s^{-1}$).[12] The reason lies in the presence of the 4-methoxyphenyl group, which lowers the nucleophilicity of the distant nitrogen (polar as well as steric effects). The break at pH 1.5 indicates a change in the rate-limiting step. At pH <0.5,

(14) (a) http://ibmlc2.chem.uga.edu/sparc/. (b) Hilal, S. H.; Karickhoff, S. W.; Carreira, L. A. *Quant. Struc. Act. Rel.* **1995**, *14*, 348–355.
(15) (a) Bunnett, J. F.; Davis, G. T. *J. Am. Chem. Soc.* **1960**, *82*, 665–674. (b) Jencks, W. P.; Carriuolo, J. *J. Am. Chem. Soc.* **1960**, *82*, 675–681. (c) Bruice, T. C.; Mayahi, M. F. *J. Am. Chem. Soc.* **1960**, *82*, 3067–3071. (d) Jencks, W. P.; Gilchrist, M. *J. Am. Chem. Soc.* **1968**, *90*, 2622–2637. (e) Blackburn, G. M.; Jencks, W. P. *J. Am. Chem. Soc.* **1968**, *90*, 2638–2645. (f) Satterthwait, A. C.; Jencks, W. P. *J. Am. Chem. Soc.* **1974**, *96*, 7018–7031. (g) Kovach, I. M.; Belz, M.; Larson, M.; Rousy, S.; Schowen, R. L. *J. Am. Chem. Soc.* **1985**, *107*, 7360–7365.
(16) Jencks, W. P. *Acc. Chem. Res.* **1976**, *9*, 425–432.
(17) Williams, A. In *Concerted Organic and Bio-organic Mechanisms*; CRC Press: Boca Raton, 2000.
(18) (a) Ilieva, S.; Galabov, B.; Musaev, D. G.; Morokuma, K.; Schaefer, H. F., III. *J. Org. Chem.* **2003**, *68*, 1496–1502. (b) Sung, D. D.; Koo, I. S.; Yang, K.; Lee, I. *Chem. Phys. Lett.* **2006**, *426*, 280–284.
(19) Holmquist, B.; Bruice, T. C. *J. Am. Chem. Soc.* **1969**, *91*, 2993–3002.
(20) Birk, J. P. *J. Chem. Educ.* **1976**, *53*, 704–707.
(21) (a) Edwards, L. J. *Trans. Faraday Soc.* **1950**, *46*, 723–735. (b) Garrett, E. R. *J. Am. Chem. Soc.* **1957**, *79*, 3401–3408.

SCHEME 3

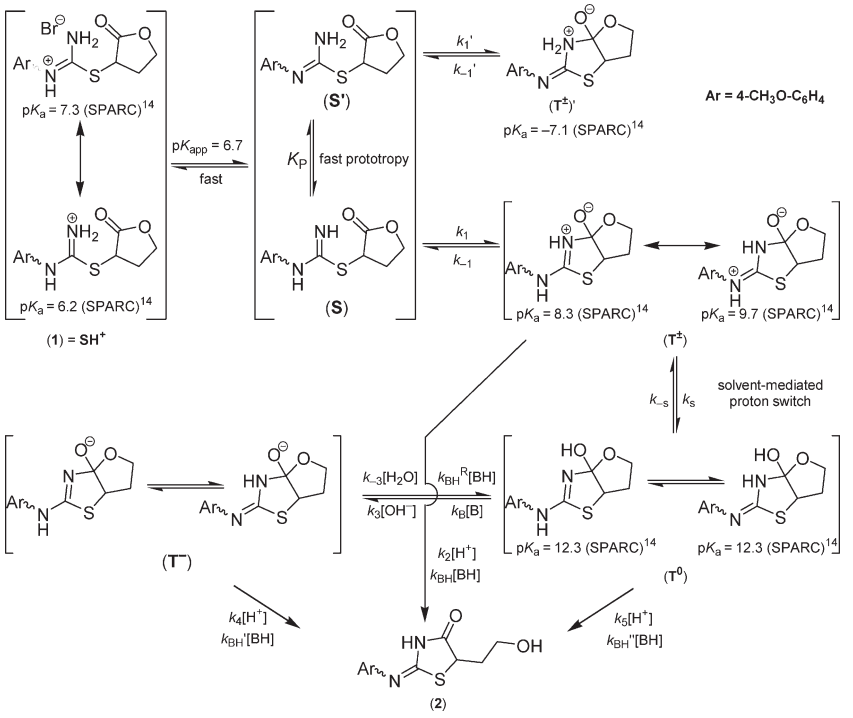

the term $k_2[H^+] \gg k_{-1}$ and eq 3 can be simplified as follows, $k_{ext} = k_1K_a/[H^+]$, and the formation of $\mathbf{T}^{\pm}$ is rate-limiting. At pH >1.5, $k_2[H^+] \ll k_{-1}$, and $k_{ext} = k_1k_2K_a/k_{-1}$ is pH-independent. The acid-catalyzed breakdown of $\mathbf{T}^{\pm}$ is now the rate-limiting step of the rearrangement. The value of the solvent kinetic isotope effect $k_{ext}^{H}/k_{ext}^{D} = 3.55$ measured in chloroacetate buffer ($c_B/c_{BH} = 1$, pH 2.67) must be consistent with the simplified form of eq 3 at pH >1.5 (plateau). It can be presumed that the solvent kinetic isotope effect for the formation and reverse breakdown of $\mathbf{T}^{\pm}$ will be negligible ($K_1^{H}/K_1^{D} \approx 1$). Solvent kinetic isotope effect for the ionization constant $K_a^{H}/K_a^{D} \approx 3$ can be estimated from fractionation factors. The value of k_2^{H}/k_2^{D} which corresponds to the H_3O^+-catalyzed breakdown of $\mathbf{T}^{\pm}$ is then 1.18. This value is substantially lesser than the value found for chloroacetic acid $k_{Buff}^{H}/k_{Buff}^{D} = 2.14$.[4c] This result can be explained by different transition-state geometry. In the case of weak acids (BH), the proton has almost a central position between $\mathbf{T}^{\pm}$ and acid in the transition state (as seen from $\alpha = -0.47$; i.e., $\mathbf{T}^{\pm}\cdots H\cdots B$), whereas in the case of much stronger H_3O^+ the transition state closely resembles reactants (early transition state $\mathbf{T}^{\pm}\cdots H{-}OH_2^+$ for which α should approach zero, as can be seen from the point falling below the straight line in Figure 5).

At pH >2.5 a new reaction pathway through $\mathbf{T}^{\mathbf{0}}$ gradually opens, and the second term in eq 2 becomes kinetically significant. k_{ext} is given by eq 4.

$$k_{ext} = \frac{k_1K_a}{k_{-1}}\left(k_2 + \frac{k_Sk_5}{k_{-S} + k_5[H^+]}\right) \qquad (4)$$

Using the parameters mentioned above, the ratios $k_{-S}/k_5 = 1.3 \times 10^{-5}$ mol·L^{-1} and $k_S/k_{-1} = 8.8 \times 10^{-4}$ were obtained by optimization of the data in pH profile. From the break at pH 4.9, it can be concluded that a change in the rate-limiting step occurs again. At pH <4.9, the formation of $\mathbf{T}^{\mathbf{0}}$ is rate-limiting, whereas at pH >4.9 its acid-catalyzed breakdown is involved. The value of solvent kinetic isotope effect $k_{ext}^{H}/k_{ext}^{D} = 1.83$ measured in acetate buffer ($c_B/c_{BH} = 1$, pH 4.61) is much less than observed in chloroacetate buffer. This observation is consistent with eq 4 under the following presumptions. Solvent kinetic isotope effect is still $K_a^{H}/K_a^{D} \approx 3$, but the ratio of fractions $(k_S^{H}k_5^{H}/(k_{-S}^{H}+k_5^{H}[H^+]))/(k_S^{D}k_5^{D}/(k_{-S}^{D}+k_5^{D}[D^+]))$ must be less than 1 because the concentration of D^+ is 3 times less than $[H^+]$ in buffer with the same c_B/c_{BH}. The value 1.83 refers to the rearrangement of $\mathbf{T}^{\pm}$ to $\mathbf{T}^{\mathbf{0}}$ (K_S^{H}/K_S^{D}) as well as to acid-catalyzed decomposition of $\mathbf{T}^{\mathbf{0}}$ (k_5^{H}/k_5^{D}).

The last reaction pathway (at pH > 5) involves the trapping of $\mathbf{T}^{\pm}$ by proton removal with a base giving $\mathbf{T}^{-}$. The nonlinear regression of all experimental data points using previously optimized parameters with eq 2 gave the values of $k_{-3}/k_4 = 2.6 \times 10^{-8}$ s^{-1} and $k_3/k_{-1} = 7 \times 10^3$ l·mol^{-1}.

Although the values of individual rate constants are not directly accessible from optimization of the measured data, they can be estimated as follows. Proton transfer from $\mathbf{T}^{\pm}$ to the strong base hydroxide ion will be thermodynamically favorable, so that the value of k_3 is taken as 10^{10} L·mol^{-1}·s^{-1} for hydroxide ion.[22] The rate constant for the reverse breakdown of $\mathbf{T}^{\pm}$ to **S** is then $k_{-1} = 1.4 \times 10^6$ s^{-1}. This value is approximately 2 orders of magnitude lesser than the estimated rate constant $k_{-1} = 6.6 \times 10^8$ s^{-1} for expulsion of amine from the related cyclic zwitterionic intermediate.[23] The value estimated by us is not totally unreasonable because our $\mathbf{T}^{\pm}$ is resonance-stabilized (Scheme 4), and therefore, its reverse breakdown would be slower. If the value of k_{-1} is 1.4×10^6 s^{-1}, then $k_2 = 7.0 \times 10^6$ L·mol^{-1}·s^{-1} and $k_S = 1260$ s^{-1}.

The two proton transfers that convert $\mathbf{T}^{\pm}$ to $\mathbf{T}^{\mathbf{0}}$ could occur either in a stepwise mechanism through $\mathbf{T}^{+}$, with the

(22) Eigen, M. *Angew. Chem., Int. Ed. Engl.* **1964**, *3*, 1–19.
(23) Barnett, R. E.; Jencks, W. P. *J. Am. Chem. Soc.* **1969**, *91*, 2358–2369.

rate constants k_{OH} and k_H (not shown in Schemes 2 and 3) or in a single concerted step with the rate constant k_S, which may include one to two water molecules. Water acts as a bifunctional catalyst for proton transfer through a five- or eight-membered ring. Experimental distinction between the two mechanisms can be done by measuring a solvent isotope effect. Bifunctional concerted catalysis is in accord with a solvent isotope effect less than 2.[24] In our case, the k_{ext}^{H}/k_{ext}^{D} obtained from linear dependences of k_{obs} *vs* c_{Buff} measured in acetate buffer (1:1) in H_2O and D_2O is only 1.83, which supports the idea of water-mediated proton switch. The values of k_S are generally in the range[4d,15f,25] $10^5-10^8\ s^{-1}$. Our value $k_S = 1260\ s^{-1}$ is quite small (perhaps due to mentioned resonance stabilization of $\mathbf{T}^{\pm}$).

An alternative mechanism is proposed in Scheme 3, together with corresponding eq 5. The only difference between mechanisms in Scheme 2 and 3 is that the cleavage of a proton proceeds from $\mathbf{T}^{\mathbf{0}}$ instead of $\mathbf{T}^{\pm}$.[4c]

$$k_{ext} = \frac{k_1\dfrac{K_a}{K_a+[H^+]}}{k_{-1}+k_2[H^+]}\left(k_2[H^+]+\frac{k_S k_5[H^+]}{k_{-S}+k_5[H^+]} + \frac{k_S k_3 k_4 K_W}{(k_{-S}+k_5[H^+])(k_{-3}[H_2O]+k_4[H^+])}\right) \quad (5)$$

Optimized values of $k_1, k_2/k_{-1}$, and k_{-S}/k_5 are the same as those obtained from eq 2. From the last two terms of eq 5 the ratios $k_S/k_{-1} = 8.0\times10^{-4}$, $k_{-3}/k_4 = 3.0\times10^{-7}\ s^{-1}$, and $k_3K_S/k_{-1} = 6\times10^4\ L\cdot mol^{-1}$ were optimized. In order to calculate the rate constants k_{-1} and k_S the value of K_S is needed. K_S can be estimated from the values of $pK_a(\mathbf{T}^{\pm}) = 8.3 - 9.7$ (cf. $pK_a(\mathbf{T}^{\pm}) = 9.8$ determined for a similar intermediate[8c]) and $pK_a(\mathbf{T}^{\mathbf{0}}) = 12.3$ which were calculated using SPARC.[14] From them, $K_S = k_S/k_{-S} = 4\times10^2 - 1\times10^4$.

If the value of k_3 is taken as $10^{10}\ L\cdot mol^{-1}\cdot s^{-1}$ and K_S is in the range $4\times10^2-1\times10^4$, then $k_{-1} = 6.7\times10^7-1.7\times10^9\ s^{-1}$, $k_2 = 3.4\times10^8-8.3\times10^9:\cdot mol^{-1}\cdot s^{-1}$, and $k_S = 5.4\times10^5-1.3\times10^6\ s^{-1}$, which conforms well with the literature mentioned above. The decision as to which mechanism is correct can be made from measurements in buffers.

In all buffer solutions, the reaction involves general acid−base catalysis; therefore, at least one buffer component must also catalyze the rearrangement of **1** to **2**, and extended kinetic eqs 6 and 7 derived from Schemes 2 and 3 can be written:

$$k_{obs} = k_{ext} + \frac{k_1\dfrac{K_a}{K_a+[H^+]}}{k_{-1}+k_{BH}[BH]}\left(k_{BH}[BH]+\frac{k_S k_{BH}'[BH]}{k_{-S}+k_{BH}'[BH]} + \frac{k_B k_{BH}''[B]}{k_{BH}^{R}+k_{BH}''}\right) \quad (6)$$

$$k_{obs} = k_{ext} + \frac{k_1\dfrac{K_a}{K_a+[H^+]}}{k_{-1}+k_{BH}[BH]}\left(k_{BH}[BH]+\frac{k_S k_{BH}'[BH]}{k_{-S}+k_{BH}'[BH]} + \frac{k_S k_B k_{BH}''[B]}{(k_{-S}+k_{BH}'[BH])(k_{BH}^{R}+k_{BH}'')}\right) \quad (7)$$

(24) Cox, M. M.; Jencks, W. P. *J. Am. Chem. Soc.* **1981**, *103*, 580–587.

SCHEME 4

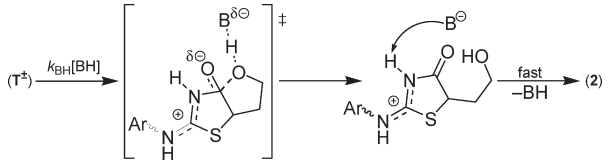

No significant general base-catalyzed reaction (k_B) was observed in substituted acetate buffers; therefore, the last term in parentheses in both eq 6 and eq 7 can be neglected. All dependences of k_{obs} *vs* c_{Buff} are linear, which means that $k_{BH}[BH] \ll k_{-1}$ (general acid BH is much weaker than H_3O^+) and $k_{BH}'[BH] \gg k_{-S}$. Equations 1 and 6 or 7 can be combined to eq 8, where $k_{BH}^{cor} = K_1k_{BH}$, $K_1 = k_1/k_{-1}$, and $k_0^{cor} = k_{ext}(K_a + [H^+])/K_a + K_1k_S$.

$$k_{cor} = k_0^{cor} + k_{BH}^{cor}[BH] \quad (8)$$

A Brønsted plot of $\log k_{BH}^{cor}$ vs $pK_a(BH)$ is linear, and the slope $\alpha = -0.47$ (Figure 5) must reflect a rate-limiting step involving proton transfer from general acid to $\mathbf{T}^{\pm}$ which is concerted with C−O bond breaking (Scheme 4). The reaction may occur by a "one-encounter" mechanism in which the same molecule of catalyzing acid (BH) donates a proton to the poorly leaving alkoxide and removes it from the nitrogen[15e] in order to avoid thermodynamically unfavorable protonated intermediate/product ($pK_a \approx -7$).

In basic amine buffers, the catalytic power of general acid BH decreases and the dependences of k_{obs} vs c_{Buff} are no longer linear because the term $k_{BH}[BH]$ is low and the term $k_{BH}'[BH]$ becomes comparable with k_{-S}. Furthermore, a general base-catalyzed pathway gradually opens in those buffers (eqs 9 and 10). Only eq 9 is consistent with the observation of linear increase of k_{cor} with c_B in concentrated buffers (Figure 6) because the eq 10 predicts saturation kinetics. The mechanism in Scheme 2 is therefore more plausible.

$$k_{cor} = k_{ext}^{cor} + K_1\left(\frac{k_S k_{BH}'[BH]}{k_{-S}+k_{BH}'[BH]} + \frac{k_B k_{BH}''[B]}{k_{BH}^{R}+k_{BH}''}\right) \quad (9)$$

$$k_{cor} = k_{ext}^{cor} + K_1\left(\frac{k_S k_{BH}'[BH]}{k_{-S}+k_{BH}'[BH]} + \frac{k_S k_B k_{BH}''[B]}{(k_{-S}+k_{BH}'[BH])(k_{BH}^{R}+k_{BH}'')}\right) \quad (10)$$

From the linear portions of nonlinear dependences (at high c_B), the slopes give $k_B' = K_1k_{BH}''k_B/(k_{BH}^{R}+k_{BH}'')$ for particular base−buffer components (Table 1). The Brønsted plot of $\log k_B'$ vs $pK_a(BH)$ is linear, and the slope $\beta_{obs} = 0.6$ (Figure 5). This value cannot be interpreted in terms of simple proton transfer from $\mathbf{T}^{\pm}$ to the base (B) because k_B' is the composite constant. It can be presumed that the dependence of $\log k_B$ vs $pK_a(BH)$ should have a slope approaching unity[4c,15e] (Eigen-type Brønsted correlation); therefore, the difference between the predicted and observed

(25) (a) Chang, K. C.; Grunwald, E. *J. Phys. Chem.* **1976**, *80*, 1422–1425. (b) Grunwald, E.; Chang, K. C.; Skipper, P. L.; Anderson, V. K. *J. Phys. Chem.* **1976**, *80*, 1425–1431. (c) Bensaude, O.; Dreyfus, M.; Dodin, G.; Dubois, J. E. *J. Am. Chem. Soc.* **1977**, *99*, 4438–4446.

slope $\Delta\beta = 0.4$ corresponds to two proton transfers (k_{BH}^{R} and k_{BH}'') from general acid to $\mathbf{T}^{-}$.

Conclusions

Treatment of the isothiuronium salt 1 (= $\mathbf{SH}^{+}$) with base produces reactive isothiourea in a fast pre-equilibrium ($pK_a = 6.7$). The resulting isothiourea can exist in the form of two prototropic tautomers (**S** and **S′**) that are rapidly interchanging with one another. In principle, both tautomers can undergo cyclization to the zwitterionic intermediate ($\mathbf{T}^{\pm}$ or $\mathbf{T}^{\pm\prime}$). However, only the tautomer **S** provides (k_1) the resonance-stabilized $\mathbf{T}^{\pm}$ whose estimated $pK_a(\mathbf{T}^{\pm}) = 8.3-9.7$ is not very different from $\mathbf{SH}^{+}$ so that there is not a large favorable free energy for proton transfer from $\mathbf{SH}^{+}$ to catalyzing base, and concerted catalysis cannot be expected for either the formation or breakdown of the zwitterionic intermediate.[3c] The stepwise process involving fast pre-equilibrium with subsequent cyclization is in accord with the "libido" rule.[1d,17,26] On the other hand, the cyclization of **S′** (k_1') would provide $\mathbf{T}^{\pm\prime}$, which is not resonance-stabilized, and its $pK_a(\mathbf{T}^{\pm\prime})$ should be around −7 (i.e., far from starting SH^{+}). Therefore, $\mathbf{T}^{\pm\prime}$ is not directly involved in reaction, but the K_P can influence the apparent ionization constant of SH^{+}. The existence of the zwitterionic intermediate $\mathbf{T}^{\pm}$ is proven by the break in pH profile (Figure 4) at pH 1.5 (see the section dealing with kinetic data evaluation). Zwitterionic intermediate $\mathbf{T}^{\pm}$ then undergoes either acid-catalyzed concerted[27] breakdown to product (pH 2−3) or water-mediated proton switch from N to O (pH 3−5). Such proton transfers between electronegative base pairs in hydroxylic solvents often occur by relay through one or more solvent molecules.[17] The last reaction pathway (pH > 5) involves the formation of anionic intermediate $\mathbf{T}^{-}$ either from $\mathbf{T}^{\pm}$ or from $\mathbf{T}^{0}$. The first possibility involving reaction $\mathbf{T}^{\pm} \rightarrow \mathbf{T}^{-}$ (Scheme 2) seems to be more likely because it is in accordance with behavior in basic amine buffers, where linear increase of the observed rate constant with c_B is observed. To the best of our knowledge, the coexistence of all three kinetically detectable intermediates $\mathbf{T}^{\pm}$, $\mathbf{T}^{0}$, and $\mathbf{T}^{-}$ in aminolysis is unique throughout the literature. We have found only one example of kinetic evidence for three species of the tetrahedral intermediate during lactonization of 4,6,8-trimethylcoumarinic acid.[28] We believe that this coexistence is possible only due to enhanced stability of all mentioned intermediates whose easy formation and slow breakdown reflects the advantage of an intramolecular reaction and the presence of a relatively poor leaving group (alkoxide) necessitating participation of an acid.

Experimental Section

Compounds. Preparation and characterization of *S*-(2-oxotetrahydrofuran-3-yl)-*N*-(4-methoxyphenyl)isothiuronium bromide (**1**) and 5-(2-hydroxyethyl)-2-[(4-methoxyphenyl)imino]-1,3-thiazolidin-4-one (**2**) was described elsewhere.[9]

Kinetic Measurements. All of the kinetic measurements were carried out in a 1 cm closable cell using a Hewlett-Packard 8453 diode array spectrophotometer at 25 ± 0.1 °C. The observed pseudo-first-order rate constants k_{obs} were calculated from absorbance−time dependences at the wavelengths of 260 and 273 nm and at the substrate concentrations of ca. 5×10^{-5} mol·L^{-1}. Ionic strength $I = 1$ mol·L^{-1} was adjusted by KCl. In all kinetic runs, the standard deviation in the fit was always less than 1% of the quoted value and was more usually between 0.2 and 0.4% of the quoted value. The pH of individual buffers was measured using PHM 93 Radiometer Copenhagen apparatus equipped with glass electrode. Redistilled water, commercially available substituted acetic acids, amines, and potassium chloride (p.a.) for adjustment of ionic strength of buffer solutions were used. The solvent kinetic isotope effect was measured in chloroacetate and acetate buffers ($c_B/c_{BH} = 1:1$) of the same composition and ionic strength which were prepared from potassium chloride, sodium hydroxide, chloroacetic anhydride/acetic anhydride, and H_2O or D_2O (99.8% D). Rapid deuteration of isothiuronium moiety in D_2O, which can cause a slight secondary kinetic isotope effect, was confirmed by ^{1}H NMR experiment. The starting salt **1** was dissolved in D_2O, and the ^{1}H NMR spectrum was measured immediately. All NH and NH_2 protons completely disappeared due to very fast exchange with solvent. This observation also proves that there is a rapid establishment of equilibrium between the salt and its conjugate base (proton transfer from/to nitrogen has the rate constant k about 10^{10} L·mol^{-1}·s^{-1}).[22]

The dissociation constant of particular buffer components (substituted acetic acids and ammonium cations) was taken from the literature.[29]

Acknowledgment. Financial support by the Ministry of Education, Youth, and Sports of the Czech Republic (Project MSM 002 162 7501) is gratefully acknowledged.

Supporting Information Available: All kinetic data (the observed rate constants measured in buffers and HCl) and selected spectral records. This material is available free of charge via the Internet at http://pubs.acs.org.

(26) Jencks, W. P. *J. Am. Chem. Soc.* **1972**, *94*, 4731–4732.
(27) Cordes, E. H.; Bull, H. G. *Chem. Rev.* **1974**, *74*, 581–603.
(28) Hershfield, R.; Schmir, G. L. *J. Am. Chem. Soc.* **1973**, *95*, 8032–8040.
(29) (a) Jencks, W. P.; Regenstein, J. In *Handbook of Biochemistry*, 2nd ed.; Sober, H. A., Ed.; Chemical Rubber Publishing Co.: Cleveland, 1970. (b) Perrin, D. D. In *Dissociation Constants of Organic Bases in Aqueous Solution*; Butterworths: London, 1965. (c) Garel, J.; Tawfik, D. S. *Chem.—Eur. J.* **2006**, *12*, 4144–4152.